COMPOUND SPECIFIC ISOTOPE ANALYSIS TO TRACK SOURCES AND TRANSFORMATION PROCESSES OF MICROPOLLUTANTS

–

INVESTIGATIONS IN ENGINEERED AND NATURAL SYSTEMS WITH A SPECIAL FOCUS ON DICLOFENAC AND CHIRAL HERBICIDES

Dissertation
der Mathematisch-Naturwissenschaftlichen Fakultät
der Eberhard Karls Universität Tübingen
zur Erlangung des Grades eines
Doktors der Naturwissenschaften
(Dr. rer. nat.)

vorgelegt von
Michael Maier
aus Nürnberg

Tübingen
2014

Gedruckt mit Genehmigung der Mathematisch-Naturwissenschaftlichen Fakultät der Eberhard Karls Universität Tübingen.

Tag der mündlichen Qualifikation:	20.05.2015
Dekan:	Prof. Dr. Wolfgang Rosenstiel
1. Berichterstatter:	PD Dr. Martin Elsner
2. Berichterstatter:	Prof. Dr. Christian Zwiener
3. Berichterstatter	Prof Dr. Thomas Ternes

TABLE OF CONTENTS

1 General Introduction 1

1.1 Global challenges related to pesticides & pharmaceuticals 2

1.1.1 Occurrence of Micropollutants in the Environment 2

1.1.2 Effects & Fate of Micropollutants in the Environment 2

1.1.3 Established Techniques to Investigate the Fate of Micropollutants 3

1.1.4 Product Counterfeiting of Pharmaceuticals 4

1.2 Principles of Enantioselective & Compound Specific Isotope Analysis (ESIA & CSIA) 4

1.2.1 Source Tracking of Micropollutants by CSIA 5

1.2.2 Isotope Fractionation during Transformation Reactions 6

1.2.3 Principles of Enantioselective Isotope Analysis (ESIA) 9

1.3 Content of the present thesis 11

1.3.1 Analytical Challenges & Objectives of CSIA and ESIA of Micropollutants 11

1.3.2 Challenge of large number of C-atoms in micropollutants 13

1.3.3 Challenge of process understanding 13

1.4 References 14

2 C & N Isotope Analysis of Diclofenac to Distinguish Oxidative and Reductive Transformation and to Track Commercial Products 18

2.1 Abstract 19

2.2 Introduction 20

2.3 Materials and Methods 21

2.3.1 Chemicals 21

2.3.2 Purification of Commercial Pharmaceutical Products and Treatment for Isotope Analysis 21

2.3.3 Aerobic Biodegradation Experiment 22

2.3.4 Dechlorination Experiment 23

2.3.5 Online Derivatization GC-IRMS Analysis 23

2.3.6 Offline Derivatization - Splitless Injection 24

2.3.7 Offline Derivatization-On-Column Injection 24

2.3.8 Extraction and Purification from River Water Samples 25

2.3.9 Post-Measurement Correction of Carbon Isotope Ratios 25

2.3.10 Evaluation of Isotope Fractionation 26
2.3.11 Evaluation of Degradation Kinetics 27
2.4 Results & Discussion 27
2.4.1 Method Validation & Quantification Limit 27
2.4.2 Source Variability and Potential for Source Tracking 29
2.4.3 Isotope Fractionation During Degradation by Aerobic River Sediment 31
2.4.4 Reductive dechlorination 33
2.4.5 Environmental Significance 34
2.4.6 Acknowledgements 35
2.5 References 36
3 Isotope Fractionation of Diclofenac in Environmental & Engineered Systems: Evidence of Different Oxidation Mechanisms 40
3.1 Abstract 41
3.2 Introduction 42
3.3 MATERIALS AND METHODS 44
3.3.1 Chemicals 44
3.3.2 Phototransformation 44
3.3.3 Ozonation 44
3.3.4 Oxidation by MnO_2 45
3.3.5 Single electron transfer by ABTS 45
3.3.6 Detection methods 45
3.3.7 Isotope analysis to evaluate (competing) transformation mechanisms 46
3.4 Results & Discussion 47
3.4.1 Phototransformation 47
3.4.2 Ozonation 48
3.4.3 Insights into oxidation mechanisms – ABTS & MnO_2 49
3.4.4 Environmental Significance 52
3.4.5 Acknowledgements 54
3.4.6 References 54
4 Enantioselective Stable Isotope Analysis (ESIA) of Polar Herbicides 58
4.1 Abstract 59
4.2 Introduction 59

4.3 Experimental 61
4.3.1 Compounds and chemicals 61
4.3.2 Derivatisation with BF3 61
4.3.3 Isotope Analysis 61
4.3.4 Calculation of the introduced methyl-group 62
4.3.5 Peak identity 63
4.3.6 DCPP transformation study 63
4.4 Results 64
4.4.1 Chromatographic Resolution 64
4.4.2 Isotope Analysis 65
4.4.3 Application of ESIA to phenoxyacids 67
4.5 Outlook 68
4.6 Acknowledgements 68
4.7 Reference 69
5 General Conclusions 71
Appendix I
Appendix A1. Compound-Specific Isotope analysis of benzotriazole and its derivatives II
Appendix A2. Combined Isotope and Enantiomer Analysis to Assess the Fate of Phenoxy Acids in a Heterogeneous Geologic Setting at an Old Landfill XVII
Appendix A3. Supporting Information of Chapter 2 XXXI
Appendix A4. Supporting Information of Chapter 3 XLII
Appendix A5. Curriculum Vitae L

ACKNOWLEDGEMENTS

An erster Stelle möchte ich mich bei Martin Elsner bedanken! Du hast immer die perfekte Balance gefunden mich zu fördern und zu fordern. Durch Dein didaktisches Geschick, hatte ich nie das Gefühl beim eigenen Unvermögen erwischt worden zu sein, sondern mich immer gefreut was gelernt zu haben! Auch weiß ich die große Freiheit zu schätzen mit der ich meine Ideen (und Utopien) ausprobieren durfte, immer mit dem Wissen dass Deine Tür offen ist. Vielen Dank!

Bedanken möchte ich mich auch bei allen Co-Autoren, insbesondere aber bei Carsten Prasse! Deine wissenschaftliche Leitlinie „Wenn Leute lachen, sind sie fähig zu denken“ deckt sich zu 100% mit meinem Verständnis von Forschung und das große Kino in Kapitel 3 wäre ohne unsere grandiose Zusammenarbeit nie gezeigt worden.

Ein großes Dankeschön geht auch an meine externen Betreuer – Christian Zwiener, Thomas Ternes und Michael Radke. Ohne die „Motivation“ aus dem Treffen in Ulm hätten die Diclofenac-Isotope den ngL^{-1} Bereich nie gesehen! Außerdem nochmal vielen Dank Michael, hätte die Diplomarbeit bei Dir nicht so viel Spaß gemacht, würde es diese Arbeit nicht geben!

Bei Rainer Meckenstock möchte ich mich herzlich für die Unterstützung und das Vertrauen bedanken, das Du mir damals beim Antrag schreiben und der Konzeption dieser Arbeit entgegen gebracht hast.

Dem ganzen IGÖ, vor allem aber der Isotopenfamilie Danke ich fürs Dasein, für die offenen Ohren, die schlauen Kommentare, die gute Laune und Armin für die fränkische Unterstützung im bayrischen Exil – Wir sind der Glubb!

Heini, vielen Dank für die allumfassenden Diskussionen, die immer hilfreich waren die Isotopenanalytik im Geschehen des 21. Jahrhunderts sowohl sportlich, wirtschaftlich, wissenschaftlich und auch kulturell richtig einzuordnen! Außerdem, vielen Dank für die einmalige Gelegenheit das frisch veröffentlichte Kapitel 4 in die große Welt der kommerziellen Isotopenanalyse zu bringen!

Vielen Dank für die großartige Zeit Thomas Spaett und Sebastian Nitsche! Ihr wart die besten Bachelorstudenten die ich je hatte! Mit Euch war „Wissen schaffen und Spaß dabei“ immer Programm!

Bei der Deutschen Bundesstiftung Umwelt und meinem dortigen Betreuer Max Hempel möchte ich mich für die finanzielle Förderung bedanken, vor allem aber auch für die grandiosen Seminare, welche sowohl fachlich und sozial ihresgleichen suchen!

Meiner Familie und insbesondere meinen Eltern und Großeltern möchte ich von ganzem Herzen für die Unterstützung Danken! Ohne Euer Vertrauen über all die Jahre wäre diese Arbeit nicht möglich gewesen!

Vielen lieben Dank Tine! Wann immer mich die Massen Spektrometer in den Wahnsinn getrieben haben, hast Du mich durch Dein Zuhören und vor allem durch Deine Liebe wieder zurückgeholt – was wäre ich ohne Dich! Vielen Dank!

ZUSAMMENFASSUNG

Arzneimittel und Pestizide gelangen über Kläranlagen und Felder in die Umwelt und zählen zu den am häufigsten nachgewiesenen Spurenstoffen in Gewässern. Es besteht daher großes Interesse herauszufinden, in welchem Ausmaß und durch welche Prozesse Spurenstoffe in der Umwelt abgebaut werden können. Allerdings ist es häufig schwierig, Abbauprozesse allein durch Konzentrationsmessungen zu bestimmen, da beispielsweise auch Verdünnungsprozesse zu einem Rückgang der Konzentrationen führen können. Dabei wird allerdings die Menge an Spurenschadstoffen in der Umwelt nicht reduziert, sondern nur ihre Gegenwart verschleiert. Außerdem können durch die Konzentrationsmessung von Spurenschadstoffen keine Abbauprozesse unterschieden werden. Dies ist zwar durch die Analyse von Transformationsprodukten (TPs) möglich, jedoch sind diese häufig nicht vollständig bekannt und können weiter abgebaut werden. Außerdem führen in manchen Fällen mehrere Prozesse zu demselben Abbauprodukt. Daher eignen sich bestehende Methoden nur bedingt zur (quantitativen) Untersuchung von Abbauprozessen in realen Systemen.

Komponentenspezifische Isotopenanalyse (CSIA) kann Transformationsprozesse unabhängig von Verdünnungseffekten nachweisen und sogar verschiedene Transformationsmechanismen unterscheiden. Dabei werden die natürlicherweise im Molekül enthaltenden Isotopenverhältnisse von $^{13}C/^{12}C$ und $^{15}N/^{14}N$ analysiert. Solange kein Abbau stattfindet, sind diese charakteristisch für die Herkunft eines Stoffes. Findet Abbau statt, so ändern sich die Isotopenverhältnisse im Substrat in Abhängigkeit vom zugrunde liegenden Reaktionstyp. Durch die alleinige Analyse der Isotopenverhältnisse des Substrats ist es dann möglich, Abbauprozesse zu untersuchen. Bisher mit diesem Ansatz allerdings noch nie Arzneimittel untersucht und außerdem war seine Anwendung auf relativ hohe Konzentrationen beschränkt. Daher wurde erstmals eine CSIA Methode für die Modellsubstanz Diclofenac entwickelt, welche sowohl in der Medizin, als auch in der Umwelt zu den am weitesten verbreiteten Arzneimitteln zählt. Diese neu entwickelte Methode wurde einerseits genutzt um die Anwendung von CSIA in den ng L^{-1} Bereich vorzuspuren. Andererseits wurde sie eingesetzt um durch CSIA von Kohlenstoff- und Stickstoffisotopen neue Erkenntnisse auf drei Ebenen zu erhalten.

(i) Da Isotopenverhältnisse durch die Wahl der Rohstoffe und des Synthesewegs beeinflusst werden konnten die meisten der getesteten Diclofenac Produkte (Tabletten, Gele) durch C und N Isotopenanalyse unterschieden werden. Dadurch können einerseits pharmazeutische Produkte mit einer

fälschungssicheren Methode verifiziert werden. Andererseits können verschiedene Quellen von Diclofenac in der Umwelt verfolgt werden, wie zum Beispiel Kläranalagen oder Gülle von Tieren, welche mit Diclofenac behandelt wurden.

(ii) CSIA konnte als neue Beweislinie für Abbauprozesse etabliert werden, welche unabhängig von der Detektion von TPs ist. Sechs verschiedene Transformationspfade wurden untersucht und alle konnten durch CSIA nachgewiesen werden. Dabei zeigte sich das interessante Bild, dass sich umweltrelevante Reaktionen durch die Analyse der C und N Isotopenverhältnisse in 2 Gruppen unterteilen lassen. Während Ozonierung und Photolyse inverse N-Isotopeneffekte verursachen, zeigen biologischer Abbau und Abbau durch Manganoxide normale N-Isotopeneffekte. Dies ist einerseits von großem Interesse, da sowohl Photolyse als auch biologischer Abbau als potentiell wichtigste Eliminationspfade in der Umwelt gelten und CSIA beide Prozesse in-situ unterschieden kann. Andererseits kann CSIA auch wertvolle Einblicke in die (Abwasser-) Aufbereitung liefern, wenn die Effizienz von biologischer Reinigung, Mangandioxid-Zugabe und/oder Ozonierung untersucht werden soll.

(iii) Dadurch, dass Isotopeneffekte Übergangszustände von Transformationsreaktionen widerspiegeln, liefern sie einzigartige Einblicke in Reaktionsmechanismen, welche durch andere Methoden unter umweltrelevanten Bedingungen nicht zugänglich sind. Das damit einhergehende Potential von CSIA wurde beim Vergleich der Reaktionen von Diclofenac mit MnO_2 und ABTS deutlich. Beide Reaktionen wurden als Modelle für Ein-Elektron-Oxidation angesehen, welche häufig bei enzymatischen Reaktionen auftritt. Allerdings zeigte CSIA, dass sich beide Reaktionen fundamental unterscheiden. Während ABTS tatsächlich durch Outer-Sphere-Ein-Elektron-Oxidation reagiert und inverse N-Isotopeneffekte verursacht, zeigte sich bei MnO_2 ein ausgeprägter normaler N-Isotopeneffekt der zudem mit dem Fraktionierungsmuster des biotischen Abbaus übereinstimmt. Ferner wurde durch CSIA deutlich, dass die ausgeprägte Isotopenfraktionierung einen wichtigen, aber noch unerforschten Transformationspfad widerspiegelt, welcher momentan nicht durch Transformationsprodukte detektierbar ist. Als weitere wichtige Reaktion Außerdem wurden mittels CSIA zum ersten Mal Transformationsprozesse bei der Ozonierung studiert. Dabei lieferte CSIA ein starkes Indiz dafür, dass das Ozonmolekül nicht am N-Atom von Diclofenac angreift, sondern am aromatischen Ring.

Neben Diclofenac wurden im Rahmen dieser Arbeit auch chirale Herbizide untersucht. Dazu wude CSIA mit enantioselektiver Trennung kombiniert um die Transformationsprozesse von chiralen Herbiziden mit einem noch vielfältigeren Ansatz zu untersuchen. Es zeigte sich, dass Isotopen- und

Enantiomerenverhältnisse komplementär verhalten. Während in dieser Studie ein Fall untersucht wurde, bei dem keine Isotopenfraktionierung, allerdings Enantiomerenfraktionierung gemessen werden konnte, wurde in einer anderen Studie genau das Gegenteil für ein Insektizid beobachtet. Interessanterweise konnten in einer ersten Feldstudie beide Prozesse parallel nachgewiesen werden.

Die vorliegende Studie hat gezeigt, dass CSIA und ESIA in vielfältiger Weise dazu beitragen können, den Abbau von Spurenschadstoffen in der Umwelt zu untersuchen und vor allem besser zu verstehen. Für Diclofenac wurde exemplarisch aufgezeigt, dass Isotopenanalyse einzigartige Einblicke in das Transformationsverhalten von Arzneimitteln geben kann. Es kann besteht daher großes Potential die in dieser Studie vorgestellte Methodik auf eines der anderen 10.000 Arzneimittel zu übertragen, welche momentan auf dem Markt sind. Auch im Bereich der chiralen Isotopenanalyse (ESIA) gibt es noch unbegrenzte Möglichkeiten. Neben der Analyse weiterer Pestizide haben nicht zuletzt die Ergebnisse für Diclofenac gezeigt, dass die Analyse eines zweiten Elements (H oder N) den Erkenntnisgewinn vervielfachen kann. Außerdem liegt die Möglichkeit auf der Hand ESIA auch auf chirale Blockbuster-Arzneimittel, wie z.B. Ibuprofen oder Metoprolol, anzuwenden.

SUMMARY

Pharmaceuticals and pesticides are among the most frequently detected micropollutants in natural waters because they enter the environment via sewage treatment plants or by application to fields. Hence, it is of great interest to know if they can be degraded in the environment and by which processes. However, the complexity of aquatic systems makes it challenging to assess the environmental fate of micropollutants by concentration measurements, because concentrations are not only affected by degradation, but also by dilution processes. In addition, concentration analysis cannot distinguish transformation processes and their underlying reaction mechanisms. To some part this can be achieved by the analysis of transformation products (TPs), but they are often not fully elucidated, can be further degraded and in some cases different reaction mechanisms yield the same transformation product.

Compound specific isotope analysis (CSIA) is an elegant alternative that is independent of dilution and can even deliver insights into reaction mechanisms. This approach is based on the detection of stable isotopes of C ($^{13}C/^{12}C$) and N ($^{15}N/^{14}N$) which are an inherent trait of all organic substances. In the absence of transformation processes, isotope ratios are preserved and can be used to verify the origin of substances. If transformation takes place, isotope ratios of the substrate are shifted and the magnitude of this shift is determined by the reaction mechanism. Consequently, transformation reactions can be directly detected by isotope analysis of the substrate and the magnitude of fractionation can deliver insight into the underlying mechanism. Before this thesis was initiated the applicability of CSIA was limited to relatively high concentrations and isotope fractionation of pharmaceuticals during transformation reactions was unexplored territory. Hence, the present thesis developed for the first time compound specific isotope analysis (CSIA) for a pharmaceutical, using diclofenac as a model compound, which is one of the most frequently consumed pharmaceuticals, but also among the most frequently detected micropollutants in the environment. First, this method was used to demonstrate its applicability to the ng L^{-1} range, which makes it one of the most sensitive CSIA methods at all. Subsequently, CSIA was used to gain insights about its fate on three levels.

(i) Since isotope ratios are determined by the resources used in synthesis and the synthesis pathway, the analysis of C and N isotope ratios could distinguish most of the tested commercial diclofenac products (tablets, gels). On the one hand this finding can be used to verify commercial

products with a fraud-resistant method. On the other hand this approach can be extended to distinguish sources of diclofenac in the environment, such as sewage treatment plants or manure that originates from diclofenac treated cattle.

(ii) CSIA could be established as a new line of evidence for transformation that is independent of TP analysis. Six transformation pathways were investigated and all of them could be tracked by CSIA. Moreover, the remarkable picture was obtained that all tested environmentally relevant transformation reactions can be separated into two groups that can be distinguished from each other by the analysis of C and N isotope ratios. Ozonation and photolysis cause inverse isotope fractionation, whereas biotransformation and MnO_2 lead to normal isotope fractionation. This is of great interest for environmental investigations, since photolysis and biotransformation are discussed as the two most important transformation pathways in the environment and CSIA delivers a direct measure for their relative importance. But CSIA can also provide insights into engineered systems, because it can be used to investigate the efficiency of biotransformation and / or ozonation during (waste-) water treatment.

(iii) Because isotope effects mirror transition states of transformation reactions, they deliver unique insights in reaction mechanisms that cannot be obtained by other methods under environmentally relevant conditions. The big potential of this approach became apparent when transformation by ABTS and MnO_2 was compared. Both processes are supposed to mimic single electron oxidation (SET), which is proposed to be of big importance in enzymatic transformation reactions. CSIA revealed that ABTS is indeed a model for SET. In contrast, MnO_2 showed a completely different isotope fractionation that was at the same time in perfect agreement with aerobic biotransformation. Moreover, it was strongly indicated that the observed isotope fractionation during MnO_2 or biotransformation, points towards an overseen transformation pathway that can only be seen by CSIA at the moment. Furthermore, CSIA was applied for the first time to study transformation processes during ozonation. There, it provided evidence that ozone rather attacks at the aromatic ring of diclofenac than at the N-atom.

(iv) Besides CSIA of diclofenac, the present thesis investigated also chiral herbicides. CSIA was combined with enantioselective separation to yield enantioselective an even more versatile approach – enantioselective stable isotope analysis (ESIA). ESIA was used for the first time to investigate the fate of the chiral herbicides and revealed that isotope ratios and enantiomeric ratios behave complementarily. In this thesis a case was studied were pronounced enantiomer fractionation, but no isotope fractionation was detected, while the opposite was found for an insecticide in another study. When ESIA was brought to the field results were even more fascinating, because isotope- and enantiomeric fractionation were observed simultaneously.

The present thesis could demonstrate that CSIA and ESIA can improve our understanding of micropollutant transformation in the environment in several ways. There is great potential when the methodology of this dissertation will be applied to one of the other 10,000 pharmaceuticals that are on the market. But also the novel area of ESIA offers plenty of possibilities, when this approach will be transferred to other pesticides and processes. Even more exciting, ESIA of carbon can be combined with the analysis of nitrogen or hydrogen and this would increase the knowledge gain dramatically as shown for CSIA of diclofenac. Moreover, ESIA should not be restricted to pesticides, but this approach urges to be extended to chiral pharmaceuticals, such as ibuprofen or metoprolol.

“Whenever a theory appears to you as the only possible one, take this as a sign that you have neither understood the theory nor the problem which it was intended to solve.”

Karl Popper - Objective Knowledge: An Evolutionary Approach

1

GENERAL INTRODUCTION

1.1 Global challenges related to pesticides & pharmaceuticals

Pesticides and pharmaceuticals increased our living standard substantially by improving crop yields and curing diseases, respectively. However, both compound classes have in common that after application their residues end up in the environment as micropollutants and constitute a potential threat to human and environmental health.[1, 2]

1.1.1 Occurrence of Micropollutants in the Environment

Micropollutants enter the environment via different pathways. The most obvious pathway is the direct application of pesticides to fields and it is estimated that between 1 and 2.5 million tons of pesticides are used in agriculture every year.[3] After their application, pesticides can be (partially) degraded, but they can also enter the water cycle via surface runoff or by leaching into groundwater.[1, 4] However, micropollutants can also indirectly enter the environment. One pathway is the consumption of pharmaceuticals by humans. After incomplete transformation in the human body,[5] pharmaceuticals reach sewage treatment plants where they are only incompletely eliminated and subsequently emitted into receiving waters.[6, 7] To illustrate the importance of this pathway one can, for example, look at the pharmaceutical consumption of Germany. In total 31,000 t of active pharmaceutical ingredients are consumed per year[8] and 328 human pharmaceuticals were applied at an amount higher than 5 t a^{-1}.[9] This number does not include pharmaceuticals like ethinyl estradiol that are consumed at a lower level (0.05 t), but have by definition an endocrine effect on organisms.[9] The second pathway concerns veterinary pharmaceuticals. After application they are excreted and distributed to fields as manure, which is used as fertilizer.[2, 10] Many of these veterinary pharmaceuticals, such as the anti-inflammatory agent diclofenac, are also applied to humans. Nevertheless, the veterinary pathway is special, because in analogy to pesticides it brings pharmaceuticals directly into the environment without passing a sewage treatment plant, where they could be at least be partially degraded. Both classes of micropollutants, pesticides and pharmaceuticals, have in common that their occurrence in the environment is abundantly documented, but their fate (distribution / further degradation) remains incompletely understood.

1.1.2 Effects & Fate of Micropollutants in the Environment

Knowledge about the self-cleaning potential of ecosystems is not only of scientific value, but affects everyone, since clean water is the basis of human- and environmental health. The necessity of terminal elimination is not only given for pesticides, which are harmful to biota by definition. Pharmaceuticals should neither be present in the environment. Besides the precautionary principle -

their longterm (eco-) toxicity is largely unknown - some candidates were shown to have ecotoxicological effects at their present level in the environment.[2, 11] For example, the pain-killer and anti-inflammatory agent diclofenac was shown to cause kidney damages in fish or inhibit mussel growth.[11-14] Moreover, it caused a drastic decrease in Indian vulture populations, because the vultures preyed cattle, which was treated with this anti-inflammatory agent.[12, 15]

The fate of micropollutants can be influenced by various processes. They can be adsorbed, diluted, transformed, finally be degraded or behave in a persistent way.[1, 2, 4] Among these processes only degradation – sometimes transformation to daughter products, in the best case mineralization to H_2O and CO_2, ensures that micropollutants do not accumulate in the environment. Depending on their structure, micropollutants can be transformed by: abiotic hydrolysis, (a)biotic oxidation, (a)biotic reduction or phototransformation. As a general trend, biodegradation and phototransformation often play the dominant role.[4] Nonetheless, the efficiency of these processes has to be assessed for each substance and each site individually. This can be illustrated at the example of diclofenac. Several studies could show in laboratory experiments that sunlight can efficiently transform diclofenac within hours. In contrast, river water/sediment batch studies have to be conducted for days to observe pronounced transformation. Therefore, it is difficult to extrapolate such findings from lab to field scale. On the one hand photo-transformation is often less efficient in the field due to turbidity, duration and intensity of sunlight or deep water bodies. On the other hand it was shown that biodegradation can be very efficient in flow-through-columns (half life time = 0.6 d) and turnover rates strongly depend on the exchange between a water body and the hyporheic zone. Consequently, robust methods are demanded to assess the self-cleaning potential of ecosystems.

1.1.3 Established Techniques to Investigate the Fate of Micropollutants

In laboratory experiments, micropollutant transformation is typically studied by measuring a decrease in concentrations over time. However, such an approach is difficult to pursue in natural systems, because concentrations are not only affected by transformation, but also by other processes, such as dilution or adsorption.[4] These processes do not lower the load of micropollutants in ecosystems, but camouflage their presence. To distinguish them from transformation, concentration measurements need to be accompanied by the application of conservative tracers and/or hydrological modeling.[16] Alternatively, transformation products (TPs) can be detected as direct proof for transformation.[17-19] However, TPs can only be detected if they are at least meta-stable, do not immediately adsorb to humic substances and they must be detectable by the applied analysis technique. Moreover, a quantitative interpretation of TP data is not only challenging due to their further transformation, but also due to a lack of reference standards that are needed for their quantification by mass spectrometry. Hence, it is often not possible to estimate the extent of transformation of the original micropollutant by the analysis of its TP.[17, 20-22] Consequently, additional tools are needed that circumvent the limitations of concentration analysis and the detection of TPs to obtain a comprehensive picture of micropollutant transformation in the environment.

1.1.4 Product Counterfeiting of Pharmaceuticals

Innovative analytical techniques are not only demanded to characterize transformation of pharmaceuticals in the environment, but also to verify their origin and to protect intellectual property. The IFPMA (International Federation of Pharmaceutical Manufacturers Association) assumes that currently 7% of all pharmaceuticals are non-genuine, and the relevance of counterfeit products is increasing.[23] This is an issue of global concern with an estimated economic loss of 75 billion US$ per year.[24] Besides products that do actually not contain the appropriate agent and are easy to detect when subjected to analysis, there is an increasing number of fakes which contain the chemically equivalent active agent in the appropriate dose.[23] In such cases conventional analysis must rely on the possible presence of different byproducts ("chemical fingerprinting"), or else there is no chance to identify a faked product.

1.2 Principles of Enantioselective & Compound Specific Isotope Analysis (ESIA & CSIA)

The analysis of stable isotope ratios (e.g. $^{13}C/^{12}C$) has unique advantages and can address the research gaps of micropollutants from a new angle. CSIA can track the origin of products and sources (1.2.1), detect transformation processes (1.2.2) and investigate transformation mechanisms (1.2.2). To this end isotope ratios are usually reported in the delta notation (Eq. 1-1, 1-2). Isotope ratios that are determined on one specific instrument ($^{12}C/^{13}C_{Sample}$, $^{15}N/^{14}N_{Sample}$) are referenced to an internationally accepted standard ($^{12}C/^{13}C_{Reference}$, $^{15}N/^{14}N_{Reference}$). This reference material is Vienna PeeDee Belemnite for C and air for N. Consequently, values can be compared even if instrument performance differs between instruments or laboratories.[25]

$$\delta^{13}C = \frac{\left(^{13}C/^{12}C_{Sample} - {}^{13}C/^{12}C_{Reference}\right)}{^{13}C/^{12}C_{Reference}} \tag{1-1}$$

$$\delta^{15}N = \frac{\left({}^{15}N/{}^{14}N_{Sample} - {}^{15}N/{}^{14}N_{Reference}\right)}{{}^{15}N/{}^{14}N_{Reference}} \tag{1-2}$$

1.2.1 Source Tracking of Micropollutants by CSIA

Looking from a broader perspective at the natural abundance of light and heavy isotopes of C and N, they seem to be constant (Tab. 1-1). However, modern isotope ratio mass spectrometry (IRMS) allows having a closer look on these ratios. In fact, high precision isotope analysis can reveal differences in the isotopic signature of a certain compound depending on its origin.[26, 27] For example, isotope ratios were used to distinguish original insecticide products from fakes[28] and delivered insight if caffeine in drinks is of natural or synthetic origin.[29] For pharmaceutical products such as aspirin, ibuprofen or naproxen, it has been shown that the analysis of stable isotope ratios of selected elements (e.g. $^{13}C/^{12}C$ or $^{15}N/^{14}N$) can be used as a fingerprint for product authentication. In one case it was even possible to determine the location of an illegal production site by isotope analysis.[24]

All these studies were based on the fact that differences in a certain production process are often reflected by isotope ratios. This is possible, because isotope ratios are determined by two factors. The first factor is the isotope ratio of the educts. This ratio is passed on to the product, provided that conversion is 100%. The second factor is the isotope effect of the commercial synthesis, which becomes important if conversion is not 100%. The underlying mechanism is called kinetic isotope effect (KIE) and described in 1.2.2. . Briefly, KIE describes that molecules which carry a light isotope at the reactive position often differ in reaction speed in comparison to molecules with a heavy isotope.[30, 31] For example, the heavier isotopologue (e.g. molecule containing ^{13}C) could react preferentially to a by-product, while the lighter isotopologue (^{12}C) ends up preferentially in the final product. The final product would then show a lighter isotope ratio than its educt(s) and the by-product would be heavier. Hence, isotope ratios can be used to prove the authenticity of (proprietary) substances, because synthesis pathways and isotope ratios of the educts often differ among producers and especially between companies and (low-budget) counterfeiters.[26-28] Moreover, in the absence of transformation processes isotope ratios behave conservative. This means that processes, such as dilution do not alter isotope ratios and as long as a compound is not transformed, it keeps its original isotopic fingerprint.[30] Consequently this approach is not restricted to industrial applications, but can also serve for source tracking of contaminants in the environment.[32, 33]

However, existing methods for isotope analysis of pharmaceuticals have limited applicability. Isotope ratios of several elements can be analyzed with high precision, if elemental analysis is coupled to isotope ratio mass spectrometry (EA-IRMS). However, it is necessary to extract large amounts of the active pharmaceutical ingredient (API) out of a formulation, which is very laborious and time consuming.[26, 27]. This can be circumvented by the coupling of liquid chromatography to IRMS (LC-IRMS). LC-IRMS can separate API from other ingredients automatically, but in return it is restricted to the analysis of carbon isotopes.[34, 35] Gas chromatography coupled to IRMS (GC-IRMS) would allow an automatic separation of ingredients, deliver an excellent quantification limit for precise isotope analysis and offers the possibility to analyze isotope ratios of C, N, H and O.[25] However, to date there is no method available to analyze isotope ratios of pharmaceuticals by GC-IRMS.

Tab. 1-1. Isotope abundance of C and N and the precision of GC-IRMS (gas chromatography - isotope ratio mass spectrometry). Adopted and modified from Elsner et al.[25].

Element	Natural abundance of the lighter isotope	Natural Abundance of heavier isotope	Typical precision of GC-IRMS (variation in the isotope ratio)
Carbon (^{12}C, ^{13}C)	98.9%	1.1%	0.5‰
Nitrogen (^{14}N, ^{15}N)	99.6%	0.4%	1.0‰

1.2.2 Isotope Fractionation during Transformation Reactions

Isotope ratios are an inherent and unique feature of substances that can be used to investigate reactions. The underlying principle is the kinetic isotope effect (KIE). The KIE describes the phenomenon that usually molecules carrying a lighter isotope at the reactive position need less activation energy than molecules with a heavy isotope (Fig. 1-1a).[30, 31] Hence, in most cases lighter isotopes are faster transformed.[36]

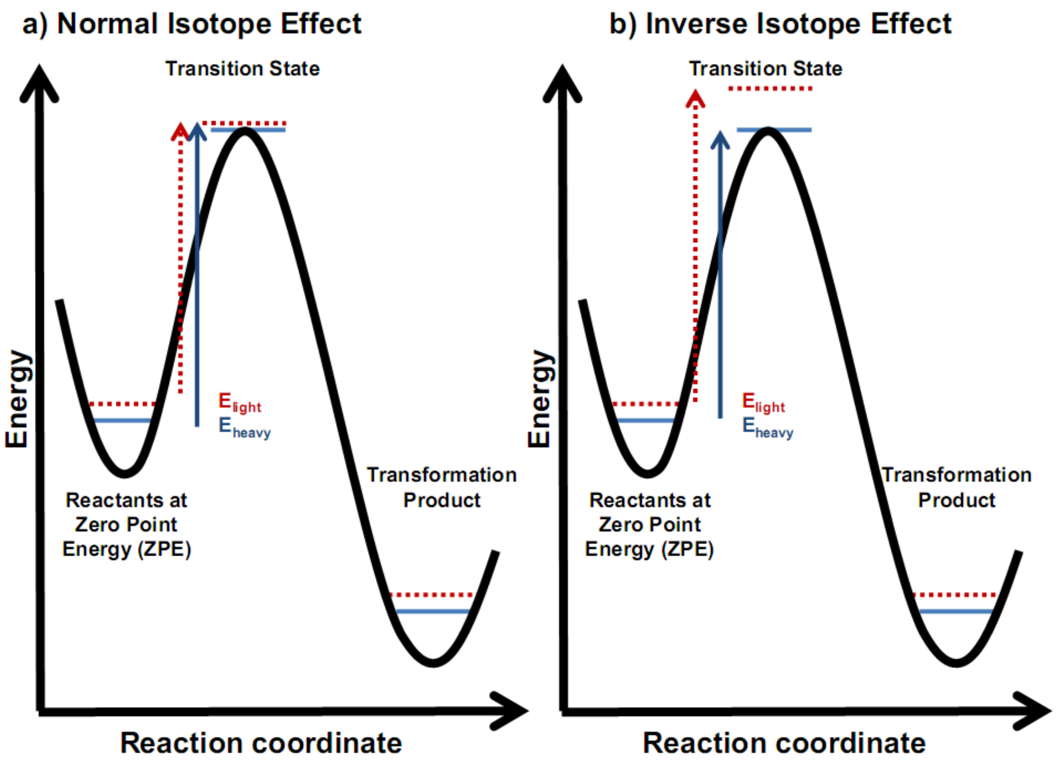
a) Normal Isotope Effect
b) Inverse Isotope Effect
Transition State
Transition State
Energy
Energy
E_{light}
E_{heavy}
E_{light}
E_{heavy}
Reactants at Zero Point Energy (ZPE)
Reactants at Zero Point Energy (ZPE)
Transformation Product
Transformation Product
Reaction coordinate
Reaction coordinate

Fig. 1-1. Difference in vibrational energies between light and heavy isotopes during a transformation reaction; a) in most cases light isotopes need less activation energy (E_{light}) than heavy isotopes (E_{heavy}) to reach the transition state and the remaining reactant gets enriched in heavy isotopes; b) if bonds are stiffer in the transition state (larger force constant in comparison to ZPE) the transformation product get enriched in heavy isotopes

This phenomenon can be explained by looking at the four different types of bond energies: electron energy, vibrational energy, translational energy and rotational energy. Although electron energy is the strongest bond energy, it does not play a role for isotope effects, because electron movement is not influenced by the nuclei-mass (Born-Oppenheimer Approximation).[36] However, there are three mass-dependent types of bond energies. Among these, vibrational energy is much more important than translational- or rotational energy. Molecules vibrate even at the lowest energy level, the so called zero point energy level (ZPE), which corresponds to 0 K.[36] If energy is added to a molecule, its vibrational energy can change in discrete steps. Looking at the vibrational energy levels of two isotopes, it becomes apparent that the ZPE of the heavier isotope is lower than the ZPE of the lighter isotope (Fig. 1-1).[36] If two isotopes undergo the same transformation reaction the heavier isotope requires more activation energy. Hence, in most cases lighter isotopes are faster transformed (Fig. 1-1a).[22, 23] This leads to an enrichment of heavy isotopes on the reactant side, while transformation products show a lighter isotope ratio (normal isotope effect). In some cases the bonds are stronger in the transition state (larger force constant) than at ZPE (Fig. 1-1b).[37, 38] This means that the difference in vibrational energy between two isotopes is larger in the transition state in comparison to the ZPE. Consequently, the lighter isotopes need more activation energy and react slower. This leads to isotopically lighter reactants and heavier transformation products (inverse isotope effect). Based on this concept isotope analysis of the reactant can deliver insight into reaction mechanisms, even if TPs cannot be detected. At the same time isotope ratios give us the opportunity to catch a glimpse on rate-limiting transition states of reactions, which is not possible by concentration measurements or TP analysis (Fig. 1-2).[22, 23]

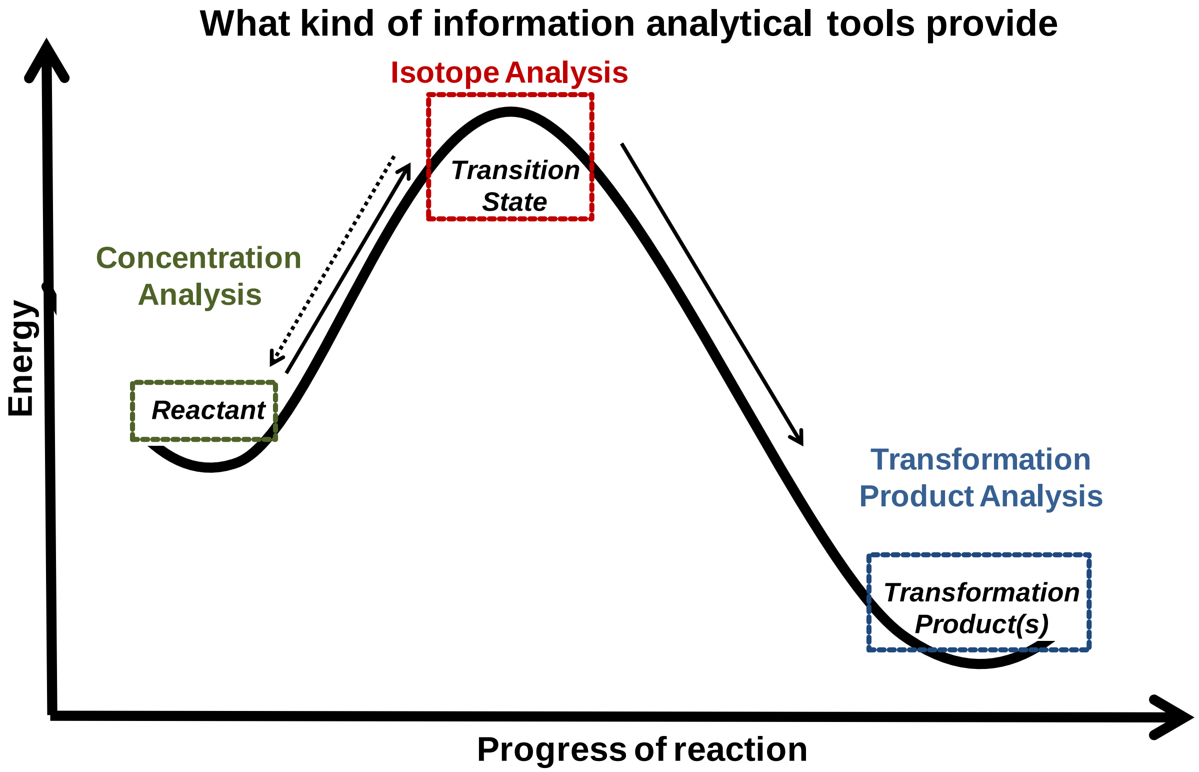
What kind of information analytical tools provide
Isotope Analysis
Transition State
Concentration Analysis
Reactant
Energy
Transformation Product Analysis
Transformation Product(s)
Progress of reaction

Fig. 1-2. While concentration analysis is restricted to the observation if reactants decrease or not, isotope ratios of the reactant reflects the transition state of a transformation reaction, even if no transformation products can be detected

Interestingly, the kinetic isotope effect is not restricted to a qualitative interpretation, but can also be used to quantify transformation. Looking at two sampling events (*0*, *t*), there is a direct correlation between the extent of transformation ($f = C_t / C_0$) and the change in isotope ratios ($\delta^{13}C_0$, $\delta^{13}C_t$) (Eq. 1-3).[22, 23]

$$\ln\left(\frac{\delta^{13}C_t + 1}{\delta^{13}C_0 + 1}\right) = \varepsilon \times \ln f \times = \varepsilon \times \ln\left(\frac{C_t}{C_0}\right) \quad (1\text{-}3)$$

The linking parameter is the enrichment factor ε, which is characteristic for specific reactions and specific elements. ε bears the information about the transition state as discussed above. If $\varepsilon < 0$ light isotopes react faster (normal isotope effect) and if $\varepsilon > 0$ heavy isotopes react faster (inverse isotope effect). Since Eq. 1-3 consists of four parameters ($\delta^{13}C_t$, $\delta^{13}C_0$, ε, f) it is sufficient to determine three parameters and calculate the fourth one. Hence, ε can be determined in the lab, where concentrations and isotope ratios can be analyzed in a closed system. Subsequently, it is possible to analyze isotope ratios in the field. With knowledge of three parameters (epsilon, $\delta^{13}C_t$, $\delta^{13}C_0$) it is then possible to determine the extent of transformation f.[39]

As described in 1.2.4 isotope ratios of micropollutants need to be analyzed by GC-IRMS to achieve maximum sensitivity. Unfortunately, this approach relies on the combustion of the target analyte to CO_2 and/or N_2. This means that site-specific information about isotope enrichment is lost during combustion and the intrinsic isotope effect of the reacting position is diluted by all the other atoms of the same element that were not involved in the reaction. Hence, measured isotope enrichment needs to be corrected for the overall number of atoms of one element (*n*)(Eq. 1-4).[31] This calculated isotope effect of the reactive position is called position-specific kinetic isotope effect (*KIE*).

$$(A)KIE = (n \times \varepsilon + 1)^{-1} \quad (1\text{-}4)$$

The *intrinsic KIE* may be masked through the presence of additional rate-limiting steps, such as adsorption to reactive surfaces in abiotic reactions or transport limitations in biological reactions. Therefore, measured isotope effects are usually stated as apparent kinetic isotope effect (*AKIE*), which implies that it could be smaller than the intrinsic KIE.[30, 31] The calculation of AKIE is important to recognize similarities or differences in the reaction mechanism of compounds that differ in *n*.

1.2.3 Principles of Enantioselective Isotope Analysis (ESIA)

Many natural and synthetic molecules contain at least one chiral center.[40, 41] In a similar way as human hands, they occur in two modifications that behave like mirror-images of each other and are called enantiomers.[42] Just as isotopologues, enantiomers share most chemical properties and cannot be separated easily.[42] However, the behavior of two enantiomers differs in terms of stereochemistry. This is of special importance in enzymatic reactions where reactivity depends strongly on the three dimensional structure of an enzyme and its substrate.[43] Hence, if enzymes are involved, enantiomers often differ in reaction kinetics, bioavailability or toxicity.[40, 44-46] There are two important processes that directly affect the ratio of two enantiomers. On the one hand enzymes can prefer one enantiomer over the other during transformation, which leads to a faster depletion of this enantiomer (Fig. 1-3).[41] On the other hand enzymes for active transport into cells can also be enantioselective.[47] This can speed up the transport of one enantiomer into a cell where it is transformed by other enzymes (Fig. 1-3). Because these processes cause a shift in the ratio of two enantiomers, they can be tracked by enantioselective analysis. Since enantiomer analysis detects molecular ratios in a similar way as isotope analysis, it is also not influenced by dilution effects and may represent a similarly robust measure for transformation. At the same time, enantiomer analysis can be expected to be complementary to CSIA. Specifically, enantiomer fractionation can occur if active transport into cells is enantioselective and rate-determining (Fig. 1-3). This is a situation where evidence from isotope fractionation would be inconclusive, because no bonds are broken or formed during transport and, hence, no isotope effects would be expected. Vice versa, isotope fractionation may be detected if enzyme transformation is rate-determining, but not enantiomer-specific – a case where enantiomer analysis would be inconclusive.

a) Transformation is rate-determining and enantioselective

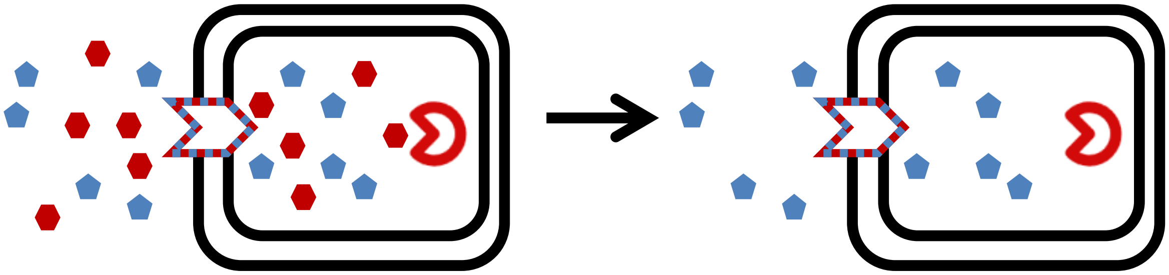

b) Uptake is rate-determining and enantioselective

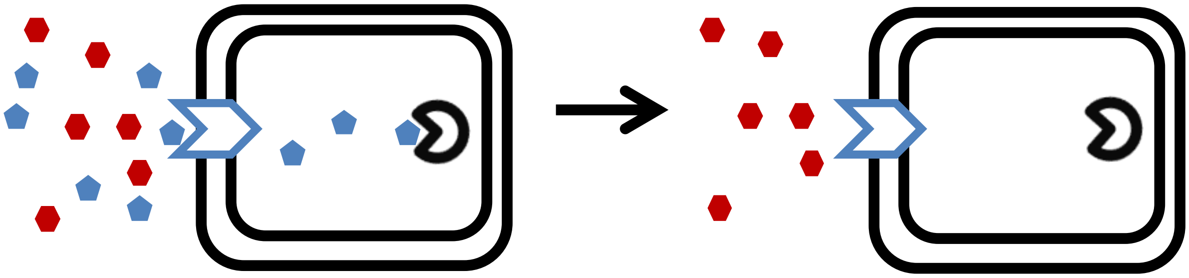

Fig. 1-3. Depending on the rate-determining step two enantiomers (blue pentagon, red hexagon) can be discriminated during (a) enzymatic transformation or (b) active transport into cells; note that in case b) no isotope fractionation would occur, because no bonds are cleaved in the rate determining step

To communicate changes in enantiomeric ratios two equal notations have been established – enantiomeric excess and enantiomeric fraction.[40, 48] In this study enantiomeric fraction (EF) is used, where the ratio of the R (Eq. 1-5) or the S enantiomer (Eq. 1-6) is expressed as percentage of the total concentration of the racemate [EF_R, EF_S]. Nearly all commercial products have either an EF of 0.5 (racemates) or 0 (enantio- pure products).

$$EF_R = \frac{[R]}{[R] + [S]} \tag{1-5}$$

$$EF_S = \frac{[S]}{[R] + [S]} \tag{1-6}$$

1.3 Content of the present thesis

CSIA and ESIA have the potential to tackle the grand challenges of micropollutants in the environment: to distinguish their sources, to proof their transformation and to investigate their transformation mechanisms. To this end five major challenges have to be mastered. In the present this was done in **Chapter 2 and 3,** where CSIA was used for the **first time to investigate the fate of pharmaceuticals** - using diclofenac as a model compound - and in **Chapter 4** where **ESIA was applied for the first time to herbicides**.

1.3.1 Analytical Challenges & Objectives of CSIA and ESIA of Micropollutants

(i) The most obvious challenge is of analytical nature and concerns the **literally low concentration range of micropollutants**. Theoretically this holds true for all analytical techniques. For CSIA it is even more difficult, because conventional mass spectrometry usually analyzes the most abundant isotope. CSIA, in contrast, must also analyze the heavier isotope, which is by far less abundant. In case of carbon this leads to an increase of the detection limit by a factor of 100 (~1% ^{13}C in C_{total}). For nitrogen this limit increases even by a factor of 600, because in addition to the low proportion of ^{15}N (~0.3% of N_{total}) two N atoms are needed to create one molecule of analyte gas (N_2).[25] Because the minor isotope must be determined with a very high precision, the real limits are even higher as described in Elsner et al.[25]. Hence, effective pre-concentration steps are needed in combination with the most sensitive analytics. To this end the limit of precise isotope analysis was determined **Chapter 2** by combining a solid phase extraction, clean-up by preparative HPLC, derivatization and on column injection, which is the most sensitive injection technique.

(ii) As stated above, the use of **gas chromatography coupled to IRMS mandatory** when highest sensitivity is needed for CSIA of micropollutants.[25] During gas chromatography target analytes have to be combusted without decay to pass through the chromatographic column. However, **many micropollutants** are at least semi-polar, because they carry a carboxyl- and/or an amine group. This causes a high boiling point, a high retention due to exchangeable hydrogen atoms and often compounds **start to decay before they are** quantitatively **transferred through the gas chromatograph**. Consequently, sensitive derivatization techniques have to be developed for micropollutants. Because derivatization is by definition a chemical reaction where bonds are broken, such a sample preparation must be conducted under absolutely controlled condition.[49] Otherwise (irreproducible) isotope effects during derivatization would impede an evaluation of isotope data.[50] Moreover, all common derivatization agents introduce at least one carbon atom into the analyte.[25, 50] Hence, isotope ratios have to be corrected for every introduced C-atom. At the same time these additional C-atoms must have a constant isotope ratio to ensure a constant C-isotope shift of all samples and the respective control standards that are used for corrections.[51] Hence, two derivatization GC-IRMS methods were established for diclofenac in **Chapter 2** facilitating either quick or sensitive analysis. In addition, the sensitive method was transferred to polar herbicides in **Chapter 4**.

(iii) For enantioselective isotope analysis a fifth requirement comes into play – the **perfect separation of enantiomers**. However, enantiomers cannot be easily separated, because they share most chemical properties. Hence, special separation techniques are demanded. For enantiomers, the use of gas chromatography offers the advantage to use an enantioselective column. In these columns analytes are not (only) separated by polarity, but also by their stereochemical properties. This concept is already known for GC-MS analysis, but again, GC-IRMS has special requirements.[44, 45] While in conventional analysis a small overlap of enantiomer peaks can be tolerated, this is not possible for GC-IRMS. The reason is the chromatographic isotope effect. Within one peak heavy and light molecules are not equally distributed, but heavy isotopologues elute at the peak front and light isotopologues elute at the peak tail.[52] This is caused by van der Waals interactions between analyte and the nonpolar column coating. Hence it is essential that each enantiomer peak is perfectly separated (Peakwidth/ (Retention time difference between two peaks) >1.5). This is even more challenging when several micropollutants with similar structures are present in one sample. One example is the herbicide DCPP, which is often detected in the field together with its TP 4-CPP or the herbicide MCPP. All three compounds are chlorinated phenoxy acids, share the same chiral center and differ only in one methyl-group or a chlorine atom, respectively. Consequently, a sensitive method was established in **Chapter 4** that is capable of analyzing isotope ratios of each single enantiomer of these herbicidal compounds.

1.3.2 Challenge of large number of C-atoms in micropollutants

The fourth challenge is the large number of C-atoms in most micropollutants. The biggest advantage of GC-IRMS is its superior detection limit for precise isotope ratios. However, the low detection limit is achieved by burning the target analyte to CO_2 and N_2 after separation. This yields a simple analyte gas that contains only one (dominant) isotope. If only one C or N atom is present in a molecule this procedure does not affect the intensity of measurable isotope effects. In cases where several atoms of the same element are present in a molecule, **isotope enrichment takes only place at one position. All other atoms from the same element dilute the measurable effect** of this reactive position. This lead to the assumption that C-isotope fractionation is not detectable any more, if molecules contain more than 14 C-atoms.[53] Because the magnitude of fractionation depends on the reactant and the reaction type it remains to be investigated**,** if this also applies for micropollutants that are in this range. This challenge was tackled in **Chapter 2 and 3** for the painkiller diclofenac (14 C atoms) and three herbicides (9 or 10 C atoms) in **Chapter 4**.

1.3.3 Challenge of process understanding

Traditionally, CSIA is applied to contaminants, whose transformation products (TPs) are well investigated, such as chlorinated ethenes.[54] In this case CSIA is used to elucidate the underlying transformation mechanism and applied as a robust measure for transformation in the field. In contrast, the mass balance between most micropollutants and their potential TPs is not closed. Hence, even if some TPs are known, it is unclear if they represent the quantitatively most important transformation pathway. Hence, a **mechanistic interpretation of isotope enrichment of micropollutants is rather challenging**, because the importance of a certain pathway can often not be deduced from TP analysis and different pathways can yield the same TP.

Consequently, **Chapter 2** investigated in a first proof of principle study, isotope fractionation of aerobic biotransformation and reductive dechlorination. In a comprehensive approach, **Chapter 3** studied the variability of isotope fractionation of diclofenac and it was tested which processes can be distinguished from each other by CSIA. To this end phototransformation and ozonation were investigated as environmentally relevant processes and transformation by MnO_2 and ABTS radicals was used to gain deeper insights into the (biotic) oxidation of diclofenac. Moreover, **Chapter 4** explored the potential of ESIA to obtain mechanistic insight into herbicide transformation.

1.4 References

1. Schwarzenbach, R. P.; Egli, T.; Hofstetter, T. B.; von Gunten, U.; Wehrli, B., Global Water Pollution and Human Health. *Annual Review of Environment and Resources* **2010,** *35*, (1), 109-136.
2. Kummerer, K., Pharmaceuticals in the Environment. In *Annual Review of Environment and Resources, Vol 35*, Gadgil, A.; Liverman, D. M., Eds. Annual Reviews: Palo Alto, 2010; pp 57-+.
3. Fenner, K.; Canonica, S.; Wackett, L. P.; Elsner, M., Evaluating Pesticide Degradation in the Environment: Blind Spots and Emerging Opportunities. *Science* **2013,** *341*, (6147), 752-758.
4. Schwarzenbach, R. P.; Gschwend, P. M.; Imboden, D. M., *Environmental organic chemistry*. second edition ed.; John Wiley & Sons, Inc.: New Jersey, 2003; p 1313.
5. Bort, R.; Macé, K.; Boobis, A.; Gómez-Lechón, M. a.-J.; Pfeifer, A.; Castell, J., Hepatic metabolism of diclofenac: role of human CYP in the minor oxidative pathways. *Biochemical Pharmacology* **1999,** *58*, (5), 787-796.
6. Ternes, T. A., Occurrence of drugs in German sewage treatment plants and rivers. *Water Research* **1998,** *32*, (11), 3245-3260.
7. Heberer, T., Tracking persistent pharmaceutical residues from municipal sewage to drinking water. *J. Hydrol.* **2002,** *266*, (3-4), 175-189.
8. Salomon, M., Pharmazeutische Wirkstoffe und Umweltschutz. *UWSF - Z Umweltchem Ökotox* **2007,** *19*, (3), 155-167.
9. BLAC, B. L. f. C., Arzneimittel in der Umwelt, Auswertung der Untersuchungsergebnisse. *Freie und Hansestadt Hamburg, Behörde für Umwelt und Gesundheit, Institut für Hygiene und Umwelt, im Auftrag des Bund/Länderausschusses für Chemikaliensicherheit (BLAC)* **2003**.
10. Ternes, T.; Römbke, Final Report Behaviour of selected human and veterinary pharmaceuticals in aquatic compartments and soil. *UBA Report* **2001**.
11. Fent, K.; Weston, A. A.; Caminada, D., Ecotoxicology of human pharmaceuticals. *Aquat. Toxicol.* **2006,** *76*, (2), 122-159.
12. Schwaiger, J.; Ferling, H.; Mallow, U.; Wintermayr, H.; Negele, R. D., Toxic effects of the non-steroidal anti-inflammatory drug diclofenac Part 1: histopathological alterations and bioaccumulation in rainbow trout. *Aquat. Toxicol.* **2004,** *68*, (2), 141-150.
13. Triebskorn, R.; Casper, H.; Scheil, V.; Schwaiger, J., Ultrastructural effects of pharmaceuticals (carbamazepine, clofibric acid, metoprolol, diclofenac) in rainbow trout (Oncorhynchus mykiss) and common carp (Cyprinus carpio). *Analytical and Bioanalytical Chemistry* **2007,** *387*, (4), 1405-1416.
14. Ericson, H.; Thorsén, G.; Kumblad, L., Physiological effects of diclofenac, ibuprofen and propranolol on Baltic Sea blue mussels. *Aquat. Toxicol.* **2010,** *99*, (2), 223-231.
15. Oaks, J. L.; Gilbert, M.; Virani, M. Z.; Watson, R. T.; Meteyer, C. U.; Rideout, B. A.; Shivaprasad, H. L.; Ahmed, S.; Chaudhry, M. J. I.; Arshad, M.; Mahmood, S.; Ali, A.; Khan, A. A., Diclofenac residues as the cause of vulture population decline in Pakistan. *Nature* **2004,** *427*, (6975), 630-633.
16. Kunkel, U.; Radke, M., Reactive Tracer Test To Evaluate the Fate of Pharmaceuticals in Rivers. *Environmental Science & Technology* **2011,** *45*, (15), 6296-6302.
17. Li, Z.; Maier, M. P.; Radke, M., Screening for pharmaceutical transformation products formed in river sediment by combining ultrahigh performance liquid chromatography/high resolution mass spectrometry with a rapid data-processing method. *Analytica Chimica Acta* **2014,** *810*, 61-70.
18. Kern, S.; Fenner, K.; Singer, H. P.; Schwarzenbach, R. P.; Hollender, J., Identification of transformation products of organic contaminants in natural waters by computer-aided prediction and high-resolution mass spectrometry. *Environ. Sci. Technol.* **2009,** *43*, (18), 7039-7046.
19. Helbling, D. E.; Hollender, J.; Kohler, H. P. E.; Singer, H.; Fenner, K., High-Throughput Identification of Microbial Transformation Products of Organic Micropollutants. *Environmental Science & Technology* **2010,** *44*, (17), 6621-6627.

20. Groning, J.; Held, C.; Garten, C.; Claussnitzer, U.; Kaschabek, S. R.; Schlomann, M., Transformation of diclofenac by the indigenous microflora of river sediments and identification of a major intermediate. *Chemosphere* **2007,** *69*, (4), 509-516.
21. Zwiener, C.; Seeger, S.; Glauner, T.; Frimmel, F. H., Metabolites from the biodegradation of pharmaceutical residues of ibuprofen in biofilm reactors and batch experiments. *Analytical and Bioanalytical Chemistry* **2002,** *372*, (4), 569-575.
22. Loffler, D.; Rombke, J.; Meller, M.; Ternes, T. A., Environmental fate of pharmaceuticals in water/sediment systems. *Environmental Science & Technology* **2005,** *39*, (14), 5209-5218.
23. Deisingh, A., Counterfeit drugs. *Chem. Ind.* **2004**, (6), 16-+.
24. Everts, S., FAKE PHARMACEUTICALS. *Chemical & Engineering News* **2010,** *88*, (1), 27-29.
25. Elsner, M.; Jochmann, M. A.; Hofstetter, T. B.; Hunkeler, D.; Bernstein, A.; Schmidt, T. C.; Schimmelmann, A., Current challenges in compound-specific stable isotope analysis of environmental organic contaminants. *Anal. Bioanal. Chem.* **2012,** *403*, (9), 2471-2491.
26. Wokovich, A. M.; Spencer, J. A.; Westenberger, B. J.; Buhse, L. F.; Jasper, J. P., Stable isotopic composition of the active pharmaceutical ingredient (API) naproxen. *J. Pharm. Biomed. Anal.* **2005,** *38*, (4), 781-784.
27. Jasper, J. P.; Weaner, L. E.; Duffy, B. J., A preliminary multi-stable-isotopic evaluation of three synthetic pathways of Topiramate. *J. Pharm. Biomed. Anal.* **2005,** *39*, (1-2), 66-75.
28. Weller, P.; Boner, M.; Foerstel, H.; Becker, H.; Peikert, B.; Dreher, W., Isotopic Fingerprinting for the Authenticity Control of Crop Protection Active Compounds using the Representative Insecticide Fipronil. *Journal of Agricultural and Food Chemistry* **2011,** *59*, (9), 4365-4370.
29. Zhang, L.; Kujawinski, D. M.; Federherr, E.; Schmidt, T. C.; Jochmann, M. A., Caffeine in Your Drink: Natural or Synthetic? *Analytical Chemistry* **2012,** *84*, (6), 2805-2810.
30. Elsner, M.; Zwank, L.; Hunkeler, D.; Schwarzenbach, R. P., A new concept linking observable stable isotope fractionation to transformation pathways of organic pollutants. *Environ. Sci. Technol.* **2005,** *39*, (18), 6896-6916.
31. Elsner, M., Stable isotope fractionation to investigate natural transformation mechanisms of organic contaminants: principles, prospects and limitations. *J. Environ. Monit.* **2010,** *12*, (11), 2005-2031.
32. Schmidt, T. C.; Zwank, L.; Elsner, M.; Berg, M.; Meckenstock, R. U.; Haderlein, S. B., Compound-specific stable isotope analysis of organic contaminants in natural environments: a critical review of the state of the art, prospects, and future challenges. *Anal. Bioanal. Chem.* **2004,** *378*, (2), 283-300.
33. Spahr, S.; Huntscha, S.; Bolotin, J.; Maier, M. P.; Elsner, M.; Hollender, J.; Hofstetter, T. B., Compound-specific isotope analysis of benzotriazole and its derivatives. *Analytical and Bioanalytical Chemistry* **2013,** *405*, (9), 2843-2856.
34. Krummen, M.; Hilkert, A. W.; Juchelka, D.; Duhr, A.; Schluter, H. J.; Pesch, R., A new concept for isotope ratio monitoring liquid chromatography/mass spectrometry. *Rapid Communications in Mass Spectrometry* **2004,** *18*, (19), 2260-2266.
35. Kujawinski, D. M.; Zhang, L.; Schmidt, T. C.; Jochmann, M. A., When other separation techniques fail: compound-specific carbon isotope ratio analysis of sulfonamide containing pharmaceuticals by high-temperature-liquid chromatography-isotope ratio mass spectrometry. *Analytical Chemistry* **2012,** *84*, (18), 7656-63.
36. Aelion, C. M.; Hohener, P.; Hunkeler, D.; Aravena, R., *Environmental Isotopes in Bioremediation and Biodegradation*. CRC Press: 2009.
37. Hartenbach, A. E.; Hofstetter, T. B.; Tentscher, P. R.; Canonica, S.; Berg, M.; Schwarzenbach, R. P., Carbon, hydrogen, and nitrogen isotope fractionation during light-Induced transformations of atrazine. *Environ. Sci. Technol.* **2008,** *42*, (21), 7751-7756.

38. Meyer, A. H.; Penning, H.; Elsner, M., C and N isotope fractionation suggests similar mechanisms of microbial atrazine transformation despite involvement of different Enzymes (AtzA and TrzN). *Environ. Sci. Technol.* **2009,** *43*, (21), 8079-8085.
39. Meckenstock, R. U.; Morasch, B.; Griebler, C.; Richnow, H. H., Stable isotope fractionation analysis as a tool to monitor biodegradation in contaminated acquifers. *J.Contam.Hydrol.* **2004,** *75*, (3-4), 215-255.
40. Wong, C., Environmental fate processes and biochemical transformations of chiral emerging organic pollutants. *Analytical and Bioanalytical Chemistry* **2006,** *386*, (3), 544-558.
41. Muller, T. A.; Kohler, H. P. E., Chirality of pollutants - effects on metabolism and fate. *Applied Microbiology and Biotechnology* **2004,** *64*, (3), 300-316.
42. Hashim, N. H.; Shafie, S.; Khan, S. J., Enantiomeric fraction as an indicator of pharmaceutical biotransformation during wastewater treatment and in the environment – a review. *Environmental Technology* **2010,** *31*, (12), 1349-1370.
43. Seffernick, J. L.; Reynolds, E.; Fedorov, A. A.; Fedorov, E.; Almo, S. C.; Sadowsky, M. J.; Wackett, L. P., X-ray Structure and Mutational Analysis of the Atrazine Chlorohydrolase TrzN. *Journal of Biological Chemistry* **2010,** *285*, (40), 30606-30614.
44. Buser, H. R.; Poiger, T.; Muller, M. D., Occurrence and environmental behavior of the chiral pharmaceutical drug ibuprofen in surface waters and in wastewater. *Environmental Science & Technology* **1999,** *33*, (15), 2529-2535.
45. Muller, M. D.; Buser, H. R., Conversion reactions of various phenoxyalkanoic acid herbicides in soil .1. Enantiomerization and enantioselective degradation of the chiral 2-phenoxypropionic acid herbicides. *Environmental Science & Technology* **1997,** *31*, (7), 1953-1959.
46. Buerge, I. J.; Poiger, T.; Muller, M. D.; Buser, H. R., Enantioselective degradation of metalaxyl in soils: Chiral preference changes with soil pH. *Environmental Science & Technology* **2003,** *37*, (12), 2668-2674.
47. Muller, R. H.; Hoffmann, D., Uptake kinetics of 2,4-dichlorophenoxyacetate by Delftia acidovorans MC1 and derivative strains: Complex characteristics in response to pH and growth substrate. *Biosci. Biotechnol. Biochem.* **2006,** *70*, (7), 1642-1654.
48. Siriphongphaew, A.; Pisnupong, P.; Wongkongkatep, J.; Inprakhon, P.; Vangnai, A.; Honda, K.; Ohtake, H.; Kato, J.; Ogawa, J.; Shimizu, S.; Urlacher, V.; Schmid, R.; Pongtharangkul, T., Development of a whole-cell biocatalyst co-expressing P450 monooxygenase and glucose dehydrogenase for synthesis of epoxyhexane. *Appl. Microbiol. Biot.* **2012,** *95*, (2), 357-367.
49. Meier-Augenstein, W., Stable isotope analysis of fatty acids by gas chromatography-isotope ratio mass spectrometry. *Analytica Chimica Acta* **2002,** *465*, (1-2), 63-79.
50. Rieley, G., Derivatization of Organic-Compounds Prior to Gas-Chromatographic Combustion-Isotope Ratio Mass-Spectrometric Analysis - Identification of Isotope Fractionation Processes. *Analyst* **1994,** *119*, (5), 915-919.
51. Reinnicke, S.; Bernstein, A.; Elsner, M., Small and Reproducible Isotope Effects during Methylation with Trimethylsulfonium Hydroxide (TMSH): A Convenient Derivatization Method for Isotope Analysis of Negatively Charged Molecules. *Analytical Chemistry* **2010,** *82*, (5), 2013-2019.
52. Cherrah, Y.; Falconnet, J. B.; Desage, M.; Brazier, J. L.; Zini, R.; Tillement, J. P., Study of deuterium isotope effects on protein binding by gas chromatography/mass spectrometry. Caffeine and deuterated isotopomers. *Biomedical & environmental mass spectrometry* **1987,** *14*, (11).
53. Morasch, B.; Richnow, H. H.; Vieth, A.; Schink, B.; Meckenstock, R. U., Stable isotope fractionation caused by glycyl radical enzymes during bacterial degradation of aromatic compounds. *Applied and Environmental Microbiology* **2004,** *70*, (5), 2935-2940.

54. Mundle, S. O. C.; Johnson, T.; Lacrampe-Couloume, G.; Perez-de-Mora, A.; Duhamel, M.; Edwards, E. A.; McMaster, M. L.; Cox, E.; Revesz, K.; Sherwood Lollar, B., Monitoring Biodegradation of Ethene and Bioremediation of Chlorinated Ethenes at a Contaminated Site Using Compound-Specific Isotope Analysis (CSIA). *Environmental Science & Technology* **2012,** *46*, (3), 1731-1738.

2

C & N ISOTOPE ANALYSIS OF DICLOFENAC TO DISTINGUISH OXIDATIVE AND REDUCTIVE TRANSFORMATION AND TO TRACK COMMERCIAL PRODUCTS

Maier, M. P.; De Corte, S.; Nitsche, S.; Spaett, T.; Boon, N.; Elsner, M., C & N Isotope Analysis of Diclofenac to Distinguish Oxidative and Reductive Transformation and to Track Commercial Products.

Environmental Science & Technology, 2014. 48, (4), 2312-2320.

Reprinted with permission. Copyright (2013) American Chemical Society.

2.1 *Abstract*

Although diclofenac is frequently found in aquatic systems, its degradability in the environment remains imperfectly understood. On the one hand, evidence from concentration analysis alone is inconclusive if an unknown hydrology impedes a distinction between degradation and dilution. On the other hand, not all transformation products may be detectable. As a new approach we therefore developed GC-IRMS (gas chromatography - isotope-ratio mass-spectrometry) analysis for carbon and nitrogen isotope measurements of diclofenac. The method uses a derivatization step that can be conducted either online or offline, for optimized throughput or sensitivity, respectively. In combination with on-column injection the latter method enables determination of diclofenac isotope ratios down to the sub-⍰gL^{-1} range in environmental samples. Degradation in an aerobic sediment-water-system showed strong nitrogen isotope fractionation (ε_N = -7.1‰), whereas reductive diclofenac dechlorination was associated with significant carbon isotope fractionation (ε_C = -2.0‰). Hence dual element isotope analysis bears potential not only to detect diclofenac degradation, but even to distinguish both transformation pathways in the environment. In an explorative survey, analysis of commercial diclofenac products showed significant differences in carbon and nitrogen isotope ratios demonstrating a further potential to track, and potentially even authenticate, commercial production batches.

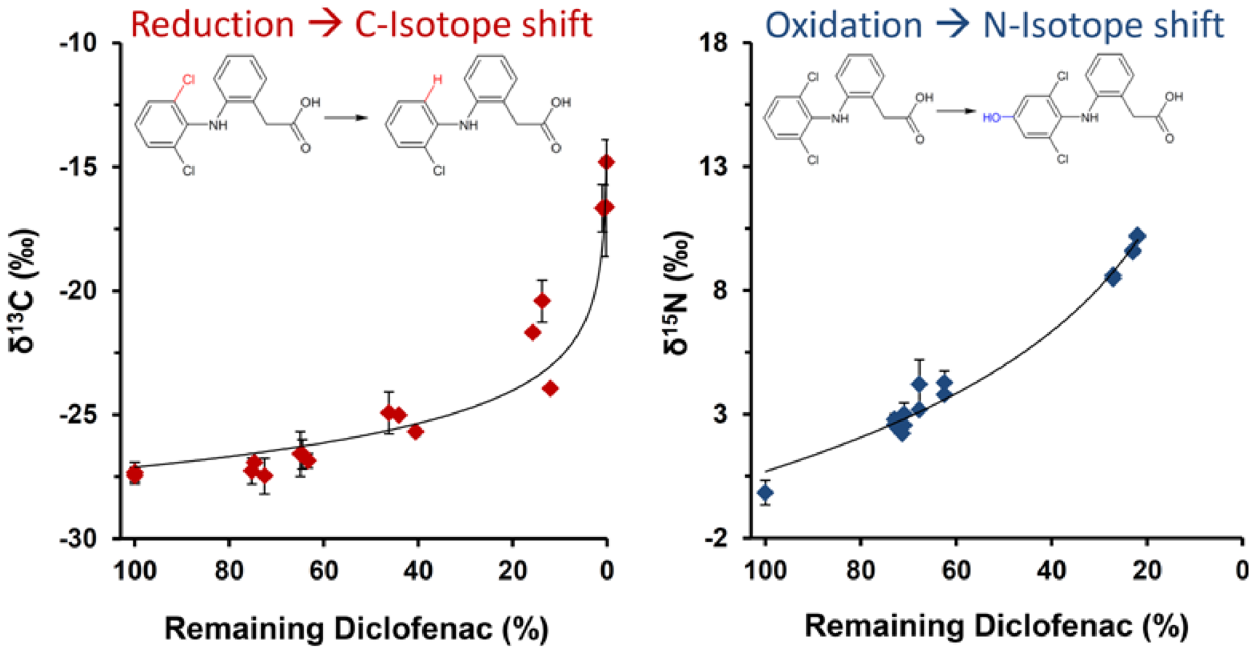

2.2 Introduction

Diclofenac is one of the most popular painkillers and anti-inflammatory agents in the world with a yearly consumption in Germany, for example, of 86 t.[1] On the downside, it enters the environment via sewage treatment plants or runoff from fields as a consequence of artificial recharge.[2-5] There, it has the potential to bioaccumulate in mussels and inhibit their growth[6], to harm rainbow trout[7], and it has been linked to the eradication of whole vulture populations.[8] While its importance is emphasized by the fact that the European Union recently proposed to add it to the list of priority pollutants[9] the assessment of its degradability in the environment remains a major challenge.

Concentration measurements alone are often inconclusive, because in rivers or groundwater it is typically difficult to obtain a closed hydraulic mass balance. To this end the hydrology has to be very well understood, including parameters like flow velocity, ex- and infiltration. Without this data it is not possible to distinguish between a concentration decrease along a stretch of a river due to degradation or due to dilution by infiltrating groundwater.[10] In addition, evidence about transformation pathways is needed, and also this information is not accessible from concentration measurements alone. Transformation products may deliver insight[11-14], but in the case of pharmaceuticals many of them are unknown and may in addition not be detectable because they are further transformed.[11, 13, 15]A common approach to assess degradation processes is the determination of degradation kinetics and the analysis of transformation products in sediment-water tests.[15-17] Although they can be used to compare the degradation kinetics of different compounds under the same conditions, the results depend strongly on the selected setup and sediment.[18] Owing to this fact, and due to the heterogeneity of geochemical boundary conditions at field sites it is very difficult to extrapolate results from those lab-scale tests to a larger scale like a river stretch.

Compound specific isotope analysis (CSIA) has the potential to provide a new, complementary handle to assess degradation of environmental pollutants.[19-21] This approach relies on isotope analysis of the original contaminant, without the need of metabolite analysis. Isotopes are contained in chemical bonds where they are not susceptible to isotopic exchange so that isotope ratios do not change in the absence of degradation. If these bonds are broken during (bio)chemical transformation, however, bonds with light isotopes typically react slightly faster than bonds with heavy isotopes (kinetic isotope effect, KIE).[22] Consequently the remaining substrate molecules contain on average increasingly more heavy isotopes. This enrichment of heavy isotopes in the original contaminant (as reflected in $^{13}C/^{12}C$, or $^{15}N/^{14}N$) may therefore provide an independent line of evidence of its degradation, even if products are not detected. Furthermore, dilution leaves isotope ratios unaffected, while it can cause false positives in assessments based on concentration data.[23] Therefore, degradation can be investigated even if the hydrological mass balance is not closed and data interpretation does not depend on hydrological investigations such as tracer tests. As additional virtue, CSIA can deliver even insight into reaction mechanisms if isotopes of two or more elements are analyzed.[22] The reason is that different (bio-) chemical reactions involve specific bonds containing different elements so that isotope effects are observed specifically for those elements in the bond that is reacting. Previous work on isoproturon, atrazine, and BAM[24-27] has shown that isotope analysis of two elements (two-dimensional isotope analysis) has the potential to elucidate different transformation pathways of pesticides. However, to date there is no study available about the investigation of pharmaceutical degradation by CSIA.

The first aim of the present study was, therefore, to establish a GC-IRMS method for diclofenac that can serve as a tool to distinguish degradation pathways by analyzing carbon and nitrogen isotope values. To this end a method was developed that features an online- or offline-derivatization step, depending on whether fast or sensitive analysis is required. The second aim was to investigate isotope fractionation in two degradation test systems. This proof of principle study was conducted (a) in an oxic sediment-water-system to assess isotope fractionation under environmentally relevant conditions and (b) for reductive dechlorination under reducing conditions. To investigate the potential for source tracking and degradation assessments in field studies, finally, we conducted two additional explorative tests. On the one hand we examined a limited number of commercial diclofenac products, as an indicator of the isotopic variability of diclofenac sources in the environment. On the other hand we made a feasibility test to investigate the potential to analyze diclofenac in low concentrations in the presence of matrix interferences from actual environmental samples.

2.3 *Materials and Methods*

2.3.1 Chemicals

A complete list of chemicals used in this study can be found in the supporting material (A3-S1).

2.3.2 Purification of Commercial Pharmaceutical Products and Treatment for Isotope Analysis

Commercial diclofenac products were directly analyzed via online-derivatization GC-IRMS (see below) after dissolving powdered tablets or gels in methanol and subsequently filtering them through

PTFE filters (0.2 µM, Carl Roth, Karlsruhe). For EA-IRMS analysis – conducted to obtain reference values for comparison with the GC-IRMS results – samples were also purified using column chromatography. This procedure was necessary to eliminate any additional carbon and nitrogen sources in the gels or tablets which are automatically separated out in the GC-method, but which would interfere in the EA-IRMS analysis. To this end, powdered tablets and gel products were dissolved in methanol and eluted through a glass column (300 x 10 mm, Lenz) filled with silica gel (40-63 µm, Merck, Darmstadt). The eluent was pentane:ethylacetate:acetic acid 70:30:1 (v/v/v). Fractions were collected and their purity was controlled with thin layer chromatography. All fractions containing diclofenac were mixed and evaporated to dryness under N_2 and subsequently analyzed on an elemental analyzer (EURO EA, Euro Vector Instruments) coupled to a Finnigan MAT 253 isotope ratio mass spectrometer (Thermo Fisher Scientific, Bremen, Germany).

2.3.3 Aerobic Biodegradation Experiment

Biodegradation of diclofenac was investigated at a concentration of 450 µg L^{-1} in river water exposed to river sediment in three 5 L replicates with one 5 L sterile control. River water and sediment were sampled from the Isar river close to Garching (Germany), wet sieved (10 mm) and filled in 5 L glass bottles (n= 4). The background concentration of diclofenac in the natural water was below the limit of detection (1 ng L^{-1}). The sediment:water ratio was 1:4 (v/v) and bottles were incubated in the dark at 12 °C on a horizontal shaker (80 rpm) and aerated with filter-sterilized air (~ 100 mL min^{-1} per bottle). The system was equilibrated at 12 °C and the sediment was allowed to settle for one week. Then the supernatant was removed and Isar water from the same sampling event was spiked with diclofenac (c= 450 µg L^{-1}) and filled into triplicate bottles each containing sediment. A sterile control was prepared by autoclaving sediment in a fourth bottle (121 °C, 20 min. 3 bar), adding Isar water containing diclofenac (c= 450 µg L^{-1}) and supplemental NaN_3 (c= 1 g L^{-1}). As expected[11], the diclofenac concentration in this sterile control remained constant over time demonstrating that neither abiotic degradation nor sorption processes were relevant for the dissipation of diclofenac (data not shown). No additional sterile controls were therefore included. During 86 days 14 samples (1.5 mL) were taken out of each bottle and filtered through PTFE filters (0.2 µm) for concentration and transformation product analysis with liquid chromatography/tandem mass spectrometry (LC/MS-MS, A3-S2). At selected time points additional samples were withdrawn for isotope analysis. Increasing sampling volumes (0.1– 2.3 L) were taken with decreasing residual concentrations to obtain sufficient amounts for precise CSIA. These samples were enriched and purified using solid phase extraction (SPE). To this end, samples were brought to pH 10.5

with NaOH (1M) and passed through Chromabond HRX-A SPE anion exchange cartridges (6 mL, 150 mg, Macherey & Nagel, Düren, Germany; for recovery rates see Supporting Information A3-S3). Subsequently, cartridges were eluted with methanol (2% formic acid), samples were evaporated, redissolved in 500 µL methanol and stored at -20 °C until GC-IRMS analysis.

2.3.4 Dechlorination Experiment

To mimic reductive dechlorination, diclofenac was transformed by H_2 in the presence of Au/Pd-nanoparticles which had been coated on microorganisms as described by De Corte et al.[28]. Briefly, a culture of *Shewanella oneidensis* was grown in Luria Bertani medium and subsequently washed and resuspended in M9 medium to an optical density of 1 at 610 nm. Pd(II) and Au(III) were added to concentrations of 50 mg L^{-1} and 1 mg L^{-1}, respectively, and then reduced by exposure to H_2 for 48 h. Diclofenac was added, resulting in an initial concentration of 20 mg L^{-1} and the headspace of the serum flasks was filled with H_2. Samples were withdrawn with a syringe, filtered through a 0.22 µm filter, and quantified by HPLC-UV according to De Corte et al.[28].

2.3.5 Online Derivatization GC-IRMS Analysis

To make the analyte diclofenac amenable to gas chromatographic analysis, the polar carboxyl-group was converted into a methyl-ester. Online derivatization with trimethylsulfonium hydroxide (TMSH, 0.25 M in methanol) was conducted as described previously[29, 30]. Previous results [29] and data of this study (see Supporting Information A3-S4) show that the molar excess of TMSH is a crucial parameter for isotope measurements; TMSH was, therefore, added to the samples prior to injection with a molar excess of at least 300. Between 1 µL and 100 µL of the analyte/TMSH mixture were injected into a temperature programmable injector (Optic 3-SC High Power Injection System, ATAS GL International B.V., Veldhoven, Netherlands) equipped with a large volume liner containing glass beads (PAS Technology, Magdala, Germany). After evaporation of the solvent, the split flow was set to zero for 5 minutes and the injector was heated from 40 °C to 300 °C at 10 °C s^{-1}. This flash heating triggered the methylation of diclofenac and transferred the formed methyl-diclofenac onto the gas chromatograph (TRACE GC Ultra gas chromatograph, Thermo Fisher Scientific, Milan, Italy) equipped with a DB-5 column (30 m × 0.25 mm or 0.32 mm, 1 µm film thickness, J&W Scientific, Folsom, Canada). The initial oven temperature was 80 °C (1min), ramped to 200 °C with a rate of 17 °C min^{-1} and then at 6 °C min^{-1} to 300 °C (held for 2 min). After chromatographic separation diclofenac was combusted in a Finnigan GC combustion interface (Thermo Fisher Scientific, Bremen, Germany) to CO_2 and N_2 with a NiO tube / CuO-

NiO reactor operated at 1030 °C (Thermo Fisher Scientific, Bremen, Germany). Isotope values of CO_2 and N_2 were determined with a Finnigan MAT 253 isotope ratio mass spectrometer (Thermo Fisher Scientific, Bremen, Germany). Three monitoring gas peaks were measured before and after every run. These monitoring gas peaks were used to correct isotope values to the international standards, Vienna PeeDee Belemnite for carbon (Eq. 2-1) and air for nitrogen isotopes (Eq. 2-2):

$$\delta^{13}C = \frac{\left({}^{13}C/{}^{12}C_{Sample} - {}^{13}C/{}^{12}C_{Reference}\right)}{{}^{13}C/{}^{12}C_{Reference}} \tag{2-1}$$

$$\delta^{15}N = \frac{\left({}^{15}N/{}^{14}N_{Sample} - {}^{15}N/{}^{14}N_{Reference}\right)}{{}^{15}N/{}^{14}N_{Reference}} \tag{2-2}$$

2.3.6 Offline Derivatization - Splitless Injection

An offline derivatization method was established as alternative to the online derivatization method to lower the limit of precise isotope analysis as described previously for polar herbicides[31]. Briefly, samples were filtered (0.22 µm) and evaporated in 2 mL amber glass vials to dryness under a gentle stream of N_2. After adding 400 µL of BF_3 (10% in methanol), the vials were incubated for 1 h at 40 °C. After cooling the remaining reactant was quenched with 400 µL MilliQ water, the methylated analytes were extracted three times with 500 µL n-hexane, transferred to a new vial and evaporated under a gentle stream of N_2 without heating. The aqueous phase was disposed of in a canister of 2 M NaOH to quench the toxicity of HF. The dried hexane extract was redissolved in 1500 µL n-hexane and between 1 µL and 8 µL were injected splitless at 280 °C into a split/splitless injector (Thermo Fisher Scientific, Milan, Italy). After one minute, the split ratio was switched to 1:10. As shown in the supporting material (A3-S5) the elevated injection volume did not bias isotope analysis. The injector was connected to the same GC-IRMS system and operational conditions, as well as data evaluation were the same as described above.

2.3.7 Offline Derivatization-On-Column Injection

Since on-column injection is known to be a most sensitive injection technique, a method established for atrazine was adapted to diclofenac.[32] Briefly, offline-derivatized samples were injected at 40 °C in a programmable injector (Optic 3-SC High Power Injection System, ATAS GL International B.V., Veldhoven, Netherlands) equipped with an on-column liner (A100129; ATAS GL International, Eindhoven, the Netherlands) pressed directly onto a fused-silica-methyl-silyl retention gap

(3 m×0.53 mm inner diameter, Chromatographie Service GmbH, Langerwehe, Germany). The injector temperature was initially at 40 °C (5 min) and then ramped to 280 °C at 2 °C s^{-1}. The column flow was set to 0.3 mL min^{-1} to gentle blow off the solvent inside the retention gap (2 min) and then ramped to 1.4 mL min^{-1} within 120 s. The GC was equipped with the same DB-5 column as above, but with a modified oven program: 40 °C (4 min) to 200 °C with 17 °C $min.^{-1}$, then ramped to 270 °C at 6 °C min^{-1} (20 min) and finally at 10 °C $min.^{-1}$ to 290°C (10 min). The operational conditions of the combustion unit and the IRMS system were as described above.

2.3.8 Extraction and Purification from River Water Samples

To determine the applicability of isotope analysis of diclofenac to field samples 10 L of spiked river water were analyzed (c = 1 μgL^{-1}). After filtration (glass fiber No.6, Schleicher & Schüll) the sample was split into ten 1 L aliquots and subjected to solid phase extraction (SPE) as described in the biodegradation experiment (splitting of the sample was conducted to prevent a potential overloading of the SPE cartridge). Unified SPE extracts were evaporated, redissolved in 1 mL MeOH:H_2O 1:1 (pH 2) and purified by preparative HPLC to minimize matrix interferences (for details see A3-S6). After offline derivatization, C- and N-isotope ratios were analyzed by on-column injection GC-IRMS as described above.

2.3.9 Post-Measurement Correction of Carbon Isotope Ratios

A crucial factor for isotope analysis is the performance of the combustion reactor in the GC-IRMS system since previous work has shown that those reactors may produce drifts in isotope values during a long sequence of samples [33]. A diclofenac lab standard was therefore frequently measured and, when necessary, used to correct sample values for such drift as described previously.[33, 34] In addition, the methylation of diclofenac introduces an extra carbon atom into the molecule changing its bulk carbon isotope ratio. To correct for this shift of $\delta^{13}C$, standards and samples were derivatized with the same batch of TMSH or methanolic BF_3, respectively, and isotope values of diclofenac were subsequently corrected using Eq. 2-3 and Eq. 2-4. Specifically, Eq. 2-3 was used to calculate the isotope ratio of the introduced methyl group ($\delta^{13}C(Me)$). We note that $\delta^{13}C(Me)$ needs not be true in absolute terms, but is a necessary parameter for the following correction of diclofenac raw data (see below), which adheres to the identical treatment of sample and standard. (i) The isotope ratio of the lab standard was determined on EA-IRMS (14 C-atoms) to obtain the isotope ratio of the diclofenac moiety ($Diclofenac_{EA}$). (ii) This value was subtracted from the GC-IRMS measurement of the methylated diclofenac standard (*Me-Diclofenac* $_{GC}$, 15 C-atoms).

$$\delta^{13}C(Me) = 15 \times \delta^{13}C(Me - Diclofenac_{GC}) - 14 \times \delta^{13}C(Diclofenac_{EA}) \tag{2-3}$$

(iii) Subsequently, isotope values of samples, $\delta^{13}C(Diclofenac_{Sample})$ were corrected using the $\delta^{13}C(Me)$ value of the standard measurements that bracketed their analysis. As can be deduced from Gaussian error propagation[31] the uncertainty of $\delta^{13}C(Me)$ in Eq. 2-3 is reduced by a factor of 14 in Eq. 2-4.

$$\delta^{13}C\left(Diclofenac_{Sample}\right) = \frac{15 \times \delta^{13}C(Me - Diclofenac_{Sample}) - 1 \times \delta^{13}C(Me)}{14} \tag{2-4}$$

2.3.10 Evaluation of Isotope Fractionation

Bulk enrichment factors (ε) were calculated using the linearized Rayleigh equation (Eq. 2-5), which links isotope ratios at the beginning ($\delta^{13}C_0$) and after time *t* ($\delta^{13}C_t$) to the remaining substrate fraction $f = (C_t/C_0)$.

$$\ln\left(\frac{\delta^{13}C_t + 1}{\delta^{13}C_0 + 1}\right) = \varepsilon \times \ln f \times = \varepsilon \times \ln\left(\frac{C_t}{C_0}\right) \tag{2-5}$$

From ε a position-specific apparent kinetic isotope effect (AKIE) can be estimated for diclofenac degradation according to

$$AKIE \quad \approx (n \times \varepsilon + 1)^{-1} \tag{2-6}$$

(Eq. 21 in Elsner et al.) [35]. Because there is only one nitrogen atom, but there are 14 carbon atoms in diclofenac, the expressions are

$$AKIE_{nitrogen} = (1 \times \varepsilon + 1)^{-1} \tag{2-7}$$

$$AKIE_{carbon} = (14 \times \varepsilon + 1)^{-1} \tag{2-8}$$

2.3.11 Evaluation of Degradation Kinetics

For the degradation experiments dissipation rates were determined with a pseudo first-order kinetic approach. To this end the logarithm was taken of the fraction $f = (C_t/C_0)$ of remaining diclofenac and plotted against time. The resulting slope of the linear regression curve represents a pseudo-first order dissipation constant (k_{dis}) which was used to calculate a dissipation time (dt50; Eq. 2-9). The standard error of k_{dis} was used to estimate the uncertainty of the dt50.

$$dt50 = \frac{\ln(2)}{k_{dis}} \tag{2-9}$$

2.4 *Results & Discussion*

2.4.1 Method Validation & Quantification Limit

Seven diclofenac products were purified on a silica column, analysed on EA-IRMS (1σ = 0.1‰[21]) and compared to parallel online-derivatization GC-IRMS measurements. Good agreement between both approaches was observed for both elements (Tab. 2-1, Fig. 2-1a, 2-1b). At the cost of slightly lower precision (see below), the online-derivatization GC-IRMS method is much faster and can facilitate high throughput analysis of commercial drugs compared to EA-IRMS. It saves resources because no offline-preparation is required except dissolving and filtering. Furthermore, GC-IRMS has a higher chromatographic resolution than the packed silica column used for preparation prior to EA-IRMS analysis. The greatest advantage of GC-IRMS, however, is its excellent sensitivity. A single EA-IRMS analysis needs 800 µg diclofenac to analyze $\delta^{13}C$ and $\delta^{15}N$ simultaneously. In contrast only 60 ng (33 ng C, 1σ = 0.4‰) are needed per injection for GC-IRMS and 3.8 µg (180 ng N, 1σ = 0.5‰) for nitrogen using online-derivatization. For even better sensitivity in the analysis of environmental samples the GC-IRMS quantification limits can be further lowered by two strategies.

(a) Online derivatization with TMSH using large volume injection. With the use of large volume injection in combination with online derivatization the solvent is evaporated in the injector prior to heating of the inlet. For isotope analysis of benzotriazole it was shown that this makes injection volumes of up to 100 µL possible.[36] While this approach is fairly easy to adapt by prolongation of the vent-phase prior to the heating of the injector, it consumes a large volume of precious sample that would be needed for replicate analysis or analysis of a second element.

Table 2-1: Isotope values of direct online-derivatization GC-IRMS analysis & silica-column purified EA-IRMS measurements; errors are given as precision of replicate measurements (n = 3-6); the total uncertainty (2σ) of the GC IRMS and EA IRMS method is 0.8‰ and 0.2‰, respectively; NA= not analyzed.

Letter	**Producer**	**Product**	**δ^{13}C GC-IRMS (‰)**	**δ^{13}C EA-IRMS (‰)**	**δ^{15}N GC-IRMS (‰)**	**δ^{15}N EA-IRMS (‰)**
A	Hexal	Diclac Dispers (2004)	-27.1 ± 0.1	-27.2 ± 0.1	-0.7 ± 0.4	-0.7 ± 0.1
B	Hexal	Diclac Dispers (2012)	-30.0 ± 0.3	-30.5 ± 0.1	-3.2 ± 0.3	-3.3 ± 0.1
C	Dolorgiet	Dolgit-Diclo	-30.3 ± 0.2	-30.2 ± 0.1	-2.2 ± 0.2	-2.6 ± 0.1
D	Betapharm	Diclo dispers	-30.3 ± 0.3	-31.0 ± 0.1	-2.3 ± 0.3	-2.0 ± 0.1
E	Novartis	Voltaren Retard	-30.6 ± 0.3	-30.9 ± 0.1	-2.6 ± 0.7	-3.2 ± 0.2
F	Novartis	Voltaren Dispers	-31.0 ± 0.2	NA	-2.8 ± 0.5	NA
G	Novartis	Voltaren Emulgel	-29.3 ± 0.5	-29.3 ± 0.1	0.0 ± 0.1	-0.3 ± 0.1
H	ratiopharm	Diclofenac-ratiopharm Gel	-28.4 ± 0.3	NA	-0.6 ± 0.5	NA
S	Sigma Aldrich	Lab standard	-26.4 ± 0.3	-26.4 ± 0.1	-1.1 ± 0.2	-1.1 ± 0.1

(b) Offline derivatization and subsequent injection into a hot splitless injector. A more efficient strategy is the combination of offline-methylation with splitless injection to maximize derivatization yield and peak sharpness in comparison to online derivatization. With this technique reliable isotope measurements have been tested, and found to be possible down to 10 ng (6 ng C, 1σ = 0.4‰) for carbon and 600 ng (30 ng N, 1σ = 0.4‰) for nitrogen (see amount-dependency plots in the Supporting Information A3-S7 as well as the finding that injecting up to 8 µL splitless does not bias isotope ratios, Supporting Information A3-S5). The quantification limit can be further lowered by offline derivatization and subsequent on-column injection as previously shown for atrazine.[32] This technique increases the quantification limit by a factor of three (3 ng C, 10 ng N) in comparison to splitless injection. These amounts correspond to 70 ng and 4 µg diclofenac that are needed in total for one sample that is subjected to carbon and nitrogen isotope analysis, respectively (final sample volume 40 µL, injection volume 2 µL).

In conclusion, the two derivatization methods complement each other nicely. If the focus is on fast and safe analysis where no HF is formed during preparation (e.g. for product analysis in laboratory studies) online-methylation is preferable. In contrast, if a low quantification limit for isotope analysis is essential, as is the case for environmental samples, offline derivatization with on-column injection delivers excellent sensitivity. Because the degradation experiments of this study were conducted in the lab without the need for extra sensitivity they were analyzed using the online-derivatization method.

2.4.2 Source Variability and Potential for Source Tracking

Knowledge about isotope ratios of diclofenac products is important to be aware of the variability of diclofenac sources the environment, such as sewage treatment plants. Moreover, it was shown that especially N-isotope analysis of micropollutants has the potential for source appointment in the environment. [36] Specifically, for pharmaceutical products such as aspirin, ibuprofen or naproxen, it has been shown that the analysis of stable isotope ratios can be used as a fingerprint for product authentication and to track sources.[37-39] In one case it was even possible to determine the location of an illegal production site by evidence from isotope analysis.[40]

Given that our method allows isotope analysis of diclofenac in complex matrices, at low concentrations (BF_3 method) and without laborious sample preparation (TMSH method), we conducted an explorative survey to investigate the typical variability of diclofenac source isotope ratios. To this end, two or three aliquots of nine products were analyzed twice by online-derivatization GC-IRMS. The results are shown in Table 2-1 and Figure 2-1c as a dual-element isotope plot. Different tablets or gel-aliquots from the same product did not show a higher deviation than replicate analysis of one aliquot, reflecting a homogeneous isotope distribution within the products. Consequently all aliquot-measurements were summarized and treated as one sample. The total range of isotope ratios was 5‰ and 4‰ for carbon and nitrogen, respectively.

This relatively low source variability is similar to the study of Jasper et al.[41] who analyzed a larger data set of 53 topiramate ($C_{12}H_{21}NO_8S$) products with EA-IRMS and found a range of 8‰ for both carbon and nitrogen. In terms of source appointment Figure 2-1c shows that the analysis of two elements clearly enhances resolution and most of the products can be distinguished in a dual isotope-plot. Isotope values of some products were quite close, e.g. of product E and F from the same producer or of E, C and D from different producers. This may be explained by the fact that diclofenac is often synthesized by the same pathway and raw materials so their isotope values may coincide. The same applies if two companies share the same supplier. In contrast, in other cases differences were greater, and in one case a clear shift of carbon and nitrogen isotope ratios was detected for exactly the same product (A+B) of the same company sold in different years. The date of expiry differed by eight years for both batches and therefore likely reflects a change in either production pathway or materials used in synthesis. An isotope shift due to aging is unlikely because peak amplitudes in analysis of equal amounts from both batches were similar. If isotope fractionation had been caused by degradation this would have been reflected in smaller peaks.

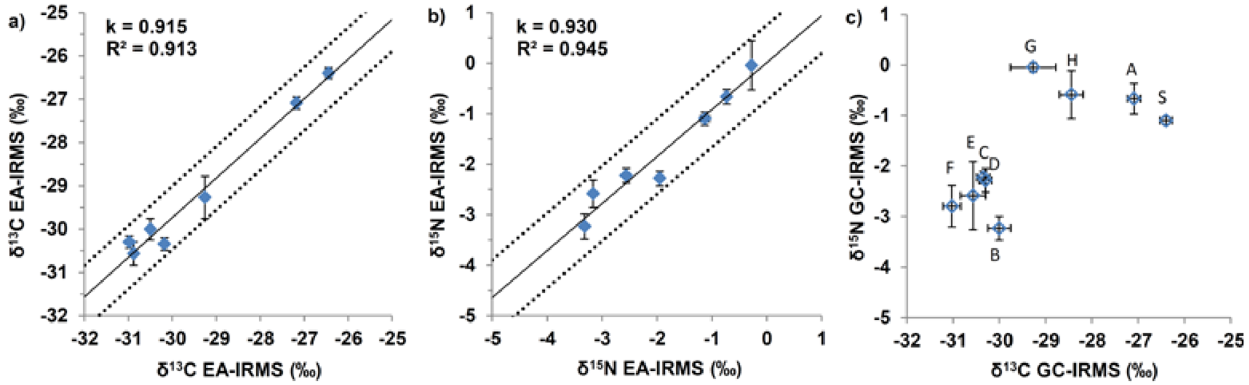

Figure 2-1. Comparison of six products and the lab standard (S) analyzed by EA-IRMS and GC-IRMS for carbon (a) and nitrogen analysis (b). In total eight products (A-H) and the reference standard (S) were measured by GC-IRMS (c) and shown as a dual isotope plot. Given are mean vales (n= 3-6) and confidence intervals (0.95) for carbon and nitrogen isotopes and the dotted line represents the uncertainty of the slope as ± 2σ.

In conclusion, although not possible in all cases, a distinction based on isotope values was accomplished for the majority of the pharmaceutical products. Our finding therefore shows the potential for producers to track batches and even to verify their products if raw materials for production are chosen carefully and isotope ratios of manufactured products are recorded. From an environmental perspective the relatively narrow isotope range has two consequences. On the one hand it limits the application of CSIA for source appointment. The reason is that except for hospital effluents, usually several producers are mixed and the uncertainty of field sample analysis is often higher than for relatively clean and highly concentrated pharmaceutical products. On the other hand this low variability is beneficial for an easier characterisation of the initial isotope ratio in degradation studies with a variable input, such as the outflow of a sewage treatment plant.

2.4.3 Isotope Fractionation During Degradation by Aerobic River Sediment

Kinetics. A proof-of-principle biodegradation experiment was conducted to investigate isotope fractionation under environmentally relevant conditions. To this end diclofenac was incubated in an aerobic sediment-water-system containing an indigenous microbial community from a river. During the experiment the diclofenac concentration in the water phase decreased by 71% within 86 days. The dissipation of diclofenac from the water phase could be described with a pseudo-first order rate resulting in a dissipation rate constant of k_{dis}= -0.015 (± 0.002) and an average dissipation time (50%; dt_{50}) of 47 d (± 4 d) (see evaluation in the Supporting Information A3-S8). The diclofenac concentration in the sterile control remained stable at the initial level. Thus, sorption to the sediment or abiotic degradation was not a significant sink in the chosen setup and dissipation can be attributed to degradation. Compared to previous studies the average dissipation time dt_{50} of 47 d falls between that of a flume experiment with river sediment (dt_{50} 3 – 9 d)[3] and bioreactors with sewage sludge, where diclofenac was not eliminated within 30 d[42] or only to a minor extent (20% degradation after 122 d).[30]

Product formation. During diclofenac degradation a hydroxylated transformation product (TP) was detected by LC-MS/MS analysis that could be identified as 4'-OH-diclofenac by comparison to an authentic standard (Fig. 2-3 and supporting material A3-S8). This TP has previously been found in sewage treatment plants[12, 14] and in river-water-test-systems.[11, 15] 4'-OH-diclofenac was not present at t=0 and appeared at low, but steadily increasing concentrations of up to 14 µg L^{-1} (A3-S8). Assuming no further degradation this amount would correspond to 3% of the transformed diclofenac; the true value may be somewhat higher, because hydroxylated diclofenac has been shown to be further biodegradable.[11, 15]

Isotope fractionation and possible mechanisms. No significant carbon isotope fractionation was observed during aerobic biodegradation (Fig. 2-2a). In contrast, nitrogen isotopes shifted from -0.2‰ to 9.4‰ corresponding to a normal isotope effect of $\varepsilon_{Nitrogen}$ = -7.1‰ ($AKIE_{nitrogen}$ of 1.007)(Fig. 2-2b). The same qualitative trend (ε_N = -10‰) was previously observed for oxidation of diphenylamine by MnO_2.[43] Two mechanistic scenarios can explain the occurrence of N-isotope fractionation (Fig. 2-3). (1) Enzymatic monohydroxylation of alkylated anilines would be in agreement with the detection of 4'-hydroxy diclofenac, which is also formed by diclofenac transformation via human CYP450 enzymes.[44] While the initial SET (single electron transfer) step Ia would be expected to cause an inverse N- isotope effect, step IIa may cause a normal N-isotope effect (Fig. 2-3).[45] This hypothesis is based on calculations for diphenylamine, which can be regarded as the molecular backbone of diclofenac, where C-N-bonds were shown to be stiffer in the radical-cation than in diphenylamine.[43] Taking steps Ia and IIa together, an observable normal N-isotope effect would result if the oxidation step (IIa) was rate limiting. (2) An alternative mechanistic hypothesis could be biotic diclofenac transformation via dioxygenation, which may also lead to a normal N-isotope effect (Fig. 3). While the N-atom is not involved in the initial reaction step (Ib), a C-N bond is broken in the second step (IIb). If this bond cleavage is rate limiting, it could explain the observed isotope fractionation. Indeed, dihydroxylation has already been investigated for diphenylamine[46] and normal N-isotope fractionation (ε_N = -1.0‰) was measured.[43]

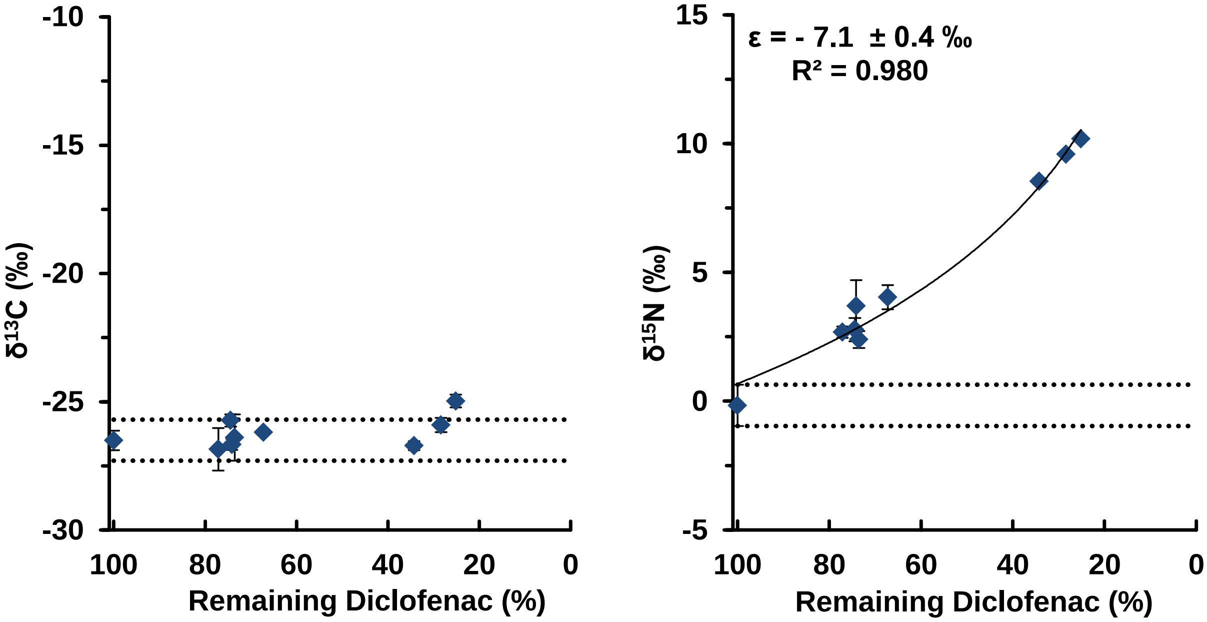

Figure 2-2. Isotope fractionation of carbon (a) and nitrogen (b) during aerobic biodegradation (three replicates). Isotope values are given as mean values with 95% confidence intervals. The slope of the regression line is equivalent to the enrichment factor ε and the dotted line represents the initial isotope value of diclofenac (t = 0) ± 2σ. The diclofenac used in this experiment had a different isotopic composition than in the dechlorination experiment.

Samples were therefore screened with LC-MS/MS for potential cleavage products, such as 2,6-dichloronaniline, 2,6-dichlorophenol and dihydroxyphenyl acetic acid, but no additional TP could be detected. Their absence may be explained by further transformation, the relatively high detection limit for 2,6-dichloronaniline (50 µg L^{-1}), or irreversible binding to humic substances as shown for 3,4-dichloroaniline.[47] Because the exclusive detection of hydroxylated products (including corresponding quinone structures) agrees with previous studies using natural sediment[11,15] or plants[48], in depth TP analysis was not further pursued.

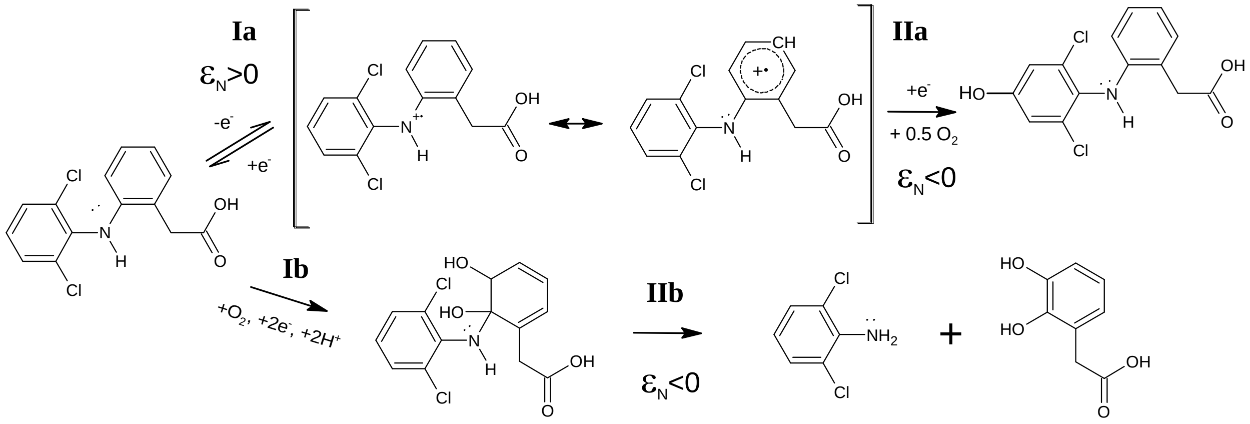

Figure 2-3. Possible reaction pathways for diclofenac: while the Monooxygenase pathway forms 4'-hydroxy diclofenac via initial single electron transfer, concerted dioxygenation (Dioxygenase-pathway) leads to 2,6-dichloroaniline and 2,3-dihydroxyphenyl acetic acid.[46]

2.4.4 Reductive dechlorination

Isotope fractionation was further investigated in a model system for reductive dehalogenation, which is an important type of environmental transformation.[49-51] In addition, this system served as an indicator if carbon isotope fractionation can be detected at all in diclofenac. Since GC-IRMS analyzes the average δ^{13}C value of all 15 C-atoms in methylated diclofenac, any potential enrichment at the reactive position is diluted by a factor of 15, so previous studies suggested that the threshold for detectable carbon isotope fractionation would be between 11 and 14 C-atoms.[52] Diclofenac was dechlorinated under anoxic conditions in the presence of hydrogen by Pd/Au-coated microorganisms [28]. This is an abiotic reaction which takes place at the outer cell wall, where microorganisms are only used as a carrier for the catalyst. After H_2 dissociates at the catalyst surface, diclofenac is also sorbed and sequentially dechlorinated.[28] Diclofenac was thereby degraded with a dt_{50} of 1.35 h ($k = 0.515\ h^{-1}$). During degradation carbon isotope values shifted from -32.1‰ to -20.1‰ corresponding to an ε_C of -2.0‰ (Fig. 4a). The magnitude of carbon fractionation ($AKIE_{carbon}$= 1.029) agrees well with previous work where an $AKIE_{carbon}$ values of around 1.03 were observed for the reductive dechlorination of tetrachloromethane by several Fe(II) bearing minerals (Streitwieser Limit 1.057).[53, 54] In contrast to carbon isotope fractionation, no nitrogen isotope fractionation was detected (Fig. 4b). This is in agreement with the reductive dechlorination mechanism, where a C-N bond is not directly involved.

The results from this model system therefore show that carbon isotope fractionation could indeed be detected in diclofenac and serve as indicator for strongly fractionating degradation processes such as reductive transformation. Reductive dechlorination was shown to be the first step of diclofenac photodegradation[13, 55] and is an important pathway for biodegradation of many chlorinated contaminants.[49-51] Such a shift in carbon isotope values could therefore indicate diclofenac dechlorination in field samples. In addition, the use of metal-catalysts to dechlorinate contaminants is discussed as a removal strategy for micropollutants in treated waste water and this process could be monitored by CSIA.[28]

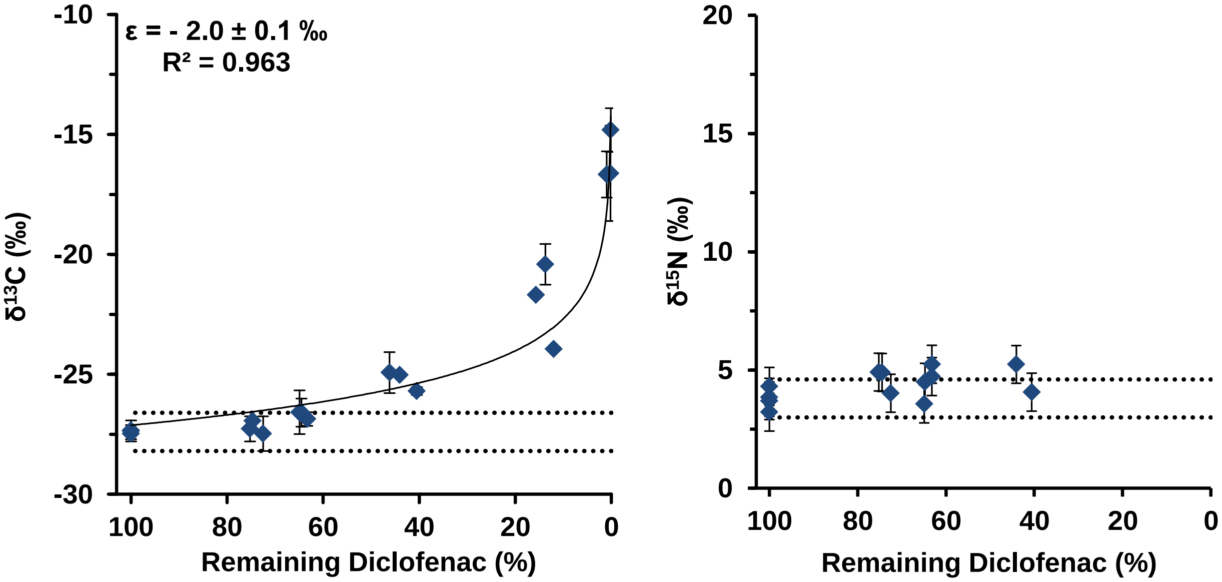

Figure 2-4. Isotope fractionation of carbon (a) and nitrogen (b) during the dechlorination experiment conducted with three replicates. Carbon isotope values are given as mean values with confidence intervals (95%). Due to the high quantification limit of nitrogen isotope analysis using online derivatization, samples could only be measured once and until 60% degradation; error bars represent the total error of the δ15N measurement (2σ = 0.8‰). The slope of the regression line is equivalent to the enrichment factor ε and the dotted line represents the value at t = 0 ± 2σ. The diclofenac used in this experiment had a different isotopic composition than in the biodegradation experiment.

2.4.5 Environmental Significance

This study is the first to explore the potential of CSIA to assess degradation of pharmaceuticals using diclofenac as a model compound. We have found that aerobic degradation by oxic river sediment was accompanied by strong nitrogen isotope fractionation, whereas reductive dechlorination showed significant carbon, but no nitrogen isotope fractionation. Consequently, the two transformation pathways may be distinguished by dual element isotope analysis. Because CSIA neither depends on transformation product analysis nor on concentration measurements, this approach delineates a new, complementary line of evidence to evaluate environmental degradation of diclofenac.

To put this observed magnitude of degradation-associated isotope fractionation into perspective, we also conducted a complementary survey of commercial diclofenac products. Their isotope values spanned a range of 5‰ and 4‰ for carbon and nitrogen, respectively. This indicates that source isotope ratios – e.g. the outflow of a sewage treatment plant – need to be well constrained in order to unequivocally detect the "on-top" changes by isotope fractionation that are caused by degradation. In the case of very pronounced isotope fractionation, however – such as for nitrogen fractionation during microbial oxidation – values may so clearly exceed the source range of 4‰ that they could allow to identify degradation even without definite knowledge of source ratios (e.g. 10‰ shift of $\delta^{15}N$ after 70% degradation).

Finally to explore the CSIA approach not only with respect to process-associated isotope fractionation ("Do we see changes in isotope values?"), but also with respect to its applicability ("Can we actually measure isotope ratios under real world conditions?") we extended our study to test the feasibility of diclofenac CSIA at low concentrations and with a complex matrix. A spiked river water sample (1 $\mu g L^{-1}$) was extracted by SPE, purified by preparative HPLC (S6)[32], and successfully analyzed after offline derivatization by on-column injection GC-IRMS. Isotope ratios were in perfect agreement with EA-IRMS data: the $\delta^{13}C$ value in river water (-26.4 ± 0.5‰) coincided with the EA-IRMS value of -26.4‰, whereas the $\delta^{15}N$ value in river water (-1.2 ± 0.4‰) was within error of the EA-IRMS value of -1.1‰ (S9). Based on this first test, the sensitivity of nitrogen isotope measurements was already in the range of sewage treatment plants outflow[4, 55] and in the case of carbon, it was even better. The high $\delta^{13}C$ peak of the sample (2500 mV, A3-S9) indicates that a peak ten times lower (250 mV), corresponding to a concentration of 100 ng L^{-1}, could be analyzed as well, which is in the range of typical diclofenac concentrations in surface waters.[3, 4, 55, 56] These limits for C- and N-isotope analysis are among the lowest reported for non-volatile compounds[21, 32] and we demonstrated that the individual techniques are suitable for isotope analysis of diclofenac. Future studies may therefore use this study as a basis to even further optimize individual steps, such as increasing the recovery rate of the SPE or by extracting larger sample volumes.

2.4.6 Acknowledgements

We acknowledge three anonymous reviewers for their valuable feedback and Lisa Douglas for reviewing the manuscript. Michael Maier is financially supported by the German Federal Environmental Foundation (DBU). Simon De Corte (aspirant) is financially supported by the Fund for Scientific Research Flanders (FWO-Vlaanderen).

Supporting information available

A3-S1 Materials; A3-S2 LC-MS/MS analysis; A3-S3 SPE Extraction; A3-S4. Influence of derivatization agent excess; A3-S5. Relationship injection volume - isotope ratio; A3-S6. Preparative HPLC-UV; A3-S7. Relationship peak amplitude - isotope ratios; A3-S8. Dissipation kinetics and transformation products during biodegradation; A3-S9. GC-IRMS analysis of spiked river water

2.5 References

1. Salomon, M., Pharmazeutische Wirkstoffe und Umweltschutz. *UWSF - Z Umweltchem Ökotox* **2007,** *19*, (3), 155-167.
2. Heberer, T., Tracking persistent pharmaceutical residues from municipal sewage to drinking water. *J. Hydrol.* **2002,** *266*, (3-4), 175-189.
3. Radke, M.; Ulrich, H.; Wurm, C.; Kunkel, U., Dynamics and Attenuation of Acidic Pharmaceuticals along a River Stretch. *Environmental Science & Technology* **2010,** *44*, (8), 2968-2974.
4. Ternes, T. A., Occurrence of drugs in German sewage treatment plants and rivers. *Water Research* **1998,** *32*, (11), 3245-3260.
5. Daughton, C. G.; Ternes, T. A., Pharmaceuticals and personal care products in the environment: Agents of subtle change? *Environmental Health Perspectives* **1999,** *107*, 907-938.
6. Ericson, H.; Thorsén, G.; Kumblad, L., Physiological effects of diclofenac, ibuprofen and propranolol on Baltic Sea blue mussels. *Aquat. Toxicol.* **2010,** *99*, (2), 223-231.
7. Schwaiger, J.; Ferling, H.; Mallow, U.; Wintermayr, H.; Negele, R. D., Toxic effects of the non-steroidal anti-inflammatory drug diclofenac Part 1: histopathological alterations and bioaccumulation in rainbow trout. *Aquat. Toxicol.* **2004,** *68*, (2), 141-150.
8. Oaks, J. L.; Gilbert, M.; Virani, M. Z.; Watson, R. T.; Meteyer, C. U.; Rideout, B. A.; Shivaprasad, H. L.; Ahmed, S.; Chaudhry, M. J. I.; Arshad, M.; Mahmood, S.; Ali, A.; Khan, A. A., Diclofenac residues as the cause of vulture population decline in Pakistan. *Nature* **2004,** *427*, (6975), 630-633.
9. Richardson, S. D.; Ternes, T. A., Water Analysis: Emerging Contaminants and Current Issues. *Analytical Chemistry* **2011,** *83*, (12), 4614-4648.
10. Kunkel, U.; Radke, M., Reactive Tracer Test To Evaluate the Fate of Pharmaceuticals in Rivers. *Environmental Science & Technology* **2011,** *45*, (15), 6296-6302.
11. Groning, J.; Held, C.; Garten, C.; Claussnitzer, U.; Kaschabek, S. R.; Schlomann, M., Transformation of diclofenac by the indigenous microflora of river sediments and identification of a major intermediate. *Chemosphere* **2007,** *69*, (4), 509-516.
12. Stulten, D.; Zuhlke, S.; Lamshoft, M.; Spiteller, M., Occurrence of diclofenac and selected metabolites in sewage effluents. *Science of The Total Environment* **2008,** *405*, (1-3), 310-316.
13. Poiger, T.; Buser, H. R.; Muller, M. D., Photodegradation of the pharmaceutical drug diclofenac in a lake: Pathway, field measurements, and mathematical modeling. *Environ. Toxicol. Chem.* **2001,** *20*, (2), 256-263.
14. Kosjek, T.; Zigon, D.; Kralj, B.; Heath, E., The use of quadrupole-time-of-flight mass spectrometer for the elucidation of diclofenac biotransformation products in wastewater. *Journal of Chromatography A* **2008,** *1215*, (1-2), 57-63.
15. Li, Z.; Maier, M. P.; Radke, M. Screening for pharmaceutical transformation products formed in river sediment by combining ultrahigh performance liquid chromatography/high resolution mass spectrometry with a rapid data-processing method. Anal. Chim. Acta **2014**, 810, 61-70.

16. Loffler, D.; Rombke, J.; Meller, M.; Ternes, T. A., Environmental fate of pharmaceuticals in water/sediment systems. *Environmental Science & Technology* **2005,** *39*, (14), 5209-5218.

17. Lin, C.; Gu, J.-G.; Qiao, C.; Duan, S.; Gu, J.-D., Degradability of atrazine, cyanazine, and dicamba in methanogenic enrichment culture microcosms using sediment from the Pearl River of Southern China. *Biology and Fertility of Soils* **2006,** *42*, (5), 395-401.

18. Kunkel, U.; Radke, M., Biodegradation of acidic pharmaceuticals in bed sediments: Insight from a laboratory experiment. *Environmental Science & Technology* **2008,** *42*, (19), 7273-7279.

19. Thullner, M.; Centler, F.; Richnow, H.-H.; Fischer, A., Quantification of organic pollutant degradation in contaminated aquifers using compound specific stable isotope analysis: Review of recent developments. *Organic Geochemistry* **2012,** *42*, (12), 1440-1460.

20. Hofstetter, T. B.; Berg, M., Assessing transformation processes of organic contaminants by compound-specific stable isotope analysis. *TrAC Trends in Analytical Chemistry* **2011,** *30*, (4), 618-627.

21. Elsner, M.; Jochmann, M. A.; Hofstetter, T. B.; Hunkeler, D.; Bernstein, A.; Schmidt, T. C.; Schimmelmann, A., Current challenges in compound-specific stable isotope analysis of environmental organic contaminants. *Anal. Bioanal. Chem.* **2012,** *403*, (9), 2471-2491.

22. Elsner, M.; Zwank, L.; Hunkeler, D.; Schwarzenbach, R. P., A new concept linking observable stable isotope fractionation to transformation pathways of organic pollutants. *Environ. Sci. Technol.* **2005,** *39*, (18), 6896-6916.

23. Meckenstock, R. U.; Morasch, B.; Griebler, C.; Richnow, H. H., Stable isotope fractionation analysis as a tool to monitor biodegradation in contaminated acquifers. *J.Contam.Hydrol.* **2004,** *75*, (3-4), 215-255.

24. Zwank, L.; Berg, M.; Elsner, M.; Schmidt, T. C.; Schwarzenbach, R. P.; Haderlein, S. B., New evaluation scheme for two-dimensional isotope analysis to decipher biodegradation processes: application to groundwater contamination by MTBE. *Environ. Sci. Technol.* **2005,** *39*, (4), 1018-1029.

25. Penning, H.; Sorensen, S. R.; Meyer, A. H.; Aamand, J.; Elsner, M., C, N, and H Isotope Fractionation of the Herbicide Isoproturon Reflects Different Microbial Transformation Pathways. *Environ. Sci. Technol.* **2010,** *44*, (7), 2372-2378.

26. Meyer, A. H.; Penning, H.; Elsner, M., C and N isotope fractionation suggests similar mechanisms of microbial atrazine transformation despite involvement of different Enzymes (AtzA and TrzN). *Environ. Sci. Technol.* **2009,** *43*, (21), 8079-8085.

27. Reinnicke, S.; Simonsen, A.; Sørensen, S. R.; Aamand, J.; Elsner, M., C and N Isotope Fractionation during Biodegradation of the Pesticide Metabolite 2,6-Dichlorobenzamide (BAM): Potential for Environmental Assessments. *Environ. Sci. Technol.* **2012,** *46*, (3), 1447-1454.

28. De Corte, S.; Sabbe, T.; Hennebel, T.; Vanhaecke, L.; De Gusseme, B.; Verstraete, W.; Boon, N., Doping of biogenic Pd catalysts with Au enables dechlorination of diclofenac at environmental conditions. *Water Research* **2012,** *46*, (8), 2718-2726.

29. Reinnicke, S.; Bernstein, A.; Elsner, M., Small and Reproducible Isotope Effects during Methylation with Trimethylsulfonium Hydroxide (TMSH): A Convenient Derivatization Method for Isotope Analysis of Negatively Charged Molecules. *Analytical Chemistry* **2010,** *82*, (5), 2013-2019.

30. Zwiener, C.; Glauner, T.; Frimmel, F. H., Biodegradation of pharmaceutical residues investigated by SPE-GC/ITD-MS and on-line derivatization. *Hrc-Journal of High Resolution Chromatography* **2000,** *23*, (7-8), 474-478.

31. Maier, M.; Qiu, S.; Elsner, M., Enantioselective stable isotope analysis (ESIA) of polar herbicides. *Analytical and Bioanalytical Chemistry* **2013,** *405*, (9), 2825-2831.

32. Schreglmann, K.; Hoeche, M.; Steinbeiss, S.; Reinnicke, S.; Elsner, M., Carbon and nitrogen isotope analysis of atrazine and desethylatrazine at sub-microgram per liter concentrations in groundwater. *Anal. Bioanal. Chem.* **2013,** *405*, (9), 2857-2867.

33. Reinnicke, S.; Juchelka, D.; Steinbeiss, S.; Meyer, A. H.; Hilkert, A.; Elsner, M., Gas chromatography-isotope ratio mass spectrometry (GC-IRMS) of recalcitrant target compounds: performance of different combustion reactors and strategies for standardization. *Rapid. Commun. Mass. Sp.* **2012,** *26*, (9), 1053-1060.
34. Werner, R. A.; Brand, W. A., Referencing strategies and techniques in stable isotope ratio analysis. *Rapid Commun. Mass Spectrom.* **2001,** *15*, 501-519.
35. Elsner, M., Stable isotope fractionation to investigate natural transformation mechanisms of organic contaminants: principles, prospects and limitations. *J. Environ. Monit.* **2010,** *12*, (11), 2005-2031.
36. Spahr, S.; Huntscha, S.; Bolotin, J.; Maier, M. P.; Elsner, M.; Hollender, J.; Hofstetter, T. B., Compound-specific isotope analysis of benzotriazole and its derivatives. *Analytical and Bioanalytical Chemistry* **2013,** *405*, (9), 2843-2856.
37. Deconinck, E.; van Nederkassel, A. M.; Stanimirova, I.; Daszykowski, M.; Bensaid, F.; Lees, M.; Martin, G. J.; Desmurs, J. R.; Smeyers-Verbeke, J.; Heyden, Y. V., Isotopic ratios to detect infringements of patents or proprietary processes of pharmaceuticals: Two case studies. *J. Pharm. Biomed. Anal.* **2008,** *48*, (1), 27-41.
38. Wokovich, A. M.; Spencer, J. A.; Westenberger, B. J.; Buhse, L. F.; Jasper, J. P., Stable isotopic composition of the active pharmaceutical ingredient (API) naproxen. *J. Pharm. Biomed. Anal.* **2005,** *38*, (4), 781-784.
39. Krummen, M.; Hilkert, A. W.; Juchelka, D.; Duhr, A.; Schluter, H. J.; Pesch, R., A new concept for isotope ratio monitoring liquid chromatography/mass spectrometry. *Rapid Communications in Mass Spectrometry* **2004,** *18*, (19), 2260-2266.
40. Everts, S., FAKE PHARMACEUTICALS. *Chemical & Engineering News* **2010,** *88*, (1), 27-29.
41. Jasper, J. P.; Weaner, L. E.; Duffy, B. J., A preliminary multi-stable-isotopic evaluation of three synthetic pathways of Topiramate. *J. Pharm. Biomed. Anal.* **2005,** *39*, (1-2), 66-75.
42. Quintana, J. B.; Weiss, S.; Reemtsma, T., Pathways and metabolites of microbial degradation of selected acidic pharmaceutical and their occurrence in municipal wastewater treated by a membrane bioreactor. *Water Research* **2005,** *39*, (12), 2654-2664.
43. Pati, S. G.; Shin, K.; Skarpeli-Liati, M.; Bolotin, J.; Eustis, S. N.; Spain, J. C.; Hofstetter, T. B., Carbon and Nitrogen Isotope Effects Associated with the Dioxygenation of Aniline and Diphenylamine. *Environmental Science & Technology* **2012,** *46*, (21), 11844-11853.
44. Bort, R.; Macé, K.; Boobis, A.; Gómez-Lechón, M. a.-J.; Pfeifer, A.; Castell, J., Hepatic metabolism of diclofenac: role of human CYP in the minor oxidative pathways. *Biochemical Pharmacology* **1999,** *58*, (5), 787-796.
45. Guengerich, F. P.; Yun, C. H.; MacDonald, T. L., Evidence for a 1-electron oxidation mechanism in N-dealkylation of N,N-dialkylanilies by cytochrome P450 2B1. *J. Biol. Chem.* **1996,** *271*, (44), 27321-27329.
46. Shin, K. A.; Spain, J. C., Pathway and Evolutionary Implications of Diphenylamine Biodegradation by Burkholderia sp. Strain JS667. *Applied and Environmental Microbiology* **2009,** *75*, (9), 2694-2704.
47. Albers, C. N.; Banta, G. T.; Hansen, P. E.; Jacobsen, O. S., Effect of Different Humic Substances on the Fate of Diuron and Its Main Metabolite 3,4-Dichloroaniline in Soil. *Environmental Science & Technology* **2008,** *42*, (23), 8687-8691.
48. Huber, C.; Bartha, B.; Schroder, P., Metabolism of diclofenac in plants - Hydroxylation is followed by glucose conjugation. *Journal of Hazardous Materials* **2012,** *243*, 250-256.
49. Griebler, C.; Adrian, L.; Meckenstock, R. U.; Richnow, H. H., Stable carbon isotope fractionation during aerobic and anaerobic transformation of trichlorobenzene. *Fems Microbiol. Ecol.* **2004,** *48*, (3), 313-321.
50. Nijenhuis, I.; Andert, J.; Beck, K.; Kastner, M.; Diekert, G.; Richnow, H. H., Stable isotope fractionation of tetrachloroethene during reductive dechlorination by *Sulfurospirillum multivorans* and

Desulfitobacterium sp. Strain PCE-S and abiotic reactions with cyanocobalamin. *Appl. Environ. Microbiol.* **2005,** *71*, (7), 3413-3419.

51. Elsner, M.; Hofstetter Thomas, B., Current Perspectives on the Mechanisms of Chlorohydrocarbon Degradation in Subsurface Environments: Insight from Kinetics, Product Formation, Probe Molecules, and Isotope Fractionation. In *Aquatic Redox Chemistry*, American Chemical Society: 2011; Vol. 1071, pp 407-439.

52. Morasch, B.; Richnow, H. H.; Vieth, A.; Schink, B.; Meckenstock, R. U., Stable isotope fractionation caused by glycyl radical enzymes during bacterial degradation of aromatic compounds. *Applied and Environmental Microbiology* **2004,** *70*, (5), 2935-2940.

53. Zwank, L.; Elsner, M.; Aeberhard, A.; Schwarzenbach, R. P.; Haderlein, S. B., Carbon isotope fractionation in the reductive dehalogenation of carbon tetrachloride at iron (hydr)oxide and iron sulfide minerals. *Environmental Science & Technology* **2005,** *39*, (15), 5634-5641.

54. Aelion, C. M.; Hohener, P.; Hunkeler, D.; Aravena, R., *Environmental Isotopes in Bioremediation and Biodegradation*. CRC Press: 2009.

55. Andreozzi, R.; Raffaele, M.; Nicklas, P., Pharmaceuticals in STP effluents and their solar photodegradation in aquatic environment. *Chemosphere* **2003,** *50*, (10), 1319-1330.

56. Tixier, C.; Singer, H. P.; Oellers, S.; Muller, S. R., Occurrence and fate of carbamazepine, clofibric acid, diclofenac, ibuprofen, ketoprofen, and naproxen in surface waters. *Environmental Science & Technology* **2003,** *37*, (6), 1061-1068.

3

ISOTOPE FRACTIONATION OF DICLOFENAC IN ENVIRONMENTAL & ENGINEERED SYSTEMS: EVIDENCE OF DIFFERENT OXIDATION MECHANISMS

Michael P. Maier, Carsten Prasse, Sarah G. Pati, Sebastian Nitsche, Thomas Hofstetter, Thomas A. Ternes, and Martin Elsner

Submitted to Environmental Science & Technology

3.1 Abstract

Diclofenac is one of the most frequently detected pharmaceuticals in natural waters, but its environmental transformation reactions remain imperfectly understood. Compound specific isotope analysis (CSIA) has been brought forward to as a new line of evidence based on isotope effect measurements. $^{15}N/^{14}N$ ratios changed during biotransformation (ε_N= -7.1‰) whereas $^{13}C/^{12}C$ ratios changed during dechlorination. This study targets further important transformation reactions in environmental and engineered systems. Photolysis caused inverse N-isotope fractionation (ε_N= +1.9‰) and can therefore be distinguished by CSIA from biotransformation. Also transformation of diclofenac by ozone was accompanied by inverse N-isotope fractionation (ε_N= +1.5‰); here, the magnitude of fractionation could even indicate the site of O_3 attack in diclofenac. Further insight into underlying oxidation mechanisms was obtained from reactions of diclofenac with ABTS radicals – a well-established outer sphere single electron transfer (SET) oxidant – and with MnO_2 – an oxidant with unknown mechanism.. While inverse nitrogen isotope fractionation (ε_N= +3.8‰) with ABTS radicals confirmed the SET mechanism, normal isotope fractionation with MnO_2 (ε_N= -7.3‰) indicated that a different reaction chemistry was at work. The similarity of nitrogen isotope effects in biodegradation and with MnO_2 may indicate a possible common pathway for which first evidence is given by CSIA.

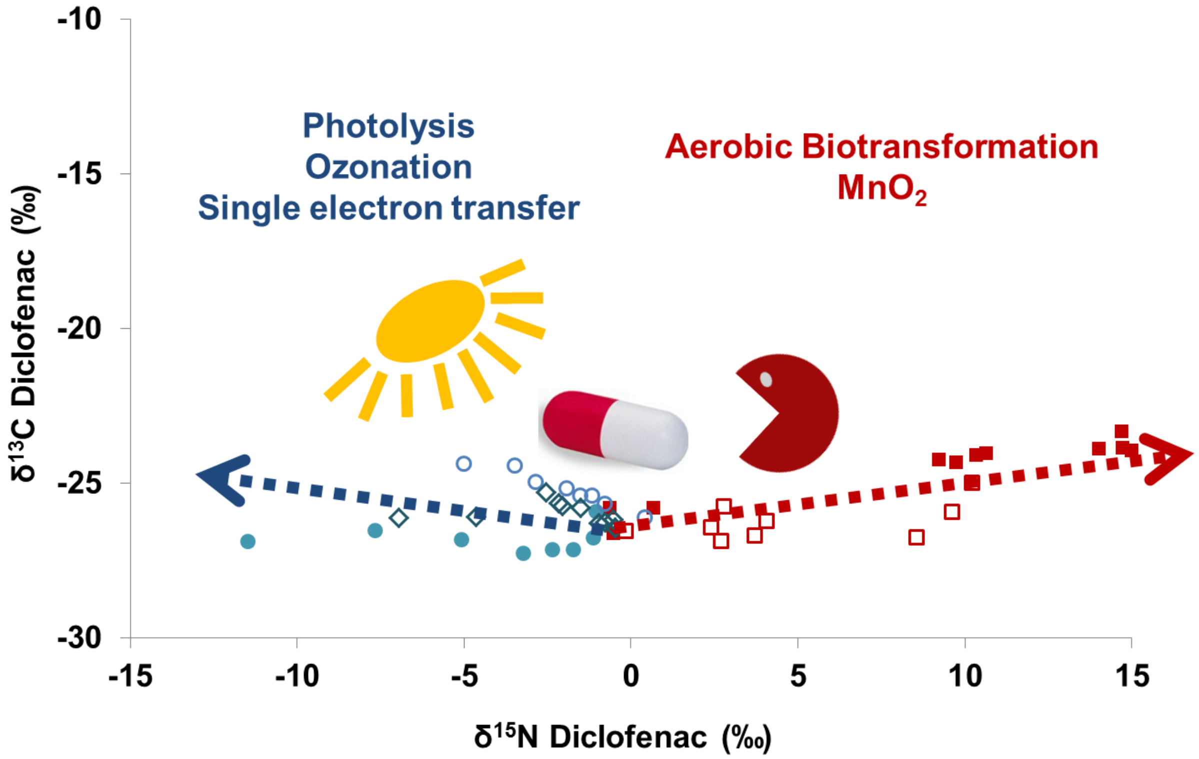

3.2 Introduction

Pharmaceuticals are used world-wide in large amounts and end up in wastewater treatment plants due to incomplete metabolization in the human body.[1, 2] The failure to remove diclofenac in wastewater treatment plants leads to a continuous emission and a steady-state exposure in rivers, surface and even ground water.[3-5] Consequently, the self-cleaning potential of aquatic ecosystems is of great interest. Even though transformation processes can be simulated in the laboratory systems including the identification of transformation products (TPs) via (high resolution) mass spectrometry and NMR, the natural transformation of many pharmaceuticals remains is not fully understood for the following reasons.[6-10] (i) In contrast to laboratory experiments, transformation in natural systems is difficult to quantify due to incomplete mass balances; (ii) transformation mechanisms are typically elusive; (iii) detectable TPs often account only for a fraction of the mass balance and the same TP can be formed by different reaction pathways (Fig. 3-1).

A prominent example is the anti-inflammatory diclofenac, one of the most widely used pharmaceuticals[11] and most frequently detected ones in the environment.[3, 12] In laboratory studies diclofenac is efficiently transformed by (sun-) light within hours.[13-16] However, it takes days to observe pronounced transformation in water/sediment batch studies.[13, 17, 18] In the case of limited sunlight availability,, phototransformation may not be the dominant way of diclofenac transformation, [14, 15] while biotransformation rates can more than double if the exchange between the water body and the hyporheic zone is increased.[19] Unfortunately, the processes that govern diclofenac transformation in the environment are still not elucidated. While TPs provide a direct evidence for transformation, their detection is challenging due to further transformation,[9, 20, 21] adsorption to humic substances[22, 23] and by lack of adequate analytical methodologies. Moreover, the lack of commercial standards often impedes a quantitative determination of TPs.[24] For example, several studies have reported the detection of hydroxylated diclofenac in laboratory experiments (Fig. 3-1 (6, 7)).[9, 10, 17, 20] Among these studies, only one has provided quantitative data for hydroxylated diclofenac, showing that it only accounts for a few percent of diclofenac transformation.[17] Therefore, there is need for a supplementary technique which does not rely on the identification and the determination of TPs, but which can nonetheless provide information on transformation processes in the environment.

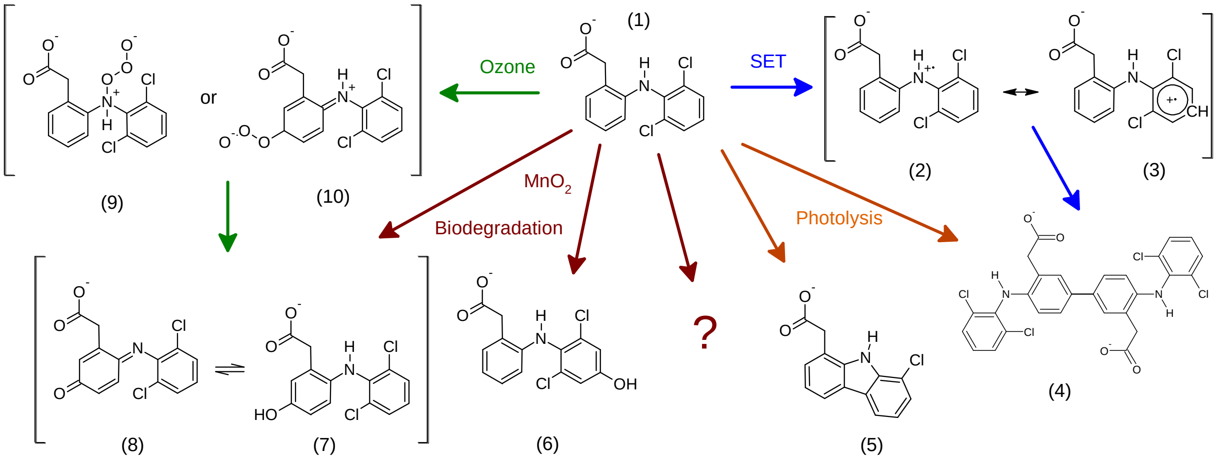

Fig.3-1. Transformation pathways of diclofenac during single electron oxidation (SET) by ABTS (2-4), photolysis[13, 25] *(4,5), ozonation*[26, 27] *(7-10) oxidation by MnO*$_2$*-*[28] *and biotransformation*[9, 17] *(6-8); TP 4-8 were also detected in this study*

Very recently compound specific isotope analysis (CSIA) has been brought forward to provide such an independent line of evidence for the transformation of diclofenac.[17] This technique analyzes the stable isotope ratios of C and N of diclofenac at natural abundance (^{13}C/^{12}C, ^{15}N/^{14}N) and detects transformation reactions by a shift in isotope ratios during transformation.[29-31] For example, biotransformation of diclofenac by river sediment was found to be by 7.1‰ slower with ^{15}N- than with ^{14}N-containing molecules (ε_N = -7.1‰) leading to progressively higher ^{15}N/^{14}N ratios in the remaining diclofenac during transformation.[17] Because this line of evidence relies on different isotopologue-specific rates in the *parent* rather than the *daughter* compound, transformation can be studied by CSIA of diclofenac without the explicit need to detect potential TPs.[32] In a second experiment targeting reductive dehalogenation of diclofenac, a similar trend was observed for ^{13}C/^{12}C ratios in diclofenac (ε_C = -2.0‰), whereas no changes in ^{15}N/^{14}N were found. These results demonstrate that CSIA delivers information on two levels. On a descriptive level, C and N isotope analysis of diclofenac can be used to simply detect oxidative and reductive transformation.[17] On a mechanistic level, isotope fractionation also allows exploring underlying transformation mechanisms, since – ultimately – isotope effects are caused by differences in transition states.[32, 33] While our recent study, therefore, highlighted the potential of CSIA, it also brought up new questions. On the one hand, there is the pragmatic interest if CSIA can track other environmentally relevant transformation pathways such as photolysis. On the other hand, there is a mechanistic interest in the observed aerobic biotransformation. How does its mechanism compare with oxidation reactions in other environmental and engineered systems? Is N-isotope fractionation during biotransformation related to the formation of hydroxylated diclofenac or does it indicate an additional transformation pathway that was so far overlooked in TP analysis?

The present study explored whether CSIA can track and even distinguish environmentally relevant transformation processes of diclofenac. To this end four additional processes were investigated. Photolysis was studied, because it may be an important elimination process in surface waters and in (waste-) water treatment. Isotope fractionation during ozonation was investigated, since it is a key technique to eliminate diclofenac in wastewater treatment plants and waterworks. Further oxidations of diclofenac were studied with MnO_2 as an environmentally relevant mineral phase and with electrochemically oxidized ABTS as an oxidative outer sphere single-electron transfer reagent.[28, 34]

3.3 MATERIALS AND METHODS

3.3.1 Chemicals

A complete list of chemicals used in this study can be found in the supporting information (A4-S1).

3.3.2 Phototransformation

Quartz glass tubes (39 cm long, 4.5 cm in diameter) were filled with 700 mL Millipore water or river water (sampled from Isar river, Germany) spiked with diclofenac (C_0 = 100 mg L^{-1}) and were exposed to sunlight from 9 a.m. to 8 p.m. on a sunny summer day (latitude 48.22° N). Samples were taken at different time points and separated for concentration and isotope analysis. For concentration and TP analysis (using LC-MS/MS) 100 µL sample aliquots were mixed with 800 µL Millipore water and 100 µL internal standard ($^{13}C_6$-diclofenac, c = 25 mg L^{-1}, in methanol) and filtered with a PTFE filter (0.22 µm). For GC-IRMS analysis larger sample volumes were taken (10-60 mL) and extracted three times with dichloromethane after addition of HCl (C_{total} ~ 0.05 M). The dichloromethane extract was evaporated to dryness and samples were methylated by BF_3/methanol as described previously.[17]

3.3.3 Ozonation

Groundwater (DOC ~ 1.5 mg L^{-1}) was spiked with diclofenac (C_0 = 30 mg L^{-1}) and different amounts of ozone to obtain O_3-diclofenac ratios between 1:7.5 and 10:1. Aqueous stock solution of ozone (approx. 1 mM) was prepared by sparging ozone-containing oxygen through deionized water cooled in an ice-bath. Ozone was generated from an O_3-geneator (Ozon generator 300, Fischer Technology, Germany). To exclude the influence of OH-radicals, duplicate experiments were also performed in the presence of *tert*-butanol (100 mM) as radical scavenger. Samples were prepared as described above for the phototransformation experiment, except that those for GC-IRMS analysis (240 mL) were freeze-dried prior to liquid-liquid extraction.

3.3.4 Oxidation by MnO_2

An MnO_2 stock solution was synthesized according to Murray et al.[35] and oxidation of diclofenac by MnO_2 was accomplished in analogy to Forrez et al.[36]. Briefly, 900 mL Millipore water were mixed with 8 mL of NaOH (1 M) and 40 mL of $NaMnO_4$ (0.1 M) under constant sparging with N_2. 60 mL of $MnCl_2$ (0.1 M) were added dropwise under continuous stirring. MnO_2 particles were allowed to settle and the supernatant was replaced by de-ionized water until the electric conductivity of the solution was below 3 µS cm^{-1}. This stock solution (final volume 1 L) was stored at 7 °C and used within one week. Diclofenac oxidation was initiated by adding 100 mL of MnO_2 stock solution to 900 mL diclofenac solution (50 mg L^{-1}, pH 6.2, 10 mM NaH_2PO_4 / Na_2HPO_4) under continuous stirring. Samples for concentration and isotope analysis (10-60 mL) were prepared as described for the phototransformation experiment, with the exception that MnO_2 particles were dissolved by addition of 20% ascorbic acid (v/v, 20 mM, pH 11) prior to filtration or extraction.

3.3.5 Single electron transfer by ABTS

Oxidation of diclofenac by ABTS was performed in an anoxic glovebox using anoxic stock and buffer solutions as described previously.[37] $ABTS^{\bullet -}$ was generated by direct electrochemical oxidation of $ABTS^{2-}$ (0.5 mM, pH 6.2, 0.1 M KH_2PO_4, 0.1 M NaCl) at a potential of 0.79 V (SHE) in an electrolysis cell described by Aeschbacher et al.[38]. The working current was monitored until a stable background value was reached. Variable amounts of $ABTS^{\bullet -}$ (0-245 µM) were immediately added to amber glass vials containing buffered diclofenac solution (30 mg L^{-1}, pH 6.2, 0.1 M KH_2PO_4, 0.1 M NaCl) resulting in different degrees of diclofenac oxidation in each of the 30 mL samples. Samples for concentration and isotope analysis (30 mL) were taken and prepared as described for the phototransformation experiment, except that no HCl was added during DCM extraction. This HCl addition had no influence on the complete extraction of diclofenac from the aqueous phase (recovery rate ~100%).

3.3.6 Detection methods

Concentrations of diclofenac, 4'OH-diclofenac, and phototransformation products were determined by LC-MS/MS (Agilent 1200 binary pump coupled to an ABSciex API 2000 Q-TRAP mass spectrometer, see also Supporting Information A4-S2). Samples from experiments with O_3, ABTS and MnO_2 were monitored for TPs using a Hybrid Linear Ion Trap-Orbitrap Mass Spectrometer (LTQ Orbitrap Velos, Thermo Scientific, Bremen, Germany) coupled to a liquid chromatography system (Accela pump and autosampler from Thermo Scientific). Full scan experiments were performed in positive electrospray ionization (ESI) and atmospheric pressure chemical ionization (APCI) mode using a mass range of 60-600 m/z. Data-dependent acquisition was used to obtain further information of the fragment ions. For this, full-scan experiments were followed by MS^2 and MS^3 scans for the two most intense ions. An external calibration was performed prior to the analysis of each batch to ensure accurate mass determinations with a resolution of (m/z)/Δ(m/z) = 60,000. A mixture of n-butylamine, caffeine, and Ultramark 1621 (mixture of fluorinated phosphazines) was used for mass calibration. The mass accuracy was always within 0.5 ppm.[39]

Isotope ratios of diclofenac were analyzed by GC-IRMS as described previously.[17] Briefly, methylated samples (in hexane) were either injected with a split ratio of 1:10 or splitless into a split/splitless injector (Thermo Fisher Scientific, Milan, Italy) at 280 °C with a flow rate of 1.4 mL min^{-1}. Separation was achieved by a gas chromatograph (TRACE GC Ultra gas chromatograph, Thermo Fisher Scientific, Milan, Italy) equipped with a DB-5 column (30 m × 0.25 mm, 1 µm film thickness, J&W Scientific, Folsom, Canada). The GC temperature was ramped from 80 °C (1 min) to 200 °C with a rate of 17 °C min^{-1} and then at 6 °C min^{-1} to 300 °C (held for 2 min). After chromatographic separation diclofenac was combusted in a Finnigan GC combustion interface (Thermo Fisher Scientific, Bremen, Germany) to CO_2 and N_2 with a NiO tube / CuO-NiO reactor operated at 1000 °C (Thermo Fisher Scientific, Bremen, Germany). Isotope values of CO_2 and N_2 were determined with a Finnigan MAT 253 isotope ratio mass spectrometer (Thermo Fisher Scientific, Bremen, Germany). For quality control, a diclofenac lab standard with known isotopic signature was analyzed in the same way as the samples at least every ninth injection. All reported isotope values were corrected to international reference materials, Vienna PeeDee Belemnite for carbon (Eq. 3-1) and air for nitrogen isotopes (Eq. 3-2).[40] $\delta^{13}C$ values were additionally corrected for the introduced methyl-group.[17]

$$\delta^{13}C = \frac{\left({}^{13}C/{}^{12}C_{Sample} - {}^{13}C/{}^{12}C_{Reference}\right)}{{}^{13}C/{}^{12}C_{Reference}} \tag{3-1}$$

$$\delta^{15}N = \frac{\left({}^{15}N/{}^{14}N_{Sample} - {}^{15}N/{}^{14}N_{Reference}\right)}{{}^{15}N/{}^{14}N_{Reference}} \tag{3-2}$$

3.3.7 Isotope analysis to evaluate (competing) transformation mechanisms

Isotope ratios of a micropollutant (R_t, R_0) are directly correlated to the extent of transformation (C_t/C_0) by the enrichment factor ε (Eq. 3-3).[32] If two processes compete with each other, e.g. biotransformation and phototransformation, the overall isotope enrichment (ε_{total}) depends on the first-order kinetic constants (k_{Photo}, k_{Bio}) and the enrichment factor (ε_{Photo}, ε_{Bio}) of both transformation pathways (Eq. 3-4).[41] In return, the share of one pathway (e.g. F_{Bio}) can be calculated if ε_{total} is determined and ε_{Bio} and ε_{Photo} are known from separate experiments (Eq. 3-5).[42]

$$ln\left(\frac{R_t}{R_0}\right) = \varepsilon \times ln\left(\frac{C_t}{C_0}\right) \tag{3-3}$$

$$\varepsilon_{total} = \varepsilon_{Photo} \times \frac{k_{Photo}}{k_{Photo} + k_{Bio}} + \varepsilon_{Bio} \times \frac{k_{Bio}}{k_{Photo} + k_{Bio}} \tag{3-4}$$

$$F_{Bio} = \frac{k_{Bio}}{k_{Photo} + k_{Bio}} = \frac{\varepsilon_{total} - \varepsilon_{Bio}}{\varepsilon_{Bio} - \varepsilon_{Photo}} \tag{3-5}$$

3.4 Results & Discussion

3.4.1 Phototransformation

Phototransformation can rapidly eliminate diclofenac. We tested if its relevance can directly be assessed by CSIA and if it can be distinguished from biotransformation. C and N isotope ratios of diclofenac were analyzed during sunlight-induced photolysis in ultrapure and river water. The half-life time of diclofenac was 2.4 ± 0.03 h in Isar river water and 2.8 ± 0.1 h in ultrapure water, which is consistent with half-lives reported in the literature.[13-16] We also detected known photolysis TPs, including 8-chlorocarbazole-1-acetic acid, which is formed by HCl elimination (Fig. 3-1. (5), supporting information A4-S3).[21, 43]

Isotope fractionation during photolysis of diclofenac was consistent for both types of water (ultra pure water: $\varepsilon_C = +1.1 \pm 0.1‰$, $\varepsilon_N = +2.0 \pm 0.1‰$; river water $\varepsilon_C = +0.7 \pm 0.1‰$, $\varepsilon_N = +1.9 \pm 0.1‰$). (Fig. 3-2, Tab. 3-1). An inverse N-isotope effect of diclofenac qualitatively agrees with the direct photolysis of atrazine, where an inverse effect was also observed ($\varepsilon_N = +4.9‰$).[44] As discussed by Hartenbach et al.[44] interpretation of isotope fractionation during photo-excitation is difficult. However, a secondary N-isotope effect appears plausible, because photo-excitation affects the N-atom as part of the π-system of diclofenac. Although further research is needed to investigate the underlying mechanism, Fig. 3-2 shows that bio- and phototransformation can be distinguished by isotope analysis of diclofenac. Consequently, CSIA can be used to investigate simultaneous bio- and phototransformation of diclofenac in rivers independent of boundary conditions and the detection of meta-stable TPs (Fig. 3-1 (5), supporting information A4-S3).[21]

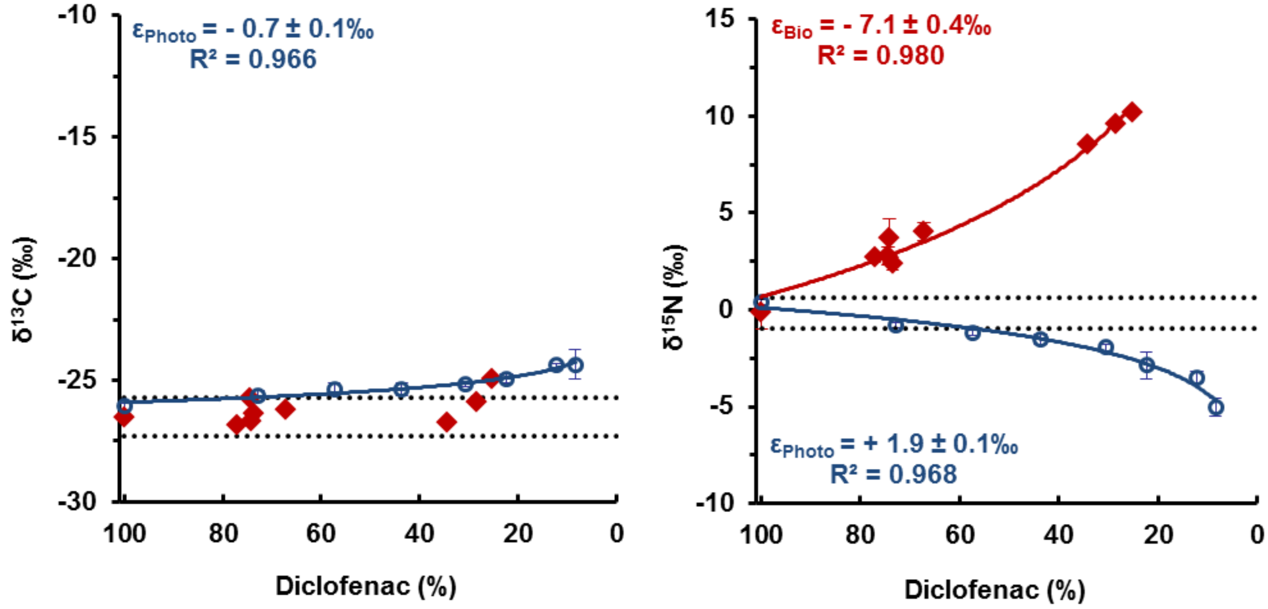

Fig. 3-2. Carbon (left) and nitrogen (right) isotope fractionation of diclofenac during photolysis in river water (this study, blues circles) and biotransformation in a river water/sediment-system (adopted from Maier et al.,[17] *red diamonds) from the same river; the dashed line represents the isotope ratio of diclofenac at* t_0 *± 2σ.*

3.4.2 Ozonation

An inverse N-isotope fractionation (ε_N = +1.5 ± 0.2‰) was observed during diclofenac ozonation together with the formation of diclofenac-2,5-iminoquinone (Fig. 3-1 (8)) and some hydroxylated TPs (Fig. 3-3, Tab. 1, supporting information A4-S4).[27, 45, 46] The direction and magnitude of isotope fractionation can be rationalized when considering possible reaction mechanisms. Two sites have been suggested for the initial attack of ozone in diclofenac. An attack at the N-atom would lead to a cationic intermediate (Fig. 3-1 (9)). Alternatively, an attack at the para-position of the non-chlorinated aromatic ring would increase the double bond character of the C-N bond as partial imine bond as shown in Fig. 3-1 (10).[37] In both cases, the bond stiffness of N is increased in the transition state which usually leads to an inverse isotope effect.[26, 27, 47] However, a direct attack at the N-atom would probably cause a primary N-isotope effect of greater magnitude. Therefore, a secondary isotope effect caused by attack at the distant para position (Fig. 3-1 (10)) appears to be more consistent with the observed, small inverse nitrogen isotope fractionation. The second mechanistic scenario is corroborated by the pathway of aniline ozonation which has been inferred from detected TPs.[27]

A further possibility involves the reaction with hydroxyl radicals generated from ozone. This reaction represent the major breakdown path during ozonation for a number of persistent pollutants.[45] However, reactions of hydroxyl radical with diclofenac can be excluded for two reasons. (1) A comparison of the pseudo-first order constants of reactions with ozone and hydroxyl radical indicates that reaction with ozone are expected to be 10^5 times faster: $k_{OH}' = 7.5 \times 10^{-3}\ s^{-1}$ versus $k_{O3}' = 10^3\ s^{-1}$ (supporting Information A4-S5). [27,48] (2) In a second experiment hydroxyl radicals were quenched with the radical scavenger tert-butanol.[26] As shown previously, less O_3 was needed to transform diclofenac but isotope fractionation showed no significant difference compared to the experiment without the radical scavenger (Fig. 3-3). Hence, isotope fractionation is clearly attributable to the reaction of diclofenac with ozone. For the first time, we demonstrated that ozonation can be tracked by a small, but significant, inverse nitrogen isotope effect. Our findings may not only be important for diclofenac but could give a first indication on the isotope fractionation of other contaminants, because many micropollutants contain aniline moieties.

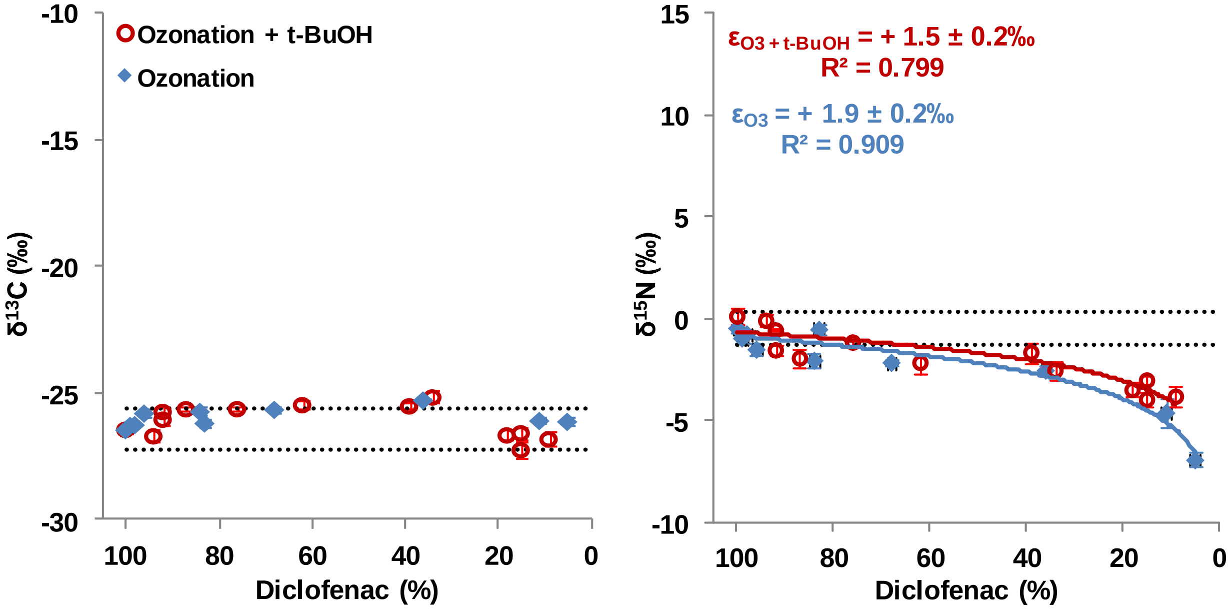

Fig. 3-3. Carbon (left) and nitrogen (right) isotope fractionation of diclofenac during ozonation with and without the hydroxyl radical scavenger tert-butanol (t-BuOH); the dashed line represents the initial isotope ratio of diclofenac ± 2σ.

3.4.3 Insights into oxidation mechanisms – ABTS & MnO_2

In a recent study[17] we investigated aerobic biodegradation of diclofenac in river sediment. Observed changes in $^{15}N/^{14}N$ ratios were opposite to the trends measured during photodegradation or ozonation

(Figure 3-1): they showed a strong, normal nitrogen isotope fractionation. Intriguingly, analysis of transformation products was unable to elucidate the underlying biotransformation pathway. The products that were detected showed a ring hydroxylation distant to the N atom which cannot explain the pronounced normal nitrogen isotope effects (Fig. 3-1 (6)).[17] Oxidative single electron transfer (SET) is frequently proposed as a putative reaction mechanism in aerobic biodegradation.[49-51] Therefore, we compared isotope fractionation during aerobic biotransformation of diclofenac with two systems for which SET was suggested previously. [28, 34]

The reaction of diclofenac with electrochemically generated ABTS radicals was studied as a well-established outer-sphere SET reagent that has previously been used to investigate SET of amines by N-isotope analysis.[34] During transformation of diclofenac by ABTS no changes in carbon isotope ratios, but pronounced *inverse* N-isotope fractionation was measured (ε_N = +5.7 ± 0.3‰). These results agree with literature data for *p*-CH_3-aniline at pH 7 where also an inverse effect N-isotope effect of ε_N = +3.8‰ was observed with ABTS.[52] In addition, we detected TPs indicative of radical coupling which typically indicates an initial one electron abstraction (Fig. 3-1 (4), supporting information A4-S6).[37]

In reaction with MnO_2, SET has also been proposed to occur, but in addition hydroxy-diclofenac and its corresponding quinone derivative have been reported, in analogy to the product we observed during biotransformation (Fig. 3-1 (7, 8)).[17] As observed previously, diclofenac transformation by MnO_2 followed a biphasic kinetics in our experiment accompanied by the formation of hydroxylated diclofenac and its corresponding quinone (A4-S4, A4-S7).[36] Because 75% of diclofenac was transformed within 10 min and the solution contained only chemicals in deionised water, a biological transformation can be ruled out. Diclofenac oxidation by MnO_2 showed small, but significant, C-isotope fractionation (ε_C = -1.5 ± 0.1‰) and pronounced *normal* N-isotope fractionation (ε_N = -7.3 ± 0.3‰). These enrichment factors are in good agreement with previously published data for the MnO_2 catalyzed oxidation of diphenylamine which has the same molecular backbone as diclofenac (ε_C = -2.3‰, ε_N = -10.0‰).[52] However, the normal N-isotope effect during the reaction with MnO_2 is in contrast to the inverse isotope fractionation during SET with ABTS. At the same time, the MnO_2 data fit well with the N-isotope enrichment of diclofenac in oxic river sediment (ε_N = -7.1‰).[17]

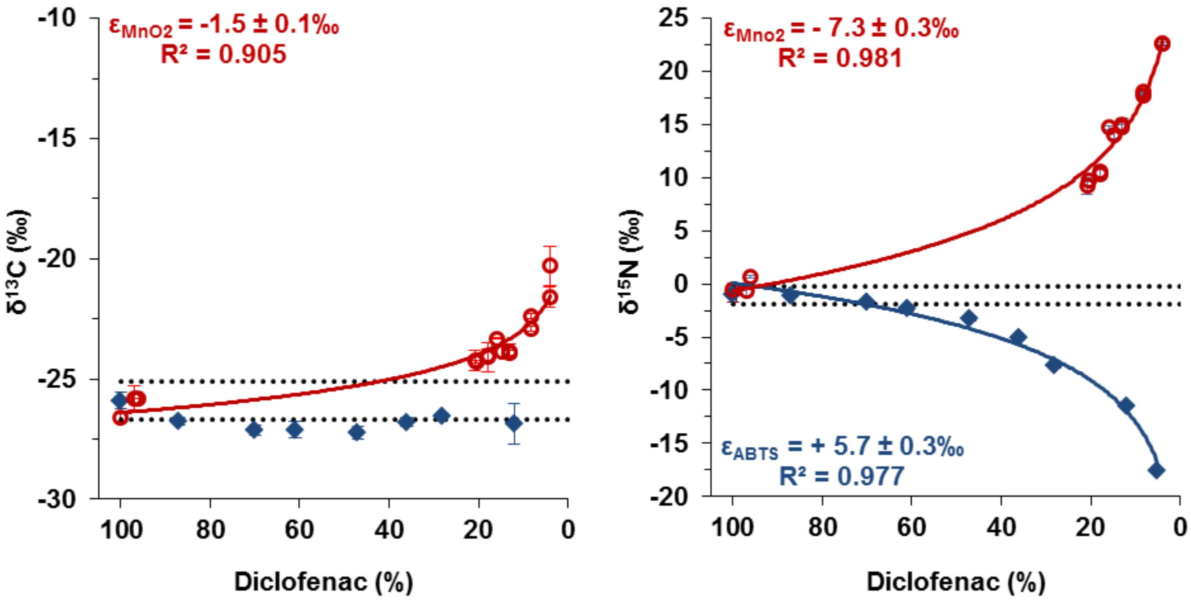

Fig. 3-4.Carbon (left) and nitrogen (right) isotope fractionation of diclofenac during transformation by MnO_2 (red circles) and ABTS (blue diamonds); the dashed line represents the isotope ratio of diclofenac at t_0± 2σ

These findings confirm that oxidation with ABTS occurs via SET which is supported by the detection of coupling TPs in experiments with ABTS. This mechanism is backed up by calculations that predict an inverse N-effect for SET.[52] Thus, we conclude that oxidation with ABTS is a good model system for outer-sphere SET, which implies that for biotransformation and oxidation by MnO_2 of diclofenac and diphenylamine an outer-sphere SET mechanism can be excluded.[52] Moreover, it appears unlikely that the formation of small amounts of mono-hydroxylated diclofenac (see supporting information A4-S7) caused the pronounced N-isotope fractionation of ε_N = -7‰ during biotic- and MnO_2 transformation of diclofenac. This is supported by recent results for benzotriazole which showed that even if an aromatic amine is exclusively transformed via hydroxylation the maximum enrichment is ε_N = -3‰.[53] Hence, we conclude that diclofenac is transformed by an unknown oxidation reaction involving the nitrogen atom, which cannot be detected by TPs, but by N-isotope fractionation.

*Tab. 3-1 Enrichments factors for diclofenac; *adopted from Maier et al.[17]; n.s. = not significant;*

System	**ε_C (‰)**	**ε_N (‰)**
ABTS	n.s.	+5.7 ± 0.3
MnO_2	-1.5 ± 0.1	-7.3 ± 0.3
Biodegradation*	n.s. (-0.7 ± 0.3)	-7.1 ± 0.4
Catalyzed Dechlorination*	-2.0 ± 0.1	n.s.
Photodegradation in ultrapure water	-1.1 ± 0.1	+2.0 ± 0.1
Photodegradation in river water	-0.7 ± 0.1	+1.9 ± 0.1
Ozonation, radical scavenger added	n.s.	+1.5 ± 0.2
Ozonation, low DOC (1.5 mg L^{-1})	n.s.	+1.9 ± 0.2

3.4.4 Environmental Significance

This study highlights the ability of CSIA to track and distinguish reaction pathways by revealing the variability of isotope fractionation in four different model reactions. N-isotope fractionation was highly reaction-specific and could, therefore, serve as a sensitive measure to identify transformation pathways of diclofenac in the environment. Since all investigated pathways showed minor or no C-isotope fractionation, this can be seen as a weak and non-specific indicator for transformation (Tab. 3-1). Hence, we provide a one-dimensional scheme for N-isotope fractionation in Fig. 5, instead of the common dual isotope plot that is plotted in the Abstract Art.

Fig. 3-5 illustrates the ability of N-CSIA to distinguish photo- and biotransformation. Both are supposed to be the most important sinks of diclofenac in the environment and CSIA can be used to investigate their relative importance. In the case that CSIA is applied as only measure for transformation, it can qualitatively distinguish photo- from biotransformation in cases where pronounced transformation occurs. If $^{15}N/^{14}N$ ratios increase, biotransformation is more important than phototransformation and vice versa in the case of $^{14}N/^{15}N$ increase. If the overall extent of transformation (C_t/C_0 of Equation 3) can in addition be determined by independent means (e.g., the combination of conservative tracers and concentration measurements),[15, 54] $\varepsilon_{N,total}$ can even be calculated, and the share of biotransformation can then directly be deduced from Fig. 5 and Eq. 5. This approach can also be used to compare the efficiency of UV-treatment and biotransformation during (waste-) water treatment.

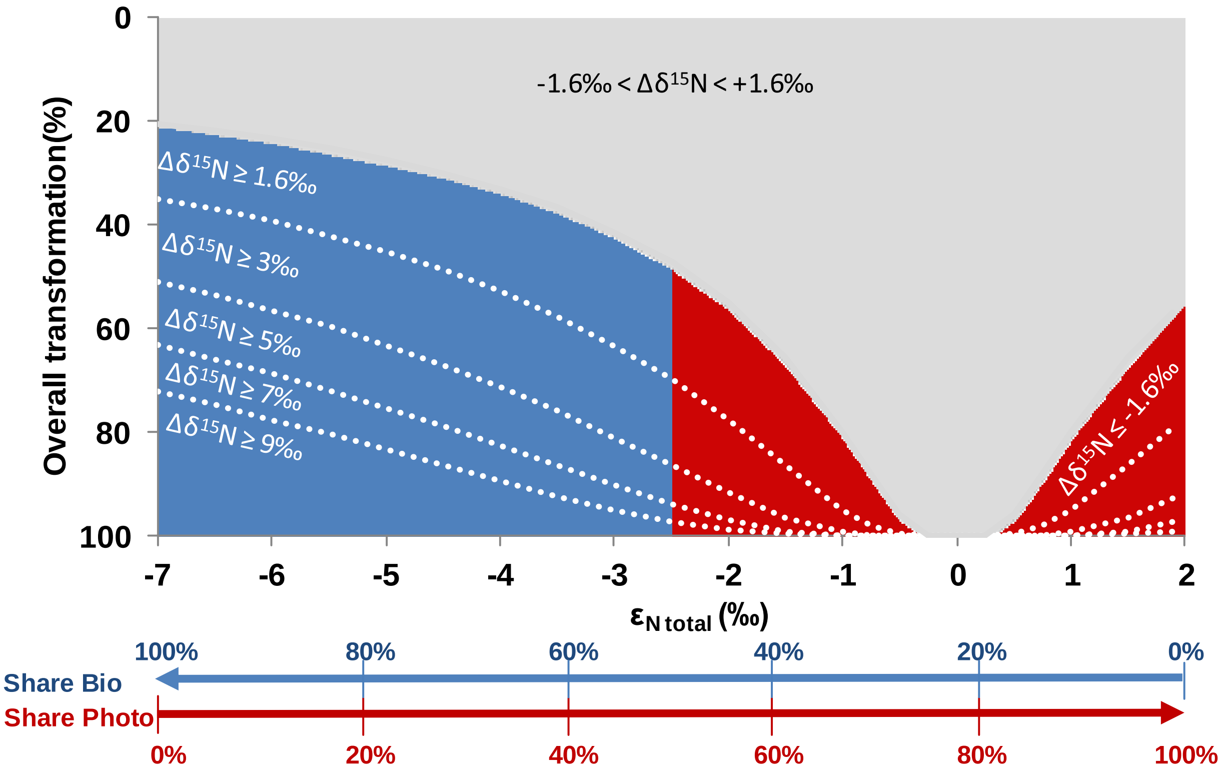

Fig. 3-5. Nitrogen isotope enrichment factors ($\varepsilon_{N,total}$) reflect the share of biotic- and photolytic transformation if both processes occur in parallel according to Eq. 3-4 (with $\varepsilon_{N,,Bio}$ = -7.1‰ vs. $\varepsilon_{N,,Photo}$ = +1.9‰); the blue and red area indicate the extent of transformation where isotope analysis is a stand-alone proof for transformation ($\Delta\delta^{15}N \geq 1.6$‰ = 4σ)

Moreover, the ability of CSIA to detect diclofenac transformation by MnO_2 is not only important for mechanistic studies with synthesized MnO_2. CSIA can also be used to detect the transformation potential of natural manganese oxides which are ubiquitously present in the environment and that were recently shown to have able to transform diclofenac.[23]

This study underlines that CSIA and TP analysis nicely complement to each other. TP analysis is important to be aware of toxic or persistent TPs and if TPs are specific for a certain reaction, they can also indicate transformation pathways. However, the mass balance between reactant and TP(s) is usually not closed when micropollutants are transformed in the environment and it is unclear if the relevant TP(s) are detected. Here, CSIA can provide an independent line of evidence and indicate if the detected TPs agree with the observed isotope fractionation, as shown for transformation of diclofenac by oxidative SET. In return, if important transformation pathways are not detectable by TP analysis, CSIA may jump in, as shown for MnO_2- and biotransformation of diclofenac.

3.4.5 Acknowledgements

We acknowledge Jan Funke for assistance with the ozonation experiments and Uwe Kunkel for his help during TP search. Michael Maier was financially supported by the German Federal Environmental Foundation (DBU).

Supporting information available

S1 Materials; S2 LC-MS/MS analysis; S3 Detection of TPs during Phototransformation; S4 Formation of diclofenac-2,5-iminoquinone in the presence of O_3, ABTS or MnO_2; S5 Calculation of pseudo-first order constants of hydroxyl radicals S6 Detection of coupling TPs during transformation by ABTS; S7 Detection of OH-diclofenac during MnO_2 transformation

3.4.6 References

1. Bort, R.; Macé, K.; Boobis, A.; Gómez-Lechón, M. a.-J.; Pfeifer, A.; Castell, J., Hepatic metabolism of diclofenac: role of human CYP in the minor oxidative pathways. *Biochemical Pharmacology* **1999,** *58*, (5), 787-796.
2. Ternes, T. A., Occurrence of drugs in German sewage treatment plants and rivers. *Water Research* **1998,** *32*, (11), 3245-3260.
3. Loos, R.; Gawlik, B. M.; Locoro, G.; Rimaviciute, E.; Contini, S.; Bidoglio, G., EU-wide survey of polar organic persistent pollutants in European river waters. *Environmental Pollution* **2009,** *157*, (2), 561-568.
4. Daughton, C. G.; Ternes, T. A., Pharmaceuticals and personal care products in the environment: Agents of subtle change? *Environmental Health Perspectives* **1999,** *107*, 907-938.
5. Heberer, T., Tracking persistent pharmaceutical residues from municipal sewage to drinking water. *J. Hydrol.* **2002,** *266*, (3-4), 175-189.
6. Helbling, D. E.; Hollender, J.; Kohler, H. P. E.; Singer, H.; Fenner, K., High-Throughput Identification of Microbial Transformation Products of Organic Micropollutants. *Environmental Science & Technology* **2010,** *44*, (17), 6621-6627.
7. Loffler, D.; Rombke, J.; Meller, M.; Ternes, T. A., Environmental fate of pharmaceuticals in water/sediment systems. *Environmental Science & Technology* **2005,** *39*, (14), 5209-5218.
8. Kern, S.; Fenner, K.; Singer, H. P.; Schwarzenbach, R. P.; Hollender, J., Identification of transformation products of organic contaminants in natural waters by computer-aided prediction and high-resolution mass spectrometry. *Environ. Sci. Technol.* **2009,** *43*, (18), 7039-7046.
9. Li, Z.; Maier, M. P.; Radke, M., Screening for pharmaceutical transformation products formed in river sediment by combining ultrahigh performance liquid chromatography/high resolution mass spectrometry with a rapid data-processing method. *Analytica Chimica Acta* **2014,** *810*, 61-70.
10. Kosjek, T.; Zigon, D.; Kralj, B.; Heath, E., The use of quadrupole-time-of-flight mass spectrometer for the elucidation of diclofenac biotransformation products in wastewater. *Journal of Chromatography A* **2008,** *1215*, (1-2), 57-63.
11. McGettigan, P.; Henry, D., Use of Non-Steroidal Anti-Inflammatory Drugs That Elevate Cardiovascular Risk: An Examination of Sales and Essential Medicines Lists in Low-, Middle-, and High-Income Countries. *Plos Medicine* **2013,** *10*, (2).

12. Pal, A.; Gin, K. Y.-H.; Lin, A. Y.-C.; Reinhard, M., Impacts of emerging organic contaminants on freshwater resources: Review of recent occurrences, sources, fate and effects. *Science of The Total Environment* **2010,** *408*, (24), 6062-6069.
13. Buser, H.-R.; Poiger, T.; Müller, M. D., Occurrence and Fate of the Pharmaceutical Drug Diclofenac in Surface Waters: Rapid Photodegradation in a Lake. *Environmental Science & Technology* **1998,** *32*, (22), 3449-3456.
14. Bartels, P.; von Tumpling, W., Solar radiation influence on the decomposition process of diclofenac in surface waters. *Science of the Total Environment* **2007,** *374*, (1), 143-155.
15. Radke, M.; Ulrich, H.; Wurm, C.; Kunkel, U., Dynamics and Attenuation of Acidic Pharmaceuticals along a River Stretch. *Environmental Science & Technology* **2010,** *44*, (8), 2968-2974.
16. Andreozzi, R.; Raffaele, M.; Nicklas, P., Pharmaceuticals in STP effluents and their solar photodegradation in aquatic environment. *Chemosphere* **2003,** *50*, (10), 1319-1330.
17. Maier, M. P.; De Corte, S.; Nitsche, S.; Spaett, T.; Boon, N.; Elsner, M., C & N Isotope Analysis of Diclofenac to Distinguish Oxidative and Reductive Transformation and to Track Commercial Products. *Environmental Science & Technology* **2014,** *48*, (4), 2312-2320.
18. Radke, M.; Maier, M. P., Lessons learned from water/sediment-testing of pharmaceuticals. *Water Research* **2014,** *55*, (0), 63-73.
19. Kunkel, U.; Radke, M., Biodegradation of acidic pharmaceuticals in bed sediments: Insight from a laboratory experiment. *Environmental Science & Technology* **2008,** *42*, (19), 7273-7279.
20. Groning, J.; Held, C.; Garten, C.; Claussnitzer, U.; Kaschabek, S. R.; Schlomann, M., Transformation of diclofenac by the indigenous microflora of river sediments and identification of a major intermediate. *Chemosphere* **2007,** *69*, (4), 509-516.
21. Poiger, T.; Buser, H. R.; Muller, M. D., Photodegradation of the pharmaceutical drug diclofenac in a lake: Pathway, field measurements, and mathematical modeling. *Environ. Toxicol. Chem.* **2001,** *20*, (2), 256-263.
22. Albers, C. N.; Banta, G. T.; Hansen, P. E.; Jacobsen, O. S., Effect of Different Humic Substances on the Fate of Diuron and Its Main Metabolite 3,4-Dichloroaniline in Soil. *Environmental Science & Technology* **2008,** *42*, (23), 8687-8691.
23. Huguet, M.; Deborde, M.; Papot, S.; Gallard, H., Oxidative decarboxylation of diclofenac by manganese oxide bed filter. *Water Research* **2013,** *47*, (14), 5400-5408.
24. Krauss, M.; Singer, H.; Hollender, J., LC-high resolution MS in environmental analysis: from target screening to the identification of unknowns. *Analytical and Bioanalytical Chemistry* **2010,** *397*, (3), 943-951.
25. Keen, O. S.; Thurman, E. M.; Ferrer, I.; Dotson, A. D.; Linden, K. G., Dimer formation during UV photolysis of diclofenac. *Chemosphere* **2013,** *93*, (9), 1948-1956.
26. Sein, M. M.; Zedda, M.; Tuerk, J.; Schmidt, T. C.; Golloch, A.; von Sonntag, C., Oxidation of diclofenac with ozone in aqueous solution. *Environmental Science & Technology* **2008,** *42*, (17), 6656-6662.
27. Von Sonntag, C.; Von Gunten, U., *Chemistry of ozone in water and waste water treatment*. IWA Publishing: London, 2012.
28. Forrez, I.; Carballa, M.; Verbeken, K.; Vanhaecke, L.; SchluÌˆsener, M.; Ternes, T.; Boon, N.; Verstraete, W., Diclofenac Oxidation by Biogenic Manganese Oxides. *Environmental Science & Technology* **2010,** *44*, (9), 3449-3454.
29. Meckenstock, R. U.; Morasch, B.; Griebler, C.; Richnow, H. H., Stable isotope fractionation analysis as a tool to monitor biodegradation in contaminated acquifers. *Journal of Contaminant Hydrology* **2004,** *75*, (3-4), 215-255.

30. Thullner, M.; Centler, F.; Richnow, H.-H.; Fischer, A., Quantification of organic pollutant degradation in contaminated aquifers using compound specific stable isotope analysis: Review of recent developments. *Organic Geochemistry* **2012,** *42*, (12), 1440-1460.
31. Hofstetter, T. B.; Berg, M., Assessing transformation processes of organic contaminants by compound-specific stable isotope analysis. *TrAC Trends in Analytical Chemistry* **2011,** *30*, (4), 618-627.
32. Elsner, M.; Zwank, L.; Hunkeler, D.; Schwarzenbach, R. P., A new concept linking observable stable isotope fractionation to transformation pathways of organic pollutants. *Environ. Sci. Technol.* **2005,** *39*, (18), 6896-6916.
33. Aelion, C. M.; Hohener, P.; Hunkeler, D.; Aravena, R., *Environmental Isotopes in Bioremediation and Biodegradation*. CRC Press: 2009.
34. Skarpeli-Liati, M.; Jiskra, M.; Turgeon, A.; Garr, A. N.; Arnold, W. A.; Cramer, C. J.; Schwarzenbach, R. P.; Hofstetter, T. B., Using nitrogen isotope fractionation to assess the oxidation of substituted anilines by Manganese Oxide. *Environ. Sci. Technol.* **2011,** *45*, (13), 5596-5604.
35. Murray, J. W., The surface chemistry of hydrous manganese dioxide. *Journal of Colloid and Interface Science* **1974,** *46*, (3), 357-371.
36. Forrez, I.; Carballa, M.; Verbeken, K.; Vanhaecke, L.; Schluesener, M.; Ternes, T.; Boon, N.; Verstraete, W., Diclofenac Oxidation by Biogenic Manganese Oxides. *Environmental Science & Technology* **2010,** *44*, (9), 3449-3454.
37. Skarpeli-Liati, M.; Pati, S. G.; Bolotin, J.; Eustis, S. N.; Hofstetter, T. B., Carbon, Hydrogen, and Nitrogen Isotope Fractionation Associated with Oxidative Transformation of Substituted Aromatic N-Alkyl Amines. *Environ. Sci. Technol.* **2012,** *46*, (13), 7189-7198.
38. Aeschbacher, M.; Sander, M.; Schwarzenbach, R. P., Novel Electrochemical Approach to Assess the Redox Properties of Humic Substances. *Environmental Science & Technology* **2010,** *44*, (1), 87-93.
39. Prasse, C.; Wagner, M.; Schulz, R.; Ternes, T. A., Biotransformation of the Antiviral Drugs Acyclovir and Penciclovir in Activated Sludge Treatment. *Environmental Science & Technology* **2011,** *45*, (7), 2761-2769.
40. Meyer, A. H.; Penning, H.; Lowag, H.; Elsner, M., Precise and accurate compound specific carbon and nitrogen isotope analysis of atrazine: critical role of combustion oven conditions. *Environ. Sci. Technol.* **2008,** *42*, (21), 7757-7763.
41. Elsner, M., Stable isotope fractionation to investigate natural transformation mechanisms of organic contaminants: principles, prospects and limitations. *J. Environ. Monit.* **2010,** *12*, (11), 2005-2031.
42. VanBreukelen, B. M., Extending the Rayleigh Equation to Allow Competing Isotope Fractionating Pathways to Improve Quantification of Biodegradation. *Environ. Sci. Technol.* **2007,** *41*, (11), 4004-4010.
43. Musa, K. A. K.; Eriksson, L. A., Photodegradation mechanism of the common non-steroid anti-inflammatory drug diclofenac and its carbazole photoproduct. *Phys. Chem. Chem. Phys.* **2009,** *11*, (22), 4601-4610.
44. Hartenbach, A. E.; Hofstetter, T. B.; Tentscher, P. R.; Canonica, S.; Berg, M.; Schwarzenbach, R. P., Carbon, hydrogen, and nitrogen isotope fractionation during light-Induced transformations of atrazine. *Environ. Sci. Technol.* **2008,** *42*, (21), 7751-7756.
45. von Gunten, U., Ozonation of drinking water: Part I. Oxidation kinetics and product formation. *Water Research* **2003,** *37*, (7), 1443-1467.
46. Huber, M. M.; Gobel, A.; Joss, A.; Hermann, N.; Loffler, D.; McArdell, C. S.; Ried, A.; Siegrist, H.; Ternes, T. A.; von Gunten, U., Oxidation of pharmaceuticals during ozonation of municipal wastewater effluents: A pilot study. *Environmental Science & Technology* **2005,** *39*, (11), 4290-4299.
47. Schramm, V. L., Enzymatic transition states and transition state analog design. *Annu. Rev. Biochem* **1998,** *67*, 693-720.

48. Huber, M. M.; Canonica, S.; Park, G. Y.; Von Gunten, U., Oxidation of pharmaceuticals during ozonation and advanced oxidation processes. *Environmental Science & Technology* **2003,** *37*, (5), 1016-1024.

49. Seto, Y.; Guengerich, F. P., Partitioning between N-dealkylation and N-oxygenation in the oxidation of N,N-dialkylarylamines catalyzed by cytochrome P450 2B1. *Journal of Biological Chemistry* **1993,** *268*, (14), 9986-9997.

50. Meunier, B.; de Visser, S. P.; Shaik, S., Mechanism of Oxidation Reactions Catalyzed by Cytochrome P450 Enzymes. *Chem. Rev.* **2004,** *104*, (9), 3947-3980.

51. Guengerich, F. P., Mechanisms of cytochrome P450 substrate oxidation: MiniReview. *J. Biochem. Mol. Toxicol.* **2007,** *21*, (4), 163-168.

52. Pati, S. G.; Shin, K.; Skarpeli-Liati, M.; Bolotin, J.; Eustis, S. N.; Spain, J. C.; Hofstetter, T. B., Carbon and Nitrogen Isotope Effects Associated with the Dioxygenation of Aniline and Diphenylamine. *Environmental Science & Technology* **2012,** *46*, (21), 11844-11853.

53. Huntscha, S.; Hofstetter, T. B.; Schymanski, E. L.; Spahr, S.; Hollender, J., Biotransformation of benzotriazoles, insights from transformation product identification and compound-specific isotope analysis. *Environmental Science & Technology* **2014**.

54. Kunkel, U.; Radke, M., Fate of pharmaceuticals in rivers: Deriving a benchmark dataset at favorable attenuation conditions. *Water Research* **2012,** *46*, (17), 5551-5565.

4

ENANTIOSELECTIVE STABLE ISOTOPE ANALYSIS (ESIA) OF POLAR HERBICIDES

Maier, M.; Qiu, S.; Elsner, M. Enantioselective stable isotope analysis (ESIA) of polar herbicides.
Analytical & Bioanalytical Chemistry, 2013. 405 (9), 2825−2831.

4.1 Abstract

Assessing the environmental fate of chiral micropollutants such as herbicides is challenging. The complexity of aquatic systems often makes it difficult to obtain hydraulic mass balances, which is a prerequisite when assessing degradation based on concentration data. Elegant alternatives are concentration-independent approaches like compound-specific isotope analysis (CSIA) or enantiospecific concentration analysis. Both detect degradation-induced changes from ratios of molecular species, either isotopologues or enantiomers. A combination of both – enatioselective stable isotope analysis (ESIA) – provides information on $^{13}C/^{12}C$ ratios for each enantiomer separately. Recently, Badea et al. demonstrated for the first time ESIA for the insecticide α-hexachlorocyclohexane. The present study enlarges the applicability of ESIA to polar herbicides such as phenoxyacids: 4-CPP (((RS)-2-(4-chlorophenoxy)-propionic acid), mecoprop (2-(4-Chloro-2-methylphenoxy)-propionic acid) and dichlorprop (2-(2,4-Dichlorophenoxy)-propionic acid). Enantioselective GC-IRMS (gas chromatography-isotope ratio mass spectrometry) was accomplished with derivatisation prior to analysis. Precise carbon isotope analysis ($2\sigma \leq 0.5‰$) was obtained with ≥ 7 ng C on column. Microbial degradation of DCPP by *Delftia acidovorans* MC1 showed pronounced enantiomer fractionation, but no isotope fractionation. In contrast, Badea et al. observed isotope fractionation, but no enantiomeric fractionation. Hence the two lines of evidence appear to complement each other. They may provide enhanced insight when combined as ESIA.

4.2 Introduction

Herbicides can help to increase crop yields by killing weeds and pests. However, after application their residues end up as micropollutants in aquatic ecosystems.[1] Since they have by definition a biological impact, they pose a potential threat to human and environmental health. It is therefore essential to understand how these compounds behave in complex environmental systems. This is a particular challenge for chiral micropollutants, where degradation behavior and toxicity often differs between single enantiomers.[2] However, in aquatic systems such as surface or ground waters the interpretation of measured concentrations relies on the possibility to obtain a closed hydraulic mass balance. Without this hydraulic information it is otherwise not possible to distinguish degradation from dilution processes. There are two elegant approaches that circumvent this difficulty by analyzing ratios that are inherent to the target molecules.

One approach is enantiospecific concentration analysis. Here the concentration of the individual enantiomers is analyzed and the enantiomer fraction (EF) is expressed as the ratio between one enantiomer and the sum of both enantiomers (e.g. EF_R=R/[R+S]). Nearly all commercial products have either an EF of 0.5 (racemates) or 0 (enatiopure products). During biological processes this ratio can be shifted. The reason is that many enzymes that are involved in transformation reactions have an enantioselective preference and favor one enantiomer over the other.[2] Hence, shifts in the EF can be a very useful tool to demonstrate that chiral compounds are degraded in complex environmental systems, particularly if other approaches (e.g. mass balances, metabolite analysis) fail.

Another promising approach to investigate sources and degradation of micropollutants in complex environmental systems is compound specific isotope analysis (CSIA). Several studies have demonstrated that changes in the isotope ratio of a compound can be used to investigate degradation of xenobiotics [3-7]. The underlying principle is that (bio-)chemical reactions are commonly associated with a kinetic isotope effect, which causes a fractionation of heavy and light isotopes. Using this approach isotope fractionation of one element can be used to quantify degradation.[8, 9]If several elements are analyzed, even the mechanisms and pathways of transformation processes can be elucidated[6, 10-12] as demonstrated recently for selected pesticides.[13-16]

CSIA and EF analysis work on the same principle that degradation can be detected because one species becomes enriched relative to the other. Despite this similarity, both approaches have been applied together in only one study. Recently Badea et al. presented a first example of enantioselective isotope analysis (ESIA) applied to the insecticide α-hexachlorocyclohexane.[17] In a biodegradation experiment they observed isotope fractionation, but no enantiomer fractionation so that the line of evidence brought forward in this particular example was similar as for conventional CSIA.

The aim of this study was to enlarge the applicability of ESIA to a broader range of substances, including polar compounds that are more challenging to analyze via GC-IRMS and for a case of biodegradation where enantiomer fractionation is well established to occur. To this end an enantiospecific stable isotope method was developed for three polar herbicides, 4-CPP ((RS)-2-(4-chlorophenoxy)-propionic acid), MCPP (mecoprop, 2-(4-Chloro-2-methylphenoxy)propionic acid) and DCPP (dichlorprop, 2-(2,4-Dichlorophenoxy)-propionic acid) to provide a tool for investigating their fate in environmental systems. For each compound the precision of the method was tested as well as the limits of precise isotope analysis. Subsequently, the method was applied to investigate microbial degradation, using the enantioselective strain *Delftia acidovorans* MC1 and the herbicide DCPP as a model compound.

4.3 Experimental

4.3.1 Compounds and chemicals

Acetonitrile (1.25% acetic acid) and n-hexane were purchased from Carl Roth (Karlsruhe, Germany) and had LC-MS grade (purity > 0.99). Acetic acid (1.25%) was purchased from Merck (Darmstadt, Germany). MCPP (mecoprop, 2-(4-Chloro-2-methylphenoxy)-propionic acid, CAS RN 7085-19-0) and BF_3 (10% in methanol) were purchased from Sigma Aldrich (St. Louis, U.S.A.). 4-CPP ((RS)-2-(4-chlorophenoxy)-propionic acid, CAS RN 3307-39-9) was purchased from Aldrich Chemistry (Milwaukee, USA) and DCPP (dichlorprop, 2-(2,4-Dichlorophenoxy) propionic acid, CAS RN 120-36-5) and R-DCPP from Dr. Ehrenstorfer GmbH (Augsburg, Germany). MilliQ water was generated with a Millipore Advantage A10 system (Millipore, Molsheim, France). (S)-2-(4-chlorophenoxy)-propionic acid methyl ester (S-4-CPP) was synthesized according to the procedure by Nittoli et al.[18] and as described in Milosevic et al.[19].

4.3.2 Derivatisation with BF3

Prior to analysis the polar carboxy-group of the analytes was methylated in a similar way as described by Chivall et al.[20] for fatty acids. To this end sterile filtered samples or standards were evaporated in 2 mL amber glass vials to dryness under a gentle stream of N_2. 400 µL of BF_3 (10% in methanol) were added, the vials were sealed with screw caps equipped with PTFE seals and incubated for 1 h at 40°C. After cooling the remaining reactant was quenched with 400 µL MilliQ water and the methylated analytes were extracted three times with 500 µL n-hexane and transferred to a new vial. If necessary, the extracted phase was reduced to 200 µL under a gentle stream of N_2 to increase the concentration for isotope analysis. The toxic aqueous phase containing HF was disposed in a canister of 2 M NaOH to quench its toxicity.

4.3.3 Isotope Analysis

Depending on the concentrations of extracts, between 1 µL and 4 µL were injected splitless at 230 °C. The gas chromatograph (TRACE GC Ultra gas chromatograph, Thermo Fisher Scientific, Milan, Italy) was equipped with a β-6TBDM column (50m x 0.25 mm, 0.25 µm film; Macherey&Nagel, Düren, Germany). The column was operated with a constant flow velocity of 29 cm s^{-1} corresponding to a He carrier flow rate of 1.4 ml min^{-1} (GC-IRMS) and 1.0 ml min^{-1} (GC-TOF-MS). Initial oven temperature was 80 °C (1 min.), ramped to 140 °C with a rate of 10 °C $min.^{-1}$, then with 1.5 °C $min.^{-1}$ to 185 °C and then with 30 °C $min.^{-1}$ to 230 °C (held for 4 min.). After separation the analytes were combusted online in a Finnigan GC combustion interface (Thermo Fisher Scientific, Bremen, Germany) to CO_2 with a NiO tube / CuO-NiO reactor operated at 1000°C (Thermo Fisher Scientific, Bremen, Germany). CO_2 isotope values were determined with a Finnigan MAT 253 isotope ratio mass spectrometer (Thermo Fisher Scientific, Bremen, Germany). Before and after every run three reference gas peaks were measured. These reference gas peaks were used to link isotope values to the international standard for carbon isotopes (Vienna PeeDee Belemnite, Eq. 4-1).

$$\delta^{13}C = \frac{\left({}^{13}C/{}^{12}C_{Sample} - {}^{13}C/{}^{12}C_{Reference}\right)}{{}^{13}C/{}^{12}C_{Reference}} \qquad (4\text{-}1)$$

To validate the results of the GC-IRMS method, in addition pure in-house standards of all compounds were characterized on an elemental analyzer (EURO EA, Euro Vector Instruments) coupled to a Finnigan MAT 253 isotope ratio mass spectrometer (Thermo Fisher Scientific, Bremen, Germany). Calibration was performed with the following organic reference materials provided by the International Atomic Energy Agency (IAEA, Vienna): IAEA 600, IAEA CH3 (cellulose), IAEA CH6 (sucrose) and IAEA CH7 (polyethylene).

4.3.4 Calculation of the introduced methyl-group

During methylation an additional carbon atom is introduced in each herbicide molecule and changes its bulk carbon isotope ratio. This shift of $\delta^{13}C$ was kept constant by using the same batch of methanolic BF_3 solution for the derivatisation of standards and samples. Values were corrected according to the common procedure as described previously.[21-23] First, the isotope ratio of the introduced methyl group was calculated ($\delta^{13}C(Me)$) (Eq. 4-2). To this end the isotope ratio of the lab standard of the respective herbicide was determined prior to methylation on EA-IRMS ($\delta^{13}C(Analyte)_{EA}$) and after methylation on GC-IRMS ($\delta^{13}C(Me\text{-}Analyte)_{GC}$). With respect to the number of C-atoms of the analyte (n), the weighted difference was then used to calculate the theoretical isotope-ratio of the introduced methyl-group (Table 4-1). Subsequently this value was used to correct samples ($\delta^{13}C(Sample)$) for the introduced methyl-group; again, with respect to the number of carbon atoms (Eq. 4-3). The inherent uncertainty of this procedure can be calculated by gaussian error propagation (Eq. 4-4). The uncertainty of the sample value (*$\Delta\delta^{13}C(Sample)$*) is strongly influenced by the uncertainty of the GC-IRMS analysis (*ΔGC)*, whereas the contribution of the methyl group calculation (*ΔMe*) is reduced by a factor of 1/9 in the case of 4-CPP and DCPP and 1/10 in the case of MCPP, respectively.

$$\delta^{13}C(Me) = (n+1)\times\delta^{13}C(Me-Analyte)_{GC} - n\times\delta^{13}C(Analyte)_{EA} \qquad (4\text{-}2)$$

$$\delta^{13}C(Sample) = \frac{(n+1)\times\delta^{13}C(Me-Analyte)_{Sample} - \delta^{13}C(Me)}{n} \qquad (4\text{-}3)$$

$$\Delta\delta^{13}C(Sample) = \sqrt{\left(\frac{\partial f(x,y)}{\partial x}\right)^2 \times \Delta x^2 + \left(\frac{\partial f(x,y)}{\partial y}\right)^2 \times \Delta y^2} = \qquad (4\text{-}4)$$

$$\sqrt{\left(\frac{n+1}{n}\right)^2 \times \Delta GC^2 + \left(\frac{1}{n}\right)^2 \times \Delta Me^2}\Delta\delta^{13}\mathrm{C(Sample)} = \sqrt{\left(\frac{\partial(\mathrm{x,y})}{\partial \mathrm{x}}\right)^2 \times \Delta \mathrm{x}^2 + \left(\frac{\partial(\mathrm{x,y})}{\partial \mathrm{y}}\right)^2 \times \Delta \mathrm{y}^2} =$$

$$\sqrt{\left(\frac{\mathrm{n}+1}{\mathrm{n}}\right)^2 \times \Delta\mathrm{GC}^2 + \left(\frac{1}{\mathrm{n}}\right)^2 \times \Delta\mathrm{Me}^2}$$

4.3.5 Peak identity

Identity of standards and samples was verified on a gas chromatograph (DANI Master-GC, Milano Italy) coupled to a time of flight mass spectrometer (DANI Master-TOF, DANI, Italy / Switzerland). The system was operated with same flow velocity, temperature conditions and the same column as described above for the GC-IRMS system, but without combustion of the samples to CO_2.

One enantiomer of each DCPP and 4-CPP was available as a pure standard, and was used to identify the respective enantiomers. There are only small molecular differences in the structure of MCPP in comparison to 4-CPP and DCPP and they are not related to the chiral center. Hence it was assumed that the elution order of 4-CPP and DCPP, where the R enantiomer elutes first, also applies to MCPP. In addition, this elution order agrees with the elution order Buser and Muller[1] determined for 4-CPP and MCPP with a similar stationary phase. Ideally, this hypothesis remains to be verified with a pure MCPP enantiomer for degradation studies with MCPP.

4.3.6 DCPP transformation study

A pure strain of *Delftia acidovorans* MC1 was used for degradation of DCPP. MC1 was first pregrown in mineral salt solution (1 L, 30°C) with 10 mg DCPP [24]. When DCPP was completely consumed by MC1, the final OD of this solution reached 0.4 at 500 nm. Using this solution, biodegradation of DCPP (60 mg L^{-1}) was conducted in duplicate non-shaken batches (200 mL each). Liquid samples (5 mL each) were collected and sterile filtered (0.22 µm). 0.5 mL sample were immediately analyzed by LC-UV as described below. The rest was stored frozen at -20°C for isotope analysis. DCPP samples were quantified using a Shimadzu LC-10A series High Performance Liquid Chromatograph equipped with an Allure C18 column, 150 × 4.6 mm, 5 µm particle size (Restek, USA) and a Ultra-Violet detector. The eluting solvents were acetonitrile with 1.25% acetic acid (solvent A) and de-ionized water with 1.25% acetic acid (solvent B). The gradient was composed of 30% solvent B (1 min) and was increased to 80% (2-10 min) and finally decreased to 30% (11-12 min) again. The flow rate was 1 mL min^{-1} and the oven temperature 45 °C. The sample injection volume was 100 µL and absorbance of DCPP was measured at 280 nm.

4.4 Results

4.4.1 Chromatographic Resolution

As shown previously by Buser and Müller,[1] chlorinated phenoxy acid herbicides can be separated on a chiral stationary phase after methylation (Fig. 4-1). We achieved this with a chromatographic resolution of $R \geq 3.0$ for the lowest tested concentrations and $R \geq 1.4$ for the highest tested concentrations when R is defined as retention time difference/ mean peak width.[25] If R is calculated using the peak width at half height[25] a chromatographic resolution between $R \geq 7.2$ and $R \geq 6.2$ was achieved. Only the highest concentrations of 4-CPP ($R \geq 1.4$) fall slightly below the conservative definition of baseline separation ($R \geq 1.5$) (Fig. 4-1b). This did not influence the isotope values (Fig. 4-2); however, in cases where values appear to be biased, samples can be diluted.

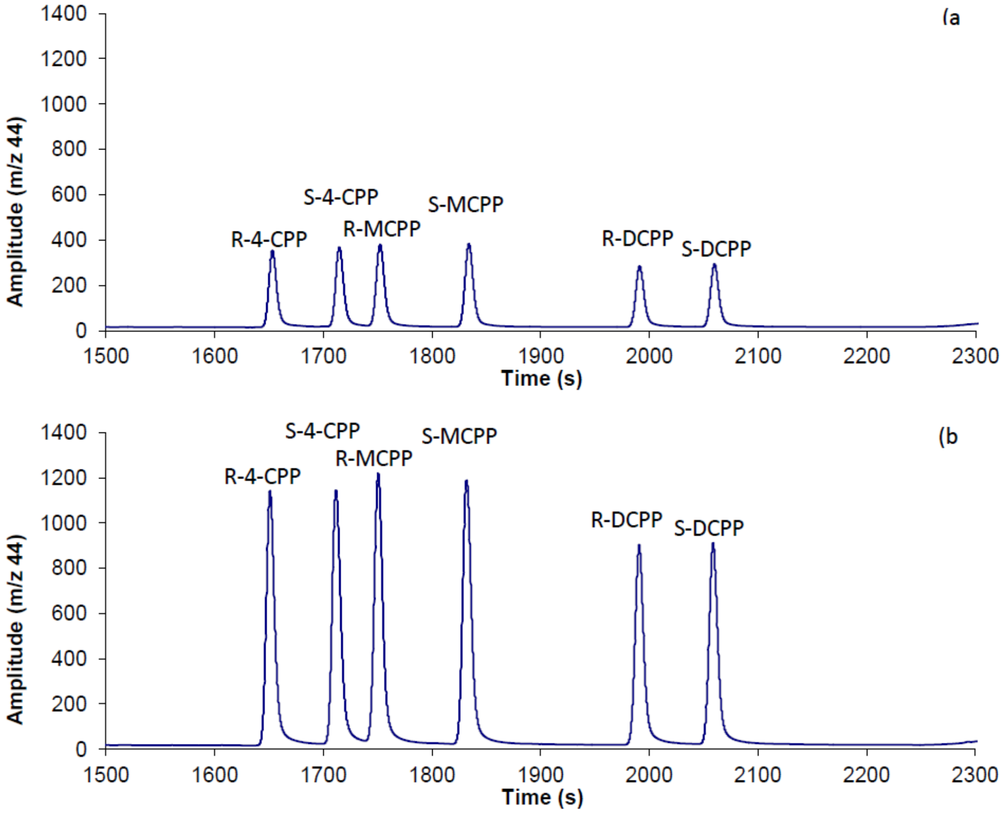

Fig. 4-1 GC-IRMS Chromatogram (m/z 44) of a racemic mix, containing 4-CPP, MCPP and DCPP; Shown are examples with an injection volume of 1 µL and concentrations per enantiomer of (a) 12.5 mg L^{-1} and (b) 50 mg L^{-1}

4.4.2 Isotope Analysis

The precision of ESIA for the three tested herbicides is comparable to other non-enantioselective studies that do not contain a derivatisation step.[12] Triplicate analysis delivered a standard deviation of 2σ ≤ 0.5‰. Although a methyl-group is introduced in the analytes during derivatisation, the isotope values of the GC-IRMS analysis (gas chromatography isotope ratio mass spectrometry) were indistinguishable from the reference values derived by elemental analysis-IRMS within the typical precision of the two methods (2σ of 0.5‰ and 0.2‰, respectively, Tab. 1). This applies for the single enantiomers as well as for the racemate value, calculated as the mean of both enantiomers. Correspondingly, the isotope ratio of the introduced methyl group was close to the isotopic composition of the target compounds (Tab. 4-1), and the methyl group-values were indistinguishable within calculated uncertainties. Because the correction scheme described above uses the isotope shift of standards for the correction of samples, it delivers precise isotope values with respect to the introduced carbon atom as well as for systematic fractionation effects that can appear during derivatization.[23] For the purposes of the linearity test we refrained from such corrections, because its focus was on the correlation of peak amplitude and isotope value and the correction term would have been the same for all samples. For degradation studies, as shown below, the additional methyl group has to be taken into account, because position-specific isotope changes are more strongly diluted by the additional carbon atom.

Tab. 4-1 Given are Isotope values of the racemate analyzed on EA-IRMS, the enantiomers analyzed on GC-IRMS, the theoretical value of the racemate calculated as the mean value of all values analyzed on GC-IRMS (R- and S- enantiomers are denoted as R and S, respectively), the lowest amount needed on column for precise isotope analysis for each enantiomer and the calculated δ13C value of the methyl-group (see Eq. 4-2) introduced during derivatisation; Uncertainties represent the standard deviation. Note that the uncertainty of the calculated isotope value of the methyl-group has only minor influence on the isotope value of samples as shown in Eq. 4-4.

Analyte	EA-IRMS $\delta^{13}C$ [‰] (n=5)	GC-IRMS $\delta^{13}C$ [‰] (n=9-13)	GC-IRMS $\delta^{13}C$ [‰] (n=9-13)	Lowest amount needed for precise isotope analysis	Calculated $\delta^{13}C$ of introduced methyl-group [‰]
4-CPP	-26.5 ± 0.1	-26.9 ± 0.3 ^{R}	-26.7 ± 0.3	62 pmol	-28 ± 3
		-26.4 ± 0.1 ^{S}		7 ng C	
MCPP	-28.6 ± 0.1	-29.2 ± 0.2 ^{R}	-28.9 ± 0.4	58 pmol	-32 ± 4
		-28.6 ± 0.2 ^{S}		7 ng C	
DCPP	-27.3 ± 0.1	-27.5 ± 0.1 ^{R}	-27.3 ± 0.2	53 pmol	-28 ± 2
		-27.2 ± 0.2 ^{S}		6 ng C	

The linear range of the method is illustrated in Fig. 4-2. For all four tested compounds the lower limit of precise $\delta^{13}C$ isotope analysis was around peak amplitudes of 200 mV. Hence we recommend that for precise ESIA only peak amplitudes higher than 200 mV should be used. This corresponds to a minimum amount of substance needed on column of ≥ 7 ng that is even below the manufacturer specification of 10 ng C.[12] A critical point for isotope data evaluation is the background correction. In most cases a 5 s interval prior to each peak is used to correct its isotope value. Because enantiomer peaks in ESIA have narrow retention times, the tailing of the first eluting enantiomer could interfere with the background used for the second eluting enantiomer. Consequently we used the background of the first enantiomer to correct peak areas of both enantiomers.

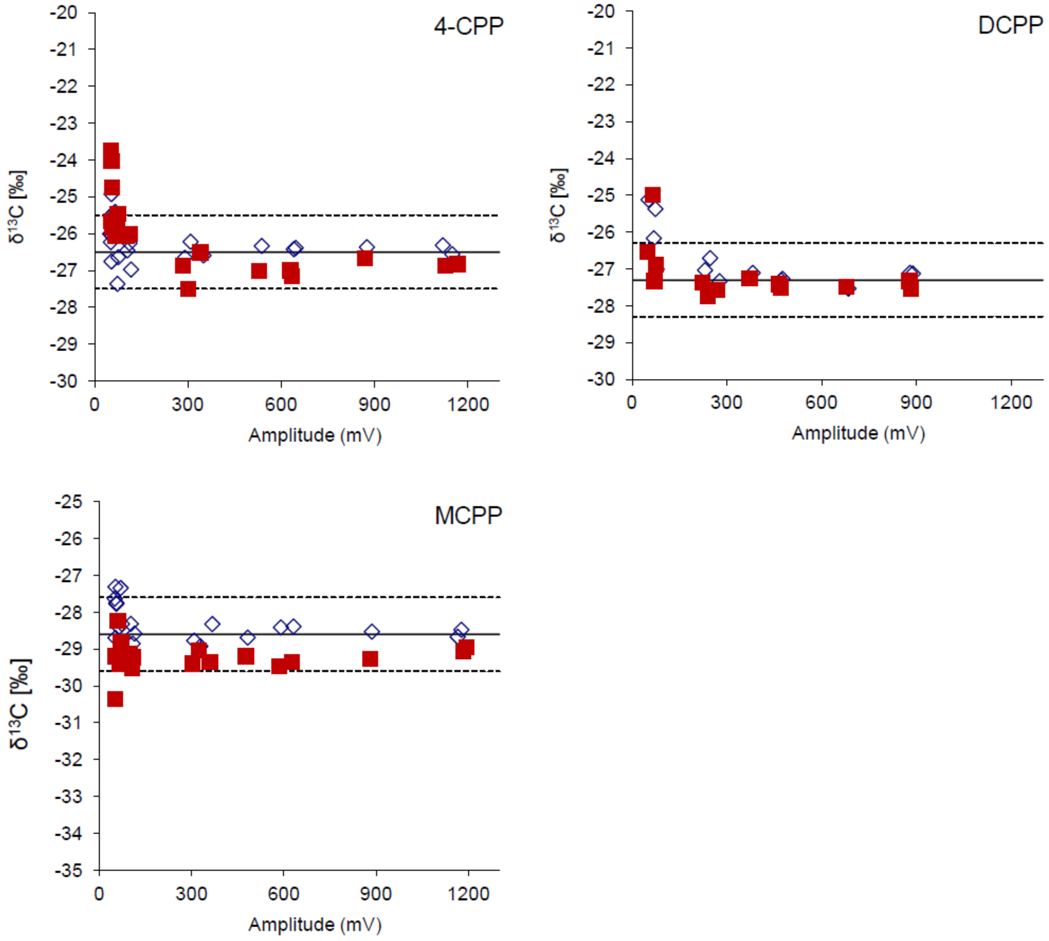

Fig. 4-2 Dependency of $\delta^{13}C$ measurements on the peak amplitude; blue diamonds indicate S-enantiomers (◇) and red squares R-enantiomers (■); the solid line represents the EA-IRMS value of the racemate

4.4.3 Application of ESIA to phenoxy acids

Biodegradation of DCPP was done in *Delftia acidovorans* MC1. Interestingly, enantioselective degradation of DCPP was observed, but no carbon isotope fractionation occurred to either enantiomer (Figure 4-3). Two scenarios can explain the absence of isotope fractionation: either the degrading enzyme has no isotopic preference, or the intrinsic kinetic isotope effect of the enzyme was masked. Such a masking effect appears if the enzymatic bond cleavage is not the rate limiting-step.[11] One example could be that transport into the cell is rate-limiting[26] as hypothesized for MC1,[24, 27] but this has to be confirmed in further studies. Our findings contrast with the observation of Badea et al. that isotope fractionation, but no enantiomeric fractionation occurred in biodegradation of α-hexachlorocyclohexane.[17] Consequently, the information of both methods (CSIA and enantiomer fractionation) appears to be complementary.

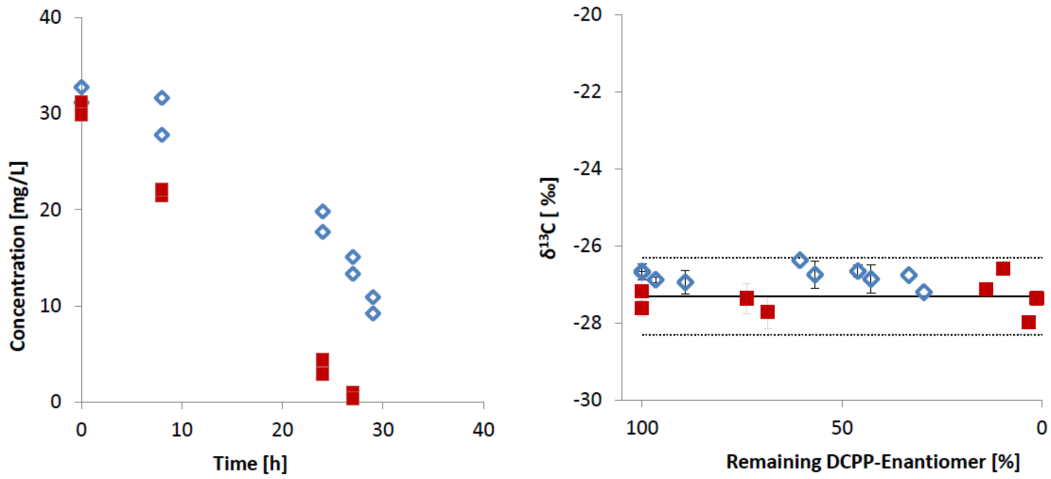

Fig. 4-3 DCPP degradation comes along with enantiomeric fractionation (left) and no isotope fractionation (right); blue diamonds indicate S-DCPP (◇) and red squares R-DCPP (■); the experiment was made as duplicate; the solid line represents the EA-IRMS value of the racemate

4.5 Outlook

With this study we provide a tool to investigate degradation of selected chiral herbicides based on the isotope analysis of enantiomers. By widening the application of ESIA to another compound class, we obtained the remarkable picture that CSIA and enantiomer fractionation do not seem to be strongly related. In other words, the methods may nicely complement each other in the assessment of contaminated sites. If only one kind of fractionation occurs – i.e. only enrichment of isotopes,[17] or only of enantiomers (our study) – ESIA presently has no unique advantage compared to CSIA and enantiomer analysis alone. In contrast, the full potential of ESIA will unfold if both processes occur in parallel. First evidence for such a scenario has been obtained in the study by Milosevic et al. where enantioselective degradation and carbon isotope fractionation of 4-CPP were observed downstream at a landfill site under anaerobic conditions.[19] There, isotope values of single 4-CPP enantiomers differed up to 3‰. Hence, much can be expected to be learned from ESIA in the future with respect to the complementarity of both lines of evidence in field applications and with respect to a better process understanding.

4.6 Acknowledgements

Michael Maier is financially supported by the German Federal Environmental Foundation (DBU). The study was supported by the Seventh Framework Program (2007–2013) of the European Commission within the GOODWATER Marie Curie Initial Training Network (grant no. 212683). We thank Heide

Bensch for her support in the synthesis of S-4-CPP. Two anonymous reviewers are acknowledged for critical comments.

4.7 Reference

1. Buser, H. R.; Muller, M. D., Occurrence and transformation reactions of chiral and achiral phenoxyalkanoic acid herbicides in lakes and rivers in Switzerland. *Environmental Science & Technology* **1998,** *32*, (5), 626-633.
2. Wong, C., Environmental fate processes and biochemical transformations of chiral emerging organic pollutants. *Analytical and Bioanalytical Chemistry* **2006,** *386*, (3), 544-558.
3. Sherwood Lollar, B.; Slater, G. F.; Sleep, B.; Witt, M.; Klecka, G. M.; Harkness, M.; Spivack, J., Stable carbon isotope evidence for intrinsic bioremediation of tetrachloroethene and trichloroethene at Area 6, Dover Air Force Base. *Environ. Sci. Technol.* **2001,** *35*, 261-269.
4. Hunkeler, D.; Aravena, R.; Butler, B. J., Monitoring microbial dechlorination of tetrachloroethene (PCE) using compound-specific carbon isotope ratios: Microcosms and field experiments. *Environ. Sci. Technol.* **1999,** *33*, (16), 2733-2738.
5. Richnow, H. H.; Annweiler, E.; Michaelis, W.; Meckenstock, R. U., Microbial in situ degradation of aromatic hydrocarbons in a contaminated aquifer monitored by carbon isotope fractionation. *Journal of Contaminant Hydrology* **2003,** *65*, (1-2), 101-120.
6. Hofstetter, T. B.; Berg, M., Assessing transformation processes of organic contaminants by compound-specific stable isotope analysis. *TrAC Trends in Analytical Chemistry* **2011,** *30*, (4), 618-627.
7. Schmidt, T. C.; Zwank, L.; Elsner, M.; Berg, M.; Meckenstock, R. U.; Haderlein, S. B., Compound-specific stable isotope analysis of organic contaminants in natural environments: a critical review of the state of the art, prospects, and future challenges. *Anal. Bioanal. Chem.* **2004,** *378*, (2), 283-300.
8. Meckenstock, R. U.; Morasch, B.; Griebler, C.; Richnow, H. H., Stable isotope fractionation analysis as a tool to monitor biodegradation in contaminated acquifers. *J.Contam.Hydrol.* **2004,** *75*, (3-4), 215-255.
9. Thullner, M.; Centler, F.; Richnow, H.-H.; Fischer, A., Quantification of organic pollutant degradation in contaminated aquifers using compound specific stable isotope analysis: Review of recent developments. *Organic Geochemistry* **2012,** *42*, (12), 1440-1460.
10. Elsner, M.; Zwank, L.; Hunkeler, D.; Schwarzenbach, R. P., A new concept linking observable stable isotope fractionation to transformation pathways of organic pollutants. *Environ. Sci. Technol.* **2005,** *39*, (18), 6896-6916.
11. Elsner, M., Stable isotope fractionation to investigate natural transformation mechanisms of organic contaminants: principles, prospects and limitations. *J. Environ. Monit.* **2010,** *12*, (11), 2005-2031.
12. Elsner, M.; Jochmann, M. A.; Hofstetter, T. B.; Hunkeler, D.; Bernstein, A.; Schmidt, T. C.; Schimmelmann, A., Current challenges in compound-specific stable isotope analysis of environmental organic contaminants. *Anal. Bioanal. Chem.* **2012,** *403*, (9), 2471-2491.
13. Meyer, A. H.; Penning, H.; Elsner, M., C and N isotope fractionation suggests similar mechanisms of microbial atrazine transformation despite involvement of different Enzymes (AtzA and TrzN). *Environ. Sci. Technol.* **2009,** *43*, (21), 8079-8085.
14. Hartenbach, A. E.; Hofstetter, T. B.; Tentscher, P. R.; Canonica, S.; Berg, M.; Schwarzenbach, R. P., Carbon, hydrogen, and nitrogen isotope fractionation during light-Induced transformations of atrazine. *Environ. Sci. Technol.* **2008,** *42*, (21), 7751-7756.
15. Penning, H.; Sorensen, S. R.; Meyer, A. H.; Aamand, J.; Elsner, M., C, N, and H Isotope Fractionation of the Herbicide Isoproturon Reflects Different Microbial Transformation Pathways. *Environ. Sci. Technol.* **2010,** *44*, (7), 2372-2378.

16. Reinnicke, S.; Simonsen, A.; Sørensen, S. R.; Aamand, J.; Elsner, M., C and N Isotope Fractionation during Biodegradation of the Pesticide Metabolite 2,6-Dichlorobenzamide (BAM): Potential for Environmental Assessments. *Environ. Sci. Technol.* **2012,** *46*, (3), 1447-1454.

17. Badea, S.-L.; Vogt, C.; Gehre, M.; Fischer, A.; Danet, A.-F.; Richnow, H.-H., Development of an enantiomer-specific stable carbon isotope analysis (ESIA) method for assessing the fate of alpha-hexachlorocyclohexane in the environment. *Rapid Communications in Mass Spectrometry* **2011,** *25*, (10), 1363-1372.

18. Nittoli, T.; Curran, K.; Insaf, S.; Di-Grandi, M.; Orlowski, M.; Chopra, R.; Agarwal, A.; Howe, A. Y. M.; Prashad, A.; Floyd, M. B.; Johnson, B.; Sutherland, A.; Wheless, K.; Feld, B.; O'Connell, J.; Mansour, T. S.; Bloom, J., Identification of anthranilic acid derivatives as a novel class of allosteric inhibitors of hepatitis C NS5B polymerase (vol 50, pg 2108, 2007). *J. Med. Chem.* **2007,** *50*, (24), 6290-6290.

19. Milosevic, N.; Qiu, S.; Elsner, M.; Einsiedl, F.; Maier, M. P.; Bensch, H. K. V.; Albrechtsen, H. J.; Bjerg, P. L., Combined isotope and enantiomer analysis to assess the fate of phenoxy acids in a heterogeneous geologic setting at an old landfill. *Water Research* **2012,** *in press*.

20. Chivall, D.; Berstan, R.; Bull, I. D.; Evershed, R. P., Isotope effects associated with the preparation and methylation of fatty acids by boron trifluoride in methanol for compound-specific stable hydrogen isotope analysis via gas chromatography/thermal conversion/isotope ratio mass spectrometry. *Rapid Communications in Mass Spectrometry* **2012,** *26*, (10), 1232-1240.

21. Reinnicke, S.; Bernstein, A.; Elsner, M., Small and Reproducible Isotope Effects during Methylation with Trimethylsulfonium Hydroxide (TMSH): A Convenient Derivatization Method for Isotope Analysis of Negatively Charged Molecules. *Analytical Chemistry* **2010,** *82*, (5), 2013-2019.

22. Pelz, O.; Hesse, C.; Tesar, M.; Coffin, R. B.; Abraham, W. R., Development of Methods to Measure Carbon Isotope Ratios of Bacterial Biomarkers in the Environment. In *Isot. Environ. Health Stud.*, Taylor & Francis: 1998; Vol. 34, pp 131-144.

23. Silfer, J. A.; Engel, M. H.; Macko, S. A.; Jumeau, E. J., Stable carbon isotope analysis of amino acid enantiomers by conventional isotope ratio mass spectrometry and combined gas chromatography/isotope ratio mass spectrometry. *Anal. Chem.* **1991,** *63*, (4), 370-374.

24. Muller, R. H.; Hoffmann, D., Uptake kinetics of 2,4-dichlorophenoxyacetate by Delftia acidovorans MC1 and derivative strains: Complex characteristics in response to pH and growth substrate. *Biosci. Biotechnol. Biochem.* **2006,** *70*, (7), 1642-1654.

25. Hübschmann, H.-J., *Handbook of GC/MS*. WILEY-VCH Verlag GmbH: Weinheim (Germany), 2001; Vol. 1.

26. Nijenhuis, I.; Andert, J.; Beck, K.; Kastner, M.; Diekert, G.; Richnow, H. H., Stable isotope fractionation of tetrachloroethene during reductive dechlorination by *Sulfurospirillum multivorans* and *Desulfitobacterium* sp. Strain PCE-S and abiotic reactions with cyanocobalamin. *Appl. Environ. Microbiol.* **2005,** *71*, (7), 3413-3419.

27. Zipper, C.; Fleischmann, T.; Kohler, H. P. E., Aerobic biodegradation of chiral phenoxyalkanoic acid derivatives during incubations with activated sludge. *FEMS Microbiology Ecology* **1999,** *29*, (2), 197-204.

5

GENERAL CONCLUSIONS

Four years ago transformation product (TP) analysis was the only way to investigate the transformation behavior of pharmaceuticals. Although compound specific isotope analysis (CSIA) was already established for well-known contaminants, such as toluene[1] or chlorinated solvents,[2] it was never used to study pharmaceutical transformation. One reason was that existing CSIA methods for non-volatile compounds were usually applied at concentrations in the mg L^{-1} or high µg L^{-1} range and even sophisticated approached using solid-phase microextraction reached "only" 80 µg L^{-1} and 2 mg L^{-1} for carbon and nitrogen, respectively.[3] Thus, applicability of CSIA was far away from typical concentrations of micropollutants. In addition, it was assumed that C-isotope fractionation cannot be detected in molecules that contain 15 C-atoms.[4] Moreover, before 2011 there was no publication on the coupling of enantioselective separation techniques with isotope ratio mass spectrometry, despite the great potential of such a method for studying transformation reactions.[5] It was, therefore, the aim of the present dissertation to develop for the first time a CSIA method for a pharmaceutical and ESIA of herbicides to obtain new insights into the fate of micropollutants:

Sources of pharmaceuticals can be traced by CSIA in the environment. In the absence of transformation processes CSIA has the potential for source appointment as shown in Chapter 2 for diclofenac and in Appendix A1 for benzotriazole. The underlying principle is that sources can vary in their isotopic composition for two reasons. On the one hand, Chapter 2 revealed that already commercial gel- and tablet formulations that contain diclofenac as active pharmaceutical ingredient vary in their isotopic composition. In addition, this finding indicated the potential for producers to track batches and to verify their products, if raw materials for production are chosen carefully and C and N isotope ratios of manufactured products are recorded (Chapter 2). On the other hand isotope ratios of different sources, such as sewage treatment plants or manure from diclofenac treated cattle, could be altered to a different extend by preceding transformation processes as described in chapter 3 and 4. Hence, CSIA has the potential to investigate different sources in the environment.

CSIA can track various transformation reactions of a pharmaceutical. In parallel to Schreglmann et al.,[6] Chapter 2 brought the application limits of CSIA down to the ng L^{-1} range. Moreover, Chapter 2 and 3 could demonstrate that CSIA of diclofenac can track aerobic biotransformation, reductive dechlorination, ozonation, photolysis, transformation by MnO_2 and single electron oxidation (SET). The big advantage of CSIA is that these processes can be monitored by the analysis of isotope ratios, even if dilution effects impede an evaluation of concentration measurements. This is important, for example, if groundwater dilutes diclofenac concentrations in a river where no transformation takes place. There, concentration measurements alone would give a false positive indication for transformation, but isotope ratios would keep constant and indicate the absence of transformation processes. Moreover, CSIA cannot only track isolated reactions, but Chapter 3 revealed that N-isotope fractionation is the key to divide all tested environmentally relevant reactions into two classes that can be distinguished by their different N isotope fractionation trends (Fig. 5-1). Transformation by river sediment and MnO_2 causes normal N-isotope fractionation, whereas SET, photolysis and ozonation cause inverse N-isotope fractionation (Chapter 2 & 3). Hence, CSIA of diclofenac can improve our understanding about key processes that eliminate diclofenac in engineered and environmental systems. In knowledge can be used in engineered systems to test the efficiency of ozonation in comparison to biotransformation or MnO_2 in (waste-) water treatment. However, the full strength of CSIA comes into play in environmental investigations. There, it is of great interest to distinguish the two (potentially) most important sinks of diclofenac in the environment - photo- and biotransformation - and this can be done by N-isotope analysis.

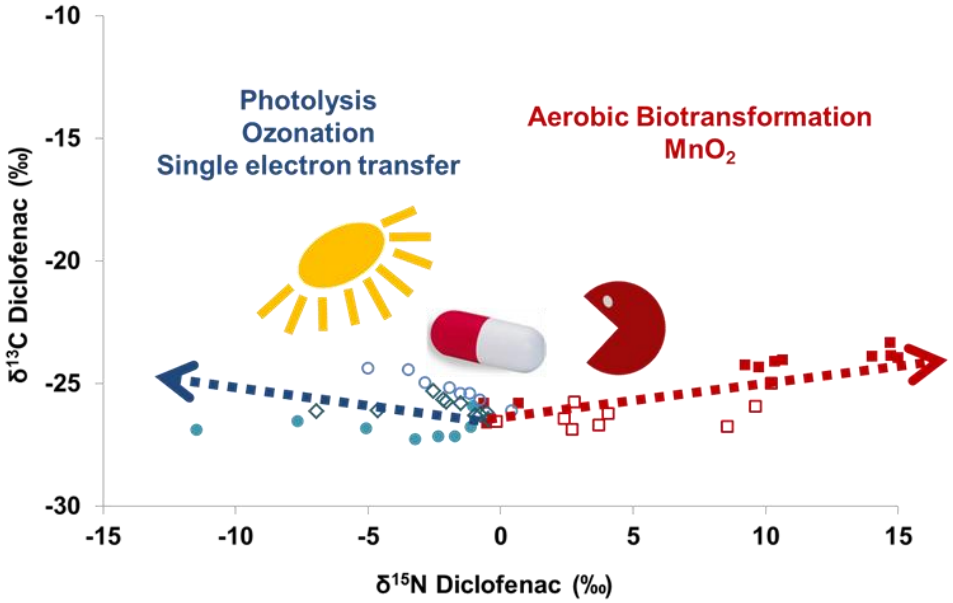

Fig. 5-1 Transformation by aerobic river sediment and MnO_2 causes normal N-isotope fractionation, whereas single electron oxidation, photolysis and ozonation cause inverse N-isotope fractionation; hence, CSIA is a valuable tool to determine dominating transformation pathways in environmental and engineered systems

CSIA delivered surprising mechanistic insights into transformation reactions. On a mechanistic level, the present thesis delivered new insights into the transformation of diclofenac, even though its environmental behavior has been under investigation for 15 years.[7] This was possible because CSIA has the unique ability to shed light on transition states of transformation reactions that are specific for a certain mechanism and cannot be accessed by other means under environmentally relevant conditions (see also 1.2.2). Chapter 3 highlighted the importance of this approach, because CSIA elucidated that ABTS oxidizes diclofenac by an outer sphere SET, whereas evidence from isotope fractionation indicated a different mechanism with MnO_2. Interestingly, the same N-isotope fractionation trend as with MnO_2 was observed in biotransformation by river sediment. Hence, CSIA indicates an unknown transformation pathway which may be similar for elimination of diclofenac by river sediment or MnO_2 and which involves nitrogen atom to a greater extent than indicated by available TP identification (ring hydroxylated species) Furthermore, in Chapter 3 CSIA was used for the first time to study micropollutant transformation by ozone and delivered strong indication that ozone attacks rather the aromatic ring of diclofenac than the N-atom. Because many micropollutants contain aniline structures, the observed N-isotope fractionation of diclofenac gives the promising outlook that CSIA could also help to understand the transformation behavior of other micropollutants during ozonation.

Isotope ratios and TPs – two complementary approaches. Transformation product analysis of Chapter 3 has shown that three different reactants – ozone, ABTS and MnO_2 – can transform diclofenac into the same TP: diclofenac-2,5-iminoquinone. At the same time CSIA revealed that this was done by at least two different reaction mechanisms. Hence, TP analysis and CSIA can be seen as complementary approaches. On the one hand CSIA shades light on the reaction mechanism (e.g. site of attack, dominant pathway) and improves our understanding of transformation processes. On the other hand TP analysis shows us the result of this mechanism, which is important because the behavior of TPs is even less investigated and in some cases they can be persistent[8] or even more toxic than their precursors.[9] However, future work should also address isotope analysis of TPs. In chapter 3 it was discussed if hydroxylation is the driver of isotope fractionation. CSIA of the hydroxylated products could show if the depletion of light isotopes in diclofenac (ε_N= -7.1‰) is reflected in an enrichment of light isotopes in the TPs (ε_N= +7.1‰ ?). In other words, CSIA offers the unique ability to correlate TP formation with reactant transformation.

ESIA combines the advantages of CSIA and enantiomer analysis and opens up new fields. Chapter 4 combined the advantages of CSIA and enantioselective analysis to provide a very robust tool that can track the fate of micropollutants, give mechanistic insight into transformation, but in addition it has also the potential to determine enzymatic activity when no isotope fractionation can be observed. Such a case was investigated in chapter 4, where microbial transformation of dichlorprop caused no isotope fractionation, but shifted enantiomeric ratios. On the one hand, this investigation showed that ESIA could track this reaction, but on the other hand it also provided ground for a deeper mechanistic interpretation. There are two hypotheses for the absence of isotope fractionation. Either the transforming enzyme shows no isotopic preference, or transport into cells limited the turnover of dichlorprop (see also Fig. 1-3). It is currently under investigation, if dichlorprop transformation by the isolated enzyme causes isotope fractionation (Qiu et al., submitted to Environmental Science & Technology). If this enzyme shows an isotopic preference, the absence of isotope fractionation in Chapter 4 would deliver a direct evidence for if transport into cells as rate-determining step in the microbial transformation of dichlorprop.

Furthermore, the application of ESIA was not restricted to lab experiments, but was already brought to the field (Appendix A2). There, the remarkable picture was obtained that enantiomer and isotope ratios of 4-CPP (TP of dichlorprop) were shifted at the same time during transformation under anaerobic conditions at a landfill site. Hence, much can be learned from ESIA in the future in field applications, but also in terms of a better process understanding. This applies especially, because ESIA was only applied to carbon isotopes. CSIA of diclofenac, atrazine[10] or isoproturon[11] has shown that the analysis of a second element can increase the possibilities of isotope analysis fundamentally. Future studies will show that this also applies for ESIA, when the $\delta^{13}C$ approach of this thesis is combined with $\delta^{2}H$ analysis.

In conclusion, this thesis highlighted the potential of isotope ratios to deliver new insights into transformation reactions by pioneering CSIA of a pharmaceutical and ESIA of herbicides. Much can be expected when future work will transfer the approach of this thesis to one of the other 10,000 pharmaceuticals on the market,[12] or when the possibilities of ESIA will be used to study chiral blockbuster drugs, such as ibuprofen or metoprolol.

References

1. Meckenstock, R. U.; Morasch, B.; Matthias, K., M.; Vieth, A.; Richnow, H. H., Assessment of bacterial degradation of aromatic hydrocarbons in the environment by analysis of stable carbon isotope fractionation. *Water, Air, & Soil Pollution: Focus* **2002,** *V2*, (3), 141-152.

2. Schmidt, T. C.; Zwank, L.; Elsner, M.; Berg, M.; Meckenstock, R. U.; Haderlein, S. B., Compound-specific stable isotope analysis of organic contaminants in natural environments: a critical review of the state of the art, prospects, and future challenges. *Anal. Bioanal. Chem.* **2004,** *378*, (2), 283-300.

3. Berg, M.; Bolotin, J.; Hofstetter, T. B., Compound-specific nitrogen and carbon isotope analysis of nitroaromatic compounds in aqueous samples using solid-phase microextraction coupled to GC/IRMS. *Anal. Chem.* **2007,** *79*, (6), 2386-2393.

4. Morasch, B.; Richnow, H. H.; Vieth, A.; Schink, B.; Meckenstock, R. U., Stable isotope fractionation caused by glycyl radical enzymes during bacterial degradation of aromatic compounds. *Applied and Environmental Microbiology* **2004,** *70*, (5), 2935-2940.

5. Badea, S.-L.; Vogt, C.; Gehre, M.; Fischer, A.; Danet, A.-F.; Richnow, H.-H., Development of an enantiomer-specific stable carbon isotope analysis (ESIA) method for assessing the fate of alpha-hexachlorocyclohexane in the environment. *Rapid Communications in Mass Spectrometry* **2011,** *25*, (10), 1363-1372.

6. Schreglmann, K.; Hoeche, M.; Steinbeiss, S.; Reinnicke, S.; Elsner, M., Carbon and nitrogen isotope analysis of atrazine and desethylatrazine at sub-microgram per liter concentrations in groundwater. *Anal. Bioanal. Chem.* **2013,** *405*, (9), 2857-2867.

7. Ternes, T. A., Occurrence of drugs in German sewage treatment plants and rivers. *Water Research* **1998,** *32*, (11), 3245-3260.

8. Björklund, E.; Anskjær, G. G.; Hansen, M.; Styrishave, B.; Halling-Sørensen, B., Analysis and environmental concentrations of the herbicide dichlobenil and its main metabolite 2,6-dichlorobenzamide (BAM): A review. *Science of The Total Environment* **2011,** *409*, (12), 2343-2356.

9. Encinas, S.; Bosca, F.; Miranda, M. A., Phototoxicity associated with diclofenac: A photophysical, photochemical, and photobiological study on the drug and its photoproducts. *Chemical Research in Toxicology* **1998,** *11*, (8), 946-952.

10. Meyer, A. H.; Penning, H.; Elsner, M., C and N isotope fractionation suggests similar mechanisms of microbial atrazine transformation despite involvement of different Enzymes (AtzA and TrzN). *Environ. Sci. Technol.* **2009,** *43*, (21), 8079-8085.

11. Penning, H.; Sorensen, S. R.; Meyer, A. H.; Aamand, J.; Elsner, M., C, N, and H Isotope Fractionation of the Herbicide Isoproturon Reflects Different Microbial Transformation Pathways. *Environ. Sci. Technol.* **2010,** *44*, (7), 2372-2378.

12. Everts, S., DRUGS IN THE ENVIRONMENT. *Chemical & Engineering News* **2010,** *88*, (13), 23-24.

APPENDIX

Appendix A1. COMPOUND-SPECIFIC ISOTOPE ANALYSIS OF BENZOTRIAZOLE AND ITS DERIVATIVES

Anal Bioanal Chem (2013) 405:2843–2856
DOI 10.1007/s00216-012-6526-1

ORIGINAL PAPER

Compound-specific isotope analysis of benzotriazole and its derivatives

Stephanie Spahr · Sebastian Huntscha · Jakov Bolotin · Michael P. Maier · Martin Elsner · Juliane Hollender · Thomas B. Hofstetter

Received: 17 September 2012 / Revised: 19 October 2012 / Accepted: 24 October 2012 / Published online: 9 December 2012
© Springer-Verlag Berlin Heidelberg 2012

Abstract Compound-specific isotope analysis (CSIA) is an important tool for the identification of contaminant sources and transformation pathways, but it is rarely applied to emerging aquatic micropollutants owing to a series of instrumental challenges. Using four different benzotriazole corrosion inhibitors and its derivatives as examples, we obtained evidence that formation of organometallic complexes of benzotriazoles with parts of the instrumentation impedes isotope analysis. Therefore, we propose two strategies for accurate $\delta^{13}C$ and $\delta^{15}N$ measurements of polar organic micropollutants by gas chromatography isotope ratio mass spectrometry (GC/IRMS). Our first approach avoids metallic components and uses a Ni/Pt reactor for benzotriazole combustion while the second is based on the coupling of online methylation to the established GC/IRMS setup. Method detection limits for on-column injection of benzotriazole, as well as its 1-CH_3-, 4-CH_3-, and 5-CH_3-substituted species were 0.1–0.3 mM and 0.1–1.0 mM for $\delta^{13}C$ and $\delta^{15}N$ analysis respectively, corresponding to injected masses of 0.7–1.8 nmol C and 0.4–3.0 nmol N, respectively. The Ni/Pt reactor showed good precision and was very long-lived (>1000 successful measurements). Coupling isotopic analysis to offline solid-phase extraction enabled benzotriazole-CSIA in tap water, wastewater treatment effluent, activated sludge, and in commercial dishwashing products. A comparison of $\delta^{13}C$ and $\delta^{15}N$ values from different benzotriazoles and benzotriazole derivatives, both from commercial standards and in dishwashing detergents, reveals the potential application of the proposed method for source apportionment.

Keywords CSIA · Gas chromatography isotope ratio mass spectrometry · Benzotriazole · Corrosion inhibitors · Micropollutants · Source identification

Introduction

The increasing contamination of water resources with organic micropollutants is a major environmental problem [1, 2]. Many of the synthetic chemicals that are currently introduced into the aquatic environment through human activity are relatively polar and therefore quite mobile [2]. Assessing the exposure of humans and the environment to aquatic micropollutants is challenging, however, because knowledge of degradation is often elusive and estimates on the amount of degraded contaminant can barely be obtained. Moreover, the widespread use of anthropogenic chemicals also leads to multiple contamination sources that are difficult to distinguish. It has therefore been proposed to use compound-specific isotope analysis (CSIA) to assess micropollutant degradation processes in individual micropollutants [3, 4].

As has been shown for *traditional* organic contaminants such as chlorinated solvents, fuel additives, and explosives,

---

Published in the topical collection *Isotope Ratio Measurements: New Developments and Applications* with guest editors Klaus G. Heumann and Torsten C. Schmidt.

Electronic supplementary material The online version of this article (doi:10.1007/s00216-012-6526-1) contains supplementary material, which is available to authorized users.

S. Spahr · S. Huntscha · J. Bolotin · J. Hollender ·
T. B. Hofstetter (✉)
Environmental Chemistry, EAWAG, Überlandstrasse 133,
8600 Dübendorf, Switzerland
e-mail: Thomas.Hofstetter@eawag.ch

M. P. Maier · M. Elsner
Institute of Groundwater Ecology, Helmholtz Zentrum München,
Ingolstädter Landstr. 1, 85764 Neuherberg, Germany

CSIA is ideally suited to contribute to the fate assessment [3–7]. Conservative isotope signatures enable source apportionment while changing isotope signatures provide robust evidence for (bio)degradation and its pathways. However, to carry out CSIA using the typical instrumentation (i.e., gas chromatography coupled to isotope ratio mass spectrometry, GC/IRMS), a series of challenges have to be addressed. (a) GC/IRMS systems exhibit rather poor sensitivity requiring extensive sample enrichment, which can, in principle, lead to isotope fractionation artifacts [5, 6, 8]. (b) Many contaminants contain polar functional groups (alcohol, amino, or carboxyl groups, N-heteroatoms) that reduce their volatility and thermal stability thus compromising their analysis by GC/IRMS. (c) Some compounds are suspected to be converted incompletely to analyte gases (i.e., CO_2 and N_2) leading to high detection limits and inaccurate isotope ratio measurements [9]. (d) Finally, several micropollutants have the potential to form organometallic complexes that may hinder isotopic analysis due to the presence of metals (e.g., stainless steel, Cu, Ni, Pt) in commercial GC/IRMS systems.

In this study, we present an approach for CSIA of benzotriazoles, representing an important class of emerging micropollutants. Because benzotriazoles are mobile and persistent, they are widely found in rivers, lakes, and groundwater in the nanograms per liter up to the low micrograms per liter range [10–15]. 1H-benzotriazole (1H-BT) and its methylated derivatives 4-methyl-benzotriazole (4-CH_3-BT) and 5-methyl-benzotriazole (5-CH_3-BT, which is often used in technical tolyltriazole mixtures including 4-CH_3-BT) are high production volume chemicals with a worldwide annual production in the range of 9000 tons/year [16]. They are widely used as corrosion inhibitors in aircraft deicing and anti-icing fluids, cooling liquids, and brake fluids as well as for silver protection in dishwashing detergents [17, 18]. Benzotriazole and its derivatives also play an important role as synthetic auxiliaries in organic chemistry [19] and are used for UV stabilization in plastics [20].

Knowledge of the processes governing benzotriazole transport and transformation in aquatic environments is, despite recent advances, scarce [21, 22]. CSIA can offer additional insight into mechanisms of transformation processes and could enable one to identify contaminant sources. It was therefore the goal of this study to provide methods for accurate, that is true and precise C and N isotope analysis of benzotriazoles by CSIA and to apply one of them for environmental analysis and supplier identification of benzotriazoles in dishwashing detergents. However, isotopic analysis of benzotriazoles by conventional GC/IRMS is challenging, because benzotriazoles are not only very polar but also exhibit low vapor pressures [13] and tend to form complexes at metal surfaces (e.g., with Cu alloys, [23, 24]), so that interactions of benzotriazoles with metal-containing parts present in GC/IRMS systems can compromise isotopic analysis. We therefore evaluated two complementary approaches including (a) the replacement of metal parts in a typical GC/IRMS system (*modified* standard setup) and (b) the derivatization of benzotriazoles to less polar and more volatile products which do not form strong metal complexes (online derivatization). The *modified* standard setup was further investigated for CSIA of 1H-BT and three methylated benzotriazole species (1-CH_3-/4-CH_3-/5-CH_3-BT) in environmental matrices and in dishwashing detergents. To this end, we tested the benzotriazole enrichment by solid-phase extraction (SPE) and its coupling to isotopic analysis in tap water, wastewater treatment plant effluent, and in activated sludge as well as in commercial dishwashing products.

Experimental section

A complete list of all used chemicals including abbreviations, purities, and suppliers, as well as a description of the sampling procedure at the wastewater treatment plant, is provided in the Electronic Supplementary Material (Table S1).

Solid-phase extraction

The performance of three commercially available SPE cartridges containing the three following adsorbent materials was compared with regard to purification and enrichment of benzotriazoles: (1) Oasis HLB (6 cm^3 cartridges, 200 mg; Waters, Milford, MA, USA), a reversed-phase sorbent, was used to retain neutral benzotriazole species (sample pH 2.0); (2) ENVI-Carb (Supelclean ENVI-Carb SPE tubes 6 cm^3, 250 and 500 mg; Supelco; Bellefonte, PA, USA), a graphitized carbon material, was tested as an alternative sorbent for neutral benzotriazole species (sample pH 2.0); and (3) Oasis MAX (6 cm^3 cartridges, 150 mg; Waters, MA, USA), a mixed-mode anion exchange sorbent, was used to retain anionic benzotriazole species (sample pH 10.6). All SPE materials were evaluated with three different matrices, namely, tap water, wastewater treatment plant effluent, and activated sludge.

Depending on the used SPE sorbent, the pH of 100-mL sample was adjusted to 2.0 ± 0.1 with 1 M HCl or to 10.6 ± 0.1 with 5 % NH_4OH. Samples were then spiked with benzotriazoles to obtain final concentrations of 0.5, 1.5, or 2.5 μM 1-CH_3-BT and 1, 3, or 5 μM 1H-BT, 4-CH_3-BT, and 5-CH_3-BT, respectively. A blank was run under identical conditions except for the addition of benzotriazoles. All samples were filtered with 0.7 µm GF-F filters (glass microfiber filters, Whatman, 47 mm) after the addition of benzotriazoles and percolated through the conditioned cartridges with a flow rate of approximately 1 mL/min. Subsequently, the cartridges were washed with 4–5 mL water, dried for at least 1 h at room temperature and benzotriazoles were eluted with 10 mL of different organic solvents. Detailed SPE protocols are provided in Table S2. For GC/MS analysis, extracts were evaporated at 30 °C under a gentle stream of N_2 to 1 mL and further diluted with ethyl acetate to obtain benzotriazole concentrations within the calibrated range of the instrument (8–40 µM). GC/IRMS analysis required further solvent evaporation to achieve a final volume of 100 µL.

Domestic dishwashing detergents

Domestic dishwashing powders and tabs from 12 commercial products were crushed with a pestle, and varying amounts (10–100 mg) were dissolved in 100 mL nanopure water. Dissolution was achieved after 15 min of sonication. Subsequently, the pH of each sample was adjusted to 2.0 ± 0.1 with 1 M HCl, and samples were enriched by SPE using Oasis HLB cartridges. For GC/MS and GC/IRMS analysis, sample extracts were evaporated under a gentle flow of N_2 to 1 mL and 100 µL, respectively.

GC/MS analysis

Modified standard setup Concentration analysis of benzotriazoles was conducted with a GC/MS system (TRACE GC Ultra/TRACE DSQ EI 250, Thermo). Liquid samples (1 µL in ethyl acetate) were injected with a Combi PAL autosampler (CTC Analytics) in a split/splitless injector operated for 1 min in splitless and then in split mode with a split flow of 50 mL/min at a temperature of 200 °C. Helium was used as carrier gas at constant pressure (100 kPa). The GC was equipped with 1 m of an OV-1701-OH deactivated fused-silica guard column (660 µm OD, 530 µm ID, BGB Analytik), a 30 m × 0.32 mm RTX-5 Amine column (Crossbond 5 % diphenyl/95 % dimethyl polysiloxane, 1 µm df, Restek), and 0.4 m OV-1701-OH deactivated fused-silica postcolumn (450 µm OD, 180 µm ID, BGB Analytik). Universal PressFit Connectors (0.3 to 0.75 mm OD, deactivated, BGB Analytik) and a Universal PressFit 4-way X-splitter (0.2 to 0.75 mm OD, deactivated, BGB Analytik) were used. The temperature program used to obtain baseline-separated analyte peaks was 1 min at 80 °C, 15 °C/min to 180 °C (10 min), and 40 °C/min to 250 °C (5 min). Benzotriazoles were quantified with external calibration using seven standard mixtures containing the four benzotriazole species in concentrations ranging from 8 to 40 µM. The mass spectrometer was operated in the full scan mode (m/z 50–400).

Online derivatization of benzotriazoles Benzotriazole online derivatization by trimethylsulfonium hydroxide (TMSH) was carried out using the same GC/MS instrument, setup, and injector (at 230 °C) described above. Each single benzotriazole standard (1 mM in ethyl acetate) was mixed with TMSH in 50-fold excess (25 mM ethyl acetate) to obtain analyte concentrations of 40 µM. Benzotriazole derivatives were identified based on GC/MS retention times and mass spectra. Tentative derivatization efficiencies were estimated from the lowest detectable concentration of underivatized benzotriazole ($c^{\mathrm{BT}}_{\mathrm{min}}$), and the theoretical concentration of benzotriazole injected with TMSH ($c^{\mathrm{BT}}_{\mathrm{theoretical,TMSH}}$), as follows:

$$\text{Derivatization efficiency} = \left(1 - \frac{c^{\mathrm{BT}}_{\mathrm{min}}}{c^{\mathrm{BT}}_{\mathrm{theoretical,TMSH}}}\right) \cdot 100\ \% \tag{1}$$

GC/IRMS analysis

Modified standard setup Analysis of δ^{13}C and δ^{15}N values of pure chemicals was carried out using a TRACE GC coupled to an isotope ratio mass spectrometer via a GC Combustion III interface (GC/IRMS 1, Thermo). C and N isotope analysis were almost identical, except for cryogenic trapping of CO_2 in liquid N_2 during δ^{15}N measurements. The GC setup and the temperature program were identical to GC/MS analysis described in Section "Modified standard setup" except for the larger postcolumn inner diameter (320 µm). The self-made oxidation reactor consisted of a ceramic tube (1.5 mm OD, 0.55 mm ID, 32 cm length, Thermo) containing two nickel wires (diameter 0.1 mm, length 30 cm, purity 99.99 %, Alfa Aesar) and one platinum wire (diameter 0.1 mm, length 30 cm, purity 99.99 %, Goodfellow). The same Ni/Ni/Pt reactor (referred to as Ni reactor in the succeeding text) operated at 1000 °C was used for C and N isotope analysis. One Ni reactor was used throughout the study covering approximately 1200 measurements. After every measurement, the reactor was reoxidized for 20 min with a continuous O_2 stream at 1000 °C after optimum reoxidation times had been evaluated between 1 and 30 min (data not shown). For reduction of nitrogen oxides, a standard reduction reactor (Thermo) containing three wires of copper was operated at 650 °C.

C and N isotope ratios are expressed in the delta notation as $\delta^{13}C$ and $\delta^{15}N$, respectively, (Eq. 2), in which the concentrations of heavy (^{h}E) and light (^{l}E) isotopologs of C and N (designated as element E) are reported relative to Vienna Pee Dee Belemnite and air, respectively.

$$\delta^{h}E\,[‰] = \frac{\left(^{h}E/^{l}E\right)_{\text{sample}}}{\left(^{h}E/^{l}E\right)_{\text{standard}}} - 1 \qquad (2)$$

To evaluate the trueness and precision of isotope measurements, the C and N isotope composition of four benzotriazole standards (1H-BT, 1-CH_3-, 4-CH_3-, 5-CH_3-BT) was measured by an elemental analyzer (EA, Carlo Erba) coupled to an IRMS (EA/IRMS, Fisons Optima, Table S4). Trueness of isotope signatures, $\Delta\delta^{h}E$, is reported as deviation of the isotope ratio measurements by GC/IRMS ($\delta^{h}E_{\text{GC/IRMS}}$) from the reference isotope signatures of four in-house working standards ($\delta^{h}E_{\text{ref}}$, Eq. 3). If not specified otherwise, isotope signatures are reported as arithmetic mean of triplicate measurements with 1 standard deviation ($\pm\sigma$) as measure for instrumental precision.

$$\Delta\delta^{h}E = \delta^{h}E_{\text{GC/IRMS}} - \delta^{h}E_{\text{ref}} \qquad (3)$$

Online derivatization approach For the online derivatization approach, a different GC/IRMS instrumentation (GC/IRMS 2) was used that is described in detail in Reinnicke et al. [25]. Online derivatization of benzotriazole with TMSH was carried out using a programmable temperature vaporizer (PTV) injector (Optic 3-SC High Power Injection System, ATAS GL International B.V.) equipped with a large-volume glassbead liner (PAS Technology). Between 1 and 100 µL of a premixed solution with 0.8 mM 1H-BT (Fluka) and TMSH (250-fold excess) in methanol was injected via a GC Pal autosampler into the glassbead liner at 40 °C. Depending on the injected sample volume, a vent time between 30 s (for 1 µL) and 630 s (for 100 µL) was used with a split flow of 50 mL/min to remove the solvent (methanol). Subsequently, the split flow was set to 0 mL/min for 60 s (column flow 1.4 mL/min) and the injector was heated with a rate of 7 °C/s to 300 °C. The GC setup and the temperature program were identical to the GC/MS analysis described in Section "Modified standard setup." A commercially available Ni tube/NiO-CuO combustion reactor with a silcosteel capillary (Thermo) operated at 1000 °C was used for $\delta^{13}C$ and $\delta^{15}N$ analysis and was reoxidized after approximately 40 injections. For reduction of nitrogen oxides, a standard reduction reactor (Thermo) was operated for N isotope measurements at 640 °C. Isotope signatures for 1H-BT were calculated as follows using the isotope values of the derivatives (1-CH_3-BT and 2-CH_3-BT) and the corresponding peak areas of mass 28 or 44 (A^{28} and A^{44}), respectively. The calculation of $\delta^{13}C$ values for 1H-BT further required correction for the introduced carbon atom through methylation ($\delta^{13}C_{\text{EA,TMSH}}$).

$$\delta^{15}N_{1\text{HBT}}\,[‰] = \frac{\delta^{15}N_{1\text{CH}_3\text{BT}} \cdot A^{28}_{1\text{CH}_3\text{BT}} + \delta^{15}N_{2\text{CH}_3\text{BT}} \cdot A^{28}_{2\text{CH}_3\text{BT}}}{A^{28}_{1\text{CH}_3\text{BT}} + A^{28}_{2\text{CH}_3\text{BT}}} \qquad (4)$$

$$\delta^{13}C_{1\text{HBT}}\,[‰] = \frac{7}{6} \cdot \left(\frac{\delta^{13}C_{1\text{CH}_3\text{BT}} \cdot A^{44}_{1\text{CH}_3\text{BT}} + \delta^{13}C_{2\text{CH}_3\text{BT}} \cdot A^{44}_{2\text{CH}_3\text{BT}}}{A^{44}_{1\text{CH}_3\text{BT}} + A^{44}_{2\text{CH}_3\text{BT}}}\right) - \frac{1}{6} \cdot \delta^{13}C_{\text{EA,TMSH}} \qquad (5)$$

Online derivatization approach vs. modified standard setup For method comparison, the online derivatization approach and the *modified* standard setup were implemented consecutively on the same GC/IRMS instrument. Therefore, GC/IRMS 2 that was used for the online derivatization approach was equipped with the same guard, chromatographic, and postcolumn as well as with the same self-made oxidation reactor than used in the *modified* standard setup. Between 1 and 100 µL benzotriazole standard compound in ethyl acetate (without TMSH) was then injected onto the GC column via the PTV injector which was heated with a rate of 5 °C/s to 230 °C.

Method detection limits Instrument linearity and method detection limits (MDLs) were determined from isotope ratio measurements of four benzotriazole working standards at different concentrations following the moving mean procedure proposed by Jochmann et al. [26]. Injected concentration ranges were 0.025–1 mM and 0.125–5 mM for $\delta^{13}C$ and $\delta^{15}N$ analysis, respectively. MDLs were determined using two different uncertainty intervals: (a) constant $\delta^{13}C$ and $\delta^{15}N$ intervals of ±0.5 and ±1 ‰, respectively (referred to as MDL), and (b) variable intervals covering $\pm 2\sigma$ of all data points used for the calculation of the moving mean ($MDL_{2\sigma}$).

Results and discussion

Analytical strategies for CSIA of benzotriazoles by GC/IRMS

Isotopic analyses of 1H-, 4-CH_3-, and 5-CH_3-benzotriazoles by standard GC/IRMS systems via on-column injection did not lead to detectable peaks even at high analyte concentrations (up to 15 mmol/L) while that of 1-CH$_3$-benzotriazole was feasible (Fig. 1a). Because the ability of benzotriazoles to form organometallic complexes requires nitrogen lone pair electrons [23, 24], our observation suggests that interactions of 1H-, 4-CH$_3$-, and 5-CH$_3$-benzotriazoles with metal parts of the GC/IRMS system, in particular with Cu in the Cu/Ni/Pt-containing oxidation reactor, impede isotopic analysis. As shown in Fig. 1b, replacing stainless steel-containing parts by silicate-based ones (PressFit Connectors, PressFit X-Splitter, Section "Modified standard setup") and removing Cu wires from the oxidation reactor enabled us to carry out CSIA of all four benzotriazole species. This approach is henceforth referred to as the *modified* standard setup which was, unless otherwise specified, implemented on GC/IRMS 1. Alternatively, as implied by the isotopic analyses of 1-CH$_3$-benzotriazole, N-methylation on the triazole ring reduces interactions of the molecule with metal surfaces [24] and thus allows one to use Cu-containing, *standard* GC/IRMS systems for benzotriazole-CSIA. An example of such a derivatization using TMSH is shown in Fig. 1c–g and the isotope analysis of derivatized benzotriazoles is discussed in Section "Benzotriazole-CSIA using online derivatization".

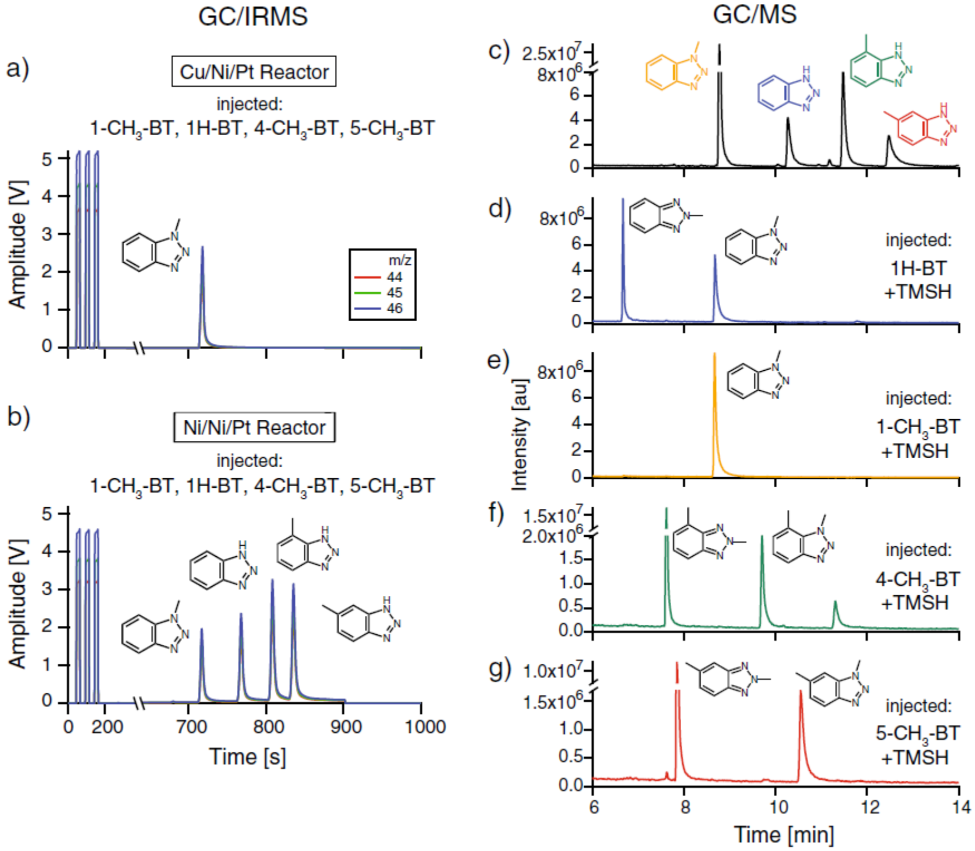

Fig. 1 GC/IRMS chromatograms (*left*): **a** 1-CH$_3$-BT was the only compound detected from a mixture of 1H-BT, 1-CH$_3$-, 4-CH$_3$-, and 5-CH$_3$-BT by conventional isotope analysis with GC/IRMS systems containing a Cu/Ni/Pt oxidation reactor; **b** all four benzotriazoles were detected when the same mixture was analyzed using the *modified* standard setup containing a Ni/Ni/Pt oxidation reactor (GC/IRMS 1). GC/MS chromatograms (*right*) of **c** four underivatized benzotriazole species, **d** derivatization products of 1H-BT methylation with trimethylsulfonium hydroxide (TMSH) identified as 1-CH$_3$-BT and 2-CH$_3$-BT with standard compounds, **e** 1-CH$_3$-BT, which was not further methylated upon derivatization, **f** derivatization products of 4-CH$_3$-BT methylation, and **g** derivatization products of 5-CH$_3$-BT. Molecular structures of derivatization products for 4-CH$_3$- and 5-CH$_3$-BT methylation are suggested based on mass spectrometric analyses without confirmation by standard compounds. Derivatization of 4-CH$_3$-BT led to a third unidentified peak of low intensity

C and N isotope analysis of benzotriazoles using the *modified* standard setup

Reproducibility More than 1000 C and N isotope measurements of the four benzotriazole working standards were carried out with the *modified* standard setup. C and N isotope signatures were highly reproducible over the whole period of analysis (Table 1, Fig. S2). Even if long-term instrumental variabilities are included, good precisions (expressed as $\pm\sigma$) of ±0.6–1.0 ‰ ($n = 79$) for C and ±0.1–0.3 ‰ ($n = 16 - 77$) for N isotope analysis were achieved. Furthermore, δ^{13}C and δ^{15}N values were consistent with reference isotope values determined by EA/IRMS. The trueness was within $\leq +0.5$ ‰ for C and ≤ -0.6 ‰ for N isotope measurements and was thus within typical uncertainties of ±0.5 ‰ and ±1 ‰ reported for GC/IRMS analysis of C and N isotope ratios, respectively [27–29]. δ^{13}C signatures of 1-CH_3-BT showed lower precision and a reproducible offset by −2.3 ± 1.8 ‰ ($n = 15$) possibly due to not fully optimized instrumental procedures at the beginning of the study. Notice the limited number of analyses owing to the depletion of our calibrated in-house standard for 1-CH_3-BT. Further analysis of 1-CH_3-BT with non-calibrated material nevertheless confirms the observed trends. C and N isotope signatures of 1-CH_3-BT did not deviate by more than ±1.5 and ±0.3 ‰ from the mean of all measurements, and precisions were ±0.5 ‰ ($n = 63$) and ±0.1 ‰ ($n = 58$) for C and N isotope measurements, respectively.

Method detection limits for accurate isotope analysis The performance of C and N isotope ratio measurements using the *modified* standard setup was determined as a function of injected benzotriazole concentration (Figs. 2 and S3). MDLs were then derived according to the moving mean procedure as the smallest analyte concentration level, for which isotope values were within predefined intervals covering the total analytical uncertainty [26]. Measures for the total analytical uncertainty of CSIA are typically ±0.5 ‰ for δ^{13}C analysis of commonly measured compounds such as (chloro)hydrocarbons, but they are poorly constrained for micropollutants and especially for their δ^{15}N measurements (±1 ‰) [6, 28, 30]. Therefore, we also calculated MDLs using an uncertainty interval of $\pm 2\sigma$ representing our measurement's precision.

For δ^{13}C analysis of benzotriazoles, MDLs of 0.1–0.3 mM (corresponding to 0.7–1.8 nmol C) were determined using an uncertainty interval of ±0.5 ‰. Except for analysis of 1-CH_3-BT, identical results were obtained if the

Table 1 Trueness and precision ($\pm\sigma$) of C and N isotope measurements of four benzotriazole working standards as well as δ^{13}C and δ^{15}N values of eight additional aromatic, N-heterocyclic compounds determined with the *modified* standard setup (GC/IRMS 1). Unless specified otherwise, isotope signatures are reported as arithmetic mean ($\pm\sigma$) of triplicate measurements

	GC/IRMS			
Compound	δ^{13}C [‰]	$\Delta\delta^{13}$C [‰][a]	δ^{15}N [‰]	$\Delta\delta^{15}$N [‰][a]
1H-BT	−26.0 ± 1.0[b]	0.5 ± 1.0[b]	−27.4 ± 0.1[c]	−0.3 ± 0.1[c]
1-CH_3-BT	−33.4 ± 1.8[d]	−2.3 ± 1.8[d]	−33.5 ± 0.1[e]	−0.2 ± 0.1[e]
4-CH_3-BT	−28.8 ± 0.6[b]	0.0 ± 0.6[b]	−4.2 ± 0.3[c]	−0.6 ± 0.3[c]
5-CH_3-BT	−27.6 ± 0.6[b]	0.0 ± 0.6[b]	−15.9 ± 0.3[c]	−0.1 ± 0.3[c]
1-CH_3OCH_2-BT	−32.6 ± 0.1	-[f]	0.9 ± 0.0	-
Benzothiazole	−28.9 ± 0.1	-	−2.1 ± 0.1	-
1-CH_2Cl-BT	−28.5 ± 0.0	-	−5.7 ± 0.1	-
Skatole	−25.2 ± 0.0	-	1.7 ± 0.1	-
Quinoline	−21.8 ± 0.1	-	3.3 ± 0.0	-
Indole	−19.5 ± 0.1	-	6.3 ± 0.2	-
5,6-$(CH_3)_2$-BT	-	-	−23.5 ± 0.3	-
1-CH_2OH-BT	-	-	−6.3 ± 0.1	-

[a] Trueness is expressed as mean deviation of isotope signatures measured with GC/IRMS from the reference isotope signatures determined by EA/IRMS

[b] $n = 79$

[c] $n = 77$

[d] $n = 15$

[e] $n = 16$

[f] Hyphen (-) = not determined

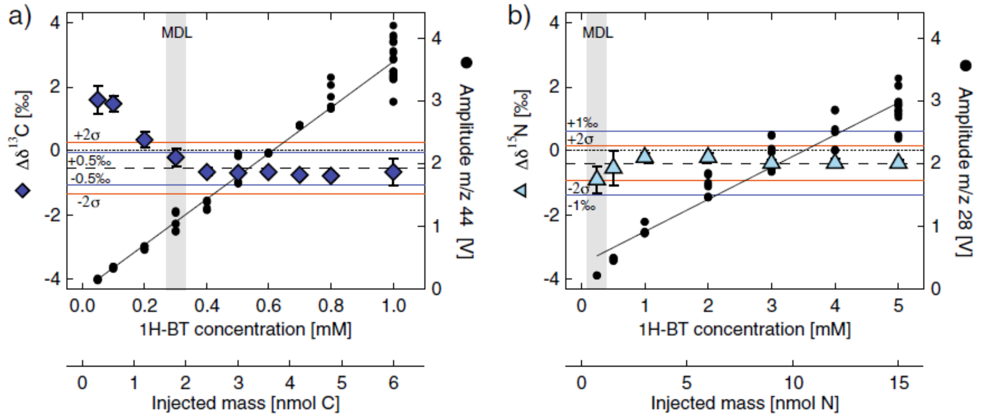

Fig. 2 Accuracies of **a** C and **b** N isotope signatures of 1H-BT determined with the *modified* standard setup (GC/IRMS 1) for a concentration range of 0.05–1 mM and 0.25–5 mM, respectively. Amplitudes increased linearly with higher injected concentrations. *Gray bars* indicate MDLs determined according to the moving mean procedure [26] with intervals of ±0.5 ‰ and ±1 ‰ for C and N isotope analysis (*blue lines*), as well as with intervals of ±2σ (*red lines*). Moving means are indicated by *dashed lines*

MDL definition was based on the ±2σ interval (Figs. 2a and S3, Table 2). MDLs for δ^{15}N analysis of benzotriazoles were derived for uncertainty intervals of ±1 ‰ and ±2σ (Fig. 2b). Due to very accurate N isotope measurements of benzotriazoles, MDLs of 0.125–0.25 mM (0.4–0.8 nmol N) coincided with the lowest measured concentrations and peak amplitudes and were, again, independent of the uncertainty definition. Only for δ^{15}N measurements of 5-CH$_3$-BT, a higher MDL$_{2\sigma}$ of 1 mM (3.0 nmol N) was determined (Table 2).

Conversion efficiency The accurate and highly reproducible C and N isotope signatures as well as low MDLs suggest an efficient conversion of benzotriazoles to analyte gases (CO$_2$ and N$_2$). To verify this hypothesis, we analyzed seven C- and N-containing in-house standards (*n*-alkanes, substituted aromatic amines, nitrobenzene, atrazine) with the *modified* standard setup. Conversion efficiencies were operationally defined as the slope of the linear regression between signal area of mass 44 and 28, respectively, per theoretical injected mass of C and N.‰ Conversion efficiencies were derived

Table 2 Method detection limits (MDL) for C and N isotope analysis of benzotriazoles with the *modified* standard setup (GC/IRMS 1) determined according to the moving mean procedure [26] with intervals of ±0.5 ‰ and 1 ‰, respectively, and ±2σ. MDLs are expressed as injected benzotriazole concentration (mM) and as corresponding mass of injected C and N (nmol). Corresponding peak amplitudes are reported in mV

	δ^{13}C			δ^{15}N		
	MDL[a]		Amp 44[c]	MDL[b]		Amp 28[c]
	[mM]	[nmol C]	[mV]	[mM]	[nmol N]	[mV]
1H-BT	0.3	1.8	1060 ± 130	0.25	0.8	210 ± 2
1-CH$_3$-BT	0.2[d]/0.1[e]	1.4/0.7	1470 ± 70[d]/750 ± 25[e]	0.125	0.4	150 ± 1
4-CH$_3$-BT	0.1	0.7	420 ± 10	0.25	0.8	220 ± 2
5-CH$_3$-BT	0.2	1.4	625 ± 50	1.0	3.0	790 ± 115

[a] Determined with an interval of ±0.5 ‰ or ± 2σ = 0.8, 1.2, 1.4, and 1.1 ‰ for 1H-BT, 1-CH$_3$-, 4-CH$_3$-, and 5-CH$_3$-BT, respectively

[b] Determined with an interval of ±1 ‰ or ± 2σ = 0.5, 0.6, 0.6, and 1.5 ‰ for 1H-BT, 1-CH$_3$-, 4-CH$_3$-, and 5-CH$_3$-BT, respectively

[c] Amplitude ±σ

[d] Interval ±0.5 ‰

[e] Interval ±2σ (=1.2 ‰)

from analysis of 1.8 to 7.2 nmol C and 1.5 to 15 nmol N per substance, resulting in signal areas between 1 and 50 Vs and amplitudes ranging from 1.2 to 10 V ($\delta^{13}C$) and 0.09 to 3.4 V ($\delta^{15}N$), respectively. Figure 3 depicts the conversion efficiencies of the tested compounds to CO_2 and N_2, respectively, grouped by substance class.

n-Alkanes are reported to be the most readily combusted and most completely converted to CO_2 [31]. Indeed dodecane showed the highest operational CO_2-conversion efficiency (5.9 Vs/nmol C). Decane conversion efficiency, in contrast, only attained 82 % of the dodecane value. The comparison of combustion efficiency ranges suggests that benzotriazole conversion to CO_2 was also high. The four benzotriazole species showed operational conversion efficiencies between 3.7 and 5.0 Vs/nmol C, which corresponded to 62–85 % of the dodecane conversion efficiency (Fig. 3a). All benzotriazole species were converted to a similar extent suggesting that the presence and position of a methyl substituent did not affect oxidation. Indeed, evidence for similar combustion properties of aliphatic and aromatic compounds has also been reported for *n*-hexane and toluene [32]. Moreover, the conversion of N-heterocycles seems favored over that of two aromatic amines (4-chloroaniline, diphenylamine), which only reached 35 % conversion to CO_2. Given that $\delta^{13}C$ values of all the N-containing compounds analyzed here can be determined accurately [30, 33–36], our data illustrate that a better conversion contributes to lower MDLs but is not prerequisite for accurate isotope analysis.

N_2-conversion efficiencies additionally support the conclusion that benzotriazoles were efficiently converted to analyte gases by the Ni/Pt reactor used in the *modified* standard setup. All benzotriazoles were most efficiently transformed to N_2 compared to amino and nitro groups in aromatic amines and nitrobenzene (Fig. 3b). It is interesting to note that atrazine, which was successfully analyzed with a similar self-made Ni/NiO reactor operated at 1150 °C in previous studies [34], could not be measured using the *modified* standard setup. We speculate that this result might be due to the lower reactor temperature used here (1000 °C).

Our comparison of conversion efficiency further underscores the need of standard materials and procedural guidelines for developing CSIA methods for organic micropollutants [6]. As illustrated here and shown previously [31, 37], conversion efficiencies strongly depend on the type and temperature of the oxidation reactor. In addition, standard materials are required that can be used under very different chromatographic conditions on a wide variety of IRMS instruments.

Benzotriazole-CSIA using online derivatization

We explored the C- and N-CSIA of benzotriazoles using an online derivatization approach with a conventional Cu/Ni/Pt reactor as the alternative to the *modified* standard setup. As shown in Fig. 1, derivatization with TMSH generates methylated benzotriazoles that do not show the same affinity to Cu and other metal-containing parts and thus can be analyzed in a conventional GC/IRMS system. As outlined in the methods section, derivatization requires one to reconcile isotope signatures measured for multiple methylation products (see tentative product identification in Fig. 1d, f, g)

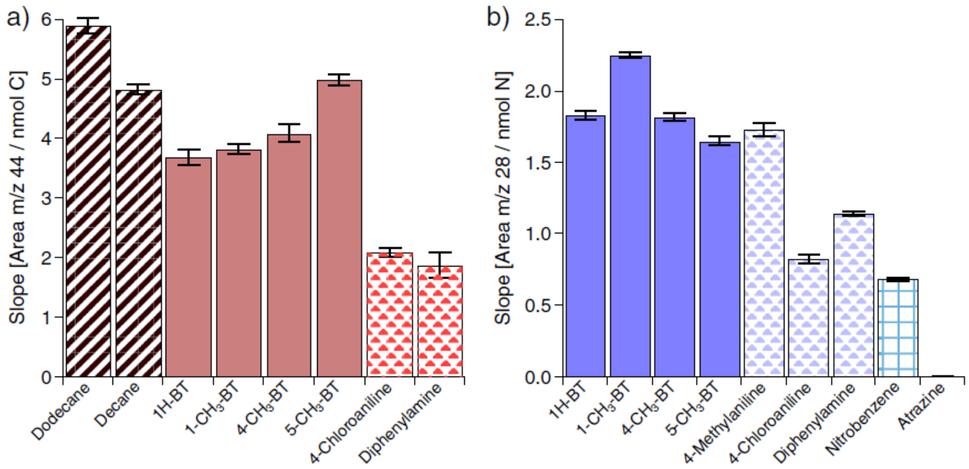

Fig. 3 Conversion of *n*-alkanes (*striped bars*), benzotriazoles (*solid bars*), substituted aromatic amines (*dotted bars*), nitrobenzene (*squared bar*), and atrazine to **a** CO_2 and **b** N_2 by the self-made Ni/Ni/Pt reactor in the *modified* standard setup (GC/IRMS 1). Conversion efficiency is expressed as slope of the linear regression between theoretical injected amount of C or N and corresponding peak area

except for 1-CH_3-BT, which remained unchanged (Fig. 1e). Unfortunately, GC/MS analysis revealed that benzotriazole methylation products have similar retention times than the other benzotriazoles investigated and co-elution would likely have compromised their isotopic analyses (Fig. 1d–g). Therefore, the following comparison of the derivatization-based approach with the *modified* standard setup focuses exclusively on 1H-BT. To enable a direct comparison of the *modified* standard setup and the derivatization approach, both methods were implemented on an identical instrument (GC/IRMS 2).

Comparison of the derivatization approach with the modified standard setup Accurate and reproducible $\delta^{13}C$ and $\delta^{15}N$ values were obtained with both approaches for 1H-BT (Fig. S4). Comparisons were made for the concentration range of 0.8–8 mM (derivatization approach) and 1–10 mM (*modified* standard setup), respectively (Fig. S5). $\delta^{13}C$ values measured with the derivatization approach were of similar trueness (±0.5 ‰ of reference value) than data acquired with the *modified* standard setup except for concentrations below 2 mM, which, on that instrument (GC/IRMS 2), only yielded satisfactory results with the derivatization approach. Both approaches performed equally well for N isotope analysis for 1H-BT concentrations between 3.5 and 10 mM but $\delta^{15}N$ values were slightly offset by −1 ‰. Notice that in contrast to typical sample injection techniques (e.g., on column, split/splitless), the derivatization approach using the PTV injector enables one to inject variable sample sizes (1–10 μL) with constant excess of TMSH. This feature might be beneficial for benzotriazole analysis in environmental samples but was not explored further in this study. Data presented in the following sections were acquired with the *modified* standard setup implemented on GC/IRMS 1.

Solid-phase extraction of benzotriazoles coupled to GC/IRMS (*modified* standard setup)

We tested three different SPE sorbents and protocols to carry out C- and N-CSIA of benzotriazoles in different aqueous matrices, that is tap water, sewage treatment plant effluent, and activated sludge as well as in consumer products. The performance of different SPE sorbents was evaluated based on isotope fractionation, analyte recovery, and interferences from the sample matrix. Regardless of the materials and protocols chosen, no influence of the sample matrix on the analyte recovery was observed as reported earlier [38].

(1) Best results were obtained using Oasis HLB cartridges that were preconditioned with hexane, ethyl acetate, methanol and water, and with sample pH values adjusted to pH 2. Using this optimized protocol (see Table S2), benzotriazole recoveries varied between 80 ± 4 % and 93 ± 5 % (Table S3) and no co-eluting substances interfered with the analytes. Notice that the latter was not the case if Oasis HLB cartridges had not been preconditioned with hexane so that interferences from the cartridge material compromised CSIA of 1-CH_3-BT and 5-CH_3-BT. Method-induced isotope fractionation, denoted as deviation $\Delta\delta^{13}C$ and $\Delta\delta^{15}N$, was negligible regardless of the sample matrices used and was within the uncertainty of analysis (Table 3). Generally, $\Delta\delta^{13}C$ and $\Delta\delta^{15}N$ values were slightly more negative than the reference value suggesting a preferential adsorption of heavy isotopologs. $\Delta\delta^{13}C$ and $\Delta\delta^{15}N$ values of 1H-BT, 4-CH_3-BT, and 5-CH_3-BT were within −0.3 ± 0.8 and −1.5 ± 0.5 ‰. The deviation of the $\delta^{13}C$ value of 1-CH_3-BT (up to −2.6 ± 1.7 ‰) was almost identical to the offset from the reference value measured without SPE (Table 1) suggesting that this deviation did not originate from the enrichment procedure.

(2) Using ENVI-Carb cartridges, benzotriazole recoveries were high (80 ± 1 % to 121 ± 11 %) (Table S3). However, co-eluting peaks impeded C isotope analysis of 1-CH_3-BT and 1H-BT after enrichment from the sludge matrix (Fig. S1). ENVI-Carb cartridges are thus only suited for N-CSIA and C-CSIA of 4-CH_3-BT and 5-CH_3-BT. $\Delta\delta^{13}C$ values of 4-CH_3-BT and 5-CH_3-BT and $\Delta\delta^{15}N$ values of all four benzotriazoles, determined after enrichment of benzotriazoles from activated sludge, showed that isotope fractionation was again negligible and within the analytical uncertainty (Table 3).

(3) SPE with Oasis MAX cartridges, which was based on anion exchange at pH 10.6, led to only low benzotriazole recoveries between 47 ± 10 % and 90 ± 1 % in particular for 1-CH_3-BT due to the lack of ionic interactions with the sorbent material. This option was therefore not considered as a viable strategy for benzotriazole enrichment.

Oasis HLB cartridges were chosen for benzotriazole enrichment prior to C- and N-CSIA, because analyte recoveries were high and neither isotope fractionation nor co-eluting substances were observed after solid-phase extraction.

Source apportionment of benzotriazoles

Isotope signatures of benzotriazoles from different suppliers We analyzed the $\delta^{13}C$ and $\delta^{15}N$ values of various commercially available benzotriazoles from six different suppliers with the *modified* standard setup. The corresponding values for six 1H-BTs, one 4-CH_3-BT, one 5-CH_3-BT,

Table 3 $\delta^{13}C$ and $\delta^{13}N$ values of four benzotriazole working standards determined with the *modified* standard setup (GC/IRMS 1) after solid-phase extraction from three different aqueous matrices using Oasis HLB or ENVI-Carb cartridges

	Oasis HLB[b]			ENVI-Carb[c]
	Tap water	Effluent	Sludge	Sludge
$\Delta\delta^{13}C$ [‰][a]				
1H-BT	−0.3 ± 0.8	−0.3 ± 0.6	−0.7 ± 0.9	–[d]
1-CH_3-BT	−2.6 ± 1.7	−1.9 ± 0.9	−2.2 ± 1.7	–[d]
4-CH_3-BT	−0.8 ± 0.5	−0.8 ± 0.1	−0.6 ± 1.2	1.3 ± 0.5
5-CH_3-BT	−1.4 ± 0.5	−1.3 ± 0.3	−1.5 ± 0.5	0.9 ± 0.7
$\Delta\delta^{15}N$ [‰][a]				
1H-BT	−0.5 ± 0.1	−0.5 ± 0.2	−0.3 ± 0.2	0.4 ± 0.8
1-CH_3-BT	−1.1 ± 0.6	−0.4 ± 0.2	−0.4 ± 0.1	−0.6 ± 0.4
4-CH_3-BT	−0.5 ± 0.4	−0.5 ± 0.4	−1.2 ± 0.5	0.0 ± 0.2
5-CH_3-BT	−0.4 ± 0.3	−0.3 ± 0.4	−0.7 ± 0.8	−0.5 ± 1.2

[a] All uncertainties correspond to $\pm\sigma$ ($n = 3$)

[b] Oasis HLB pH 2 hexane (ethyl acetate elution)

[c] 250 mg, MeOH elution

[d] Co-eluting peaks from the sludge matrix impeded $\delta^{13}C$ analysis

and one tolyltriazole (mixture of 4-CH_3- and 5-CH_3-BT) are reported in Fig. 4a, b and Table S5. While $\delta^{13}C$ of all compounds were confined to the range of −24.8 ‰ to −30.6 ‰, $\delta^{15}N$ values varied considerably more from −4.2 ‰ to −27.5 ‰. This observation is consistent with the reported synthetic routes of benzotriazoles, which involve multistep reactions at N-functional groups of various N-containing precursor materials whereas the carbon skeleton of benzene remains unchanged (see detailed discussion below). In fact, the observed $\delta^{13}C$ values of 1H-, 4-CH_3-, and 5-CH_3-BT correspond to the typical carbon signatures for benzene from petrochemical sources [39]. In contrast, $\delta^{15}N$ values of 1H-BT clustered around −10 ‰ (Ciba and Bayer), −15 ‰ (Ehrenstorfer), −20 ‰ (Aldrich), and −27 ‰ (Fluka) (Fig. 4a). Notice that uncertainties of $\delta^{15}N$ measurements were due to not fully optimized analytical procedures at the very beginning of this study and additional measurements would result in typical variations by ±2 ‰. The observed variability of $\delta^{15}N$ values can arise, in principle, from different precursor materials and/or isotope fractionation during benzotriazole production [40].

Figure 5 depicts reported benzotriazole production pathways. 2-Chloronitrobenzene (compound **1**) is reacted with ammonia to 2-nitroaniline (**2**), which is then reduced to the benzotriazole precursor *o*-phenylenediamine (**3**) [41]. A ring closing diazotization reaction of *o*-phenylenediamine with nitrous acid in dilute sulfuric acid or with sodium nitrite and acetic acid leads to the formation of 1H-BT [41, 42]. The ^{15}N content of all N-containing precursor substances, especially of the direct reactants (*o*-phenylenediamine and NO_2^-) contributes to the measurable N isotope signature of 1H-BT. Besides, the $\delta^{15}N$ value of benzotriazole might be significantly affected by potential N isotope fractionation associated with bond breaking reactions during the production process or incomplete reactant conversion. No specific enrichment factors are reported for the amination reaction, *o*-phenylenediamine synthesis, and subsequent diazotization. Bulk ^{15}N enrichment factors between −30 ‰ and −46 ‰ reported for the reduction of nitrobenzene to aniline [43–45], however, indicate single-reaction steps during 1H-BT production to be strongly fractionating. The same reason is valid for 4-CH_3-BT and 5-CH_3-BT that are produced via the same pathway as 1H-BT (Fig. 5). Indeed C isotope signatures were in the typical range of −24.8 ‰ to −30.6 ‰, whereas N isotope signatures showed higher variations (Fig. 4b).

The variations of $\delta^{15}N$ values imply that an identification of benzotriazole suppliers might be possible by N-CSIA, while $\delta^{13}C$ data are less indicative. A comparison of two 1H-benzotriazoles from Aldrich also suggests that there may be variabilities between different production lots through the use of different raw materials or modifications in the production process (Fig. 4a). Consequently, analysis of additional specimen from the same supplier will be necessary to confirm our interpretation.

Isotope signatures of benzotriazoles in domestic dishwashing detergents The $\delta^{13}C$ and $\delta^{15}N$ values of benzotriazoles were determined in 12 domestic dishwashing tabs and powders by SPE-GC/IRMS, and their concentrations were quantified by GC/MS. Seven of the 12 dishwashing detergents analyzed contained between 0.3 ± 0.1 and 1.5 ± 0.2 mg/g of

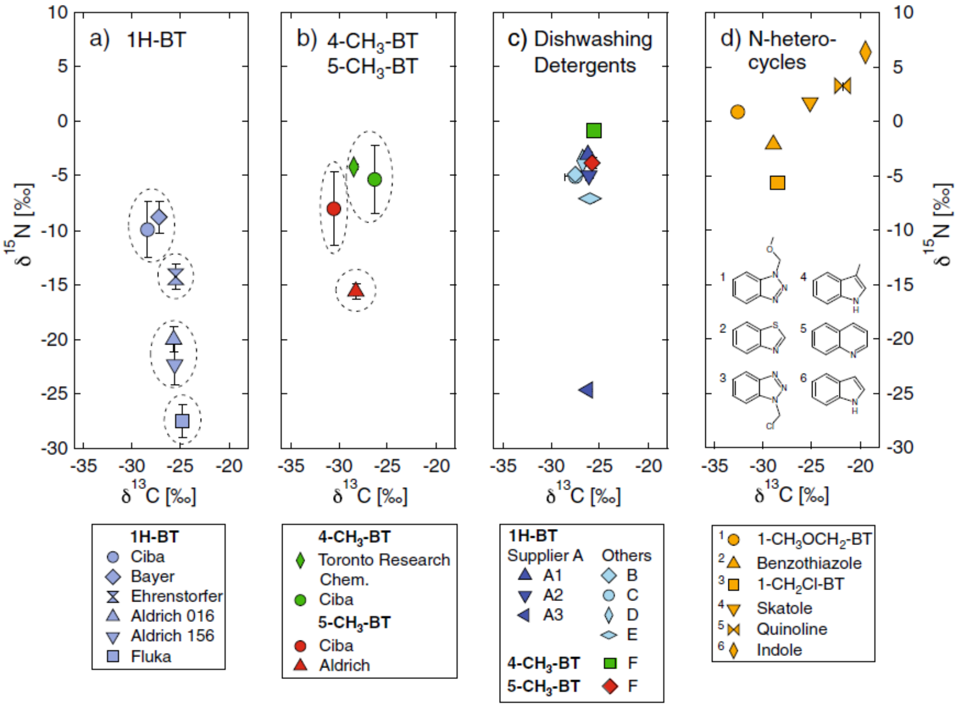

Fig. 4 δ^{13}C and δ^{15}N values of **a** 1H-benzotriazole and **b** 4-CH$_3$-BT and 5-CH$_3$-BT from different suppliers. Clusters with similar C and N isotope ratios are indicated by *dashed circles*. δ^{13}C and δ^{15}N values of **c** 1H-BT, 4-CH$_3$-BT, and 5-CH$_3$-BT in domestic dishwashing detergents from different retailers (A–F) and **d** further aromatic, N-heterocyclic compounds (numbers 1–6 indicate structural formulas). All measurements were conducted with the *modified* standard setup (GC/IRMS 1). Standard deviations of triplicate C isotope measurements are usually <0.5 ‰ and smaller than marker size

1H-BT, while 4-CH$_3$-BT and 5-CH$_3$-BT were detected in only one dishwashing tab (0.8 ± 0.2 mg/g, see Table S6). Four specimens did not contain measurable concentrations of benzotriazoles (<0.01 mg/g from 100 mg of detergent). δ^{13}C of the detected benzotriazole species was confined to values between −25.6 and −27.5 ‰ (Fig. 4c), that is in the typical range for δ^{13}C values reported for different benzotriazole suppliers (Fig. 4a, b). Six out of seven 1H-BT-

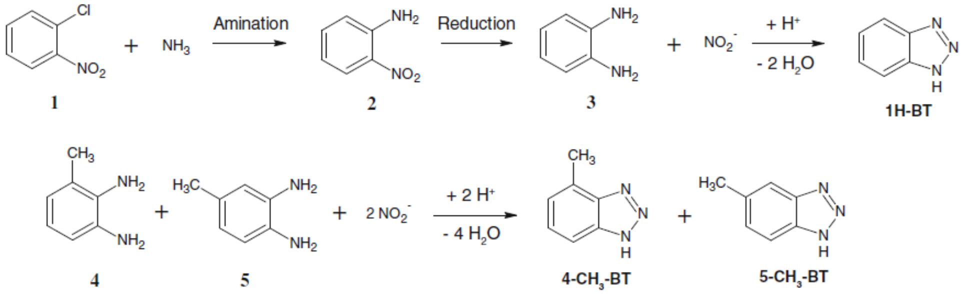

Fig. 5 Synthetic routes to benzotriazole by reaction of *o*-phenylenediamine (**3**) with nitrous acid in dilute sulfuric acid or acetic acid [41, 42]. Synthesis of *o*-phenylenediamine is reported from reduction of 2-nitroaniline (**2**), which is produced by amination of 2-chloronitrobenzene (**1**) [41]. *Lower panel*: Synthesis of tolyltriazole (4-CH$_3$- and 5-CH$_3$-BT) by reaction of *o*-toluylenediamine (a mixture of 2,3-diaminotoluene (**4**) and 3,4-diaminotoluene (**5**)) with nitrite in acidic solution [46]

containing dishwashing detergents exhibited similar $\delta^{15}N$ values between −3.0 ‰ and −7.1 ‰. Only one tab (A3) had a distinctly different N isotope signature of −24.6 ‰.

Even though this sampling campaign was not based on a representative selection of dishwashing detergent manufacturers and retailers, a tentative source apportionment of benzotriazole supplies can be made from CSIA data. The $\delta^{15}N$ data obtained for different dishwashing detergents cluster around -5 ± 2 ‰ suggesting a common origin. Based on the $\delta^{15}N$ of 1H-BT in dishwashing detergents, their 1H-BT seems closely related to that produced by Ciba (−9.9 ‰) and Bayer (−8.8 ‰), while the $\delta^{15}N$ of one dishwashing tab (A3) agrees with data for 1H-BT from Aldrich and Fluka (Fig. 4a, c). The $\delta^{13}C$ and $\delta^{15}N$ values of tolyltriazole in dishwashing detergent F can also be tentatively related to 4-CH_3-BT and 5-CH_3-BT from Ciba (Fig. 4b, c). We detected slightly more positive $\delta^{15}N$ of benzotriazoles in dishwashing detergents compared to the pure chemicals. Based on our limited data set, it is currently unclear whether these differences arise from isotope fractionation during dishwashing detergent production or are an indication of benzotriazoles produced by other suppliers.

Isotope analysis of further aromatic, heterocyclic compounds The applicability of our instrumental approach for the CSIA of benzotriazoles was tested with the analysis of additional, substituted aromatic N-heterocycles of similar molecular structures. Isotope signatures of chloromethyl- and methoxymethyl-benzotriazole as well as benzothiazole, indole, skatole, and quinoline are shown in Fig. 4d and corresponding isotope values are listed in Table 1. 2-Aminobenzimidazole could not be analyzed while measurements of 1-hydroxymethyl- and 5,6-dimethyl-benzotriazole were successful for N isotopes only. In contrast to benzotriazoles, $\delta^{13}C$ values of six aromatic N-heterocycles spanned over a larger range (-19.5 ± 0.1 to -32.6 ± 0.1 ‰) suggesting that in addition to benzene, alternative C-based precursor materials may have been used in synthesis. $\delta^{15}N$ values partly matched the values of benzotriazoles from dishwashing detergents ($+6.3 \pm 0.2$ and -5.7 ± 0.1 ‰, Fig. 4d) but were generally more enriched in ^{15}N than the pure benzotriazoles (Fig. 4a). Note, however, that the range of chemicals investigated was rather limited and a more comprehensive study is needed to establish isotopic fingerprinting of these chemicals.

Environmental significance

Our study shows that the applicability of CSIA can be expanded towards more polar organic micropollutants through modifications of standard approaches to GC/IRMS. Because of the excellent long-term performance and good precision of Ni-based combustion reactors, this approach is likely to work equally well with other polar organic compounds such as nitro- and aminoaromatic compounds, whose isotopic composition is presently analyzed by conventional means [30, 47].

The coupling of solid-phase extraction to the *modified* standard setup used here for the source apportionment of benzotriazoles in dishwashing detergents is an important first step towards analyzing this emerging class of micropollutants in aquatic systems. Given the limited knowledge of benzotriazole (bio)degradation pathways, our work provides the foundations for accurate measurements of isotope fractionation trends in laboratory experiments, which will enable the identification of transformation mechanisms [4, 7]. In addition, this study offers new avenues for further method development for benzotriazole-CSIA in environmental samples. Typical 1H-benzotriazole concentrations in groundwater, rivers, and sewage treatment plant effluents (0.2–2 µg/L [14, 48–50]), however, illustrate that substantial preconcentration of up to 10^5-fold will be necessary to reach MDLs proposed here. Optimizing SPE procedures for a selective benzotriazole enrichment from environmental samples is one of the major challenges of CSIA.

Acknowledgements We acknowledge the financial support from the Swiss Federal Office for the Environment and the German Federal Environmental Foundation (DBU).

References

1. Schwarzenbach RP, Escher BI, Fenner K, Hofstetter TB, Johnson CA, von Gunten U, Wehrli B (2006) The challenge of micropollutants in aquatic systems. Science 313:1072–1077
2. Schwarzenbach RP, Egli T, Hofstetter TB, von Gunten U, Wehrli B (2010) Global water pollution and human health. Annu Rev Environ Resour 35:109–136
3. Hofstetter T, Berg M (2011) Assessing transformation processes of organic contaminants by compound-specific stable isotope analysis. TrAC-Trends Anal Chem 30:618–627
4. Elsner M (2010) Stable isotope fractionation to investigate natural transformation mechanisms of organic contaminants: principles, prospects and limitations. J Environ Monit 12:2005–2031
5. Schmidt TC, Zwank L, Elsner M, Berg M, Meckenstock RU, Haderlein SB (2004) Compound-specific stable isotope analysis of organic contaminants in natural environments: a critical review of the state of the art, prospects, and future challenges. Anal Bioanal Chem 378:283–300
6. Elsner M, Jochmann MA, Hofstetter TB, Hunkeler D, Bernstein A, Schmidt TC, Schmimmelmann A (2012) Current challenges in compound-specific stable isotope analysis of environmental organic contaminants. Anal Bioanal Chem 403:2471–2491
7. Hofstetter TB, Schwarzenbach RP, Bernasconi SM (2008) Assessing transformation processes of organic compounds using stable isotope fractionation. Environ Sci Technol 42:7737–7743

8. Blessing M, Jochmann MA, Schmidt TC (2008) Pitfalls in compound-specific isotope analysis of environmental samples. Anal Bioanal Chem 390:591–603
9. Reinnicke S, Juchelka D, Steinbeiss S, Meyer A, Hilkert A, Elsner M (2012) Gas chromatography-isotope ratio mass spectrometry of recalcitrant target compounds: performance of different combustion reactors and strategies for standardization. Rapid Commun Mass Spectrom 26:1053–1060
10. Bi E, Schmidt TC, Haderlein SB (2006) Sorption of heterocyclic organic compounds to reference soils: column studies for process identification. Environ Sci Technol 40:5962–5970
11. Bi E, Schmidt TC, Haderlein SB (2007) Environmental factors influencing sorption of heterocyclic aromatic compounds to soil. Environ Sci Technol 41:3172–3178
12. Bi E, Zhang L, Schmidt TC, Haderlein SB (2009) Simulation of nonlinear sorption of N-heterocyclic organic contaminates in soil columns. J Contam Hydrol 107:58–65
13. Voutsa D, Hartmann P, Schaffner C, Giger W (2006) Benzotriazoles, alkylphenols and bisphenol A in municipal wastewaters and in the Glatt River, Switzerland. Environ Sci Pollut Res 13:333–341
14. Giger W, Schaffner C, Kohler H-PE (2006) Benzotriazole and tolyltriazole as aquatic contaminants. 1. Input and occurrence in rivers and lakes. Environ Sci Technol 40:7186–7192
15. Reemtsma T, Miehe U, Duennbier U, Jekel M (2010) Polar pollutants in municipal wastewater and the water cycle: occurrence and removal of benzotriazoles. Water Res 44:596–604
16. Weiss S, Jakobs J, Reemtsma T (2006) Discharge of three benzotriazole corrosion inhibitors with municipal wastewater and improvements by membrane bioreactor treatment and ozonation. Environ Sci Technol 40:7193–7199
17. Cornell JS, Pillard DA, Hernandez MT (2000) Comparative measures of the toxicity of component chemicals in aircraft deicing fluid. Environ Toxicol Chem 19:1465–1472
18. Kiss A, Fries E (2009) Occurrence of benzotriazoles in the rivers Main, Hengstbach, and Hegbach (Germany). Environ Sci Pollut Res 16:702–710
19. Katritzky AR, Lan X, Yang JZ, Denisko OV (1998) Properties and sythetic utility of N-substituted benzotriazoles. Chem Rev 98:409–548
20. Hart DS, Davis LC, Erickson LE, Callender TM (2004) Sorption and partitioning parameters of benzotriazole compounds. Microchem J 77:9–17
21. Liu Y-S, Ying G-G, Shareef A, Kookana RS (2011) Biodegradation of three selected benzotriazoles under aerobic and anaerobic conditions. Water Res 45:5005–5014
22. Mawhinney DB, Vanderford BJ, Snyder SA (2012) Transformation of 1H-benzotriazole by ozone in aqueous solution. Environ Sci Technol 46:7102–7111
23. Allam NK, Nazeer AA, Ashour EA (2009) A review of the effects of benzotriazole on the corrosion of copper and copper alloys in clean and polluted environments. J Appl Electrochem 39:961–969
24. Finsgar M, Milosev I (2010) Inhibition of copper corrosion by 1,2,3-benzotriazole: a review. Corros Sci 52:2737–2749
25. Reinnicke S, Bernstein A, Elsner M (2010) Small and reproducible isotope effects during methylation with trimethylsulfonium hydroxide (TMSH): a convenient derivatization method for isotope analysis of negatively charged molecules. Anal Chem 82:2013–2019
26. Jochmann MA, Blessing M, Haderlein SB, Schmidt TC (2006) A new approach to determine method detection limits for compound-specific isotope analysis of volatile organic compounds. Rapid Commun Mass Spectrom 20:3639–3648
27. Hunkeler D, Bernasconi SM (2010). In: Aelion CM, Höhener P, Hunkeler D, Aravena R (eds) Environmental isotopes in biodegradation and bioremediation. CRC Press, Boca Raton, pp 23–42
28. Sherwood Lollar B, Hirschorn SK, Chartrand MMG, Lacrampe-Couloume G (2007) An approach for assessing total instrumental uncertainty in compound-specific carbon isotope analysis: implications for environmental remediation studies. Anal Chem 79:3469–3475
29. Sessions AL (2006) Isotope-ratio detection for gas chromatography. J Sep Sci 29:1946–1961
30. Skarpeli-Liati M, Turgeon A, Garr AN, Arnold WA, Cramer CJ, Hofstetter TB (2011) pH-dependent equilibrium isotope fractionation associated with the compound specific nitrogen and carbon isotope analysis of substituted anilines by SPME-GC/IRMS. Anal Chem 83:1641–1648
31. Merritt DA, Freeman KH, Ricci MP, Studley SA, Hayes JM (1995) Performance and optimization of a combustion interface for isotope ratio monitoring gas chromatography/mass spectrometry. Anal Chem 67:2461–2473
32. Schmitt J, Glaser B, Zech W (2003) Amount-dependent isotopic fractionation during compound-specific isotope analysis. Rapid Commun Mass Spectrom 17:970–977
33. Skarpeli-Liati M, Pati SG, Bolotin J, Eustis SN, Hofstetter TB (2012) Carbon, hydrogen, and nitrogen isotope fractionation associated with oxidative transformation of substituted *N*-alkyl amines. Environ Sci Technol 46:7189–7198
34. Meyer AH, Penning H, Lowag H, Elsner M (2008) Precise and accurate compound specific carbon and nitrogen isotope analysis of atrazine: critical role of combustion oven conditions. Environ Sci Technol 42:7757–7763
35. Hofstetter TB, Spain JC, Nishino SF, Bolotin J, Schwarzenbach RP (2008) Identifying competing aerobic nitrobenzene biodegradation pathways using compound-specific isotope analysis. Environ Sci Technol 42:4764–4770
36. Pati SG, Shin K, Skarpeli-Liati M, Bolotin J, Eustis SN, Spain JC, Hofstetter TB (2012) Carbon and nitrogen isotope effects associated with the dioxygenation of aniline and diphenylamine. Environ Sci Technol 46:11844–11853
37. Merritt DA, Hayes JM (1994) Nitrogen isotopic analyses by isotope-ratio-monitoring gas chromatography/mass spectrometry. J Am Soc Mass Spectrom 5:387–397
38. Weiss S, Reemtsma T (2005) Determination of benzotriazole corrosion inhibitors from aqueous environmental samples by liquid chromatography-electrospray ionization-tandem mass spectrometry. Anal Chem 77:7415–7420
39. Smallwood BJ, Philp RP, Allen JD (2002) Stable carbon isotopic composition of gasolines determined by isotope ratio monitoring gas chromatography mass spectrometry. Org Geochem 33:149–159
40. Philp RP (2007) The emergence of stable isotopes in environmental and forensic geochemistry studies: a review. Environ Chem Lett 5:57–66
41. Smiley RA (2002) Ullmann's encyclopedia of industrial chemistry. Wiley-VCH Verlag GmbH & Co. KGaA, Weinheim
42. Chan MS, Hunter WE (1981) United States Patent 4,299,965. Preparation of benzotriazole. pat. 4,299,965
43. Gorski CA, Nurmi JT, Tratnyek PG, Hofstetter TB, Scherer MM (2010) Redox behavior of magnetite: implications for contaminant reduction. Environ Sci Technol 44:55–60
44. Hartenbach AE, Hofstetter TB, Aeschbacher M, Sander M, Kim D, Strathmann TJ, Arnold WA, Cramer CJ, Schwarzenbach RP

(2008) Variability of nitrogen isotope fractionation during the reduction of nitroaromatic compounds with dissolved reductants. Environ Sci Technol 42:8352–8359

45. Hartenbach AE, Hofstetter TB, Berg M, Bolotin J, Schwarzenbach RP (2006) Using nitrogen isotope fractionation to assess abiotic reduction of nitroaromatic compounds. Environ Sci Technol 40:7710–7716
46. Schnegg U, Bormann U (1990) United States Patent 4,918,195. Process for preparing triazoles fused with aromatic systems by reaction of *o*-arylenediamines with nitrites. pat., 4,918,195
47. Berg M, Bolotin J, Hofstetter TB (2007) Compound-specific nitrogen and carbon isotope analysis of nitroaromatic compounds in aqueous samples using solid-phase microextraction coupled to GC/IRMS. Anal Chem 79:2386–2393
48. Janna H, Scrimshaw MD, Williams RJ, Churchley J, Sumpter JP (2011) From dishwasher to tap? Xenobiotic substances benzotriazole and tolytriazole in the environments. Environ Sci Technol 45:3858–3864
49. Wolschke H, Xie Z, Möller A, Sturm R, Ebinghaus R (2011) Occurrence, distribution and fluxes of benzotriazoles along the German large river basins into the North Sea. Water Res 45:6259–6266
50. Huntscha S, Singer HP, McArdell CS, Frank CE, Hollender J (2012) Multiresidue analysis of 88 polar organic micropollutants in ground, surface and wastewater using online mixed-bed multilayer solid-phase extraction coupled to high performance liquid chromatography-tandem mass spectrometry. J Chromatogr A 1268:74–83

Appendix A2. COMBINED ISOTOPE AND ENANTIOMER ANALYSIS TO ASSESS THE FATE OF PHENOXY ACIDS IN A HETEROGENEOUS GEOLOGIC SETTING AT AN OLD LANDFILL

WATER RESEARCH 47 (2013) 637–649

Available online at www.sciencedirect.com

SciVerse ScienceDirect

journal homepage: www.elsevier.com/locate/watres

Combined isotope and enantiomer analysis to assess the fate of phenoxy acids in a heterogeneous geologic setting at an old landfill

N. Milosevic [a,*], S. Qiu [b], M. Elsner [b], F. Einsiedl [a], M.P. Maier [b], H.K.V. Bensch [b], H.-J. Albrechtsen [a], P.L. Bjerg [a]

[a] Department of Environmental Engineering, Technical University of Denmark (DTU), Miljoevej, Building 113, DK-2800 Kgs. Lyngby, Denmark
[b] Institute of Groundwater Ecology, Helmholtz Zentrum München, Ingolstädter Landstr. 1, 85764 Neuherberg, Germany

ARTICLE INFO

Article history:
Received 27 June 2012
Received in revised form
20 September 2012
Accepted 14 October 2012
Available online 30 October 2012

Keywords:
4-CPP
Dichlorprop
Clay till
CSIA
Chiral
Degradation mechanism

ABSTRACT

Phenoxy acid herbicides and their potential metabolites represent industrial or agricultural waste that impacts groundwater and surface waters through leaching from old landfills throughout the world. Fate assessment of dichlorprop and its putative metabolite 4-CPP (2-(4-chlorophenoxy)propionic acid) is frequently obstructed by inconclusive evidence from redox conditions, heterogeneous geologic settings (e.g. clay till) and ambiguous parent–daughter relationships (i.e. 4-CPP may be daughter product or impurity of dichlorprop). For the first time, a combination of four methods was tested to assess transformation of phenoxy acids at a contaminated landfill (Risby site): analysis of (i) parent and daughter compound concentrations, (ii) enantiomer ratios (iii) compound-specific isotope analysis and (iv) enantiomer-specific isotope analysis. Additionally, water isotopes and chloride were used as conservative tracers to delineate two distinct groundwater flow paths in the clay till. Metabolite concentrations and isotope ratios of chlorinated ethenes demonstrated dechlorination activity in the area with highest leachate concentrations (hotspot) indicating favorable conditions also for dechlorination of dichlorprop to 4-CPP and further to phenoxypropionic acid. Combined evidence from concentrations, enantiomer ratios and isotope ratios of dichlorprop and 4-CPP confirmed their dechlorination in the hotspot and gave evidence for further degradation of 4-CPP downgradient of the hotspot. A combination of 4-CPP enantiomer and isotope analysis indicated different enantioselectivity and isotope fractionation, i.e. different modes of 4-CPP degradation, at different locations. This combined information was beyond the reach of any of the methods applied alone demonstrating the power of the new combined approach.

© 2012 Elsevier Ltd. All rights reserved.

1. Introduction

Hundreds of thousands of landfill sites throughout the world may leach pollutants with long-term and local-to-regional impact on groundwater and surface waters (Kjeldsen et al., 2002; Schwarzenbach et al., 2010). Often former landfill sites contain substances whose use has subsequently been banned or restricted, such as phenoxy acid herbicides like dichlorprop

---

* *Corresponding author*. Tel.: +45 45252174; fax: +45 45932850.
E-mail address: nemm@env.dtu.dk (N. Milosevic).

0043-1354/$ – see front matter © 2012 Elsevier Ltd. All rights reserved.
http://dx.doi.org/10.1016/j.watres.2012.10.029

(2-(2,4-dichlorophenoxy)propionic acid, CAS RN 120-36-5) (Baun et al., 2004). Moreover, phenoxy acids and impurities in their production and/or transformation products such as 4-CPP (2-(4-chlorophenoxy)propionic acid, CAS RN 3307-39-9) (Reitzel et al., 2004) are commonly found in groundwater (Malaguerra et al., 2012). Thus, a proper understanding of the fate of phenoxy acids is crucial for risk assessment at landfill sites and for groundwater quality protection and management in general.

In addition to chemical variability of landfill contaminants, leachate indicators in groundwater samples collected beneath landfills may reflect a complex spatial distribution of the deposited waste at old landfill sites, including secondary sources of the same chemical (Kjeldsen and Christophersen, 2001). In landfill leachate plumes in such complex pattern, fate assessment of different xenobiotic organic compounds is complicated (Baun et al., 2003; Eganhouse et al., 2001; Rügge et al., 1995). Heterogeneous underlying geologic settings such as fractured rock or clay sediments can also complicate the spreading of contaminants. In Scandinavia and parts of North America clay till is a common geologic setting. This is glacially deposited clay with very low permeability and with preferential groundwater flow paths through vertical fractures and mostly horizontally interbedded sand lenses (e.g. Gerber et al., 2001; Hendry et al., 2004; McKay et al., 1998).

In addition to spatial complexity, physiochemical properties of the contaminants, degradability of the contaminants and redox conditions at the site may govern the attenuation of different contaminants. Physical attenuation such as sorption/desorption of xenobiotics in clay till settings (Stringfellow et al., 2011) may affect their availability for microorganisms. Microbial attenuation, e.g. reductive dechlorination of chlorinated hydrocarbons such as chlorinated ethenes is primarily expected under reducing, anaerobic conditions. The depletion of electron acceptors alone cannot be used as proof of degradation of xenobiotic compounds in a landfill leachate plume, because it is mostly driven by the turnover of general organic matter rather than the specific contaminants. The use of normalization with a conservative compound such as chloride may also fail, because of more than one chloride source in the landfill or in the plume (Bjerg et al., 1995; Tuxen et al., 2003). Thus, in avoiding the challenges of uncertainty over chloride concentrations in the source, the fate assessment of xenobiotics requires information that is specific of their transformation (Bjerg et al., 2011), such as parent-to-daughter compound concentration ratios, enantiomer ratios of chiral compounds and compound-specific isotope analysis (CSIA) (Eganhouse et al., 2001; Reitzel et al., 2004; Richnow et al., 2003).

Phenoxy acid herbicides are generally expected to be recalcitrant under strongly anaerobic conditions (Rügge et al., 1999), but prone to biodegradation under nitrate reducing or aerobic conditions (see review by Buss et al., 2006; Reitzel et al., 2004). Presence of 4-CPP might indicate dechlorination of dichlorprop (Fig. 1) in the same way as less chlorinated ethenes give evidence of dechlorination of more chlorinated ethenes. However, the presence of metabolites may be ambiguous, since proven or suggested degradation products can be present as an impurity in the production of the source compound, which is the case for dichlorprop and 4-CPP (Reitzel et al., 2004; Tuxen et al., 2003). 4-CPP might be further dechlorinated, transforming to a non-chlorinated compound. This pathway was indicated by an abiotic chemical reaction under laboratory conditions with reductive electron transfer (Azzena and Pittalis, 2011). Reductive dechlorination of chlorobenzenes resembling dichlorprop and 4-CPP (without the propionic acid entity) has been proven (Liang et al., 2011; Nelson et al., 2011).

Phenoxy acids are chiral compounds consisting of two isomeric molecules that differ only in the spatial orientation of their atoms (Fig. 1). Their enantioselective microbial degradation has been shown in laboratory conditions (Heron and Christensen, 1992; Reitzel, 2005) and in the field (Harrison et al., 1998; Reitzel, 2005; Williams et al., 2003; Zipper et al., 1998, 1999) and was found to be dependent on redox conditions (Harrison et al., 2003; Reitzel et al., 2004). (S)-4-CPP-preferential enzymes and deracemizing enzymes (i.e. enzymes which can invert the spatial orientation of one 4-CPP enantiomer in a mixture with equal quantities of each enantiomer) have been identified by Kato et al. (2010). Both processes result in the preferential occurrence of one enantiomer form. Compared to metabolic analysis, where the same metabolite can derive from different parent compounds, enantiomer analysis has the advantage that it is compound-specific. The use of enantioselective concentration measurements fails, however, if an enzyme happens to degrade both enantiomers equally well or if both (S)- and (R)-preferential enzymes are present.

Compound-specific isotope analysis (CSIA) is a fate assessment tool with an increasing number of applications in recent fate assessment studies of different contaminant groups (Elsner, 2010; Thullner et al., 2012). CSIA measures the stable isotope ratios of a compound (e.g. $^{13}C/^{12}C$, $^{2}H/^{1}H$, $^{15}N/^{14}N$, etc.) at natural abundance. Isotope ratios, such as $R_{sample} = {}^{13}C/^{12}C$, are expressed in the delta notation relative to that of an international reference $R_{reference}$.

$$\delta^{13}C = \frac{R_{sample} - R_{reference}}{R_{reference}} \tag{1}$$

where a difference of, e.g., $-0.028 = -28‰$ indicates that the sample contains 28 per mille less $^{13}C/^{12}C$ than the reference.

During a biochemical reaction, molecules with light isotopes tend to be degraded faster than molecules possessing a heavy isotope in the reactive position (because the bond is slightly weaker), leading to an enrichment of heavy isotopes in the remaining substrate ($\delta^{13}C$ becomes more positive) (Bigeleisen and Wolfsberg, 1958; Wolfsberg et al., 2010). This enables the detection of *in situ* biodegradation of organic contaminants. Furthermore, if the isotope enrichment factor (ε) of a specific compound is determined in laboratory experiments based on the Rayleigh equation, it can be used to estimate the extent of biodegradation of that compound from changes in isotope ratios of field samples (Hunkeler et al., 2008).

The carbon-based CSIA has recently been extended to assess microbial degradation of different pesticides (Badea et al., 2009; Penning et al., 2010; Reinnicke et al., 2012) and the method was very recently optimized for phenoxy acids (Reinnicke et al., 2010). CSIA has been widely used for degradation assessment of chlorinated ethenes and monoaromatic petroleum hydrocarbons such as benzene, toluene, ethylbenzene, m-,o- and p-xylene (BTEX) on different typical contaminated sites, and the literature on their natural attenuation and isotope fractionation is extensive (Thullner et al., 2012). Richnow et al. (2003) used CSIA to examine the fate of

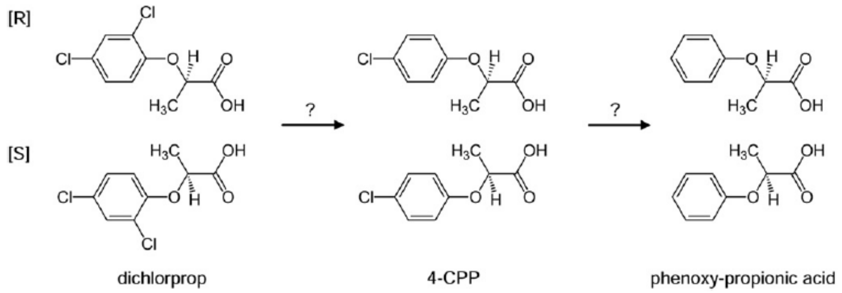

Fig. 1 – Structural formulas and possible anaerobic degradation (dechlorination) pathways of the phenoxy acid dichlorprop and the putative metabolite/impurity 4-CPP.

BTEX in landfill leachate, but to date no CSIA study has been reported on the fate of phenoxy acids using environmental samples. Similar to enantiomer analysis, the isotope fractionation process is specific for a certain compound, and may change with redox conditions. The advantage of isotope over enantiomer analysis is that it works for a wider range of compounds (also for non-chiral molecules and non-enantiomer-specific reactions). A disadvantage is that CSIA does not work if the rate-limiting step in the degradation reaction does not show an isotope effect, for example if the first limiting step is the transport inside a cell (Elsner, 2010). Very recently, a study has, therefore, brought forward enantioselective stable isotope analysis as innovative approach, but only for a single compound (alpha-hexachlorocyclohexane) and not yet tested in the field (Badea et al., 2011).

In a previous study Milosevic et al. (2012) identified dichlorprop and 4-CPP as well as other xenobiotic organic compounds at the Risby Landfill, but the actual fate of the phenoxy acids was not investigated in the leachate-contaminated groundwater. In the present study we elucidated the potential for degradation of phenoxy acids (dichlorprop and 4-CPP) at the Risby Landfill using for the first time a combination of metabolite, enantiomer and compound-specific carbon isotope analysis. We investigated whether this assessment would improve insight compared to conventional approaches. The specific aims were (1) to infer the potential for dichlorprop degradation to 4-CPP in the source zone of the landfill by evaluating the degradation potential of other xenobiotics (BTEX, chlorinated ethenes) based on metabolite and compound-specific isotope analysis, (2) to evaluate further degradation of 4-CPP downstream of the source zone by a combination of enantiomer and compound-specific isotope analysis of 4-CPP and (3) to combine this assessment with a water isotopes-based characterization of hydraulic flow paths to aid in the spatial interpretation of observed reactivity patterns.

2. Materials and methods

2.1. Field site and conceptual site model

The study site was the Risby Landfill, Denmark, characterized by heterogeneous geologic settings dominated by glacial deposits of clay till with interbedded sand stringers and lenses (Milosevic et al., 2012) (Fig. 2). The initial waste deposition (from 1959 until approximately 1970) was uncontrolled and it is likely that chemical waste has been disposed in the northern part of the landfill (see review of the site in Thomsen et al., in press). In a hotspot in the clay till setting beneath the landfill several contaminants were found: dichlorprop and 4-CPP, chlorinated ethenes (PCE (tetrachlorethene), TCE (trichlorethene), cis-DCE (cis-dichlorethene), vinyl chloride) and BTEX. The flow direction in the clay till during the period 2009–2011 was constant from south to north and the landfill leachate impacted the stream immediately north of the landfill (Milosevic et al., 2012). The measurement of groundwater chemistry showed a significant variability in concentrations of the contaminants and redox parameters. Groundwater conditions in 2010 and 2011 were anaerobic ranging from methanogenic to nitrate reducing and dissolved organic carbon was identified as the driver of redox processes (Milosevic et al., 2012; selected parameters in Table 1).

2.2. Sampling

A groundwater and stream water sampling network was developed encompassing all hydrogeologic units of the landfill site (hotspots beneath the landfill, groundwater flow paths in the underlying clay till, groundwater/surface water interface and the local Risby Stream) after the sampling procedure described by Milosevic et al. (2012). Chemical analysis included water isotopes, major anions and cations, redox sensitive compounds (e.g. sulfate), phenoxy acids, chlorinated ethenes and BTEX. On-site field measurements included electric conductivity (EC), pH and dissolved oxygen.

2.3. Chemical analysis

Concentrations of dichlorprop and 4-CPP were measured using an Agilent 1200 LC coupled to a Q-trap mass spectrometer (Applied Biosystems) through a Lux 3u Cellulose-3 column (250 mm × 4.60 mm, Phenomenex). Liquid samples (20 μL) were injected via a Pal autosampler (CTC, Zwingen, Switzerland). A binary element consisting of solution A (Acetonitrile, ≥99.95%) and solution B (water with 1.25% acetic acid) were applied for eluting the analytes. 60% of solution A

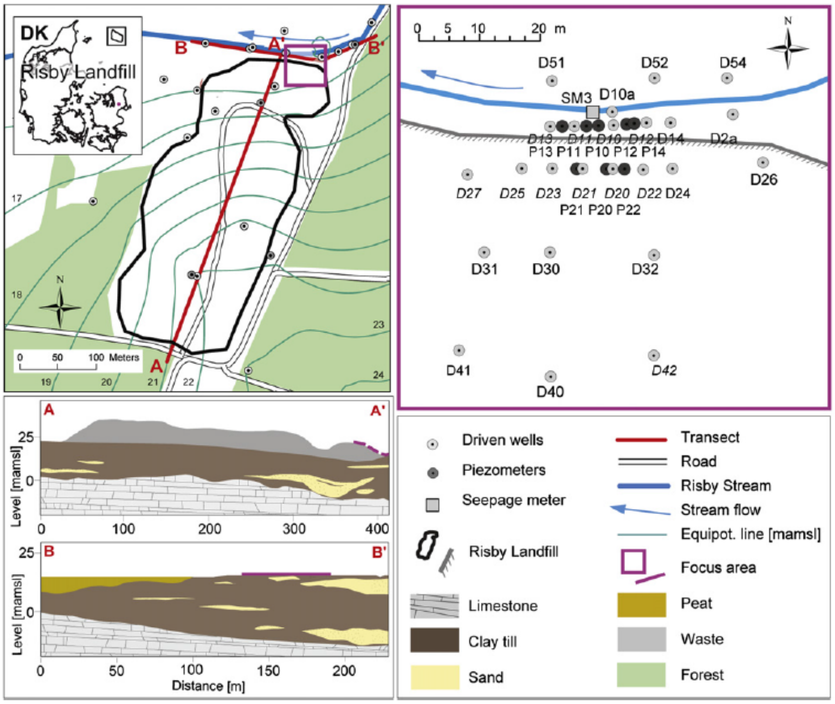
DK
Risby Landfill
A
A'
B
B'
N
0 50 100 Meters
17
18
19
20
21
22
23
24
0 5 10 20 m
D51
D52
D54
SM3
D10a
D13
D11
D10
D12
D14
D2a
P13 P11 P10 P12 P14
D27
D25
D23
D21
D20
D22
D24
D26
P21 P20 P22
D31
D30
D32
D41
D40
D42
Level [mamsl]
25
0
100
200
300
400
50
150
Distance [m]
Driven wells
Piezometers
Seepage meter
Risby Landfill
Limestone
Clay till
Sand
Transect
Road
Risby Stream
Stream flow
Equipot. line [mamsl]
Focus area
Peat
Waste
Forest

Fig. 2 – General geology and hydrology at the Risby Landfill site. Plan view (up left) and geologic transects (down left) at the site show horizontal and vertical heterogeneity of geologic settings (clay till, sand and peat) in the upper layer and groundwater flow direction going from the landfill toward the stream. Leachate is delineated at transect B–B′ between the landfill and the stream, and the focus sampling area (up right) includes hotspots in the south (transects D3x and D4x), a groundwater transport flow path (wells and piezometers (P) at transects D1x and D2x), the hyporheic zone (well D10a and seepage meter) and north of the stream with low hydraulic connectivity with the landfill (transect D5x). Driven wells with screens in clay used only for delineation (not in sampling campaign) are marked italic.

and 40% of solution B were used with a flow rate of 1 mL/min for 20 min. An electrospray ionization source was operated in the negative ion mode (ESI^-). The optimized parameters for the ESI were: Ion source temperature 450 °C, collision energy −18 eV, declustering potential −21 V, entrance potential −5 V, collision cell exit potential −2 V, ion spray voltage −4500 V, curtain gas 50, and ion source gas 60. MS/MS modes (Product Ion Scan (PIS) and Multiple Reaction Monitoring (MRM)) were applied on the mass spectrometer. MRM precursor ion-to-product ion transitions for analysis of dichlorprop and 4-CPP were m/z 232.8 to 160.8 and 198.9 to 140.9, respectively. Analytical uncertainty of 4-CPP and dichlorprop concentrations was estimated based on standard deviations of the duplicate sample measurements. Detection limit for phenoxy acids was lower than 1 μg/L.

The concentrations of BTEX and chlorinated solvents were measured by a Gas Chromatograph coupled to a Flame Ionization Detector (GC/FID) (Hewlett Packard, 5890 Seris II). Headspace (1 mL) samples were injected via a Combi PAL autosampler. A Vocol column (30 × 0.25 mm, 1.5 μm film, SUPELCO, Bellefonte, PA) was used with the following temperature program: 80 °C (hold 1 min), ramp 30 °C/min to 160 °C and ramp 60 °C/min to a final temperature of 200 °C (hold 6 min).

2.4. *Isotope analysis*

The water isotopes $\delta^{18}O$ and $\delta^{2}H$, which are reported relative to Vienna Standard Mean Ocean Water standards, were analyzed by laser spectroscopy using a Picarro isotope analyzer. The analytical precision and reproducibility was 0.1‰ for O and 0.5‰ and for H. One measurement was performed per sample.

Samples for CSIA on phenoxy acids were extracted in a 200 mg solid phase extraction column CHROMABOND® EASY, conditioned by 2 × 2 ml acetone, then 2 × 2 ml ultra pure water. The pH value of 1 L water samples was adjusted to pH = 2.0 using sulfuric acid and then passed through the extraction column at a rate of 1.5 h/L. Dried columns were eluted by 2 × 2 ml methanol–acetone (1:1, v/v) prior to analysis and eluates were used for isotope-ratio measurement.

The enantiomer-specific carbon stable isotope compositions ($\delta^{13}C$) of dichlorprop and 4-CPP, as well as the compound-specific isotope analysis of chlorinated ethenes and BTEX were measured using a GC–C–IRMS, which consisted of a TRACE GC Ultra gas chromatograph (GC) (Thermo Fisher Scientific, Milan, Italy) coupled to a Finnigan MAT 253 isotope ratio mass spectrometer (IRMS) (Thermo Fisher

Table 1 – Chemical analysis of groundwater samples at different transects at the Risby Landfill and of water samples along the Risby Stream in July 2011. Values of basic physical parameters (pH and temperature), leachate indicators (electric conductivity (EC) and chloride) and redox indicators (nitrate and sulfate) are shown at different transect along the groundwater flow direction.

	EC [mS/cm]	pH	T [°C]	O_2 [mg/L]	Cl^- [mg/L]	NO_3^- (N) [mg/L]	SO_4^{2-} (S) [mg/L]
Hotspot 30 m upgradient of the stream (transects D3x, D4x)							
D30	11.5	6.7	13.8	0.1	1771	<0.2	2.1
D31	4.1	6.7	16.3	<0.1	319	<0.2	<0.2
D32	2.1	6.7	16.8	0.1	158	<0.2	0.3
D40	3.1	6.8	17.7	0.1	218	<0.2	0.1
D41	2.5	6.9	15.7	1.9	130	<0.2	n.m.
D42	n.m.	n.m.	n.m.	n.m.	n.m.	n.m.	n.m.
D2x transect 15 m upgradient of the stream							
P20	3.7	6.7	13.3	<0.1	556	<0.2	0.1
P21	4.1	6.6	11.7	<0.1	779	<0.2	0.1
P22	3.5	6.5	11.3	0.1	477	<0.2	0.3
D24	3.6	6.8	16.7	<0.1	547	<0.2	0.1
D26	3.6	6.8	11.6	<0.1	271	<0.2	0.2
D1x transect 2 m upgradient of the stream							
D2a	2.0	6.9	11.2	<0.1	335	<0.2	3.2
D14	3.6	7.2	12.6	0.1	284	<0.2	0.2
P10	4.4	6.8	11.7	0.3	869	<0.2	0.1
P11	4.3	6.7	11.6	0.1	900	<0.2	<0.2
P12	3.6	7.1	14.5	0.1	246	<0.2	0.7
P13	4.0	6.7	11.6	<0.1	848	<0.2	0.2
P14	3.7	7.1	12.1	<0.1	293	<0.2	0.2
Hyporheic zone							
D10a	4.0	6.7	12.6	<0.1	659	<0.2	n.m.
SM3	1.6	n.m.	n.m.	n.m.	248	<0.2	n.m.
Risby Stream							
St 1	n.m.	n.m.	n.m.	n.m.	62	<0.2	n.m.
St 9	n.m.	n.m.	n.m.	n.m.	85	<0.2	n.m.
St 12	n.m.	n.m.	n.m.	n.m.	88	<0.2	n.m.
St 14	n.m.	n.m.	n.m.	n.m.	109	<0.2	n.m.
St 17	n.m.	n.m.	n.m.	n.m.	113	<0.2	n.m.
St 20	n.m.	n.m.	n.m.	n.m.	90	<0.2	n.m.
D5x transect 2 m downgradient of the stream							
D51	1.7	6.9	13.1	<0.1	282	<0.2	1.0
D52	1.0	7.0	13.6	0.2	141	<0.2	11.7
D54	0.9	7.0	12.8	<0.1	132	<0.2	8.6

n.m.: not measured.
b.d.l.: below detection limit.

Scientific, Bremen, Germany) via a Finnigan GC Combustion III interface. For dichlorprop and 4-CPP, samples were first dissolved in TMSH (trimethylsulfonium hydroxide, CAS no.: 17287-03-5, Sigma Aldrich, Taufkirchen, Germany) for online derivatization (Reinnicke et al., 2010). Liquid samples (4 μL) were then injected via a GC Pal autosampler (CTC, Zwingen, Switzerland). The analytical column was a hydrodex-β-6TBDM (50 m × 0.25 mm; 0.25 μm film; J&W Scientific, Folsom; CA). The GC program was as follows: 80 °C (hold 1 min), ramp 20 °C/min to 35 °C and ramp 5 °C/min to a final temperature of 220 °C. For chlorinated ethenes and BTEX, liquid samples (30 mL) were injected via a Velocity XPT purge and trap (P&T) sample concentrator with an AQUATek 70 liquid autosampler (Teledyne Tekmar) connected to the GC–IRMS. The analytical column was a DB-624 (60 m × 0.25 mm; 1.4 μm film; J&W Scientific, Agilent Technologies; USA). The GC program was as follows: 40 °C (hold 3 min), ramp 5 °C/min to 95 °C (hold 1 min) and ramp 10 °C/min to 145 °C (hold 1 min) and ramp 20 °C/min to a final temperature of 240 °C (hold 3 min). The combustion reactor used was a commercial ceramic tube filled with CuO/NiO/Pt-wire (Thermo Fischer Scientific, Bremen, Germany) that was operated at 940 °C.

The $\delta^{13}C$ are reported relative to Vienna PeeDee Belemnite (VPDB) standard. CO_2 reference gas was calibrated to V-PDB and was introduced at the beginning and the end of each run. Carbon isotope standards of chlorinated ethenes, BTEX and phenoxyacids were measured regularly to ensure the accuracy of measured isotope values. Compound derivatization and associated isotope value corrections were based on (Reinnicke et al., 2010). $\delta^{13}C_{4\text{-CPP}}$ and $\delta^{13}C_{\text{dichlorprop}}$ were measured in duplicates and the analytical uncertainty was estimated based on the standard deviation of 4-CPP and dichlorprop standards measured along with the field samples. An enantio-pure form of (S)-4CPP was synthesized from 4-chlorophenol, (R)-methyl-2-hydroxypropanoate (98% optical purity, 96% enantiomeric excess purity and the final product purity 87%) and triphenylphosphine (Nittoli et al., 2007). This authentic standard was taken to verify the identity of peaks in the GC–IRMS chromatogram. For information on the synthesis, see section 4 in the Supporting Information.

The peak intensities of (R) and (S) peaks of dichlorprop and 4-CPP in GC–IRMS chromatograms were also used to calculate the enantiomer excess (EE) where the values range between −100% and 100% (Eq. (2)) and zero is avoided as equation denominator (Nic et al., 2006).

$$EE = \frac{R - S}{R + S} \cdot 100\% \qquad (2)$$

3. Results and discussion

3.1. *Groundwater flow paths from hotspot to stream*

To investigate the decrease in xenobiotic organic compound concentrations due to dilution, the contaminant concentrations were compared with concentrations of conservative tracers. Chloride and water isotopes were used to identify groundwater flow paths, the dilution factor between the hotspot and the hyporheic zone and the groundwater origin in the highly heterogeneous Risby Landfill site. A hotspot of inorganic and organic xenobiotic compounds (phenoxy acids, chlorinated ethenes and BTEX) was identified by Milosevic et al. (2012) in the D30-D32 and D40-D42 wells (Fig. 2). Due to heterogeneity, the exact hotspots could not be identified, and the actual hotspot probably extended east from the main hotspot D30 toward D32, and south from the D3x transect the D2x transect.

Chloride decreased from D30 (1771 mg/L) along the groundwater flow (246–900 mg/L) to the hyporheic zone (248 mg/L) (Fig. 3). The decrease in chloride concentration may reflect the dilution and a dilution factor was calculated after Lyngkilde and Christensen (1992). Chloride showed distinct western and eastern groundwater flow paths, with approximately 400 mg/L of chloride as a separation value between the flow paths. The chloride concentrations decreased from D30 to D2x transect (15 m distance) by approximately 85% in the eastern and by approximately 60% in the western flow path, and remained quite constant until the D1x transect. The dilution factor between the hotspot and the hyporheic zone was 3–6 times in the eastern flow path and 1.5–2.5 times in the western flow path.

Water isotopes values $\delta^{18}O = -9.0‰$ and $\delta^{2}H = -61.4‰$ also indicated groundwater flow paths, but the position of the separation line was slightly different from the chloride concentrations' separation line (Figs. 3 and 4). Therefore the exact separation line between the groundwater flow paths in clay till could not be distinguished, and two separation lines formed a strip with the intermediate values of conservative tracers.

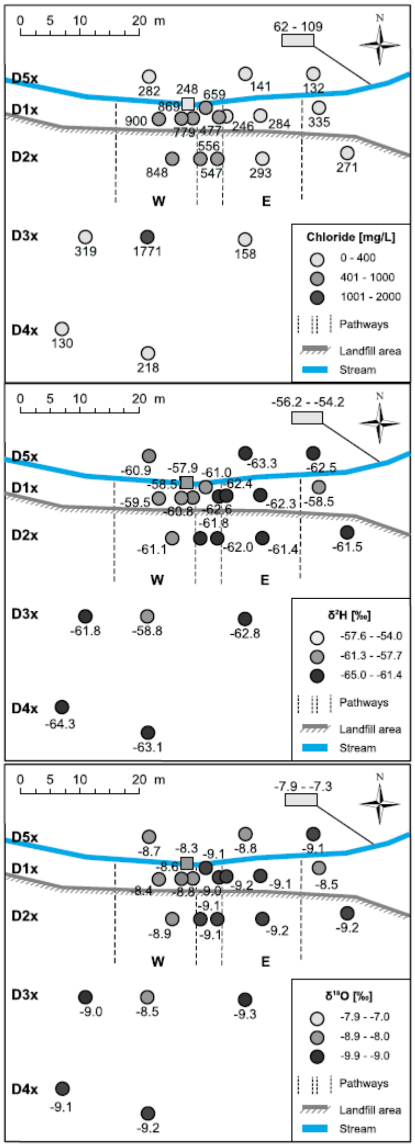

Fig. 3 – Chloride and water isotopes, measured as conservative tracers in July 2011, are shown on the map of the focus area at the Risby Landfill site (Fig. 1). Two groundwater flow paths emerge in the sand lens in the clay till, beginning approximately below the hotspot area (D3x, D4x) and ending in the groundwater-gaining Risby Stream. Sodium data show the same trend whereas bromide values were below the detection limit except in D30 (Table 1).

Water isotopes were used for identification of the groundwater origin. The global meteoric water line (GMWL: $\delta^{2}H = 8^{*}\delta^{18}O + 10$) shows the typical isotope ratio for groundwater. The evaporation line (EL: $\delta^{2}H = 5^{*}\delta^{18}O$) (Dansgaard, 1964) shows the trend toward more ^{2}H and ^{18}O expected in evaporated samples. The strong enrichment of both isotopes in the stream water confirms the more or less stagnant stream flow conditions observed during the sampling campaign. A considerable difference in water isotope values between the flow paths indicated infiltration of the percolated rainwater through the landfill surface and waste layers in one of the flow paths. There was no considerable potential for stream recharge (losing stream) into the groundwater with a high hydraulic gradient toward the stream (Milosevic et al., 2012) and evaporation was unlikely to shift the water isotope values toward more negative numbers in the wells (4–9 m below surface). The hyporheic exchange can not be excluded (Keery et al., 2007) but stream recharge into groundwater has never been investigated in detail.

Chloride concentrations and water isotope values enabled an approximate distinction between two groundwater flow paths. A detailed analysis of the xenobiotic organic compounds' degradation based only on concentrations was not conclusive due to possible undetected chloride sources in the landfill and due to the uncertainty related to the groundwater origin. Therefore, alternative methods (parent to daughter compound concentrations, enantiomer ratios, compound-specific isotope analysis and enantiomer-specific isotope analysis) were applied as degradation indicators at the complex Risby Landfill site. For water isotope data from the Risby Stream and the hyporheic zone see section 3 in Supporting Information.

3.2. *Fate of contaminants in the hotspot*

3.2.1. *Degradation of dissolved organic carbon (DOC) and BTEX*

In the hotspot of the Risby Landfill the redox conditions are anaerobic, and the concentration of DOC is high (1600 mg/L) (Milosevic et al., 2012). BTEX compounds were detected only on D3x transect, mostly in the range 100–10,000 μg/L (Fig. 5) and the values were in accordance with previous measurements (Milosevic et al., 2012). Summed BTEX concentration in the main hotspot D30 (400 mg/L) comprised 25% of DOC concentration and in general toluene dominated in the molar fractions of BTEX. These high concentrations indicate a separate phase of gasoline compounds nearby. There was an overall trend of more positive $\delta^{13}C_{BTEx}$ at low concentrations (Fig. 5), indicating degradation-associated isotope fractionation and giving evidence of microbial activity and DOC oxidation outside the main hotspot, in D31 and D32.

3.2.2. *Chlorinated ethene dechlorination*

To investigate the potential for dechlorination activity, we investigated chlorinated ethenes. Chlorinated ethenes (PCE and TCE) and the products from their microbially mediated reductive dechlorination (cis-DCE, VC and ethene) were also detected only within the landfill hotspot (Table 2). We calculated their molar fractions within the dechlorination sequence to assess the extent of the degradation. To this end, the relative proportion of the degradation products cis-DCE and VC was compared to that of the putative parent compounds TCE and PCE (see section 1 in Supporting Information). Similarly, the degree of dechlorination was calculated from the total number of chlorine atoms that had been cleaved off (e.g. Heimann et al., 2007) (see section 2 in Supporting Information). Both calculations showed reductive dechlorination with cis-DCE and VC as the predominant compounds, which suggests that also dechlorination of dichlorprop to 4-CPP in the hotspot is possible.

3.2.3. *Evidence of fresh contaminant input*

In addition, we measured isotope values of chlorinated ethenes to detect not only dechlorination, but also to infer a possible inflow from a non-degraded source. Concentrations and isotope values of chlorinated ethenes can be used for assessment of originally deposited compounds and sequential dechlorination kinetics. However, the modeled isotope values of TCE could not be reconciled with reported $\delta^{13}C_{TCE}$ ranges and enrichment factors (Hunkeler et al., 2008; Meckenstock et al., 2004; Shouakar-Stash et al., 2003). Such situations – i.e., when isotope values for TCE observed in the field are more negative than expected – this is typically attributed to the mixing of a residual fraction of TCE that was exposed to degradation (more positive) with non-degraded original contaminant TCE (Hunkeler et al., 1999; Morrill et al., 2005, 2009; Song et al., 2002). This evidence of inflow of non-degraded TCE indicated that contaminants in the hotspot were continuously introduced from a separate phase source. The inflow was corroborated by evidence of water isotopes which indicated enhanced infiltration in the hotspot. Therefore, the inflow of non-degraded TCE also may indicate a potential for input of non-degraded dichlorprop in the hotspot.

3.2.4. *Origin and fate of dichlorprop and 4-CPP*

The phenoxy acids dichlorprop and 4-CPP were detected in the hotspot at the Risby Landfill (Fig. 6a). They had the highest concentrations in well D30, whereas only 4-CPP was found ubiquitously throughout the site. Therefore the focus of this

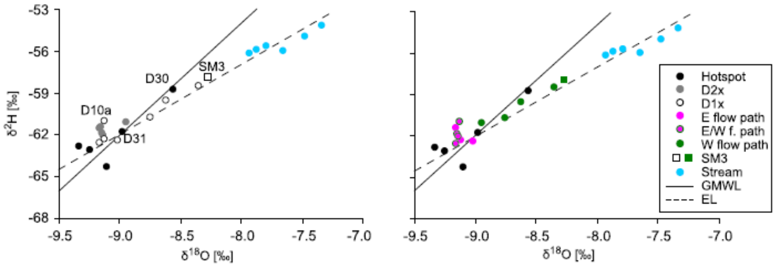

Fig. 4 – Hydrogen and oxygen isotope values measured in groundwater and stream water, grouped in transects perpendicular to the groundwater flow (left), in groundwater flow paths (E and W) and the strip between the flow paths (E/W) (right; Fig. 1).

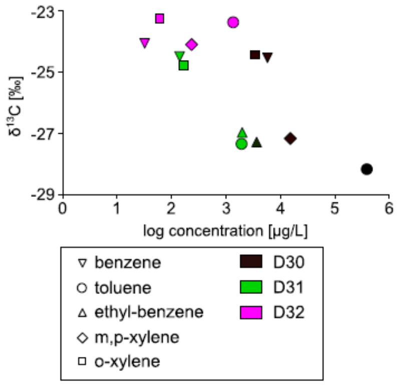

Fig. 5 – Dependence of isotope values ($\delta^{13}C$) [‰] on concentrations [µg/L] of BTEX in the hotspot area (D30, D31 and D32) measured in July 2011.

study was 4-CPP and the investigation of other compounds was a support for assessing the fate of 4-CPP. In order to investigate whether 4-CPP was present as an impurity in industrial production of the herbicide dichlorprop or as a product of its dechlorination, we combined different *in situ* indicators of degradation as discussed in the introduction.

The first indicator of dichlorprop degradation was the 4-CPP/dichlorprop ratio. The maximum estimated content (yield in weight) of 4-CPP as impurity in dichlorprop is 7% (Reitzel et al., 2004), which can be regarded as the maximum 4-CPP/dichlorprop ratio to be expected in the landfill leachate. However, this scenario was exceeded approximately 3 times in D30 with dichlorprop concentration of 42,000 µg/L (see section 5 in Supporting Information) and 4-CPP 8160 µg/L (Fig. 6a). Dichlorprop was close to, or below the limit of detection outside the hotspot and dilution can be expected to be the same for both compounds. This indicates either (i) dichlorprop transformation to 4-CPP, (ii) dichlorprop transformation to other compounds while 4-CPP stayed non-degraded, or (iii) dichlorprop attenuation by sorption/diffusion into the clay matrix. The latter is not plausible without sorption/diffusion of 4-CPP as well, because dichlorprop and 4-CPP have very similar physiochemical characteristics (Hansch et al., 1995). Therefore, the metabolite ratio gave evidence for dichlorprop dechlorination to 4-CPP, as supported also by the evidence of chlorinated ethene dechlorination (see Section 3.2.2).

Table 2 – Molar concentrations [µM] and isotope values ($\delta^{13}C$) [‰] of chlorinated ethenes that were measured in the hotspot of the Risby Landfill.

	PCE	TCE	cis-DCE	VC	Ethene
Molar concentrations [µM]					
D30	b.d.l.	0.6	0.5	369	n.a.
D31	0.7	0.01	b.d.l.	138	n.a.
D32	b.d.l.	0.2	b.d.l.	0.3	n.a.
Isotope values ($\delta^{13}C$) [‰]					
D30	b.d.l.	−26.7	−10.9	−20.0	b.d.l.
D31	−27.4	b.d.l.	b.d.l.	−31.6	b.d.l.
D32	b.d.l.	b.d.l.	b.d.l.	b.d.l.	b.d.l.

n.a.: not analyzed.
b.d.l.: below detection limit.

Enantiomer excess (EE) was the second indicator of dichlorprop degradation. $EE_{dichlorprop}$ in D30 was zero (±1%), showing a racemic mixture with equal (S)- and (R)-dichlorprop concentrations (data not shown). Dichlorprop was deposited within the focus area before the time of industrial production of pure (S) or (R)-forms of dichlorprop (Müller and Buser, 1997). Therefore zero excess could not confirm, but also did not rule out the microbial degradation of dichlorprop in the hotspot for which independent evidence was obtained by the 4-CPP/dichlorprop ratio. Likewise, the very negative isotope value of dichlorprop in D30 (−33.1‰) (see section 5 in Supporting Information) appears to indicate its recalcitrance in the hotspot, but also does not rule out a situation where inflow of non-degraded dichlorprop masks the isotope fractionation of ongoing degradation, similar to the situation for TCE (see Section 3.2.3).

3.2.5. *Further degradation of 4-CPP*

The enantiomer ratio of 4-CPP was highest in D30 ($EE_{4\text{-}CPP} = 49\%$). Preferential formation of (R)-4-CPP from (R)-dichlorprop is an unlikely reason, because a corresponding enrichment of (S)-dichlorprop was not observed in D30 ($EE_{dichlorprop} = 0 \pm 1\%$). Therefore, the enantiomeric excess of 49% in 4-CPP indicates (S)-4-CPP-preferential degradation in the hotspot. The same conclusion (i.e., 4-CPP degradation in the hotspot) is obtained from a positive difference of +1.5‰ between $\delta^{13}C_{4\text{-}CPP}$ (−31.6‰) (Fig. 6c) and $\delta^{13}C_{dichlorprop}$ (−33.1‰): if 4-CPP is formed from dichlorprop, and if it is not further degraded, it should have a more negative isotope value than dichlorprop; a more positive value, therefore, indicates further 4-CPP degradation.

Again the same conclusion is obtained from our enantiomer-specific isotope analysis on herbicides in field samples. $\delta^{13}C$ differed between 4-CPP enantiomers in D30 (Fig. 6d), supporting an (S)-4-CPP-preferential degradation. In a plot of enantiomer-specific concentrations and isotope values (Fig. 7a), degradation without isotope fractionation would show a trend from right to the left – decreasing concentrations without changes of isotope values. Isotope fractionation, in contrast would be reflected by an ascending slope from the right to the left – less negative isotope values as concentrations decrease. Dilution, finally, would show the same trend as degradation without isotope fractionation, but it is the same for different enantiomers and therefore does not affect the ratio between them. The general trend in the hotspot was that (S) enantiomers contained more ^{13}C, corresponding to a slope from the right to the left and confirming the evidence of 4-CPP degradation (Fig. 7a). In conclusion, the combined enantiomer and isotope analysis in the hotspot indicated non-enantiospecific transformation of dichlorprop and confirmed (S)-preferential degradation of 4-CPP under anaerobic conditions as shown by e.g. Reitzel et al. (2004).

3.3. *Fate of 4-CPP downgradient of the hotspot*

3.3.1. *Evidence from 4-CPP concentrations*

After observing indications for degradation of dichlorprop and 4-CPP in the hotspot, we focused on evidence of further

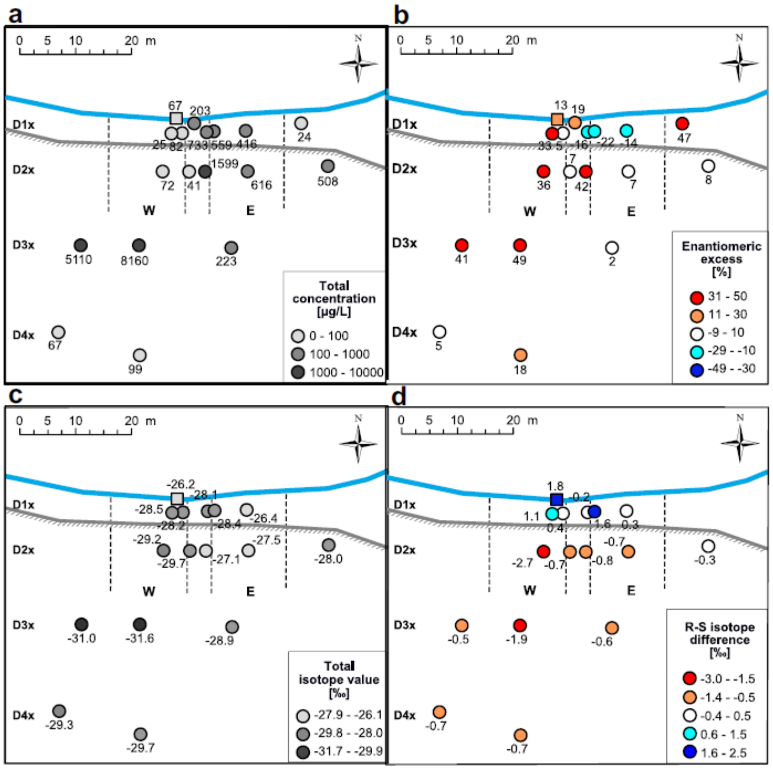
a
b
c
d
0 5 10 20 m
N
D1x
D2x
D3x
D4x
W
E
67
203
25
82
733
559
416
24
1599
72
41
616
508
5110
8160
223
67
99
Total concentration [µg/L]
0 - 100
100 - 1000
1000 - 10000
13
19
33
5
-16
-22
-14
47
7
36
42
7
8
41
49
2
5
18
Enantiomeric excess [%]
31 - 50
11 - 30
-9 - 10
-29 - -10
-49 - -30
-26.2
-28.1
-28.5
-28.2
-28.4
-26.4
-29.2
-27.5
-29.7
-27.1
-28.0
-31.0
-31.6
-28.9
-29.3
-29.7
Total isotope value [‰]
-27.9 - -26.1
-29.8 - -28.0
-31.7 - -29.9
1.8
-0.2
1.1
0.4
1.6
0.3
-0.7
-2.7
-0.7
-0.8
-0.3
-0.5
-1.9
-0.6
-0.7
-0.7
R-S isotope difference [‰]
-3.0 - -1.5
-1.4 - -0.5
-0.4 - 0.5
0.6 - 1.5
1.6 - 2.5

Fig. 6 – Maps of 4-CPP in the focus area of the Risby Landfill site: (a) Total concentration [µg/L] (summed (R) and (S) enantiomer concentrations), (b) Enantiomeric excess of (R)-form shows (S)-preferential degradation (red) and enantiomeric excess of (S)-form shows (R)-preferential degradation (blue), with values ranging from 100% for pure (R)-form to −100% for pure (S)-form (Fig. 7), (c) Total isotope values [‰] (weighted average of (R) and (S) isotope values) and (d) Difference of isotope values between (R) and (S) enantiomers. The analytical uncertainty of isotope values was estimated according to the standard deviations of 0.7‰. Seepage meter values are shown as a square in the stream at the end of the western groundwater flow path. (For interpretation of the references to colour in this figure legend, the reader is referred to the web version of this article.)

degradation of 4-CPP throughout the site. The average DOC concentrations decreased by approximately 97.5% (to approximately 40 mg/L), within 15 m downgradient from the hotspot, and remained in this range until the hyporheic zone in both groundwater flow paths (Fig. 8). The decrease in concentration of biodegradable compounds reveals their degradation if the decrease is faster than calculated by the dilution factor. The decrease of DOC (97–98%) was 5–20 times stronger than the dilution factor (85% in the eastern and 60% in western flow path) supporting that DOC was degraded, and explaining the consumption of electron acceptors. The product of DOC degradation, bicarbonate, decreased approximately 65% within 15 m from the hotspot and varied ±5% further on. The decrease was equal or smaller than the dilution factor, indicating bicarbonate production, and supporting DOC degradation.

Although downgradient from the hotspot redox conditions stayed anaerobic, the average indicators' values showed slightly less reducing conditions in the eastern groundwater flow path. The average values of bicarbonate and dissolved iron did not have clear trends between 15 and 30 m in one or both groundwater flow paths. The redox environment in the hyporheic zone was intermediate between the values from two groundwater flow paths (Fig. 8). It indicated a mixing of more reduced groundwater from the eastern flow path (discharged upstream the seepage meter) with the less reduced groundwater from the western flow path (discharged at the seepage meter). Redox parameters in groundwater could confirm anaerobic conditions as shown by Milosevic et al. (2012), but could not provide evidence that degradation of a specific organic xenobiotic compounds takes place.

We compared 4-CPP concentrations with the conservative tracers. 4-CPP was detected outside the hotspot but the concentrations decreased by approximately 90% (from >8000 µg/L) within 15 m from the hotspot in the eastern flow path (616 µg/L) and approximately 99% in the western flow

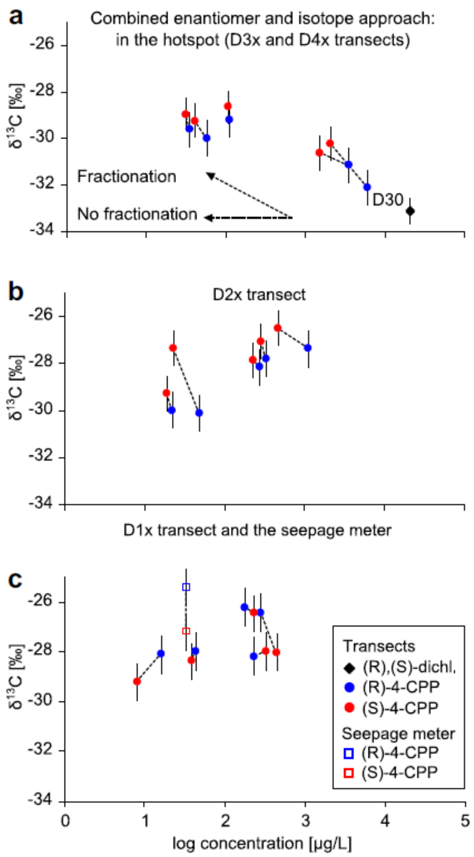

Fig. 7 – Combined isotope and enantiomer approach for dichlorprop and 4-CPP at the Risby Landfill. Isotope values [‰] and the natural logarithm of concentrations [µg/L] of 4-CPP and dichlorprop are shown for the different transects and the seepage meter placed in the Risby Stream (Fig. 1). Values of the two enantiomers from a given sample are connected by a dashed line. (a) Isotope values and enantiomer concentrations of 4-CPP and dichlorprop in the hotspot at transects D3x and D4x, (b) Isotope values and enantiomer concentrations of 4-CPP at transect D2x and (c) Isotope values and enantiomer concentrations of 4-CPP at transect D1x and seepage meter. The analytical uncertainty of concentrations was estimated based on the standard deviations of the duplicate sample measurements and of isotope values was estimated according to the standard deviations of 0.7‰ calculated from the dichlorprop and 4-CPP standards measured along with the field samples.

path (41–72 µg/L), and stayed in this range until the hyporheic zone (67 µg/L). 4-CPP concentrations generally decreased more than chloride (50–70% in the western flow path and 70–85% in the eastern flow path), implying degradation of 4-CPP. However, possible undetected additional sources of chloride in the landfill ruled out the usage of chloride as a conservative tracer for comparison of its concentration with that of the compound of interest. Additionally, another potential product of dichlorprop degradation (Reitzel et al., 2004), 2,4-dichlorophenol (CAS RN 120-83-2) was mostly below the detection limit of 0.12 µg/L in previous campaigns in 2009–2011 it was found close to the stream in concentrations 0.31–0.91 µg/L (data not shown). It may originate as an impurity of dichlorprop or as a product of its aerobic degradation, but does not provide evidence that transformation of dichlorprop to 4-CPP takes place. Therefore we used enantiomer analysis, compound-specific isotope analysis and enantiomer-specific isotope analysis to indicate the degradation of 4-CPP along the groundwater flow.

3.3.2. *Evidence from enantiomer ratios and from compound-specific isotope analysis*

In order to investigate whether anaerobic degradation of 4-CPP and alterations in the degradation mechanisms along the groundwater flow take place, we initially applied the enantiomer and isotope methods individually.

Enantiomer excess gradually decreased from D30 along the groundwater flow path, indicating 4-CPP degradation with a shift from (S)- to (R)-enantioselectivity. EE stayed positive at D2x transect, giving evidence of a still highly (S)-enantioselective degradation. The excess decreased to negative values in the eastern flow path at D1x transect, giving evidence of (R)-enantioselective degradation close to the stream (Fig. 6b). Redox conditions were slightly less reduced (nitrate-reducing) in the eastern transect (Fig. 8) where seasonal infiltration of oxygen might occur and affect the shallow groundwater (D1x wells, 2.25 m below surface). Despite varying values, EE remained in the same range along the western pathway: 36% at D2x transect, 5–33% at D1x transect (3.00 m b. s.) and 13% in the seepage meter (Fig. 6b). Hence 4-CPP degradation is indicated, but an alteration of the (S)-preferential degradation mechanism in the western flow path or in the hyporheic zone can not be claimed using enantiomer concentrations individually.

Compound-specific isotope values of 4-CPP generally became less negative downgradient of the hotspots (Fig. 6c), supporting the conclusion of 4-CPP degradation based on enantiomer excess. Interestingly, this isotope fractionation was most pronounced in the eastern flow path where the concentrations were higher and where some wells showed similar concentrations of (S)- and (R)-CPP so that evidence from concentrations or EE alone would not have been conclusive. Isotope fractionation (Fig. 6c) could, therefore, serve as a second, even stronger line of evidence to confirm the degradation of 4-CPP (and the change in the degradation mechanism), which was indicated by enantiomer excess (Fig. 6b). Smaller, but still significant changes in isotope values were observed in the western flow path where degradation was indicated by EE and the concentrations were very low (approximately 0.1% of D30).

Therefore, individual application of enantiomer and isotope methods complemented each other. Enantiomer excess gave evidence of degradation in parts of the eastern flow path, where isotope fractionation was low. On the other hand, a rather constant EE in the western flow path and the hyporheic zone was a rather weak degradation indicator compared to isotope fractionation.

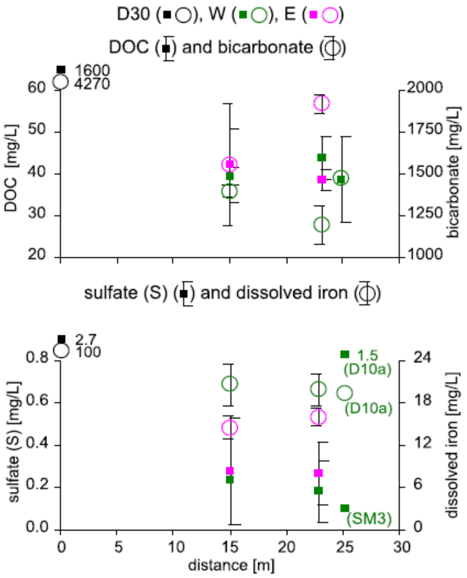

Fig. 8 – Selected redox parameters measured in 2010 (Milosevic et al., 2012) are plotted as a function of distance along the groundwater flow from hotspot (D30, black) over eastern (E, pink) and western (W, green) flow paths to the hyporheic zone in the end of the western flow path (SM3 and D10a, green). Dissolved organic carbon (DOC) is plotted as square with its oxidation product bicarbonate as circle (upper plot). Sulfate is plotted as square and dissolved iron as circle (lower plot). (For interpretation of the references to colour in this figure legend, the reader is referred to the web version of this article.)

3.3.3. *Evidence from enantiomer-specific isotope analysis*

In addition to enantiomer analysis on the one hand, and compound-specific isotope analysis on the other hand (i.e., isotope values integrated over (R) and (S) forms together), we also performed the enantiomer-specific isotope analysis (i.e., isotope values of (R) and (S) forms individually) in field samples of 4-CPP. Due to the analytical uncertainty of the isotope measurement (standard deviation ±0.75‰) conclusions must be drawn carefully. However, some trends can nonetheless be discerned. (R) and (S) pairs in almost all samples showed a trend from the lower right to the upper left in Fig. 7 (see Section 3.2.5). This means that the enantiomer which was less abundant and was, therefore, expected to have reacted to a greater extent, also consistently contained more ^{13}C. This enrichment of ^{13}C could thereby provide an additional, independent evidence of degradation suggesting that the EE was not caused by, e.g., deracemization. In addition, enantiomer-specific isotope values also strongly confirm the trend of a change in the degradation mechanism throughout the site. Whereas (S)-4-CPP preferential degradation (red symbols toward the upper left in Fig. 7a and b) was observed in samples of D4x, D3x and the D2x transect, a change toward (R)-preferential degradation (blue symbols toward the upper left in Fig. 7c) was observed in some samples of the transect D1x. This change in enantiomer fractionation may be caused by an alteration of degradation mechanism (Williams et al., 2003; Zipper et al., 1998). For a combined approach using enantiomer analysis and integrated values for isotopes over both enantiomers see section 5 in Supporting Information.

The combined approach described the degradation process at different locations, therefore providing superior insight in degradation mechanisms. Joint usage of the methods was in particular advantageous when the changes in redox parameters could not be related to the substrate degradability (throughout the site) and when the isotope fractionation, substrate concentrations and changes of the enantiomer excess were small (western groundwater flow path including the hyporheic zone).

4. Conclusion

Our combined evidence of (i) parent and daughter compound concentrations, (ii) enantiomer ratios (iii) compound-specific isotope analysis and (iv) enantiomer-specific isotope analysis showed the following results at the Risby Landfill:

- Reductive dechlorination of dichlorprop to 4-CPP, further degradation of 4-CPP and inflow of non-degraded dichlorprop were indicated in the hotspot. These processes were assessed based on isotope and concentration measurements of the two phenoxy acids (enantiospecific), chlorinated solvents and BTEX.
- Anaerobic degradation of 4-CPP was detected along two groundwater flow paths downgradient of the hotspot. An alteration of the degradation mechanism was indicated close to the stream in both flow paths.
- The challenge of geologic and chemical complexity at the Risby Landfill was overcome by combination of conservative tracers such as chloride and water isotopes. Groundwater flow paths were revealed in clay till settings, enabling an estimation of dilution and in particular framing the degradation assessment. This approach is expected to be useful at other sites with complex hydrogeological conditions.

From a methodological point of view the study for the first time showed the simultaneous use of compound- and enantiomer-specific concentration and isotope analysis for fate assessment of phenoxy acids, let alone the use of isotope analysis on the fate of phenoxy acids in environmental samples. The methods complemented and supported each other in the identification of initial contaminants, assessment of their isotope values and their degradation in the hotspot and along the flow paths. The combined approach could pinpoint a change of enantioselective degradation at low 4-CPP concentrations, at low isotope fractionation, at small changes of the enantiomer excess and when the redox parameters could not be related to the substrate degradability.

Finally, also the integrated use of insight gained from different groups of contaminants (phenoxy acids, chlorinated ethenes and BTEX) proved useful. In particular, reductive dechlorination was shown for chlorinated ethenes in the hotspot, supporting reductive dechlorination processes for phenoxy acids.

Acknowledgments

We thank our colleagues from DTU Environment Bent Henning Skov, Susanne Kruse and Jens Schaarup Sørensen for field work and laboratory analysis. Julie C. Chambon is greatly acknowledged for coupled modeling of dechlorination and isotope fractionation of chlorinated ethenes. We thank Kristen Thoreson and Armin Meyer from Helmholtz Zentrum München for support in the laboratory and concerning the usage of GC–FID and GC–IRMS methods, respectively. The study was supported by the Seventh Framework Program (2007–2013) of the European Commission within the GOODWATER Marie Curie Initial Training Network (grant no. 212683) and the Riskpoint project funded by the Danish Research Council.

Appendix A. Supplementary data

Supplementary data related to this article can be found at http://dx.doi.org/10.1016/j.watres.2012.10.029.

REFERENCES

Azzena, U., Pittalis, M., 2011. Electron-transfer-induced reductive cleavage of chlorinated aryloxyalkanoic acids. Tetrahedron 67 (19), 3360–3362.

Badea, S.-L., Vogt, C., Weber, S., Danet, A.-F., Richnow, H.-H., 2009. Stable isotope fractionation of gamma-hexachlorocyclohexane (lindane) during reductive dechlorination by two strains of sulfate-reducing bacteria. Environmental Science & Technology 43 (9), 3155–3161.

Badea, S.-L., Vogt, C., Gehre, M., Fischer, A., Danet, A.-F., Richnow, H.-H., 2011. Development of an enantiomer-specific stable carbon isotope analysis (ESIA) method for assessing the fate of alpha-hexachlorocyclohexane in the environment. Rapid Communications in Mass Spectrometry 25 (10), 1363–1372.

Baun, A., Reitzel, L.A., Ledin, A., Christensen, T.H., Bjerg, P.L., 2003. Natural attenuation of xenobiotic organic compounds in a landfill leachate plume (Vejen, Denmark). Journal of Contaminant Hydrology 65 (3–4), 269–291.

Baun, A., Ledin, A., Reitzel, L.A., Bjerg, P.L., Christensen, T.H., 2004. Xenobiotic organic compounds in leachates from ten Danish MSW landfills – chemical analysis and toxicity tests. Water Research 38 (18), 3845–3858.

Bigeleisen, J., Wolfsberg, M., 1958. Theoretical and experimental aspects of isotope effects in chemical kinetics. Advances in Chemical Physics 1, 15–76.

Bjerg, P.L., Rügge, K., Pedersen, J.K., Christensen, T.H., 1995. Distribution of redox sensitive groundwater quality parameters downgradient of a landfill (Grindsted, Denmark). Environmental Science & Technology 29, 1387–1394.

Bjerg, P.L., Tuxen, N., Reitzel, L.A., Albrechtsen, H.J., Kjeldsen, P., 2011. Natural attenuation processes in landfill leachate plumes at three Danish sites. Ground Water 49 (5), 688–705.

Buss, S.R., Thrasher, J., Morgan, P., Smith, J.W.N., 2006. A review of mecoprop attenuation in the subsurface. Quarterly Journal of Engineering Geology and Hydrogeology 39, 283–292.

Dansgaard, W., 1964. Stable isotopes in precipitation. Tellus 16 (4), 436–468.

Eganhouse, R.P., Cozzarelli, I.M., Scholl, M.A., Matthews, L.L., 2001. Natural attenuation of volatile organic compounds (VOCs) in the leachate plume of a municipal landfill: using alkylbenzenes as process probes. Ground Water 39 (2), 192–202.

Elsner, M., 2010. Stable isotope fractionation to investigate natural transformation mechanisms of organic contaminants: principles, prospects and limitations. Journal of Environmental Monitoring 12 (11), 2005–2031.

Gerber, R.E., Boyce, J.I., Howard, K.W.F., 2001. Evaluation of heterogeneity and field-scale groundwater flow regime in a leaky till aquitard. Hydrogeology Journal 9 (1), 60–78.

Hansch, C., Hoekman, D., Leo, A., Zhang, L.T., Li, P., 1995. The expanding role of quantitative structure-activity-relationships (QSAR) in toxicology. Toxicology Letters 79 (1–3), 45–53.

Harrison, I., Leader, R.U., Higgo, J.J.W., Williams, G.M., 1998. A study of the degradation of phenoxy acid herbicides at different sites in a limestone aquifer. Chemosphere 36 (6), 1211–1232.

Harrison, I., Williams, G.M., Carlick, C.A., 2003. Enantioselective biodegradation of mecoprop in aerobic and anaerobic microcosms. Chemosphere 53 (5), 539–549.

Heimann, A.C., Friis, A.K., Scheutz, C., Jakobsen, R., 2007. Dynamics of reductive TCE dechlorination in two distinct H(2) supply scenarios and at various temperatures. Biodegradation 18 (2), 167–179.

Hendry, M.J., Kelln, C.J., Wassenaar, L.I., Shaw, J., 2004. Characterizing the hydrogeology of a complex clay-rich aquitard system using detailed vertical profiles of the stable isotopes of water. Journal of Hydrology 293 (1–4), 47–56.

Heron, G., Christensen, T.H., 1992. Degradation of the herbicide mecoprop in an aerobic aquifer determined by laboratory batch studies. Chemosphere 24 (5), 547–557.

Hunkeler, D., Aravena, R., Butler, B.J., 1999. Monitoring microbial dechlorination of tetrachloroethene (PCE) in groundwater using compound-specific stable carbon isotope ratios: microcosm and field studies. Environmental Science & Technology 33 (16), 2733–2738.

Hunkeler, D., Meckenstock, R.U., Sherwood Lollar, B., Schmidt, T.C., Wilson, J.T., 2008. A Guide for Assessing Biodegradation and Source Identification of Organic Ground Water Contaminants Using Compound Specific Isotope Analysis (CSIA). US EPA. 600/R-08/148.

Kato, D., Yoshida, H., Takeo, M., Negoro, S., Ohta, H., 2010. Purification and gene cloning of an enantioselective thioesterification enzyme from Brevibacterium ketoglutamicum KU1073, a deracemization bacterium of 2-(4-Chlorophenoxy)propanoic acid. Bioscience Biotechnology and Biochemistry 74 (12), 2405–2412.

Keery, J., Binley, A., Crook, N., Smith, J.W.N., 2007. Temporal and spatial variability of groundwater-surface water fluxes: development and application of an analytical method using temperature time series. Journal of Hydrology 336 (1–2), 1–16.

Kjeldsen, P., Christophersen, M., 2001. Composition of leachate from old landfills in Denmark. Waste Management & Research 19 (3), 249–256.

Kjeldsen, P., Barlaz, M.A., Rooker, A.P., Baun, A., Ledin, A., Christensen, T.H., 2002. Present and long-term composition of MSW landfill leachate: a review. Critical Reviews in Environmental Science and Technology 32 (4), 297–336.

Liang, X., Howlett, M.R., Nelson, J.L., Grant, G., Dworatzek, S., Lacrampe-Couloume, G., Zinder, S.H., Edwards, E.A., Lollar, B.S., 2011. Pathway-dependent isotope fractionation during aerobic and anaerobic degradation of monochlorobenzene and 1,2,4-trichlorobenzene. Environmental Science & Technology 45 (19), 8321–8327.

Lyngkilde, J., Christensen, T.H., 1992. Fate of organic contaminants in the redox zones of a landfill leachate pollution plume (Vejen, Denmark). Journal of Contaminant Hydrology 10 (4), 291–307.

Malaguerra, F., Albrechtsen, H.J., Thorling, L., Binning, P.J., 2012. Pesticides in water supply wells in Zealand, Denmark: a statistical analysis. Science of the Total Environment 414, 433–444.

McKay, L.D., Balfour, D.J., Cherry, J.A., 1998. Lateral chloride migration from a landfill in a fractured clay-rich glacial deposit. Ground Water 36 (6), 988–999.

Meckenstock, R.U., Morasch, B., Griebler, C., Richnow, H.H., 2004. Stable isotope fractionation analysis as a tool to monitor biodegradation in contaminated acquifers. Journal of Contaminant Hydrology 75 (3–4), 215–255.

Milosevic, N., Thomsen, N.I., Juhler, R.K., Albrechtsen, H.-J., Bjerg, P.L., 2012. Identification of discharge zones and quantification of contaminant mass discharges into a local stream from a landfill in a heterogeneous geologic setting. Journal of Hydrology 446–447, 13–23.

Morrill, P.L., Lacrampe-Couloume, G., Slater, G.F., Sleep, B.E., Edwards, E.A., McMaster, M.L., Major, D.W., Lollar, B.S., 2005. Quantifying chlorinated ethene degradation during reductive dechlorination at Kelly AFB using stable carbon isotopes. Journal of Contaminant Hydrology 76 (3–4), 279–293.

Morrill, P.L., Sleep, B.E., Seepersad, D.J., McMaster, M.L., Hood, E.D., LeBron, C., Major, D.W., Edwards, E.A., Lollar, B.S., 2009. Variations in expression of carbon isotope fractionation of chlorinated ethenes during biologically enhanced PCE dissolution close to a source zone. Journal of Contaminant Hydrology 110 (1–2), 60–71.

Müller, M.D., Buser, H.R., 1997. Conversion reactions of various phenoxyalkanoic acid herbicides in soil. 1. Enantiomerization and enantioselective degradation of the chiral 2-phenoxypropionic acid herbicides. Environmental Science & Technology 31 (7), 1953–1959.

Nelson, J.L., Fung, J.M., Cadillo-Quiroz, H., Cheng, X., Zinder, S.H., 2011. A role for Dehalobacter spp. in the reductive dehalogenation of dichlorobenzenes and monochlorobenzene. Environmental Science & Technology 45 (16), 6806–6813.

Nic, M., Jirat, J., Kosata, B., 2006. Enantiomer Excess. IUPAC Compendium of Chemical Terminology, ISBN 0-9678550-9-8. http://dx.doi.org/10.1351/goldbook.E02070. http://goldbook.iupac.org/E02070.html.

Nittoli, T., Curran, K., Insaf, S., DiGrandi, M., Orlowski, M., Chopra, R., Agarwal, A., Howe, A.Y.M., Prashad, A., Floyd, M.B., Johnson, B., Sutherland, A., Wheless, K., Feld, B., O'Connell, J., Mansour, T.S., Bloom, J., 2007. Identification of anthranilic acid derivatives as a novel class of allosteric inhibitors of hepatitis C NS5B polymerase. Journal of Medicinal Chemistry 50 (9), 2108–2116.

Penning, H., Sorensen, S.R., Meyer, A.H., Aamand, J., Elsner, M., 2010. C, N, and H isotope fractionation of the herbicide isoproturon reflects different microbial transformation pathways. Environmental Science & Technology 44 (7), 2372–2378.

Reinnicke, S., Bernstein, A., Elsner, M., 2010. Small and reproducible isotope effects during methylation with trimethylsulfonium hydroxide (TMSH): a convenient derivatization method for isotope analysis of negatively charged molecules. Analytical Chemistry 82 (5), 2013–2019.

Reinnicke, S., Simonsen, A., Sorensen, S.R., Aamand, J., Elsner, M., 2012. C and N isotope fractionation during biodegradation of the pesticide metabolite 2,6-dichlorobenzamide (BAM): potential for environmental assessments. Environmental Science & Technology 46 (3), 1447–1454.

Reitzel, L.A., Tuxen, N., Ledin, A., Bjerg, P.L., 2004. Can degradation products be used as documentation for natural attenuation of phenoxy acids in groundwater? Environmental Science & Technology 38 (2), 457–467.

Reitzel, L.A., 2005. Quantification of Natural Attenuation Using Analytical-chemical Tools, PhD thesis., Technical University of Denmark, Department of Environmental Engineering.

Richnow, H.H., Meckenstock, R.U., Reitzel, L.A., Baun, A., Ledin, A., Christensen, T.H., 2003. *In situ* biodegradation determined by carbon isotope fractionation of aromatic hydrocarbons in an anaerobic landfill leachate plume (Vejen, Denmark). Journal of Contaminant Hydrology 64 (1–2), 59–72.

Rügge, K., Bjerg, P.L., Christensen, T.H., 1995. Distribution of organic-compounds from municipal solid-waste in the groundwater downgradient of a landfill (Grindsted, Denmark). Environmental Science & Technology 29 (5), 1395–1400.

Rügge, K., Bjerg, P.L., Mosbæk, H., Christensen, T., 1999. Fate of MCPP and atrazine in an anaerobic landfill leachate plume (Grindsted, Denmark). Water Research 33 (10), 2455–2458.

Schwarzenbach, R.P., Egli, T., Hofstetter, T.B., von Gunten, U., Wehrli, B., 2010. Global water pollution and human health. Annual Review of Environment and Resources 35, 109–136.

Shouakar-Stash, O., Frape, S.K., Drimmie, R.J., 2003. Stable hydrogen, carbon and chlorine isotope measurements of selected chlorinated organic solvents. Journal of Contaminant Hydrology 60 (3–4), 211–228.

Song, D.L., Conrad, M.E., Sorenson, K.S., Alvarez-Cohen, L., 2002. Stable carbon isotope fractionation during enhanced *in situ* bioremediation of trichloroethene. Environmental Science & Technology 36 (10), 2262–2268.

Stringfellow, A.M., Simoes, A., Smallman, D., Beaven, R., Powrie, W., Potter, H.A.B., 2011. Sorption of mecoprop by two clay landfill liner materials: Oxford clay and Mercia mudstone. Quarterly Journal of Engineering Geology and Hydrogeology 44, 321–329.

Thomsen, N.I., Milosevic, N., Bjerg, P.L. Application of a contaminant mass balance method at an old landfill to assess the impact on water resources. Waste Management, in press.

Thullner, M., Centler, F., Richnow, H.-H., Fischer, A., 2012. Quantification of organic pollutant degradation in contaminated aquifers using compound specific stable isotope analysis – review of recent developments. Organic Geochemistry 42 (12), 1440–1460.

Tuxen, N., Ejlskov, P., Albrechtsen, H.J., Reitzel, L.A., Pedersen, J.K., Bjerg, P.L., 2003. Application of natural attenuation to ground water contaminated by phenoxy acid herbicides at an old landfill in Sjoelund, Denmark. Ground Water Monitoring and Remediation 23 (4), 48–58.

Williams, G.M., Harrison, I., Carlick, C.A., Crowley, O., 2003. Changes in enantiomeric fraction as evidence of natural attenuation of mecoprop in a limestone aquifer. Journal of Contaminant Hydrology 64 (3–4), 253–267.

Wolfsberg, M., Van Hook, W.A., Paneth, P., 2010. Isotope Effects in the Chemical, Geological and Bio Sciences. Springer, Dordrecht, Heidelberg, London, New York.

Zipper, C., Suter, M.J.F., Haderlein, S.B., Gruhl, M., Kohler, H.P.E., 1998. Changes in the enantiomeric ratio of (R)- to (S)-mecoprop indicate *in situ* biodegradation of this chiral herbicide in a polluted aquifer. Environmental Science & Technology 32 (14), 2070–2076.

Zipper, C., Fleischmann, T., Kohler, H.P.E., 1999. Aerobic biodegradation of chiral phenoxyalkanoic acid derivatives during incubations with activated sludge. FEMS Microbiology Ecology 29 (2), 197–204.

Appendix A3. SUPPORTING INFORMATION OF CHAPTER 2

Contents

A3-S1 Materials

A3-S2 LC-MS/MS analysis

A3-S3 SPE extraction

A3-S4 Influence of derivatization agent excess

A3-S5 Relationship injection volume - isotope ratio

A3-S6 Preparative HPLC-UV

A3-S7 Relationship peak amplitude - isotope ratios

A3-S8 Dissipation kinetics and transformation products during biodegradation

A3-S9 GC-IRMS analysis of spiked river water

References

A3-S1 Materials

Methanol, acetonitrile, n-hexane, water (0.1% acetic acid), pentane, formic acid and acetic acid were purchased from Carl Roth (Karlsruhe, Germany) and had LC-MS grade (purity > 0.99). Ethyl acetate, diclofenac sodium (CAS Nr. 15307-79-6), BF3 (10% in methanol), 2,6-dichloroaniline and TMSH (0.25 M in methanol) were purchased from Sigma Aldrich (St. Louis, U.S.A.).

A3-S2 LC-MS/MS analysis

Filtered samples of the biodegradation experiment were quantified and screened for transformation products without enrichment with a LC-MS/MS system consisting of an Agilent 1200 binary pump and an ABSciex API 2000 Q-TRAP mass spectrometer. The system was equipped with a Luna C18(2) column (100 x 2 mm, 5 µm particle size, Phenomenex, Aschaffenburg, Germany), and operated at a flow rate of 300 µL min.$^{-1}$. A gradient of acetic acid (0.1%, A) and acetonitrile (B) was used for separation as following: A:B = 85:15 (0-3 min.) then to A:B = 30:70 (3-24 min.) and set back to A:B = 85:15 after 24 min. (held until 29 min.). Ionization was achieved with positive and negative electrospray ionization and the screened molecular- and fragment-masses can be found in Table A3-S2.

*Tab. A3-S2. LC-MS/MS settings; Diclofenac (Dic); 4'-hydroxy Diclofenac (4'-OH-Dic); 5-QID (5-benzoquinone diclofenac); dihydroxyphenly acetic acid (DHPA); 2,6-dichlorophenol (2,6-DCP); 2,6-dichloroaniline (2,6-DCA); note that due to poor fragmentation for 2,6-DCP & 2,6-DCA the non-fragmented molecule was detected in Q3; * 2,6-DCA was analyzed in postive electrospray ionization mode.*

Analyte	**Diclofenac/ $^{13}C_6$-Dic**	**4'-OH-Dic**	**5-BQID**	**DHPA**	**2,6-DCP**	**2,6-DCA***
Molecular mass $[M-H]^-$	294 / 300	310	308	167	161	162 *
Fragment mass $[M-H]^-$	250 / 256	266	264	123	161	162 *
Declustering potential	-16	-16	-16	-16	-56	26
Extraction potential	-6	-7,5	-7.5	-7.5	-12	12
Cell exit potential	-16	-18	-18	-18	-10	12
Collision energy	-12	-12	-12	-12	-5	5
Cell exit potential	-2	-4	-3	-3	-3	4
Ion spray voltage	-4500 V	-4500 V	-4500 V	-4500 V	-4500 V	+5500 V
Source temperature	350 °C	350 °C	350 °C	350 °C	350 °C	350 °C

A3-S3 SPE extraction

Tab. A3-S3. Recovery rates of the SPE in tap water and Isar water; elevated salt concentrations had no adverse effects on the efficiency

500mL Test solution spiked with Diclofenac (c = 666 µg L^{-1})	Recovery Rate
Spiked tap water	101% ± 1%
Spiked tap water + salt [1]	95% ± 1%
Spiked Isar water	68% ± 2%
Spiked Isar water + salt [1]	77% ± 5%

[1] *Salt added to 500mL:*

82.5 mg NaCl (corresponding to 100 mgL^{-1} Cl); 79 mg Na_2SO_4 (corresponding to 100 mgL^{-1} SO_4^{2-});
40.7 mg KNO_3 (corresponding to 50 mgL^{-1} NO_3^-)

A3-S4 Influence of derivatization agent excess

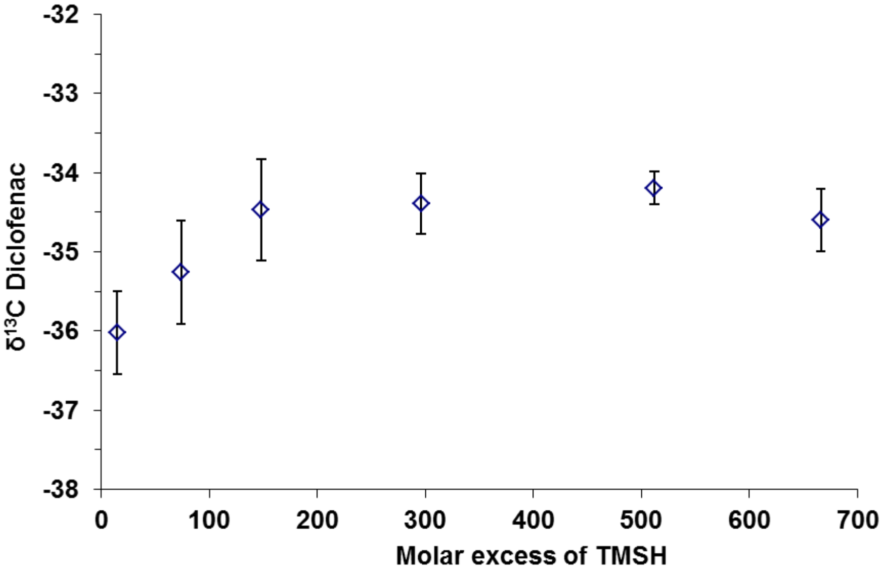

Fig. A3-S4. A minimum molar excess of Diclofenac:TMSH 1:150 is needed to obtain reproducible $\delta^{13}C$ values. Note that values were not corrected for the introduced methyl-group.

S5 Relationship injection volume - isotope ratio

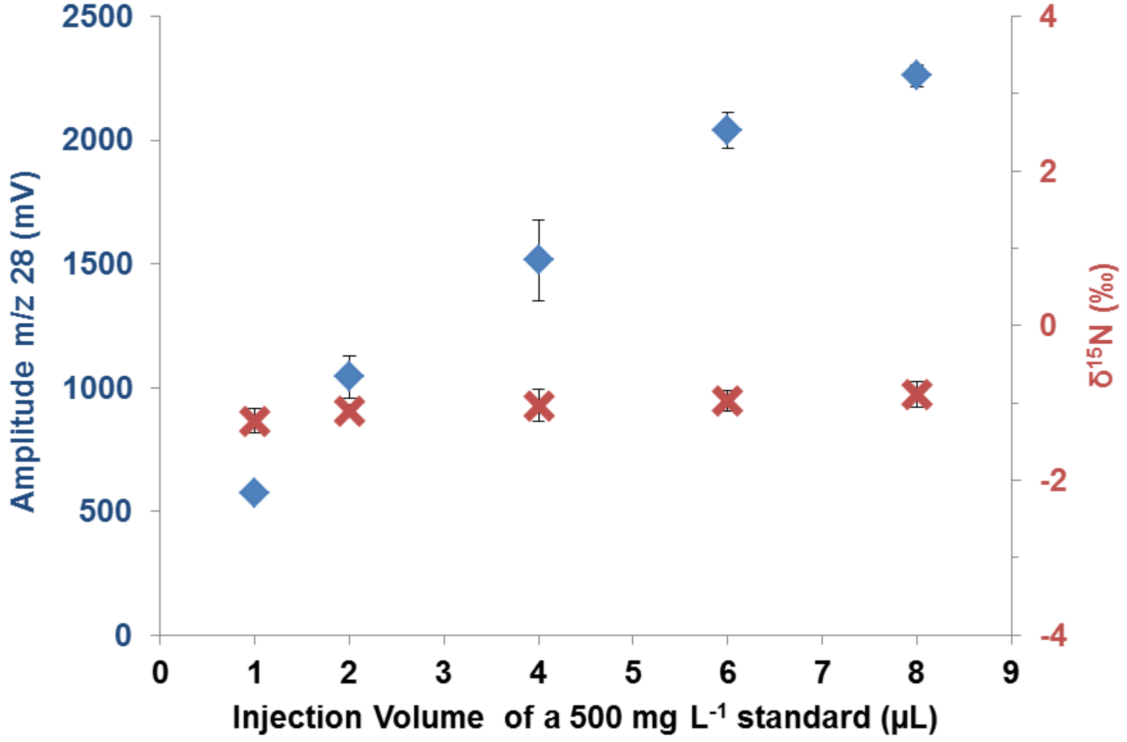

Fig. A3-S5. Increasing Injection volume (blue squares) of a 500 mg L^{-1} standard does not affect δ^{15}N isotope ratios (red crosses)(reference value EA-IRMS: -1.1‰). Injection volumes higher than 2 µL do not increase the amplitude gain linearly. Given are mean values and standard deviation (n=4).

A3-S6 Preparative HPLC-UV

To purify an enriched sample after extraction by SPE preparative HPLC was conducted. The system consisted of a Shimadzu LC-10A HPLC-UV that was equipped with an Allure C18 column (150 x 4.6 mm, 5 µm particle size, Restek, Bellefonte, U.S.A.) and a fraction collector FRC-10A. It was operated at a flow rate of 800 µL min^{-1} and a gradient of phosphoric acid (5mM A) and acetonitrile (B) was used for separation as following: A:B = 90:10 (0-1 min) then to A:B = 20:80 (1-25 min) hold for 3 min (25-28min) and then set back to A:B = 90:10 for 5 min (28 - 33 min). Diclofenac was detected at 220 nm. The sample was purified by injecting 333µL aliquots manually into a 500 µL loop and a 2 mL fraction was collected as shown in the chromatogram below (S4). The collected fractions were unified and dried before derivatization.

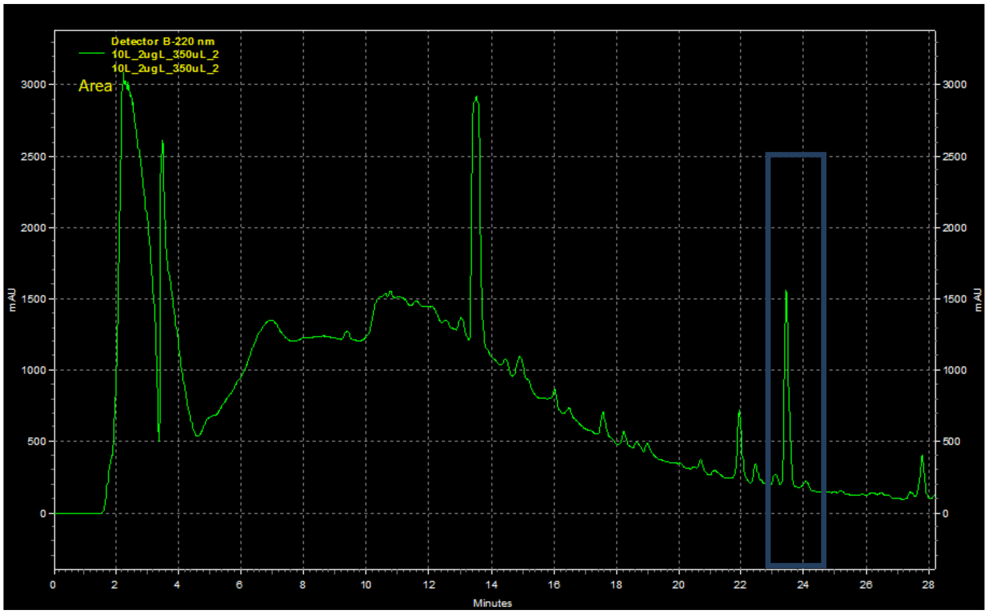

Fig. A3-S6. HPLC-UV Chromatogram of diclofenac (220 nm, RT 23.5 min) conducted after SPE. The blue box (22.5 - 25 min) indicates the fraction that was collected and subsequently dried and derivatized for on-column-GC-IRMS analysis .

A3-S7 Relationship peak amplitude - isotope ratios

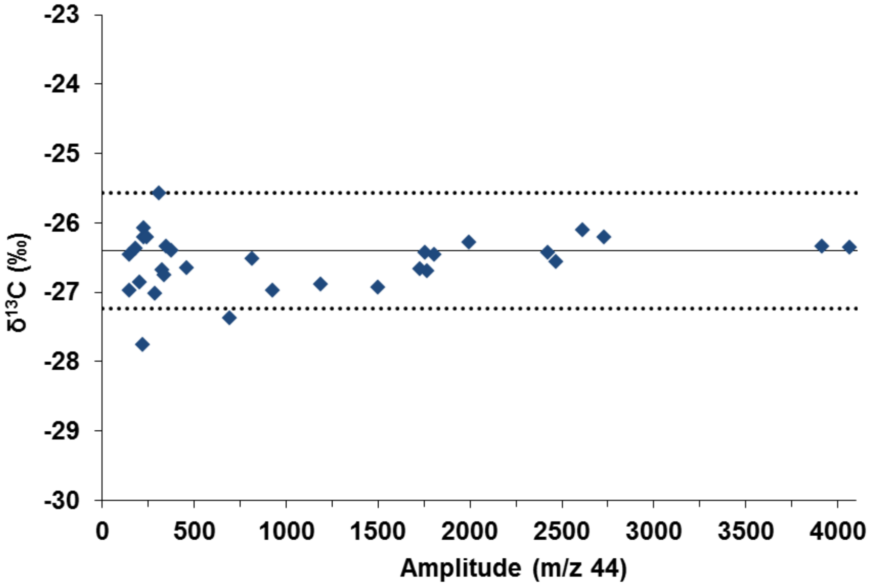

Fig. A3-S7a. Carbon isotope ratios show no dependency on amplitude height; solid line stands for EA-IRMS values and the dotted line for 2σ (0.8‰)

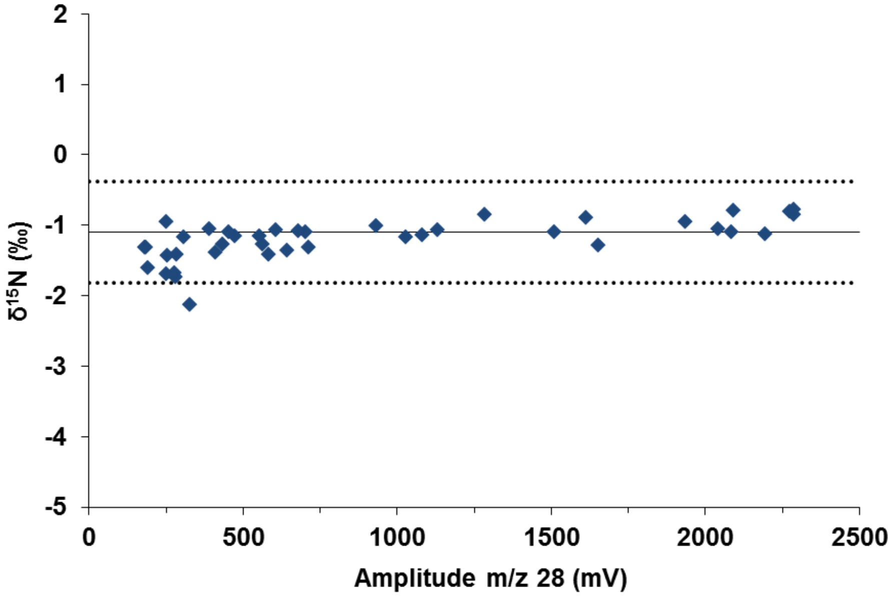

Fig. A3-S7b. Nitrogen isotope ratios show no dependency on amplitude height; solid line stands for EA-IRMS value and the dotted line for 2σ (0.8‰)

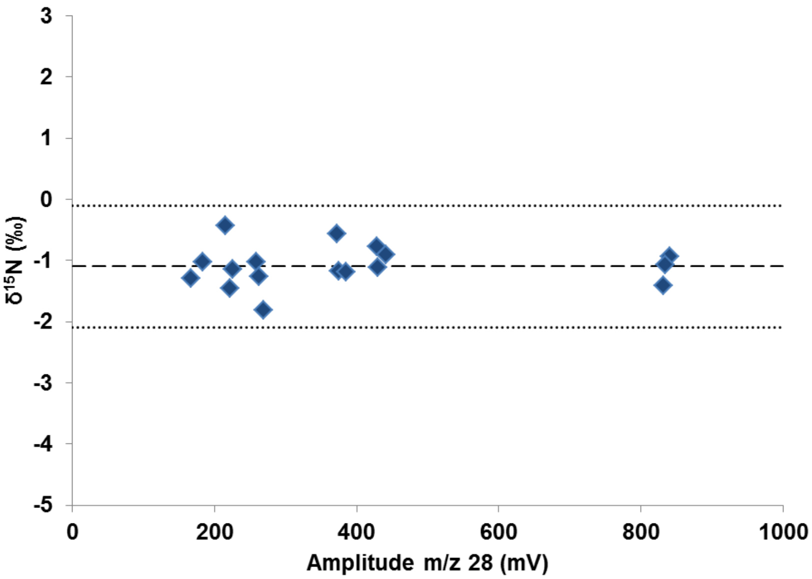

Fig. A3-S7c. Nitrogen isotope ratios using on column injection technique show no dependency on amplitude height; solid line stands for EA-IRMS value and the dotted line for 2σ (0.8‰); lowest analyzed standards had a diclofenac concentration of 200 mg L^{-1}. This analysis was done as a first test for the applicability of the on-column technique on an established system 1 and differed from the final GC method by: using a RXI-5MS column (60 m × 0.25 mm, 1 µm film thickness, Restek, Bad Homburg, Germany); the GC program started at 40 °C (240 s) and was ramped at 10 °C min^{-1} to 290 °C (600 s).

A3-S8 Dissipation kinetics and transformation products during biodegradation

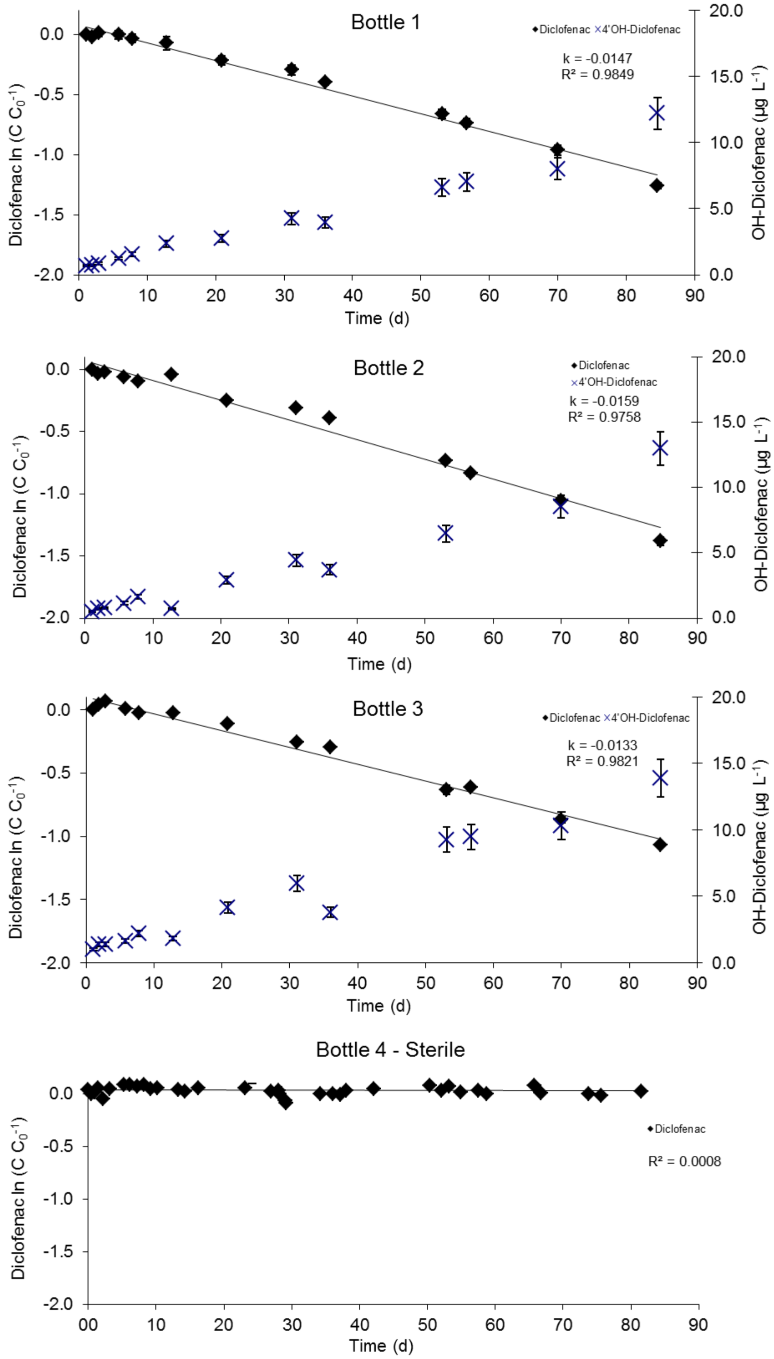

Fig. A3-S8a. Dissipation behavior of diclofenac and formation of 4'-OH-diclofenac during oxidative transformation in three replicates with river water and sediment (Bottle 1-3) and in the sterile control.

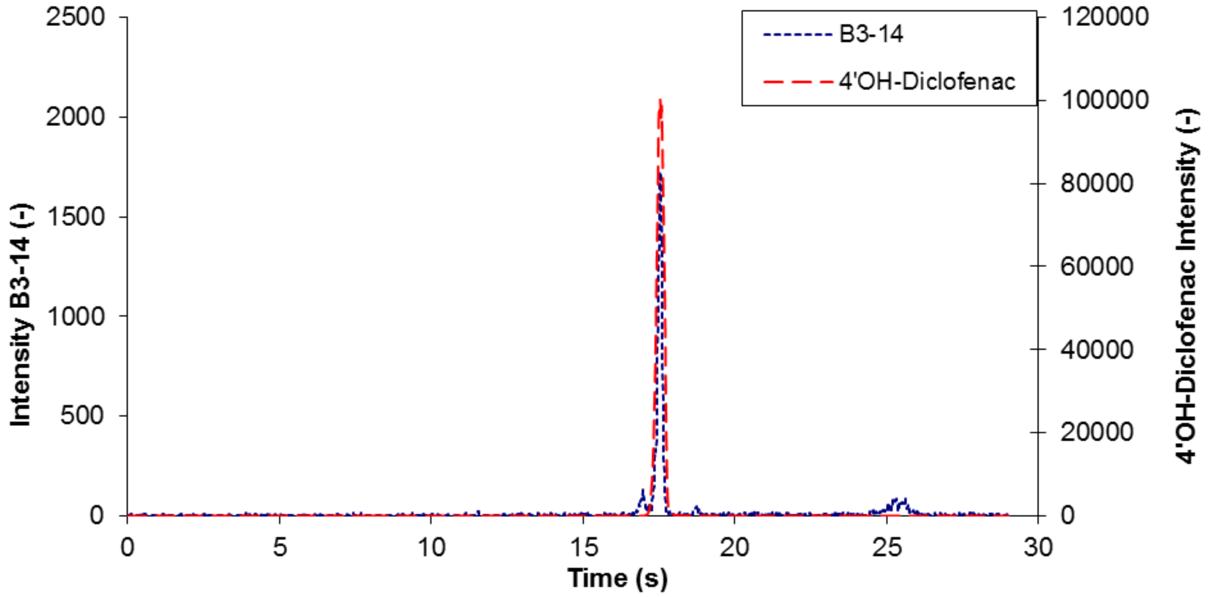

Fig. A3-S8b. LC-MS/MS Chromatogram ($[m/z]^-$ 310/266) of a 4'-hydroxy diclofenac standard (red) and sample B3-14 at the end of the incubation (86 d); corresponding mass spectra can be found in S8b.

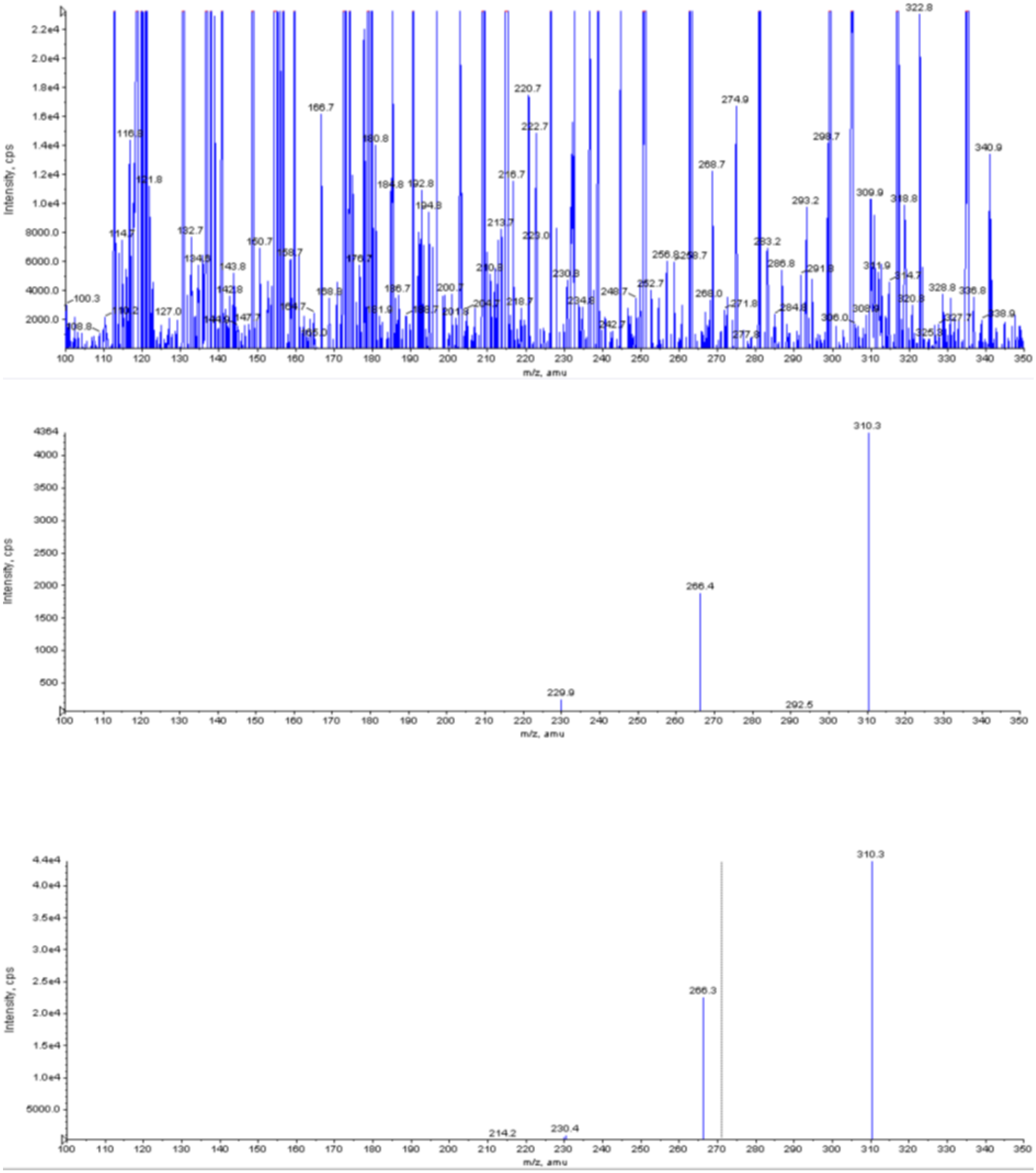

Fig. A3-S8c. mass spectra of sample B3-14, top to bottom, mas: (1) full scan (background subtracted) of TP peak at 17.8 min. and the (2) corresponding product ion scan of m/z 310 at 17.8 min.; (3) product ion scan of m/z 310 at 17.7 min of a 4'-hydroxy-diclofenac standard. All dominant fragment-ions of the standard are present at a similar ratio in the sample: [M-H]$^-$ m/z 310, [M-H-CO2]$^-$ m/z 266, [M-H-CO2-HCl]$^-$ m/z 230.

S9. GC-IRMS analysis of spiked river water

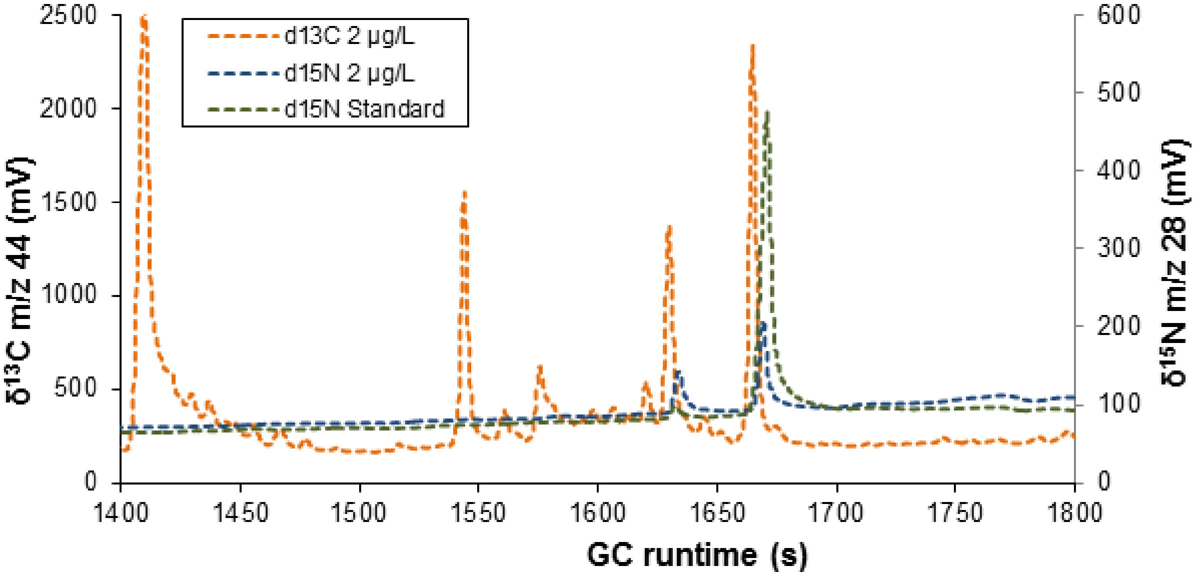

Fig. A3-S9. GC-IRMS Chromatogram of spiked river water (c(diclofenac) = 1 µg L^{-1}) and a methylated diclofenac lab standard. The retention time (RT = 1668 ± 2 s) agrees well between the sample (δ^{13}C (orange), δ^{15}N (blue)) and the lab standard (δ^{15}N (green)). Isotope ratios were in perfect agreement with EA-IRMS data: δ13C river water -26.4 ± 0.5‰ (EA-IRMS: -26.4‰) δ^{15}N river water -1.2 ± 0.4‰ (EA-IRMS: -1.1‰).

References

1. Schreglmann, K.; Hoeche, M.; Steinbeiss, S.; Reinnicke, S.; Elsner, M., Carbon and nitrogen isotope analysis of atrazine and desethylatrazine at sub-microgram per liter concentrations in groundwater. Anal. Bioanal. Chem. 2013, 405, (9), 2857-2867.

Appendix A4. SUPPORTING INFORMATION OF CHAPTER 3

Contents

A4-S1 Materials

A4-S2 LC-MS/MS analysis

A4-S3 Detection of TPs during Phototransformation

A4-S4 Formation of diclofenac-2,5-iminoquinone in the presence of O_3, ABTS or MnO_2

A4-S5 Calculation of pseudo-first order constants of hydroxyl radicals

A4-S6 Detection of coupling TPs during transformation by ABTS

A4-S7 Detection of OH-diclofenac during MnO_2 transformation

References

S1 Materials

Methanol, acetonitrile, n-hexane, water (0.1% acetic acid) and acetic acid were purchased from Carl Roth (Karlsruhe, Germany) and had LC-MS grade (purity > 0.99). Diclofenac sodium (CAS Nr. 15307-79-6), $^{13}C_6$-diclofenac, 4’hydroxyl-diclofenac and BF_3 (10% in methanol) were purchased from Sigma Aldrich (St. Louis, U.S.A.).

S2 LC-MS/MS analysis

Filtered samples were quantified and screened for transformation products without enrichment with a LC-MS/MS system consisting of an Agilent 1200 binary pump and an ABSciex API 2000 Q-TRAP mass spectrometer. The system was equipped with a Luna C18(2) column (100 x 2 mm, 5 µm particle size, Phenomenex, Aschaffenburg, Germany), and operated at a flow rate of 300 µL min^{-1}. A gradient of acetic acid (0.1%, A) and acetonitrile (B) was used for separation as following: A:B = 85:15 (0-3 min) then to A:B = 30:70 (3-24 min) and set back to A:B = 85:15 after 24 min (held until 29 min). Ionization was achieved with negative electrospray ionization and the screened molecular- and fragment-masses can be found in Table A4-S2.

Tab. S2. LC-MS/MS settings for Diclofenac (Dic), 4’-hydroxy Diclofenac (4’-OH-Dic), 8-chlorocarbazole acetic acid (TP1), carbazole acetic acid (TP2a) and 8-hydroxycarbazole acetic acid (TP2b)

Analyte	**Diclofenac / $^{13}C_6$-Dic**	**4’-OH-Dic**	**TP1**	**TP2a**	**TP2b**
Molecular mass [M-H]-	294 / 300	310	258	224	240
Fragment mass [M-H]-	250 / 256	266	214	180	196
Declustering potential	-16	-16	-16	-16	-16
Extraction potential	-6	-7,5	-6	-6	-6
Cell exit potential	-16	-18	-16	-16	-16
Collision energy	-12	-12	-12	-12	-12
Cell exit potential	-2	-4	-2	-2	-2
Ion spray voltage	-4500 V	-4500 V	-4500 V	-4500 V	-4500 V
Source temperature	350 °C	350 °C	350 °C	350 °C	350 °C

S3 Detection of TPs during Phototransformation

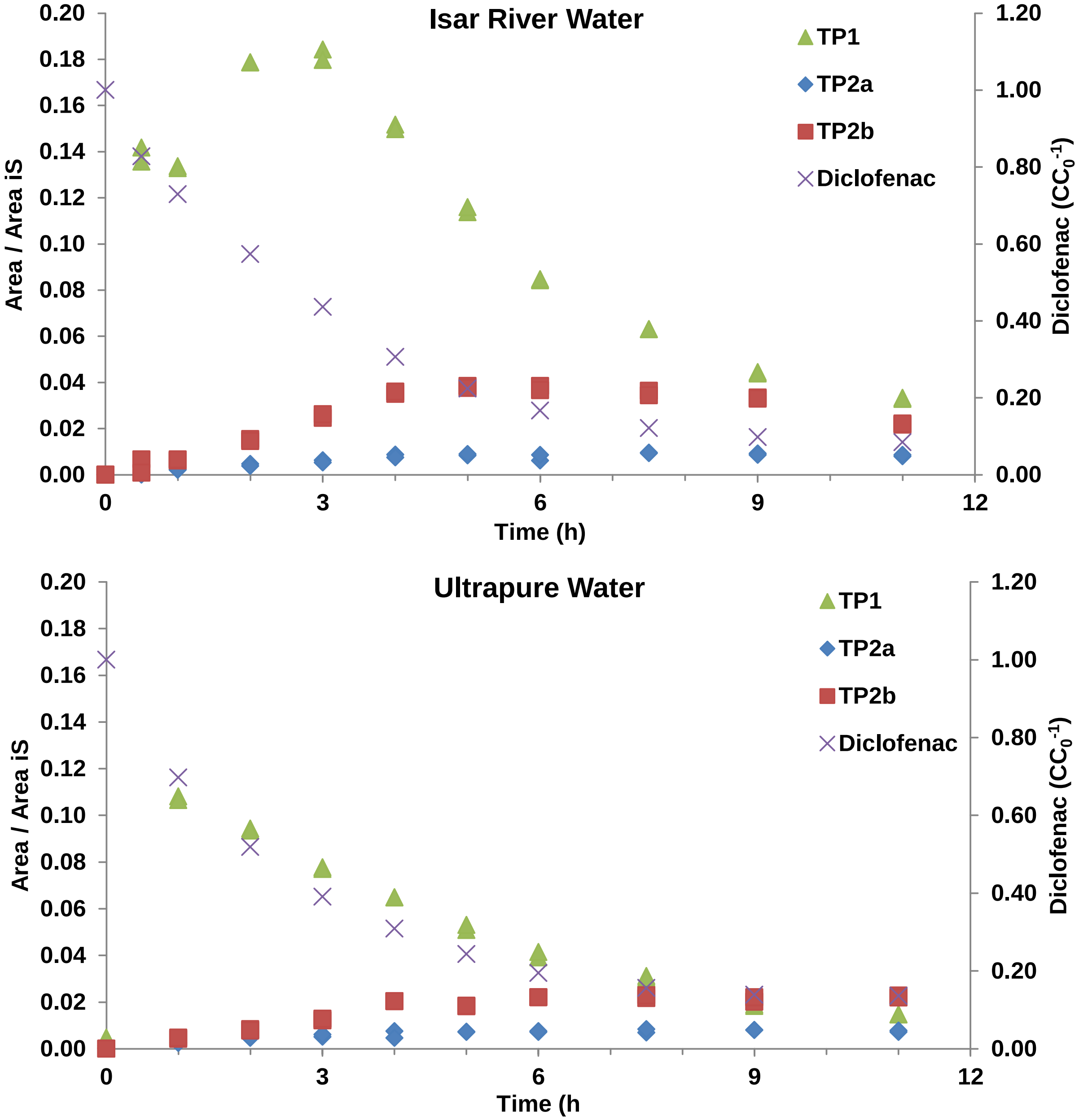

Fig. S3a. Time series of diclofenac (right axis) phototransformation in river and ultra-pure water and formation of three TPs (left axis): 8-chlorocarbazole acetic acid (TP1), carbazole acetic acid (TP2a) and 8-hydroxycarbazole acetic acid (TP2b)

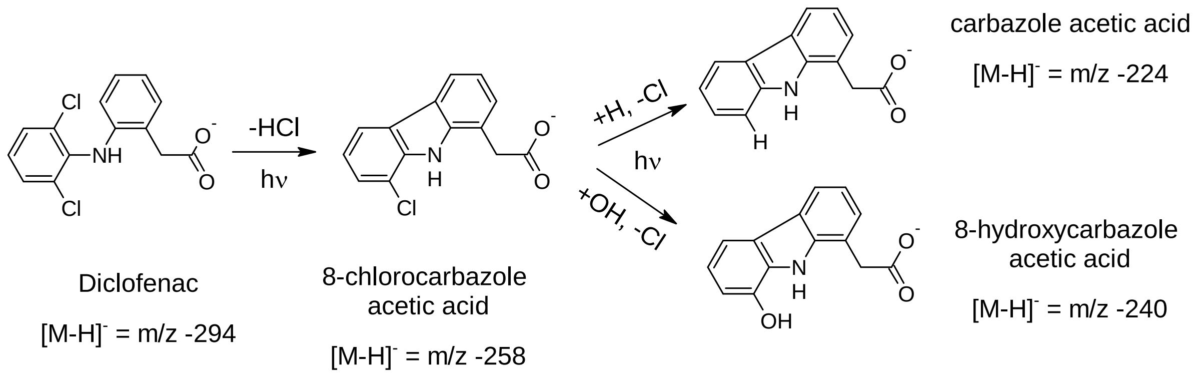
Cl
NH
Cl
O-
O
-HCl
hν
N
H
Cl
O-
O
+H, -Cl
hν
+OH, -Cl
N
H
H
O-
O
N
H
OH
O-
O
Diclofenac
[M-H]- = m/z -294
8-chlorocarbazole acetic acid
[M-H]- = m/z -258
carbazole acetic acid
[M-H]- = m/z -224
8-hydroxycarbazole acetic acid
[M-H]- = m/z -240

Fig. S3b. Reactions scheme of diclofenac during phototransformation[1]

S4. Formation of diclofenac-2,5-iminoquinone in the presence of O3, ABTS or MnO2

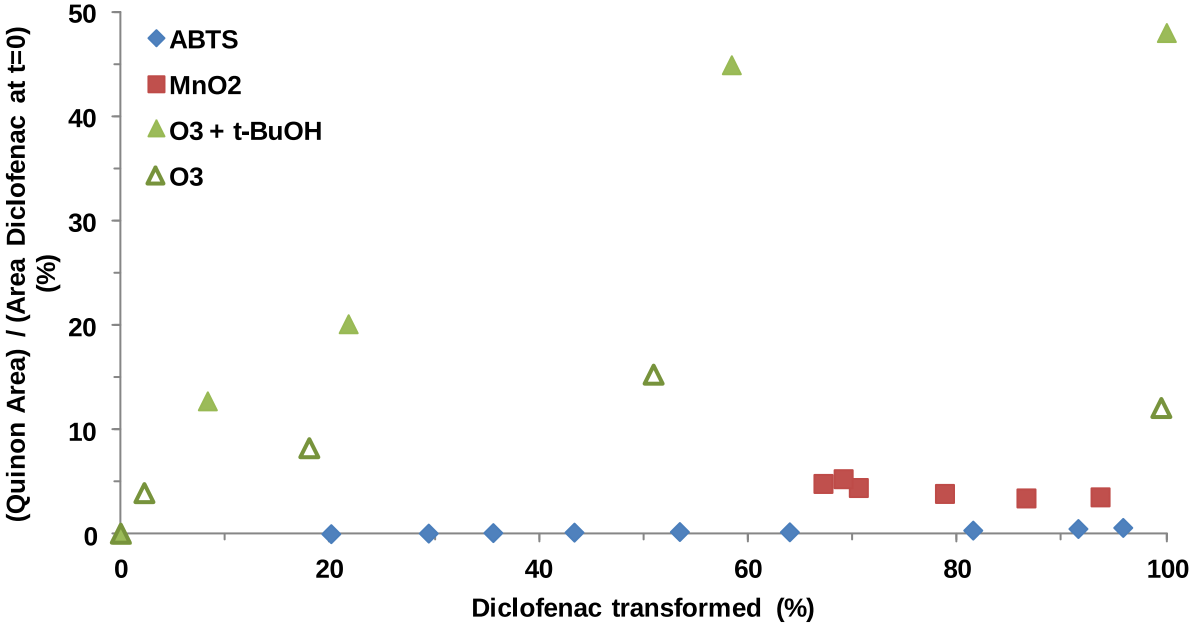

Fig. S4. Formation of diclofenac-2,5-iminoquinone ($[M+H]^+$ = 310.002 ± 0.005 Da) during transformation by ABTS and MnO_2 and during ozonation with and without the hydroxyl-radical scavenger tert-butanol (t-BuOH); the y-axis can be interpreted as an approximate yield of TP formation, although ionization efficiency may be different for diclofenac and diclofenac-2,5-iminoquinone; diclofenac-2,5-iminoquinone was also found by Forrez et al.[2] *during MnO_2 transformation and by Sein et al.*[3] *during ozonation*

S5 Calculation of pseudo-first order constants of hydroxyl radicals

A comparison of the pseudo-first order constants of reactions with ozone and hydroxyl radical indicates that reaction with ozone are expected to be 10^5 times faster:

$$k_{OH}' = [\mathrm{OH(dot)}]\cdot k_{OH} = 7.5 \times 10^{-3}\ \mathrm{s}^{-1} \tag{A4-1}$$

$[\mathrm{OH(dot)}] = 10^{-12}$ M ; [4] $k_{OH} = 7.5 \times 10^{9}\ \mathrm{M}^{-1}\ \mathrm{s}^{-1}$; [5]

$$k_{O3}' = [\mathrm{O_3}]\cdot k_{O3} = 10^{3}\ \mathrm{s}^{-1} \tag{A4-2}$$

$[\mathrm{O_3}] = 10^{-3}$ M ; $k_{O3}\cdot = 10^{6}\ \mathrm{M}^{-1}\ \mathrm{s}^{-1}$; [5]

S6 Detection of coupling TPs during transformation by ABTS

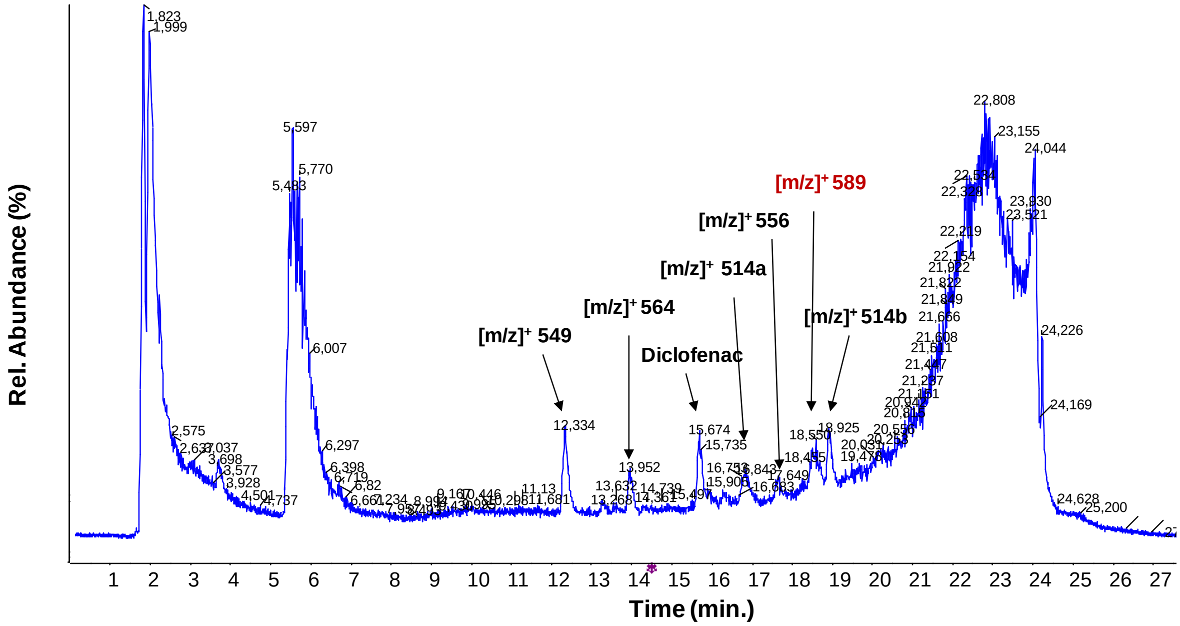

Fig. S5a. LC-Orbitrap Full scan of ABTS experiment (positive ESI); several coupling products with high molecular mass appear when diclofenac is transformed by ABTS; none of these TPs is present at t=0 (data not shown)

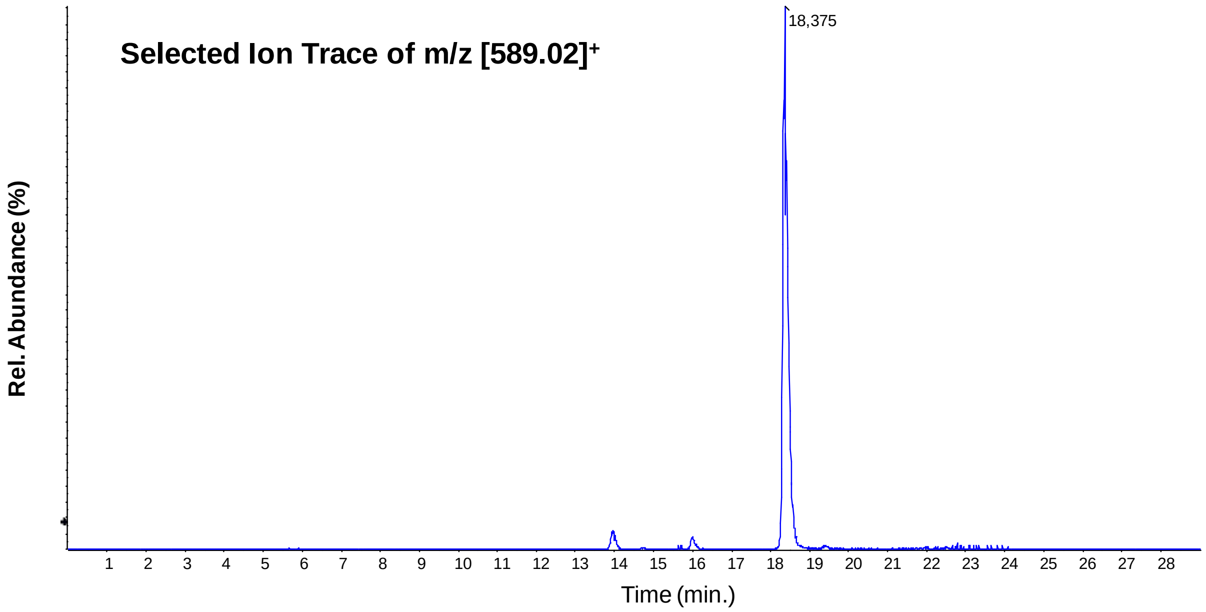

Fig. S5b. Selected ion trace chromatogram of m/z 589.02 (positive LC-ESI-Orbitrap analysis) and the diclofenac dimer peak at 18.38 min

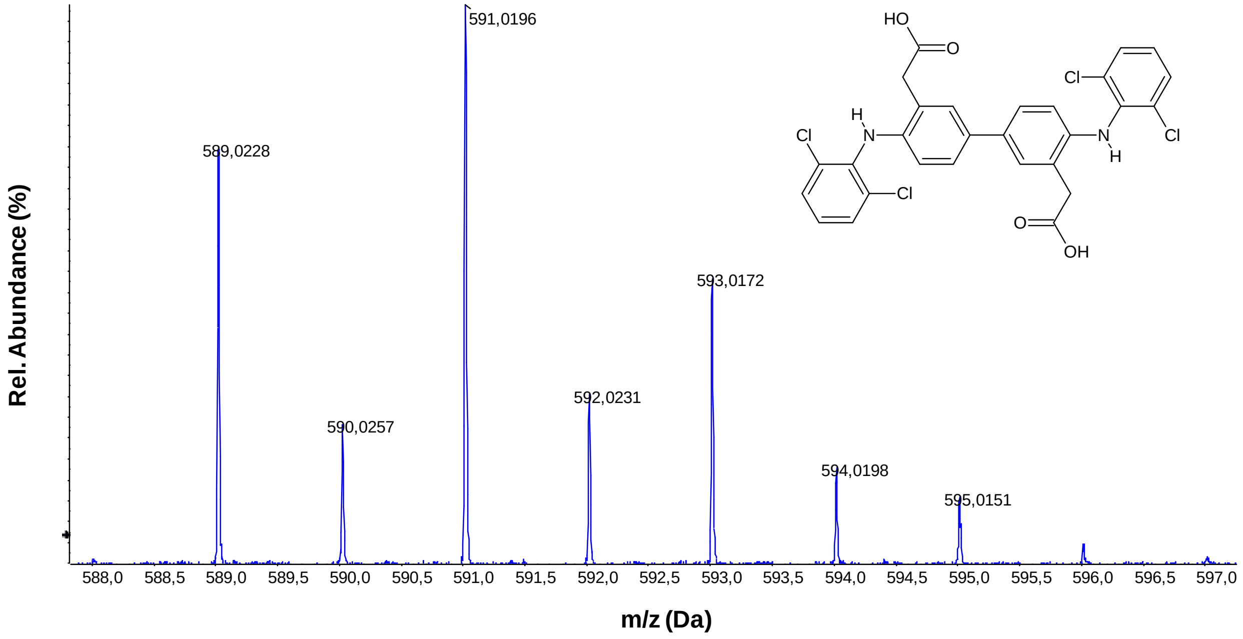

Fig. S5c. Spectrum of diclofenac-dimer peak at 18.38 min; the molecular mass fits perfectly to the proposed molecular mass of $[M+H]^+$ (589.025) and the chlorine isotope pattern is in perfect agreement with the presence of four Cl-atoms; note that the given molecular structure is only a suggestion, since the coupling position was not elucidated

S7. Detection of OH-diclofenac during MnO_2 transformation

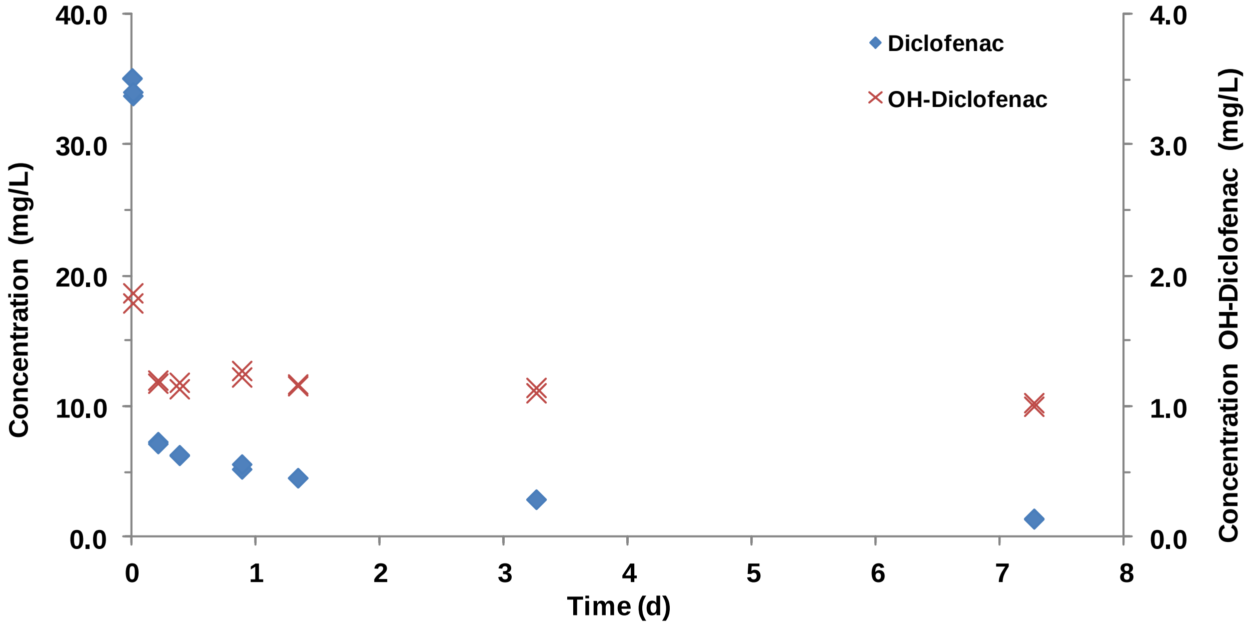

Fig. S6. Concentrations of diclofenac (left axis) and hydroxy-diclofenac (right axis) during oxidation by MnO_2; note that hydroxy-diclofenac was not present at t = 0 min, but its first data point corresponds to t = 10 min.; hydroxylated diclofenac was quantified with a 4'hydroxy-diclofenac standard

References

1. Poiger, T.; Buser, H. R.; Muller, M. D., Photodegradation of the pharmaceutical drug diclofenac in a lake: Pathway, field measurements, and mathematical modeling. *Environ. Toxicol. Chem.* **2001,** *20*, (2), 256-263.
2. Forrez, I.; Carballa, M.; Verbeken, K.; Vanhaecke, L.; Schlul̀ˆsener, M.; Ternes, T.; Boon, N.; Verstraete, W., Diclofenac Oxidation by Biogenic Manganese Oxides. *Environmental Science & Technology* **2010,** *44*, (9), 3449-3454.
3. Sein, M. M.; Zedda, M.; Tuerk, J.; Schmidt, T. C.; Golloch, A.; von Sonntag, C., Oxidation of diclofenac with ozone in aqueous solution. *Environmental Science & Technology* **2008,** *42*, (17), 6656-6662.
4. Von Sonntag, C.; Von Gunten, U., *Chemistry of ozone in water and waste water treatment*. IWA Publishing: London, 2012.
5. Huber, M. M.; Canonica, S.; Park, G. Y.; Von Gunten, U., Oxidation of pharmaceuticals during ozonation and advanced oxidation processes. *Environmental Science & Technology* **2003,** *37*, (5), 1016-1024.

Appendix A5. CURRICULUM VITAE

2010 - 2014	**PhD at the Institute of Groundwater Ecology** (Helmholtz-Centre Munich), supported by a fellowship of the Federal German Environmental Foundation (DBU), supervised by PD Dr. Martin Elsner, Prof. Dr. Christian Zwiener, Prof. Dr. Thomas Ternes and PD Dr. Michael Radke
2012 / 2013	Occasional **analytical measurements** (non-target analysis and Isotope analysis) for **Isodetect GmbH**
2010	**Initiative planning of a PhD project** and application for third-party funding in cooperation with PD Dr. Martin Elsner, Institute of Groundwater Ecology (Helmholtz-Centre Munich)
2004 – 2010	**Study of Environmental Sciences** (dt.: Geoökologie) at the University of Bayreuth (Germany)
2009 / 2010	**Diploma Thesis**: Evaluation of degradation kinetics and identification of transformation products of pharmaceuticals using a sediment water test system; supervised by Dr. Michael Radke; University of Bayreuth, Department of Hydrology
2009	**Research stay** at the Institute of Applied Environmental Sciences (Stockholm, Sweden) in the group of Prof. Michael McLachlan; supported by a fellowship of the German Academic Exchange Service (DAAD)
2008	**Student apprentice** at British American Tobacco (Bayreuth, Germany), Department **Quality Management – Analytical Technical Services**
2005 – 2008	**Student worker** in DFG (German Research Foundation) **Research Group** 562: Dynamics of soil processes at extreme meteorological boundary conditions
2003 / 2004	**Civil Service** at the Albert Schweitzer Sternstundenhaus in Rückersdorf (Germany)
1994 - 2003	**High School and A-level (Abitur)** at the Christoph-Jacob-Treu-Gymnasium-Lauf (Germany)
1983	**Born in Nuremberg,** Germany